

# Symmetries and Correlations in Strongly Interacting One-dimensional Quantum Gases

**Jean DECAMP**

Institut de Physique de Nice

**Submitted for the title of Doctor of Physics of** Université Côte d'Azur

**Supervised by** Patrizia Vignolo and Mathias Albert

**Defended on:** September 25, 2018

**Before the jury composed of:**

**Mathias Albert**, Associate professor, Institut de Physique de Nice (Université Côte d'Azur)

**George Batrouni**, Professor, Institut de Physique de Nice (Université Côte d'Azur)

**Leonardo Fallani**, Professor, University of Florence

**Maxim Olchanyi**, Professor, University of Massachusetts at Boston

**Ludovic Pricoupenko**, Professor, Laboratoire de Physique Théorique de la Matière Condensée (Université Pierre et Marie Curie)

**Patrizia Vignolo**, Professor, Institut de Physique de Nice (Université Côte d'Azur)

**Nikolaj T. Zinner**, Associate professor, Aarhus Institute of Advanced Studies (Aarhus University)



# Symmetries and Correlations in Strongly Interacting One-dimensional Quantum Gases

*Symétries et corrélations dans les gaz quantiques fortement interagissants à une dimension*

Jury:

Reviewers

**Maxim Olchanyi**, Professor, University of Massachusetts at Boston

**Ludovic Pricoupenko**, Professor, Laboratoire de Physique Théorique de la Matière Condensée (Université Pierre et Marie Curie)

Examiners

**George Batrouni**, Professor, Institut de Physique de Nice (Université Côte d'Azur)

**Leonardo Fallani**, Professor, University of Florence

**Nikolaj T. Zinner**, Associate professor, Aarhus Institute of Advanced Studies (Aarhus University)

Thesis supervisors

**Mathias Albert**, Associate professor, Institut de Physique de Nice (Université Côte d'Azur)

**Patrizia Vignolo**, Professor, Institut de Physique de Nice (Université Côte d'Azur)



# Symétries et corrélations dans les gaz quantiques fortement interagissants à une dimension

## Résumé

L'objectif principal de cette thèse est l'étude théorique de mélanges quantiques fortement interagissants à une dimension et soumis à un potentiel externe harmonique. De tels systèmes fortement corrélés peuvent être réalisés et testés dans des expériences d'atomes ultrafroids. Leurs propriétés de symétrie par permutation non triviales sont étudiées, ainsi que leurs effets sur les corrélations.

Exploitant une solution exacte pour des interactions fortes, nous extrayons des propriétés générales des corrélations encodées dans la matrice densité à un corps et dans les distributions des impulsions associées, dans les mélanges fermioniques et de Bose-Fermi. En particulier, nous obtenons des résultats substantiels sur le comportement à courtes distances, et donc les queues à haute impulsions, qui suivent des lois en  $k^{-4}$  typiques. Les poids de ces queues, dénotés contacts de Tan, sont liés à de nombreuses propriétés thermodynamiques des systèmes telles que les corrélations à deux corps, la dérivée de l'énergie par rapport à la longueur de diffusion unidimensionnelle, ou le facteur de structure statique. Nous montrons que ces contacts universels de Tan permettent également de caractériser la symétrie spatiale des systèmes, et constitue donc une connexion profonde entre les corrélations et les symétries. En outre, la symétrie d'échange est extraite en utilisant une méthode de théorie des groupes, à savoir la méthode de la somme des classes (*class-sum method* en anglais), qui provient à l'origine de la physique nucléaire. De plus, nous montrons que ces systèmes suivent une version généralisée du fameux théorème de Lieb-Mattis. Souhaitant rendre nos résultats aussi pertinents expérimentalement que possible, nous dérivons des lois d'échelle pour le contact de Tan en fonction de l'interaction, de la température et du confinement transverse. Ces lois présentent des effets intéressants liés aux fortes corrélations et à la dimensionnalité.

**Mots clés :** Gaz quantiques, atomes ultrafroids, dimension un, mixtures quantiques, symétrie d'échange, théorie des groupes, méthode de la somme des classes, fermionisation, corrélations à un corps, contact de Tan, lois d'échelle

## Symmetries and Correlations in Strongly Interacting One-dimensional Quantum Gases

### Abstract

The main focus of this thesis is the theoretical study of strongly interacting quantum mixtures confined in one dimension and subjected to a harmonic external potential. Such strongly correlated systems can be realized and tested in ultracold atoms experiments. Their non-trivial permutational symmetry properties are investigated, as well as their interplay with correlations.

Exploiting an exact solution at strong interactions, we extract general correlation properties encoded in the one-body density matrix and in the associated momentum distributions, in fermionic and Bose-Fermi mixtures. In particular, we obtain substantial results about the short-range behavior, and therefore the high-momentum tails, which display typical  $k^{-4}$  laws. The weights of these tails, denoted as Tan's contacts, are related to numerous thermodynamic properties of the systems such as the two-body correlations, the derivative of the energy with respect to the one-dimensional scattering length, or the static structure factor. We show that these universal Tan's contacts also allow to characterize the spatial symmetry of the systems, and therefore is a deep connection between correlations and symmetries. Besides, the exchange symmetry is extracted using a group theory method, namely the class-sum method, which comes originally from nuclear physics. Moreover, we show that these systems follow a generalized version of the famous Lieb-Mattis theorem. Wishing to make our results as experimentally relevant as possible, we derive scaling laws for Tan's contact as a function of the interaction, temperature and transverse confinement. These laws display interesting effects related to strong correlations and dimensionality.

**Keywords:** Quantum gases, ultracold atoms, one dimension, quantum mixtures, exchange symmetry, group theory, class-sum method, fermionization, one-body correlations, Tan's contact, scaling laws



---

# Acknowledgements

---

There are many people I should thank in these acknowledgments, and for many different reasons. I will certainly not be exhaustive in what follows, but I hope that those who made this adventure possible realize how grateful I am for this.

First of all, I would like to thank George Batrouni, Leonardo Fallani, Maxim Olshanii, Ludovic Pricoupenko and Nikolaj T. Zinner for agreeing to be part of my jury and for their enthusiasm for this work. In particular, I thank the two people who guided me during these three years of PhD, my supervisors Patrizia and Mathias. Both of you have always managed to be available when I needed it, and to share enthusiastic discussions about Physics, but not only. I feel lucky that I had you as my supervisors, and I thank you for that.

I should thank the other permanent members of the *Institut de Physique de Nice* (INPHYNI) for bringing such a good atmosphere to the lab. Thank you to the researchers with whom I had the chance to have interesting discussions during a lunch, a coffee break, or in the corridors: Mario, Frédéric, Thierry, Robin, William, among others. A special thanks to Guillaume and Xavier, with whom I have learned so much about the Magnus effect (let's put it this way). I do not forget the members of the administrative and computer staffs: thank you Nathalie, Isabelle, François-Régis and Christian for your kindness and patience, you needed it with me!

I also thank all the PhD students, postdocs and interns of the INPHYNI for being such nice traveling companions: Abdoulaye, Bruno, François, Thibaut, Ali, Simona, Antoine, Samir, Tao, Cristina, Michelle, Patrice, Aurélien, Guido, Axel, Guillaume *1145B*, Pierre, Romain, Patrizia, Marius, Anna, Julian, Vittorio, Florent, Alexis, and of course my compatriot Antonin. While writing your names I am thinking about the good moments I have shared with all of you, thank you for this! In particular, I thank Thibaut for the nice discussions and memorable moments we have shared together. Simona, for all the laughs, surrealistic debates about dragons, and for having enough imagination for both of us. Guillaume *1145B*, for the passionate discussions about Science and for the *petites sœurs*. My buddies of the "G. crew", Patrice and Aurélien, for all the games we have invented during breaks and for never leaving room for boredom in our office. I especially thank our "daddy" Patrice for taking care of Aurélien and I, who really needed it — I honestly wonder how we could have survived without you. And Aurélien, if Patrice is our daddy, you are with no doubt my brother: I feel like we have experienced the same things, good or bad, at the same moments during these three years. And every time, you were there when I needed to. More than thank you, I want to say: *bien joué Aurélien !*

There are also people who were there before my doctoral studies, who are still here now, and whom I would like to thank for their support and just for being a part of my life. First, the very good friends I have met during my studies, starting with my *vieux frère* Manu and the *trois frères* Hugo, Mickael and Romain during my unforgettable years of *classe prépa*, followed by my *grand Ami* Etienne (who is not only a great friend but also was kind enough to read and make spelling corrections to part of this manuscript) and my *copain* Will at the *magistère*, without forgetting my friends Audrey, Nathaniel, Jérémy and Anne-Charlotte (among others) of the *prépa agreg*. Besides, I thank Roch, Philippe, and all the great teachers I was fortunate to have in *classe prépa* and after, to be largely responsible for the choices that led me to do this thesis today.

I also thank my weird family<sup>1</sup>, for teaching me to always be curious about the world. In particular, I thank my brother François, whom I nicknamed Science-Boy at the time, for having forced me to sit in front of our white board and to learn too-advanced-for-my-age science when I was young. I also want to thank my other brother Manu, who taught me the importance of having a balanced life. Moreover, I am grateful to my partner's extravagant family to have welcomed me with such kindness among theirs.

Last but not least, I thank the two loves of my life, my partner Lorène and my daughter Ambre, for bringing me joy every day. Lorène, needless to say that a "thank you" is far from being enough, seeing all that you have done for me, especially during this last year. And Ambre, starting each day by seeing your smile is the best gift I could have dreamed of.

---

<sup>1</sup>admit it, you guys are a bit weird!



*We were on a walk and somehow began to talk about space. I had just read Weyl's book  
Space, Time and Matter, and under its influence was proud to declare that space was  
simply the field of linear operations.  
"Nonsense," said Heisenberg, "space is blue and birds fly through it."*

---

Felix Bloch

*Heisenberg and the early days of quantum mechanics*



---

# Contents

---

<b>Introduction</b> .....	15
<b>CHAPTER I — Strongly interacting one-dimensional quantum gases</b> .....	19
<b>I.1 Generalities on one-dimensional quantum gases</b> .....	20
I.1.1 Some theoretical peculiarities of one dimension .....	20
I.1.2 Experimental aspects .....	23
I.1.2.1 Cooling atoms .....	23
I.1.2.2 Trapping ultracold atoms .....	24
I.1.2.3 Tuning the interactions .....	25
I.1.2.4 Spin mixtures .....	27
I.1.3 The two-body problem .....	28
I.1.3.1 Scattering length and pseudo-potential .....	28
I.1.3.2 Interactions in one dimension .....	30
I.1.3.3 The cusp condition .....	31
<b>I.2 Strongly-interacting systems</b> .....	31
I.2.1 The Tonks-Girardeau gas .....	32
I.2.1.1 Model .....	32
I.2.1.2 Bose-Fermi mapping .....	32
I.2.2 Strongly interacting multi-component systems in atomic traps ..	34
I.2.2.1 Model .....	34
I.2.2.2 A perturbative ansatz .....	35
<b>CHAPTER II — Symmetry analysis</b> .....	43
<b>II.1 Generalities</b> .....	44
II.1.1 Symmetries in physics .....	44
II.1.1.1 What is symmetry? .....	44
II.1.1.2 Importance in physics .....	45
II.1.2 Exchange symmetry .....	48
II.1.2.1 Identical particles .....	48
II.1.2.2 The symmetric group and its representations .....	49

II.2	<b>Symmetry analysis of strongly interacting quantum mixtures</b> . . . . .	52
II.2.1	One-dimensional $SU(\kappa)$ quantum gases and quantum magnetism . . . . .	52
II.2.2	The class-sum method . . . . .	54
II.2.2.1	Class-sums and central characters . . . . .	54
II.2.2.2	Description of the method . . . . .	56
II.2.2.3	Implementation for $N = 6$ mixtures and first observations . . . . .	60
II.2.3	Ordering of energy levels . . . . .	63
II.2.3.1	The Lieb-Mattis theorem . . . . .	63
II.2.3.2	Analysis in our system . . . . .	69
<b>CHAPTER III — One-body correlations. Tan's contact</b> . . . . .		73
III.1	<b>One-body correlations</b> . . . . .	74
III.1.1	Generalities . . . . .	74
III.1.1.1	Definitions . . . . .	74
III.1.1.2	Experimental probes . . . . .	76
III.1.2	Exact one-body correlations for strongly repulsive systems . . . . .	77
III.1.2.1	A formula for the one-body density matrix . . . . .	77
III.1.2.2	Density profile analysis . . . . .	79
III.1.2.3	Momentum distributions . . . . .	82
III.2	<b>Short-range correlations: Tan's contact</b> . . . . .	84
III.2.1	Introduction . . . . .	85
III.2.1.1	Brief historical review . . . . .	85
III.2.1.2	Asymptotic behavior of the momentum distributions in one-dimensional quantum gases . . . . .	85
III.2.1.3	Tan sweep theorem . . . . .	87
III.2.2	Exact results in the fermionized limit . . . . .	88
III.2.2.1	Exact contact from the perturbative ansatz . . . . .	88
III.2.2.2	Discussion: Tan's contact as a symmetry probe . . . . .	90
III.2.3	Scaling laws for Tan's contact . . . . .	90
III.2.3.1	Contact at finite interaction strength . . . . .	90
III.2.3.2	Contact at finite temperature . . . . .	95
III.2.3.3	Influence of the transverse confinement . . . . .	99
<b>Conclusion</b> . . . . .		109
<b>Appendices</b> . . . . .		<b>113</b>
<b>APPENDIX A — Coordinate Bethe ansatz</b> . . . . .		115
A.1	<b>Model and first considerations</b> . . . . .	115

A.2	<b>One-component Bose gas: the Lieb-Liniger model</b> .....	117
A.2.1	Deriving the Bethe ansatz equations .....	117
A.2.2	The ground state .....	118
A.2.3	Finite temperature thermodynamics .....	120
A.3	<b>Extension to the multi-component case</b> .....	121
A.3.1	Scattering operators and consistency .....	121
A.3.2	Two-component fermions: the Gaudin-Yang model .....	123
A.3.2.1	The Bethe-Yang hypothesis .....	123
A.3.2.2	Bethe ansatz equations and ground state .....	126
A.3.3	General case: the nested Bethe ansatz .....	127
A.3.3.1	Bethe ansatz equations .....	127
A.3.3.2	Strong-coupling expansion in the balanced fermionic case	128
A.3.4	Thermodynamic Bethe ansatz .....	130
APPENDIX B — <b>List of publications</b> .....		133



---

# Introduction

---

One of the greatest challenges of modern physics is to understand the so-called *strongly correlated systems*, where particles have so much influence over each other that completely new paradigms have to be involved in order to describe them. Indeed, free models are pretty well understood, and in many systems the correlations can be treated as a *perturbation* of the non-interacting model. However, in other ones, interactions are so strong that they cannot be treated perturbatively and lead to totally different properties than their weak-coupling counterparts. In solid state physics for instance, many phenomena are associated or believed to be associated with electron-electron interactions, including the very debated *high-temperature superconductivity* [Auerbach 1994]. The realization of a common framework in order to treat strong correlations appears to be such a complicate but groundbreaking task that it is sometimes referred as a *third quantum revolution*.

Among the possible classes of strongly correlated systems that one could think of, there is one whose strongly correlated nature is present even for very weak interactions, which is the class of one-dimensional systems [Giamarchi 2003]. This can be understood pretty easily by the fact that, because of the dimensional constraint, particles cannot avoid each other. Thus, even the slightest particle excitation will directly turn into a collective one. Therefore, physics in one dimension must be addressed in a whole different way than in higher dimensions, and is rich of counter-intuitive and interesting phenomena.

Inseparable from the notion of quantum correlations is the notion of *indistinguishability*, a counter-intuitive aspect of quantum physics which makes the quantum many-body problem even harder to treat, at least conceptually, than the classical  $n$ -body problem. In quantum physics, particles with the same intrinsic properties (mass, charge, spin...) are said identical and cannot be distinguished with each other. Therefore, permuting two identical particles should not change the physical properties of the system, and can thus only change the many-body wave function describing it by a phase factor. Depending on the spin of these identical particles, one can show that this phase factor is either  $+1$  or  $-1$ , corresponding respectively to a *symmetric* and an *anti-symmetric* exchange [Schwinger 1951]. This discriminates identical particles into two classes, the so-called *bosons* and *fermions*, depending on their symmetrical or anti-symmetrical nature.

The consequences of the symmetrization postulate of identical particles are striking. On a purely conceptual point of view, it implies that all identical particles are, in a certain way, correlated, even if they are not interacting. For fermions, it implies that two identical particles cannot be in the same quantum state — for instance, all the

electrons of the Universe are in different states! This fact, known as the *Pauli exclusion principle*, explains a huge variety of properties of everyday life, such as for instance the fact that ordinary matter does not collapse [Dyson 1967]. The implications are even more spectacular for bosons. They have indeed the tendency to accumulate in their lowest energy state, at the origin of the celebrated *Bose-Einstein condensation* phenomenon at ultracold temperatures, where millions of particles behave as a single macroscopic wave. The bosonic symmetry is also related to other surprising quantum phases of matter, such as *superfluids*, a type of fluids which has zero viscosity, or *superconductors*, a type of materials with zero resistance where electrons form bosonic *Cooper pairs*.

Thus, the study of strongly correlated systems is extremely intricate. As we have previously stated, they cannot be treated perturbatively, and the exponential growth of their complexity with increasing number of particles makes it extremely difficult to access by exact analytical or numerical calculations. In order to face this problem, Feynman suggested in the eighties to make use of *quantum simulators* [Feynman 1982, Feynman 1986]. The idea is to create a clean and controllable experimental system with a given Hamiltonian coming from other branches of physics such as condensed matter, quantum chemistry or high-energy physics.

Following Feynman's direction, huge progresses have been done in the field of ultracold atomic physics after the realization of the first atomic Bose-Einstein condensate in the nineties [Tollett 1995, Petrich 1995, Davis 1995, Anderson 1995, Bradley 1995]. Using only lasers and magnetic fields, experimentalists are now able to prepare their systems in various external potentials, to tune the interactions between the strongly attractive to the strongly repulsive regimes, with almost no coupling to the environment [Bloch 2008, Bloch 2012]. They have then been able to simulate a large number of strongly correlated systems, such as the *Bose-Hubbard model* [Greiner 2002], the quantum Hall effect [Lin 2011] (making use of *artificial gauge fields* in order to circumvent the fact that atoms are neutral particles), and even cosmological models such as a black hole-like system in a Bose-Einstein condensate [Lahav 2010] or Universe's expansion [Eckel 2018], among many others.

Moreover, by making the external trapping potential very anisotropic, experimentalists have been able to access the one-dimensional regime, allowing to test some of surprising predictions of low-dimensional quantum physics [Cazalilla 2011]. Many experiments have been performed on spinless bosons, and the exceptional control over interactions has allowed to observe, for instance, the *fermionization* of bosons at very large repulsions [Paredes 2004, Kinoshita 2004]. However, a lot of typically one-dimensional phenomena, such as the *spin-charge separation* between the spin and density excitations, are expected to happen in one-dimensional fermionic spin mixtures [Voit 1995].

Recently, a one-dimensional fermionic mixture with up to six spin-components was realized in the experimental group of Leonardo Fallani in the LENS [Pagano 2014], paving the way for the verification of many hitherto untested theoretical predictions. Their experiment was performed using fermionic Ytterbium atoms, whose ground-state has a purely nuclear spin. This implies that particles are subjected to the same external and interaction potentials regardless of their spin-orientation, and that there are no spin-flipping collisions. This confers the so-called  $SU(\kappa)$  symmetry to the system, where  $\kappa$  is the number of spin-components [Gorshkov 2010], making it an ideal quantum simu-



lator for the Yang-Mills gauge theories involved in the standard model of elementary particles [Banerjee 2013, Zohar 2013, Tagliacozzo 2013].

This thesis is devoted to the theoretical study of one-dimensional quantum mixtures (fermionic, bosonic, or mixed), in the fermionized regime of very strong repulsions. As in the LENS experiment, the particles have the same mass, are subjected to the same (harmonic) external potential and ( $\delta$ -type) interaction potential whatever their species, and the number of particle per species is fixed. As one can see, many aspects of strongly correlated systems are tackled, namely the strong interactions, low-dimensionality, and the question of exchange symmetry and quantum statistics. During this work, we have tried to link these concepts together and analyze their effects, always keeping in mind the experimental aspects. The central question that we address is the following: How to characterize, both theoretically and experimentally, the exchange symmetry in our system? Indeed, although the *total* symmetry of the particles is fixed by their fermionic or bosonic nature, the fact that they have different spin orientations allows to obtain other kinds of *spatial* exchange symmetries.

This manuscript is organized as follows.

Chapter I is an introduction to the concepts and techniques related to strongly interacting one-dimensional quantum mixtures. After describing some of the theoretical peculiarities and experimental aspects of one-dimension, we explain the effects of strong interactions and the so-called fermionization. In particular, we describe the method we implemented in order to obtain exact analytical results for few-body systems, which is based on a mapping to a non-interacting fermionic problem combined with a perturbative expansion performed over the inverse of the coupling strength. Besides, we give an interpretation of this method in terms of graph theory.

In chapter II, we explain how, given an exact solution obtained by the aforementioned perturbative method, we are able to characterize its exchange symmetry. To do so, we adapt the so-called *class-sum method*, which is originally due to Dirac. We try to present it in a pedagogical but mathematically rigorous way, with the hope that this manuscript can serve as a good introduction to this method. The exchange symmetry of various few-body mixtures are then analyzed. We show in particular that the class-sum method can serve to generalize the so-called *Lieb-Mattis theorem*, which allows to compare the ordering of the energy levels associated to certain symmetry classes.

In chapter III, we study the correlations in our system, and more precisely the *one-body correlations*, which embed the density distributions of the particles in real and momentum space and are easily accessible in a cold atom experiment. First, we analyze the effects of interactions and symmetries on few-body systems, and show that the density and momentum profiles can be qualitatively deduced from symmetry arguments. Second, we focus on the so-called *Tan's contact*, an observable that governs the high-momentum behavior of shortly-interacting quantum gases. We show in particular that a measurement of Tan's contact allows to deduce uniquely the exchange symmetry of the system. Then, in order to be as experimentally relevant as possible, we derive scaling laws for Tan's contact, as a function of the interaction strength, number of particles and components, temperature, and transverse confinement.

The so-called *coordinate Bethe ansatz*, which allows to obtain exact results in the absence

of an external potential but for any value of the interaction strength, is explained in details in appendix [A](#). Appendix [B](#) contains the list of publications of the author of this thesis.

# CHAPTER I

---

## Strongly interacting one-dimensional quantum gases

### Contents

---

<b>I.1</b>	<b>Generalities on one-dimensional quantum gases</b> .....	<b>20</b>
I.1.1	Some theoretical peculiarities of one dimension .....	20
I.1.2	Experimental aspects .....	23
I.1.2.1	Cooling atoms .....	23
I.1.2.2	Trapping ultracold atoms .....	24
I.1.2.3	Tuning the interactions .....	25
I.1.2.4	Spin mixtures .....	27
I.1.3	The two-body problem .....	28
I.1.3.1	Scattering length and pseudo-potential .....	28
I.1.3.2	Interactions in one dimension .....	30
I.1.3.3	The cusp condition .....	31
<b>I.2</b>	<b>Strongly-interacting systems</b> .....	<b>31</b>
I.2.1	The Tonks-Girardeau gas .....	32
I.2.1.1	Model .....	32
I.2.1.2	Bose-Fermi mapping .....	32
I.2.2	Strongly interacting multi-component systems in atomic traps .	34
I.2.2.1	Model .....	34
I.2.2.2	A perturbative ansatz .....	35

---

What makes one-dimensional systems extremely interesting for theoretical physicists is divided in two main reasons. First, due to the extreme complexity of many-body physics, these systems are usually easier to solve analytically than many-body systems in higher dimensions. Second, and perhaps more interestingly, phenomena in one-dimension are often very different from what our three-dimensional intuition may suggest us. Indeed, many of the theories that work extremely well in higher dimensions have to be completely modified in order to tackle their one-dimensional counterparts. Finally, besides these two historical reasons, what makes this research area even more exciting is the huge progresses realized in ultracold atom physics, that allow to engineer and probe various one-dimensional systems with an incredible precision.

This chapter is devoted to the study of the models describing strongly interacting one-dimensional ultracold atomic gases. First, in section I.1, we provide a very general description of one-dimensional systems, from their theoretical peculiarities and modelization to their main experimental realization techniques. Then, in section I.2, we focus on the case of strongly interacting one-dimensional quantum gases in the experimentally relevant case of a harmonic external potential, and describe an exact analytic solution that we will extensively use throughout this thesis.

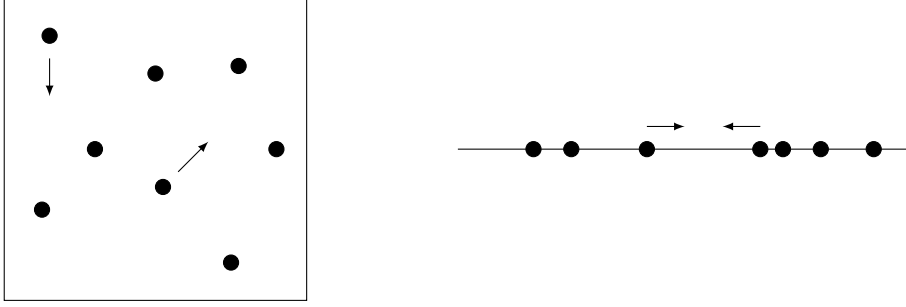
## I.1. Generalities on one-dimensional quantum gases

In this introductory section, we discuss some general aspects of ultracold atomic gases in one dimension. First, we are going to review some of the very peculiar theoretical features of one dimension in I.1.1. Then, we briefly present how experimental physicists are able to create highly clean and tunable ultracold atomic systems that can be modeled by one-dimensional theories in I.1.2. Finally, in I.1.3, we focus on the theoretical description of interactions in one-dimensional ultracold atomic gases, whose diluted nature reduce the problem to two-body interactions. This last part will serve as a preliminary for the rest of the chapter, by justifying precisely the form of the interaction potential and its consequence on the many-body wave function.

### I.1.1. Some theoretical peculiarities of one dimension

The one-dimensional (1D) world is, on many aspects, profoundly distinct from higher dimensions [Giamarchi 2003]. Many quantum theories that have proven to be very efficient in higher dimensions, such as the Landau-Fermi liquid theory describing interacting electrons [Landau 1957] simply breakdown in 1D. It could naively seem strange that models that work perfectly well in two (2D), three (3D) and, formally, any dimension  $d \geq 2$ , fail so dramatically in 1D. On a mathematical point of view, this is a reflect of the very peculiar topological properties of low-dimensional spaces. Physically, for a many-body one-dimensional system, the dimensional constraint is actually very simple to understand: contrary to higher dimensions, particles do not have the possibility to avoid each other (see Fig. I.1.1).

This very simple observation has dramatic impacts. First, 1D systems are strongly corre-



**Figure I.1.1:** Classical interpretation of the dimensional constraint. In the 2D gas (left), particles are free to avoid each other, which is not the case in 1D (right).

lated, even if the interactions between particles are weak. It seems clear then that naive mean-field approaches will not succeed to describe it. Second, a single-particle excitation will automatically lead to a collective excitation. This explains why the Landau-Fermi liquid paradigm fails to describe 1D systems. Indeed, Landau's description is based on the idea that a Fermi liquid behaves essentially as a free Fermi gas, but with "dressed" particles, that is whose dynamical properties such as the mass or the magnetic moment are renormalized due to interactions. This so-called *adiabatic connection* implies that the elementary excitations of a Fermi liquid can be treated very similarly to the individual excitations of a free Fermi gas, as quasi-particles with a very long life time  $\tau$ . Due to the collective nature of excitations in 1D, such a description by essentially free quasi-particles clearly becomes irrelevant.

The 1D counterpart of the Landau-Fermi liquid universality class is the so-called Tomonaga-Luttinger liquid universality class [Haldane 1981]. The Tomonaga-Luttinger liquid theory describes the low-energy excitations of a large number of 1D models, by mean of the so-called *bosonization* method. It consists in linearizing the energy spectrum  $\epsilon_k$  around the two Fermi points  $+k_F$  and  $-k_F$  writing  $\epsilon_k \simeq \pm \hbar v_F (k - k_F)$ . This implies the following low-energy effective description for the Hamiltonian  $\hat{H}_0$  of the free Fermi gas:

$$\hat{H}_0 = \sum_k \hbar v_F k \left( \hat{c}_k^{R\dagger} \hat{c}_k^R - \hat{c}_k^{L\dagger} \hat{c}_k^L \right), \quad (\text{I.1.1})$$

where  $\hat{c}_k^{R/L\dagger}$ ,  $\hat{c}_k^{R/L}$  are the usual fermionic creation/annihilation operator, the  $R/L$  exponents standing for right/left moving particles. Motivated by the long wavelength collective behavior of low-energy excitations, we define the density fluctuation operators as

$$\hat{\rho}_q^{R/L\dagger} = \sum_k \hat{c}_{k+q}^{R/L\dagger} \hat{c}_k^{R/L} \quad (\text{I.1.2})$$

and

$$\hat{\rho}_q^{R/L} = \sum_k \hat{c}_{k-q}^{R/L} \hat{c}_k^{R/L}. \quad (\text{I.1.3})$$

We then use the associated field operators  $\hat{\rho}^{R/L}(x)$  to define the current and density

fields as the following bosonic fields<sup>1</sup>:

$$\begin{aligned}\phi(x) &= -\pi \left( \hat{\rho}^R(x) + \hat{\rho}^L(x) \right), \\ \Pi(x) &= \hat{\rho}^R(x) - \hat{\rho}^L(x).\end{aligned}\tag{I.1.4}$$

Then, Eq. (I.1.1) can be re-written

$$\hat{H}_0 = \frac{\hbar}{2} \int dx v_F \left[ \pi \Pi(x)^2 + \frac{1}{\pi} (\partial_x \phi(x))^2 \right].\tag{I.1.5}$$

When interactions are taken into account, Haldane has shown that the total Hamiltonian  $\hat{H}$  is very similar to Eq. (I.1.5):

$$\hat{H} = \frac{\hbar}{2} \int dx u \left[ \pi K \Pi(x)^2 + \frac{1}{\pi K} (\partial_x \phi(x))^2 \right],\tag{I.1.6}$$

where  $u$  is the sound velocity and the so-called *Luttinger parameter*  $K$  controls the long-distance behavior of the correlation functions. More generally, we can define the Tomonaga-Luttinger liquids as the class of 1D liquids described by an Hamiltonian of the form of Eq. (I.1.6). It is then sufficient to determine the model-dependent parameters  $K$  and  $u$  to obtain precious information about the low-energy and low-momentum behavior of the system, hence the power of this method. Moreover, although derived at first for spinless fermions, it also allows to describe spinless bosonic systems as well as spin mixtures.

If we consider a mixture of different spin species, another striking effect of the dimensionality occurs. In the case of a spin- $\frac{1}{2}$  mixture, we can define respectively the charge and spin fields as the following spin-symmetric and spin-anti-symmetric operators:

$$\begin{aligned}\phi_{c/s}(x) &= \frac{1}{\sqrt{2}} [\phi_{\uparrow}(x) \pm \phi_{\downarrow}(x)], \\ \Pi_{c/s}(x) &= \frac{1}{\sqrt{2}} [\Pi_{\uparrow}(x) \pm \Pi_{\downarrow}(x)],\end{aligned}\tag{I.1.7}$$

where  $c/s$  are respectively associated with  $+/-$ . It can be shown that the Hamiltonian can be written:

$$\hat{H} = \hat{H}_c + \hat{H}_s = \sum_{\nu=c,s} \frac{\hbar}{2} \int dx u_{\nu} \left[ \pi K_{\nu} \Pi_{\nu}(x)^2 + \frac{1}{\pi K_{\nu}} (\partial_x \phi_{\nu}(x))^2 \right].\tag{I.1.8}$$

To put it in words, the excitations in 1D are completely decoupled between charge and spin excitations! This counter-intuitive effect is known as the *spin-charge separation*. It is intimately connected with the collective nature of excitations.

Another very surprising property of 1D systems is that they are more interacting at low densities. This can be understood with a simple dimensional argument: if we denote the atomic lineic density by  $n$  and the interaction strength by  $g$ , the typical interaction and kinetic energies per particle are respectively given by  $E_{int} \sim ng$  and  $E_K \sim \hbar^2 n^2 / 2m$ .

---

<sup>1</sup>The following expressions are only true in the thermodynamic limit  $L \rightarrow \infty$ . Finite-size definitions are more involved and make use of a cut-off parameter.

Thus, the ratio of these energies is  $\gamma \sim E_{int}/E_K \sim g/n$ . It is then clear that the interactions will have a more important influence on the system for low  $n$ .

Let us finish this introduction to the beauty of one-dimensional physics by a very profound and important theorem known as the Mermin-Wagner-Hohenberg theorem [Mermin 1966, Hohenberg 1967]. It states that, because of the too important long-range fluctuations induced by the dimensional constraint, there is no phase transition with spontaneous breaking of a continuous symmetry at non-zero temperatures (see section II.1.1.2). This implies, in particular, the absence of the celebrated Bose-Einstein condensation in 1D, which is associated with the breakdown of the phase symmetry  $U(1)$  [Pitaevskii 2016].

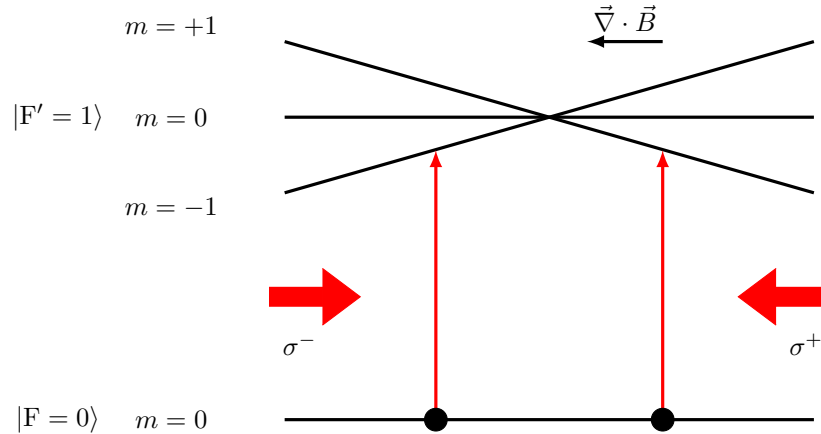
## I.1.2. Experimental aspects

Although very interesting on a purely theoretical point of view, it would be a little bit unsatisfying if one-dimensional physics was only a set of mathematical *toy models* without any experimental significance. Fortunately, wonderful progress has been achieved in the domain of ultracold gases ([Bloch 2008] and references therein), allowing to access the 1D world with an incredible degree of experimental control [Moritz 2003, Stöferle 2004]. This motivates a very stimulating interplay between theoretical and experimental physicists. We thus briefly take the time to present some of the experimental techniques used to address 1D physics with ultracold gases. The probing techniques will be exposed in the chapter devoted to one-body correlations (chapter III). Remark that other physical experimental systems can be modeled by 1D theories, ranging from edge states in the quantum hall effect [Milliken 1996], to carbon nanotubes [Bockrath 1999] or quantum wires [Auslaender 2005] and spin chains [Lake 2005]. However these systems don't offer the experimental control of ultracold atomic physics. We focus on the latter in the following.

### I.1.2.1. Cooling atoms

The main tool in order to cool atoms is the so-called *magneto-optical trap* (MOT), whose principle was suggested by Jean Dalibard in the eighties, and whose first experimental realization was reported in [Raab 1987]. It allows to cool atoms at the order of a few  $\mu\text{K}$ .

There are two main ingredients in a MOT: first, the atoms are illuminated by counter-propagating *red-detuned* laser beams, i.e. with a lower frequency than the resonant frequency of the atoms. Because of the Doppler effect, when an atom moves, it will absorb a photon coming from the opposite direction and carrying a momentum  $\vec{p}$ , thus reducing the momentum of the atom. The second ingredient of the MOT is a spatially varying magnetic field generated by magnetic coils in anti-Helmholtz configuration. This causes a Zeeman splitting of the energy levels of the atoms, which increases with the distance from the center of the trap, and therefore shifts the atomic resonance closer to the frequency of the lasers. Thus, atoms are more likely to absorb a "photon kick" when far from the trap center. Moreover, by choosing the laser polarizations so that photons



**Figure I.1.2:** Schematic diagram of a MOT. The magnetic gradient generates a Zeeman splitting of the  $|F' = 1\rangle$  state. The red-detuned counter-propagating lasers have opposite circular polarizations. Because of the atomic selection rules, each laser can only induce a transition to a single Zeeman level. Thus, the atoms are slowed down and pushed toward the center of the MOT.

interact with the correct energy levels, these photon kicks are always pushing the atoms toward the center. A schematic diagram of a MOT is given in Fig. I.1.2.

However, the cooling induced by a MOT is limited by the fact that atoms spontaneously emit the photons previously absorbed during the cooling process, which in result will heat the atoms. In order to reach the ultracold limit (around 100 nK), the next step is the *evaporative cooling*. It consists in trapping the atoms in a magnetic trap of finite depth  $\epsilon$ . The "hot" atoms with energies higher than  $\epsilon$  will then escape from the trap, resulting in a reduced average temperature of the atoms remaining in the trap. It is the exact analog of cooling a hot drink by blowing on it! This technique was employed in order to obtain the first Bose-Einstein condensate with ultracold atoms [Tollett 1995, Petrich 1995, Davis 1995, Anderson 1995, Bradley 1995].

### I.1.2.2. Trapping ultracold atoms

The basic way of generating 1D atomic traps is to manipulate the atomic potential in order to make it very anisotropic. In a typical harmonic oscillator potential characterized by frequencies  $\omega_x = \omega_y = \omega_\perp$  and  $\omega_z$ , we want the *aspect ratio*  $\lambda = \omega_z/\omega_\perp$  to be sufficiently small, so that the typical energy of a particle is smaller than the energy of the first transverse excited state. This way, the so-called *quasi-1D* regime is achieved, with no transverse excited modes and all the dynamics occurring in the  $z$  direction [Olshanii 1998]. The main ways to generate atomic potentials are discussed below.

There are two main methods in order to trap ultracold atoms: *optical* and *magnetic* trapping. The optical trapping is based on interference patterns created by a superposition of laser beams. More precisely, the electric fields generated by the light will interact with the atom and generate a small dipole moment. The resulting dipolar force  $\vec{F}$  between



the atom and the laser of frequency  $\omega_L$  has the form [Grimm 2000]:

$$\vec{F}(\vec{r}) = \frac{1}{2}\alpha(\omega_L)\nabla \left[ |\vec{E}(\vec{r})|^2 \right], \quad (\text{I.1.9})$$

where  $\alpha(\omega_L)$  is the polarizability. If  $\omega_L$  is close to the resonance frequency  $\omega_0$  between the ground  $|g\rangle$  and excited state  $|e\rangle$  of the atom, it can be shown that the polarizability has the form:

$$\alpha(\omega_L) \simeq \frac{|\langle e | \hat{d}_{\vec{E}} | g \rangle|^2}{\hbar(\omega_0 - \omega_L)}, \quad (\text{I.1.10})$$

where  $\hat{d}_{\vec{E}}$  is the dipole operator in the direction of the field. Therefore, we see that the atoms will be attracted to regions of high light intensity when the laser is *red detuned* ( $\omega_L < \omega_0$ ) and to regions of weak light intensity when the laser is *blue detuned* ( $\omega_L > \omega_0$ ). An example of 2D optical lattice allowing to generate 1D traps is given in figure I.1.3.

The magnetic trapping techniques are based on the Zeeman coupling between an external magnetic field  $\vec{B}(\vec{r})$  and the total spin  $\vec{S}$  of the atom. In 1D, the magnetic field is generally generated by a so-called *atom chip*, which consists in a surface where wires were deposited with high-precision micro-fabrication techniques [Reichel 1999, Jacqumin 2011]. If we denote the magnetic moment of the atom by  $\vec{\mu}$ , the atomic potential is given by [Folman 2002]:

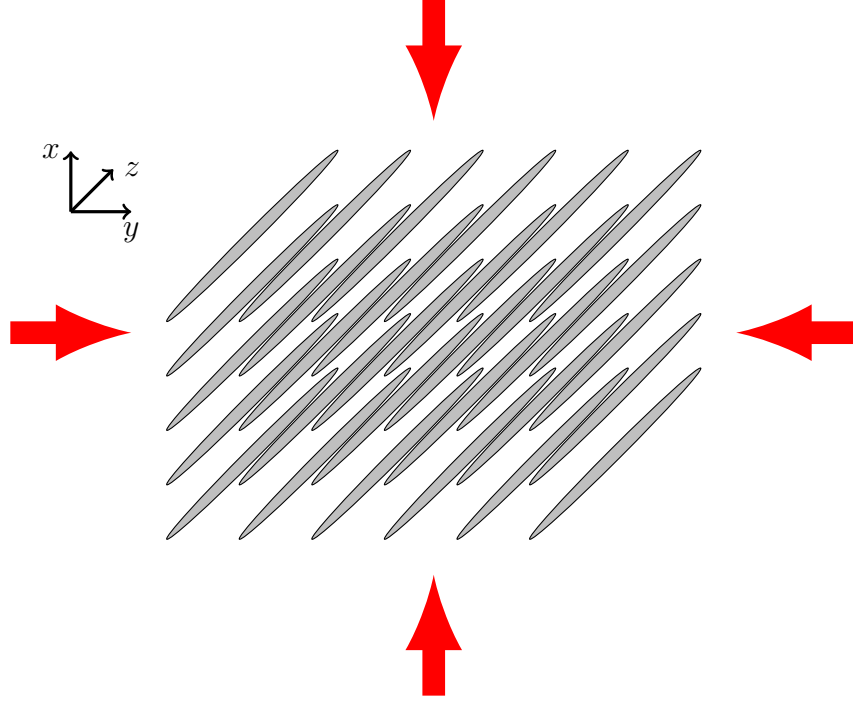
$$V_{mag}(\vec{r}) = -\vec{\mu} \cdot \vec{B}(\vec{r}), \quad (\text{I.1.11})$$

which is simply proportional to  $\|\vec{B}(\vec{r})\|$  when  $\vec{B}(\vec{r})$  is sufficiently slowly varying. Similarly to the case of the optical trapping, there are two cases, depending if  $\vec{\mu}$  is in the same direction as  $\vec{B}$  ( $V_{mag} < 0$ ) or in the opposite direction ( $V_{mag} > 0$ ). In these two so-called *strong field seeking* (resp. *weak field seeking*) states, the atoms are attracted by maxima (resp. minima) of  $\|\vec{B}(r)\|$ . Due to a theorem by Earnshaw which states that there cannot be maxima of the magnetic field in free space, the source of the field must be inside the trapping region in the strong field seeking case [Ketterle 1992]. This is the reason why the weak field seeking state is more used. However, it has the inconvenient of preventing the use of strong magnetic fields, which can be useful in order to tune the interactions (see section I.1.2.3).

### I.1.2.3. Tuning the interactions

Ultracold gases offer a very powerful tool that allows to tune the interactions very precisely, and even to change the sign of the interactions, namely the Feshbach resonances [Feshbach 1958, Fano 1961]. The basic idea is to generate, via an external magnetic field<sup>2</sup>, a resonance between a bound-state in a close channel and the scattering continuum of an open channel. Typically, given two atoms, these two states correspond to different two-spin configurations. When the two atoms are scattering together, this induced resonance will result in a quasi-bound state which will considerably modify the (3D) scattering length  $a_{3D}$  (a precise definition of the scattering length will be given in

<sup>2</sup>Alternatively, one could also use an external optical field [Fedichev 1996].



**Figure I.1.3:** A 2D optical lattice: the superposition of two standing waves generates 1D traps. The hopping time between these tubes has to be significantly greater than the characteristic time of the experiment.

section I.1.3). Phenomenologically, this resonance can be described for the scattering length by [Bloch 2008]:

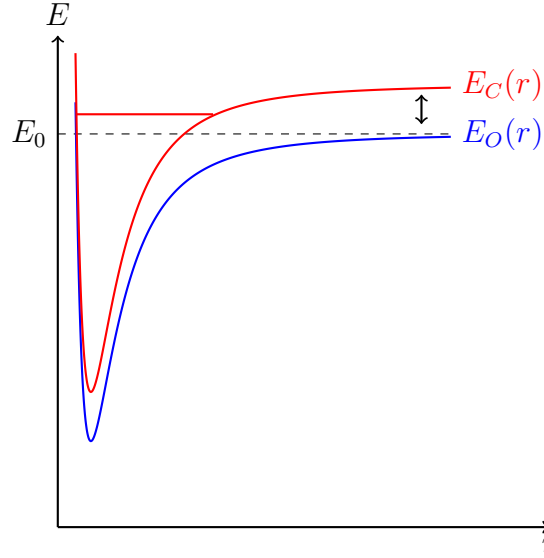
$$a_{3D}(B) = a_{bg} \left[ 1 - \frac{\Delta B}{B - B_0} \right], \quad (\text{I.1.12})$$

where  $a_{bg}$  is the background scattering length in the absence of the external magnetic field  $B$ , and  $\Delta B$  and  $B_0$  are respectively the width and position of the magnetic resonance. We can see in Eq. (I.1.12) that a Feshbach resonance even allows to change the sign of  $a_{3D}$ , and to tune it from  $-\infty$  to  $+\infty$  just by changing the external magnetic field [Tiesinga 1993]. For a graphical interpretation of a two-channel Feshbach resonance, see Fig. I.1.4.

There are alternative methods in order to tune the interactions that are specific to 1D. First, as seen in section I.1.1, one way to change the interaction regime in 1D is given by the atomic density  $n$ : the lower the density, the stronger the interactions. Moreover, it can be shown [Olshanii 1998] that when the system is in the quasi-1D regime (see section I.1.2.2), the scattering processes can be described by an effective interaction potential  $U(x) = g_{1D}\delta(x)$  where the effective coupling parameter is

$$g_{1D} = \frac{-2\hbar^2}{ma_{1D}} = \frac{2\hbar^2 a_{3D}}{ma_{\perp}^2} \left( 1 - C \frac{a_{3D}}{a_{\perp}} \right)^{-1}, \quad (\text{I.1.13})$$

where  $a_{1D}$  is the effective 1D scattering length,  $a_{\perp} = \sqrt{\hbar/m\omega_{\perp}}$  is the transverse harmonic oscillator length and  $C = |\zeta(1/2)|/\sqrt{2} \simeq 1.0326$ ,  $\zeta$  being the Riemann zeta function. Then, by varying  $\omega_{\perp}$ , we see that we can approach a *confined induced resonance* when  $a_{\perp} \simeq Ca_{3D}$ . This method was achieved experimentally, see e.g. [Peano 2005].



**Figure I.1.4:** Two-channel model for a Feshbach resonance. When varying an external magnetic field  $\vec{B}_{ext}$ , the incident energy  $E_0$  of the particle in the open channel  $E_O$  can be in resonance at short inter-atomic distance  $r$  with the energy of a bound state of the closed channel  $E_C$ .

The theoretical aspects of two-body interactions in 1D quantum gases will be discussed in more detail in section I.1.3.

#### I.1.2.4. Spin mixtures

In this thesis, we will mainly focus on quantum mixtures, i.e. ultracold atomic gases with different spin components. On the experimental side, a huge breakthrough was made in an experiment made in the LENS (European Laboratory for Nonlinear Spectroscopy) in Florence by the team of L. Fallani [Pagano 2014]. We briefly describe it here, as a paradigmatic realization of the system we studied in this thesis.

L. Fallani and coworkers realized a 1D fermionic mixture of  $^{173}\text{Yb}$  atoms with a tunable number  $\kappa \in \{1, \dots, 6\}$  of components. The ground state of  $^{173}\text{Yb}$  atoms has a nuclear spin  $I = 5/2$  and a zero electronic angular momentum  $J = 0$ . This last property, which is also common to all alkaline-earth atoms [Gorshkov 2010], implies that the electronic wave function is independent of the nuclear spin state — there is no hyperfine structure. Therefore, the interactions between atoms of different nuclear spin states  $\sigma \neq \sigma'$ , which depends only on their electronic wave functions, are the same regardless of the choice of  $\sigma \neq \sigma'$ . Moreover, it implies the absence of spin-flipping collisions. Thus, their system is invariant by any permutation of the  $\kappa \in \{1, \dots, 6\}$  spin populations, which is referred as the  $SU(\kappa)$  symmetry (see chapter II).

Moreover, the system can be initialized with a given number  $\kappa < 6$  of spin-components with an equal number of atoms per component, starting from an equally populated six-component mixture. The idea is the following: the first excited state ( $I = 5/2, J = 1$ ) is Zeeman-split by mean of a magnetic field. Then, they can optically pump out the population of a given spin state  $\sigma$  to another spin state  $\sigma \pm 1$  through polarized

beams resonant on a specific Zeeman component of the excited state. The unwanted populations are then put in an optically closed transition and removed by evaporation.

Because the spin of  $^{173}\text{Yb}$  is purely nuclear, spin-resolved detection cannot be done by mean of a standard magnetic Stern-Gerlach procedure [Gerlach 1922]. In order to circumvent this problem, an *optical* Stern-Gerlach experiment is performed [Taie 2010], by misaligning a laser beam on the atomic cloud. The Gaussian profile of the laser generates an electric gradient. The atoms will then interact with the laser in a similar way as described in expression I.1.9, but with a polarizability depending on the spin-state, thus splitting the populations.

It is important to note that when  $\kappa > 2$ , interactions cannot be tuned using Feshbach resonances if one wants to preserve the  $SU(\kappa)$  symmetry. Experimentalists have to rely on the other methods (decreasing the atomic density or generating confined induced resonances) in order to reach the strongly interacting regime. In the LENS experiment, interactions are typically in the intermediate regime.

### I.1.3. The two-body problem

In this section we discuss the properties of interactions in ultracold quantum gases. We will justify the form of the interaction Hamiltonian on the one hand, and on the other hand we will discuss its consequence on the many-body wave function, known as the *cusp condition*.

#### I.1.3.1. Scattering length and pseudo-potential

Since atoms are neutral particles, they interact via van der Waals forces [Dzyaloshinskii 1961]. Typically, at large distance  $r$  the interaction potential  $U(r)$  is of the type  $\propto -1/r^6$  and at distances lower than the so-called *van der Waals contact distance*  $r_0$ , the electronic clouds will lead to a strong contact repulsion. The systems we consider are ultracold and diluted: therefore,  $r_0$  can be considered negligible as compared to the de Broglie wavelength  $\lambda_{\text{dB}}$  and the inter-atomic separation  $n^{-1/3}$  (where  $n$  is the atomic density). This property, together with the fact that the temperatures are very low, explains why the system can be effectively described by low energy two-body collisions, and by a single parameter, namely the *s*-wave scattering length  $a_{3D}$  [Pitaevskii 2016]. Considering spinless particles, the two-body problem can be written:

$$\left(-\frac{\hbar^2}{2\mu}\Delta + U(r) - E\right)\psi(\vec{r}) = 0, \quad (\text{I.1.14})$$

where  $\vec{r} = \vec{r}_1 - \vec{r}_2$  and  $\mu = m/2$  is the reduced mass. In the asymptotic region  $r \gg r_0$ , the solution can be written as the superposition of an incident plane wave in the  $x$  direction and a spherical scattered wave:

$$\psi(\vec{r}) \simeq e^{ikx} + f(\theta, k)\frac{e^{ikr}}{r}, \quad (\text{I.1.15})$$

where

$$k = \sqrt{\frac{2\mu E}{\hbar^2}}, \quad (\text{I.1.16})$$

$\theta$  is the angle between  $\vec{r}$  and the  $x$ -axis, and  $f$  is defined as the *scattering amplitude*. Expanding  $\psi$  in the natural basis of Legendre polynomials  $P_l$  yields:

$$\psi(\vec{r}) = \sum_{l=0}^{\infty} P_l(\cos \theta) \frac{\chi_{kl}(r)}{kr}, \quad (\text{I.1.17})$$

where  $\chi_{kl}(r)$  satisfies

$$\frac{d^2 \chi_{kl}(r)}{dr^2} - \frac{l(l+1)}{r^2} \chi_{kl}(r) + \frac{2\mu}{\hbar^2} (E - U(r)) \chi_{kl}(r) = 0. \quad (\text{I.1.18})$$

In the asymptotic region  $r \gg r_0$ , one can neglect the  $\propto 1/r^2$  term, which yields the simple expression:

$$\chi_{kl}(r) = A_l \sin \left( kr - \frac{\pi l}{2} + \delta_l(k) \right), \quad (\text{I.1.19})$$

where  $\delta_l(k)$  are defined as *phase shifts*. Then, an appropriate choice for  $A_l$  gives after some simple algebra:

$$f(\theta, k) = \frac{1}{2ik} \sum_{l=0}^{\infty} (2l+1) P_l(\cos \theta) (e^{2i\delta_l} - 1). \quad (\text{I.1.20})$$

Thus, the scattering cross-section  $\sigma$ , related to  $f(\theta, k)$  through  $\sigma = \frac{4\pi}{k} \text{Im}[f(0, k)]$ , is given by:

$$\sigma(k) = \frac{4\pi}{k^2} \sum_{l=0}^{\infty} (2l+1) \sin^2 \delta_l(k). \quad (\text{I.1.21})$$

For low energy collisions and momenta  $k \ll 1/r_0$ , one can prove that only the  $s$ -wave  $l = 0$  term will be relevant. Therefore, Eq. (I.1.20) simply becomes:

$$f(\theta, k) \simeq \frac{e^{2i\delta_0} - 1}{2ik} = \frac{1}{k \cot \delta_0(k) - ik}. \quad (\text{I.1.22})$$

We define the  $s$ -wave scattering length  $a_{3D}$  as

$$a_{3D} = - \lim_{k \rightarrow 0} \frac{\tan \delta_0(k)}{k}, \quad (\text{I.1.23})$$

which implies that  $\sigma \simeq 4\pi a_{3D}^2$ . Intuitively, this can be interpreted as if the system had the same low energy scattering properties as a hard sphere of radius  $a_{3D}$ .

In the case where we consider the spin-statistics, we can observe an important effect. Indeed, because of the (anti-)symmetrization of the two-body wave function for identical (fermions) bosons, it implies that only the (odd) even  $l$  terms in Eq. (I.1.20) will contribute to the cross-section  $\sigma$ . Thus, in the  $s$ -wave scattering limit of low energy and for distances  $r \ll r_0$ , identical fermions are not interacting.

In the previous discussion, we have never used a precise expression for the interaction potential  $U(r)$  in Eq. (I.1.14), but instead showed that, in our regime, all the physics is

captured by the  $s$ -wave scattering asymptotic behavior and thus  $a_{3D}$ . It is then sufficient to replace  $U(r)$  by a simpler *pseudopotential*  $U_{\text{pseudo}}(r)$  which has the same long distance  $s$ -wave scattering properties than  $U(r)$ . It was shown in [Huang 1957] that the following pseudo-potential has the right properties:

$$U_{\text{Huang}}(r) = g_{3D} \delta(\vec{r}) \frac{\partial}{\partial r}(r \cdot), \quad (\text{I.1.24})$$

where  $g_{3D} = 4\pi\hbar^2 a_{3D}/m$  is the coupling constant. The  $\frac{\partial}{\partial r}(r \cdot)$  is useful in order to remove the  $1/r$  divergence in Eq. (I.1.15).

### I.1.3.2. Interactions in one dimension

In the quasi-1D case where the atoms are in a highly elongated trap in the  $x$  direction, Eq. (I.1.14) becomes, in the pseudo-potential approximation:

$$\left( -\frac{\hbar^2}{2\mu} \frac{\partial^2}{\partial x^2} + U_{\text{Huang}}(r) + \hat{H}_{\perp} - E \right) \psi(\vec{r}) = 0, \quad (\text{I.1.25})$$

where

$$\hat{H}_{\perp} = -\frac{\hbar^2}{2\mu} \left( \frac{\partial^2}{\partial y^2} + \frac{\partial^2}{\partial z^2} \right) + \frac{1}{2} \mu \omega_{\perp}^2 (y^2 + z^2) \quad (\text{I.1.26})$$

and  $\omega_{\perp}$  is the radial confinement frequency, which is such that  $\hbar\omega_{\perp}$  is sufficiently higher than the other typical energies so that the quasi-1D regime can be achieved. This case was studied in [Olshanii 1998]. Then, considering that the incident wave is in the ground state  $\phi_0(y, z)$  of  $\hat{H}_{\perp}$ , the analogue of Eq. (I.1.15) for the asymptotic form of the scattered wave function is:

$$\Psi(\vec{r}) \simeq \left( e^{ik_x x} + f_{\text{even}}(k) e^{ik_x |x|} + f_{\text{odd}}(k) \text{sign}(z) e^{ik_x |x|} \right) \phi_0(y, z). \quad (\text{I.1.27})$$

The scattering amplitudes can then be calculated analytically, by correctly taking into account the *virtual* transverse excited states during the collision process. This gives  $f_{\text{odd}} = 0$  and, in the  $k_x a_{1D} \ll 1$  limit:

$$f_{\text{even}}(k) = -\frac{1}{1 + ik_x a_{1D} + \mathcal{O}((k_x a_{1D})^3)}, \quad (\text{I.1.28})$$

where the 1D effective scattering length is defined as in Eq. (I.1.13) by

$$a_{1D} = -\frac{a_{\perp}^2}{a_{3D}} \left( 1 - C \frac{a_{3D}}{a_{\perp}} \right). \quad (\text{I.1.29})$$

As stated in section I.1.2.3, the analogue of Huang's pseudo-potential that captures the correct even wave scattering behavior in 1D is

$$U_{\text{pseudo}}(x) = g_{1D} \delta(x), \quad (\text{I.1.30})$$

where  $g_{1D} = -\frac{2\hbar^2}{ma_{1D}}$ .

### I.1.3.3. The cusp condition

Here we prove a very important corollary to the fact that the 1D two-body interactions can be described by the potential (I.1.30). Let us consider a strictly 1D Schrödinger equation for two atoms of equal masses  $m$  and coordinates  $x_1, x_2$ :

$$\left( -\frac{\hbar^2}{2m} \left( \frac{\partial^2}{\partial x_1^2} + \frac{\partial^2}{\partial x_2^2} \right) + g_{1D} \delta(x_1 - x_2) + V_{ext}(x_1, x_2) - E \right) \psi(x_1, x_2) = 0, \quad (\text{I.1.31})$$

where  $V_{ext}$  is an arbitrary (continuous) external potential. We then define the relative coordinate by  $x_{12} = x_1 - x_2$  and the center-of-mass coordinate by  $X_{12} = \frac{x_1 + x_2}{2}$ . Eq. (I.1.31) then becomes:

$$\left( -\frac{\hbar^2}{2M} \frac{\partial^2}{\partial X_{12}^2} - \frac{\hbar^2}{2\mu} \frac{\partial^2}{\partial x_{12}^2} + g_{1D} \delta(x_{12}) + V_{ext}(x_{12}, X_{12}) - E \right) \psi(X_{12}, x_{12}) = 0, \quad (\text{I.1.32})$$

with  $M = 2m$  and  $\mu = m/2$ . Let us now integrate this equation in the vicinity  $[-\epsilon, +\epsilon]$  of  $x_{12} = 0$ . If we suppose that  $\psi$  is continuous, the only relevant terms in the  $\epsilon \rightarrow 0$  limit are:

$$-\frac{\hbar^2}{2\mu} \int_{-\epsilon}^{\epsilon} \frac{\partial^2 \psi(X_{12}, x_{12})}{\partial x_{12}^2} dx_{12} + g_{1D} \int \delta(x_{12}) \psi(X_{12}, x_{12}) dx_{12}. \quad (\text{I.1.33})$$

Thus, we obtain the *cusp condition* for the two-body wave function in  $x_1 = x_2$ :

$$\frac{\partial \psi}{\partial x_{12}}(X_{12}, 0^+) - \frac{\partial \psi}{\partial x_{12}}(X_{12}, 0^-) = \frac{2\mu g_{1D}}{\hbar^2} \psi(X_{12}, 0). \quad (\text{I.1.34})$$

This simple discontinuity condition on the wave function has extremely important consequences, and will be used crucially throughout this thesis.

On a side note, it is interesting to remark that if the two atoms are identical fermions, the anti-symmetrization requirement on Eq. (I.1.34) will imply that  $\psi(X_{12}, 0) = 0^3$ . This means that, even if identical fermions do not interact in experiments (see section I.1.3), it will not change the physics to consider a  $\delta$ -type interaction between them *a priori*, as the symmetry properties will naturally cancel its effect.

## I.2. Strongly-interacting systems

When we consider the more realist case where the system is confined by an external harmonic potential  $V_{ext}(x) = \frac{1}{2}m\omega^2 x^2$  along the longitudinal direction, quantum integrability breaks down and the system can no longer be directly solved by Bethe ansatz. Indeed, since the system is not translation invariant anymore, the scattering events will also depend on where they took place in the trap, so that the system is no longer *integrable* (c.f. appendix A). In the limit of very strong repulsion however, one can obtain exact analytical solutions using the so-called *fermionization* property, as first pointed

---

<sup>3</sup>Note that in this case, there is no cusp on the many-body wave-function.

out in [Girardeau 1960] for a gas of impenetrable bosons, or Tonks-Girardeau gas<sup>4</sup>. In this section, we will first explain the notion of fermionization for this simple model in I.2.1. Then, we will turn to a more general method developed in [Volosniev 2014] that is valid for any choice of the mixture in I.2.2. The last one has a central role in this thesis, as it is the one we used in order to obtain exact analytic expressions for the many-body wave functions.

## I.2.1. The Tonks-Girardeau gas

### I.2.1.1. Model

As a pedagogical example of a simple strongly interacting system, we briefly present here the solution of the so-called Tonks-Girardeau gas. It consists in a gas of identical impenetrable bosons. It can be described, for an arbitrary external potential  $V_{ext}$ , by the following equation:

$$\left[ \sum_{j=1}^N \left( -\frac{\hbar^2}{2m} \frac{\partial^2}{\partial x_j^2} + V_{ext}(x_j) \right) - E \right] \psi_B = 0, \quad (\text{I.2.1})$$

together with the boundary conditions:

$$\psi_B(x_1, \dots, x_N) = 0 \quad \text{if} \quad x_i = x_j, \quad 1 \leq i < j \leq N. \quad (\text{I.2.2})$$

Alternatively, one can say that the Tonks-Girardeau gas is the hardcore limit  $g_{1D} \rightarrow \infty$  of the (trapped) Lieb-Liniger gas:

$$\left[ \sum_{j=1}^N \left( -\frac{\hbar^2}{2m} \frac{\partial^2}{\partial x_j^2} + V_{ext}(x_j) \right) + g_{1D} \sum_{i < j} \delta(x_i - x_j) - E \right] \psi_B = 0. \quad (\text{I.2.3})$$

Notice that the resulting cusp condition (see e.g. Eq. (I.1.34)) implies Eq. (I.2.2) in the  $g_{1D} \rightarrow \infty$  limit. Experimentally, observation of a 1D Tonks-Girardeau gas was first reported in [Paredes 2004, Kinoshita 2004].

### I.2.1.2. Bose-Fermi mapping

Girardeau's idea in order to solve this problem was to remark that the many-body wave function of a spinless gas of fermions  $\psi_F$  that satisfies Eq. (I.2.1) also satisfies Eq. (I.2.2). Because of the Bose statistics, the solution for the Tonks-Girardeau gas can then be written [Girardeau 1960]:

$$\psi_B(x_1, \dots, x_N) = A(x_1, \dots, x_N) \psi_F(x_1, \dots, x_N), \quad (\text{I.2.4})$$

where  $A(x_1, \dots, x_N) = \prod_{i > j} \text{sign}(x_i - x_j) = \pm 1$  compensates the anti-symmetrization of  $\psi_F$ . This observation, known as the *Bose-Fermi mapping* or more generally as the

---

<sup>4</sup>Tonks studied the classical gas of hard spheres in [Tonks 1936].



*fermionization* of bosons, maps a strongly interacting problem onto a (simpler!) non-interacting one.

Since  $\psi_B$  and  $\psi_F$  both satisfy Eq. (I.2.1), their energy spectrum are identical. In the homogeneous case  $V_{ext} = 0$  on a ring of size  $L$  with periodic boundary conditions, one finds for the ground-state many-body wave function:

$$\psi_B^0(x_1, \dots, x_N) = \sqrt{\frac{2^{N(N-1)}}{N!L^N}} \prod_{i < j} \sin\left(\frac{\pi}{L}|x_i - x_j|\right), \quad (\text{I.2.5})$$

with the associated ground-state energy:

$$E_0 = \left(N - \frac{1}{N}\right) \frac{\hbar^2 \pi^2 n^2}{6m}, \quad (\text{I.2.6})$$

with  $n = N/L$  the particle density. Note that in the thermodynamic limit this relation corresponds to the  $\gamma \rightarrow \infty$  limit in Eq. (A.2.16). In the case where the particles are trapped in a harmonic potential, Eq (I.2.1) becomes:

$$\left[ \sum_{j=1}^N \left( -\frac{\hbar^2}{2m} \frac{\partial^2}{\partial x_j^2} + \frac{1}{2} m \omega^2 x_j^2 \right) - E \right] \psi_B = 0 \quad (\text{I.2.7})$$

This case is solved in [Girardeau 2001] and [Forrester 2003]. The fermionic solution  $\psi_F$  of Eq. (I.2.7) is given by the well-known Slater determinant:

$$\psi_F(x_1, \dots, x_N) = \frac{1}{\sqrt{N!}} \det [\phi_j(x_i/a_0)]_{i \in \{1, \dots, N\}, j \in \{0, \dots, N-1\}}, \quad (\text{I.2.8})$$

where the eigenstates  $\phi_j$  of the single-particle Hamiltonian  $\hat{H}_1 = -\frac{\hbar^2}{2m} \frac{\partial^2}{\partial x^2} + \frac{1}{2} m \omega^2 x^2$  are defined by:

$$\phi_j(x/a_0) = \frac{e^{-(x/a_0)^2/2} H_j(x/a_0)}{\sqrt{\sqrt{\pi} 2^j j!}}, \quad (\text{I.2.9})$$

where  $a_0 = \sqrt{\hbar/m\omega}$  is the harmonic oscillator length and  $H_j$  is the  $j$ th Hermite polynomial. Using a Vandermonde determinant formula and Eq. (I.2.4), Forrester *et al.* deduced the expression for the ground-state of the harmonically trapped Tonks-Girardeau gas:

$$\psi_B^0(x_1, \dots, x_N) = \frac{1}{a_0^{N/2} \sqrt{N!} \prod_{m=0}^{N-1} 2^{-m} \sqrt{\pi} m!} \prod_{k=1}^N e^{-(x_k/a_0)^2/2} \prod_{1 \leq j < k \leq N} |x_j - x_k|. \quad (\text{I.2.10})$$

The Bose-Fermi mapping can be further exploited by noticing that  $|\psi_B| = |\psi_F|$ . Thus, the density profiles  $n(x)$  defined by

$$n(x) = N \int dx_2 \cdots dx_N |\psi(x, x_2, \dots, x_N)|^2 \quad (\text{I.2.11})$$

and measuring the probability (normalized to  $N$ ) of finding a particle at a point  $x$  are the same for the Tonks-Girardeau gas and spinless fermions. More explicitly, the density profile in the harmonic trap is given by [Vignolo 2000, Kolomeisky 2000]:

$$n_F(x) = \frac{1}{\sqrt{\pi} a_0} \sum_{k=0}^{N-1} \frac{1}{2^k k!} H_k^2(x/a_0) e^{-(x/a_0)^2}. \quad (\text{I.2.12})$$

This analogy between hardcore bosons and non-interacting fermions is also true, for example, for the pair distribution functions defined by

$$D(x, y) = N(N - 1) \int dx_3 \cdots dx_N |\psi(x, y, x_3, \dots, x_N)|^2, \quad (\text{I.2.13})$$

which measures the joint probability (normalized to  $N(N - 1)$ ) of finding one atom in  $x$  and another in  $y$  [Vignolo 2001].

However, if we consider the off-diagonal correlations or the momentum distributions, the symmetry plays an important role, and the analogy is no longer true. The one-body correlations will be discussed in details in chapter III.

## I.2.2. Strongly interacting multi-component systems in atomic traps

Here we generalize the previous considerations and turn to the main Hamiltonian that we studied in this thesis.

### I.2.2.1. Model

We consider a strongly interacting system of  $N$  particles divided in  $\kappa$  different spin species with populations  $N_1, \dots, N_\kappa$ . The species can be either fermions or bosons. We impose that all the particles:

1. Have the same mass  $m$ ;
2. Interact via a  $\delta$ -type potential of same strength  $g_{1D}$ ;
3. Are submitted to the same external potential  $V_{ext}(x) = \frac{1}{2}m\omega^2 x^2$ .

In the case of a fermionic mixture, note that Florence's experiment with  $^{173}\text{Yb}$  atoms [Pagano 2014] described in section I.1.2.4 fulfills these conditions, with  $\kappa \in \{2, \dots, 6\}$  and  $N_1 = \dots = N_\kappa \simeq 10^4$ . In the case of Bose-Fermi mixtures, these assumptions are demanding, but can however be considered as good approximations in the case of isotopes, as realized in [Fukuhara 2009] with an  $^{173}\text{Yb} - ^{174}\text{Yb}$  mixture.

The stationary Schrödinger equation for this system is given by:

$$\left[ \sum_{j=1}^N \left( -\frac{\hbar^2}{2m} \frac{\partial^2}{\partial x_j^2} + \frac{1}{2} m \omega^2 x_j^2 \right) + g_{1D} \sum_{i < j} \delta(x_i - x_j) - E \right] \psi = 0. \quad (\text{I.2.14})$$

As stated in previous sections (see e.g. section I.1.3.3), it is not necessary to specify the mixture in this equation, since the Pauli principle for identical fermions is naturally obtained by Eq. (I.1.34), that we recall here for any couple of particles  $i, j$ :

$$\left( \frac{\partial \psi}{\partial x_i} - \frac{\partial \psi}{\partial x_j} \right) \Big|_{x_{ij}=0^+} - \left( \frac{\partial \psi}{\partial x_i} - \frac{\partial \psi}{\partial x_j} \right) \Big|_{x_{ij}=0^-} = \frac{mg_{1D}}{\hbar^2} \psi \Big|_{x_{ij}=0}, \quad (\text{I.2.15})$$

with  $x_{ij} = x_i - x_j$ . Eq. (I.2.14) is the main equation studied in this thesis.

As in the Tonks-Girardeau gas of section I.2.1, in the impenetrable limit the system will fermionize, since the  $g_{1D} \rightarrow \infty$  limit in the cusp condition (I.2.15) implies that  $\psi = 0$  whenever two particles are at the same point. The system can thus be again mapped onto a spinless fermionic gas. In particular, the Slater determinant  $\psi_F$  of Eq. (I.2.8) has the right nodes and energy  $E_0$  as the ground state. Since all the systems have the same eigenspectrum as the free Fermi gas regardless of their composition and symmetry when  $g_{1D} = \infty$ , these points of the energy spectrum are often called *degenerate manifolds* [Harshman 2014]. The question is, if we consider that  $g_{1D}$  is in the vicinity of the  $g_{1D} = \infty$  point, how will this degeneracy be removed as a function of the mixture's symmetry?

### I.2.2.2. A perturbative ansatz

#### Method

The method developed in [Volosniev 2013, Volosniev 2014] allows to answer last paragraph's question. Although it works for any confining potential  $V_{ext}$ , I focus here on the harmonic case. We switch to natural units of  $a_0 = \sqrt{\hbar/m\omega}$  for length and  $\hbar\omega$  for energy.

The first idea is to use the aforementioned fact that the Slater determinant  $\psi_F$  has the right nodes in the  $g_{1D} \rightarrow \infty$  limit. Then, in order to have a solution  $\psi$  that respects the symmetry of the considered mixture, Volosniev *et al.* proposed the following ansatz:

$$\psi(x_1, \dots, x_N) = \sum_{P \in \mathfrak{S}_N} a_P \theta(x_{P_1} < \dots < x_{P_N}) \psi_F(x_1, \dots, x_N), \quad (\text{I.2.16})$$

where  $\mathfrak{S}_N$  is the permutation group of  $\{1, \dots, N\}$  (see section II.1.2.2) and  $\theta(x_1 < \dots < x_N)$ , the indicator function of the sector  $\{x_1 < \dots < x_N\} \subset \mathbb{R}^N$ , is equal to 1 if  $x_1 < \dots < x_N$  and 0 otherwise. This ansatz is very much in the spirit of the Bethe ansatz (cf Eq. (A.1.5)), except that the asymptotic plane wave basis in the last one is replaced with the fermionic Slater determinant here.

Because of the (anti-)symmetrization constraint imposed for identical (fermions) bosons, the choice of a given mixture  $N_1, \dots, N_\kappa$  will reduce the number of independent  $a_P$  coefficient in Eq (I.2.16) to the multinomial coefficient:

$$D_{N_1, \dots, N_\kappa} = \binom{N}{N_1, N_2, \dots, N_\kappa} = \frac{N!}{N_1! N_2! \dots N_\kappa!}. \quad (\text{I.2.17})$$

The number  $D_{N_1, \dots, N_\kappa}$  corresponds to the number of linearly independent states that can be written in terms of  $\psi_F$ . Since  $\psi_F$  is associated with the ground state energy  $E_0$ ,  $D_{N_1, \dots, N_\kappa}$  is in fact the dimension of the degenerate manifold at  $g_{1D} = \infty$ . Instead of writing the solution in one of the  $N!$  sectors of  $\mathbb{R}^N$ , this observation encourages to write the solution in one of the  $D_{N_1, \dots, N_\kappa}$  so-called *snippets* [Deuretzbacher 2008, Fang 2011] of  $\text{Sect}(\mathbb{R}^N)/\mathcal{R}$ , where  $\text{Sect}(\mathbb{R}^N)/\mathcal{R}$  is the quotient set of all sectors of  $\mathbb{R}^N$  by the equivalence relation  $\mathcal{R}$ : 'two sectors are equivalent if they are equal up to permutations of *identical* particles'. This operation considerably reduces the dimension of the problem.

In order to determine these  $a_P$  coefficients, the idea is to remove the degeneracy by analyzing the system in the vicinity of the degenerate point  $g_{1D} = \infty$ . In other words, one has to consider a linear perturbation in the energy around  $1/g_{1D} = 0$ :

$$E(1/g_{1D}) \underset{+\infty}{=} E_0 + \frac{1}{g_{1D}}(-K) + o(1/g_{1D}). \quad (\text{I.2.18})$$

The *energy slope*  $K = -\lim_{g_{1D} \rightarrow \infty} \frac{\partial E}{\partial g_{1D}^{-1}} = g_{1D}^2 \frac{\partial E}{\partial g_{1D}}$  will be different for different states of the degenerate manifold, and is then a functional of the  $a_P$  coefficients. Using the Hellmann-Feynman theorem [Feynman 1939] on the Hamiltonian of Eq. (I.2.14), one gets:

$$K = \lim_{g_{1D} \rightarrow \infty} g_{1D}^2 \frac{\sum_{i < j} \int dx_1 \dots dx_N \delta(x_i - x_j) |\psi|^2}{\int dx_1 \dots dx_N |\psi|^2}, \quad (\text{I.2.19})$$

where the  $g_{1D}$ -dependence is removed by the cusp condition (I.2.15), yielding

$$K = \frac{1}{4} \frac{\sum_{i < j} \int dx_1 \dots dx_N \delta(x_i - x_j) \left| \left( \left( \frac{\partial}{\partial x_i} - \frac{\partial}{\partial x_j} \right) \Big|_{x_{ij}=0^+} - \left( \frac{\partial}{\partial x_i} - \frac{\partial}{\partial x_j} \right) \Big|_{x_{ij}=0^-} \right) \psi \right|^2}{\int dx_1 \dots dx_N |\psi|^2}, \quad (\text{I.2.20})$$

with  $x_{ij} = x_i - x_j$ . Then, using Eq. (I.2.16) and normalizing  $\psi$  to unity, one gets:

$$K = \sum_{P, Q \in \mathfrak{S}_N} (a_P - a_Q)^2 \alpha_{P, Q}, \quad (\text{I.2.21})$$

where  $\alpha_{P, Q}$  is defined by

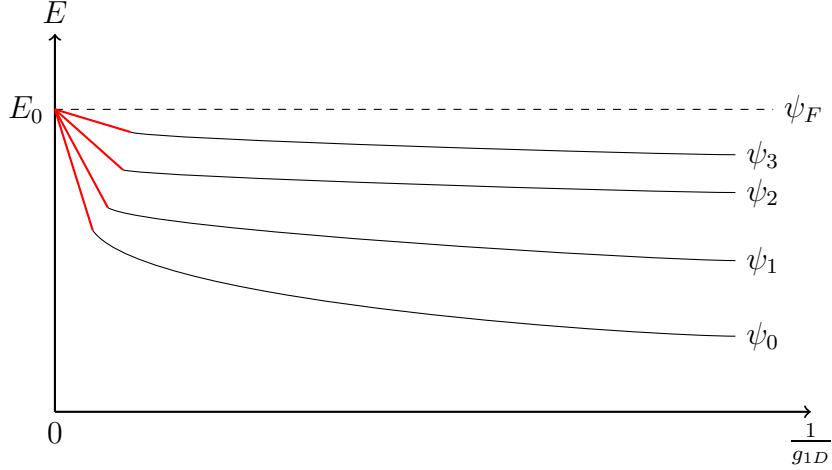
$$\alpha_{P, Q} \equiv \alpha_k = \int dx_1 \dots dx_N \theta(x_1 < \dots < x_N) \delta(x_k - x_{k+1}) \left| \frac{\partial \psi_F}{\partial x_k} \right|^2 \quad (\text{I.2.22})$$

if  $P = Q(k, k+1)$  (that is to say  $P$  and  $Q$  are equal up to a transposition in  $k$  and  $k+1$ ), where the particles in  $k$  and  $k+1$  are not identical fermions, and  $\alpha_{P, Q} = 0$  otherwise. These  $\alpha_k$  coefficients can be seen as the energy cost of an exchange of particles at positions  $k$  and  $k+1$  in the trap, and are sometimes called *nearest-neighbor exchange constants* [Deuretzbacher 2014, Laird 2017]. Note that the parity invariance of the harmonic potential implies that  $\alpha_k = \alpha_{N-k}$ , reducing the number of different  $\alpha_k$  coefficients to  $\lfloor N/2 \rfloor$ . As seen in section I.2.1, expression for  $\psi_F$  is given by [Girardeau 2001, Forrester 2003]:

$$\psi_F(x_1, \dots, x_N) = \frac{1}{\sqrt{N! \prod_{m=0}^{N-1} 2^{-m} \sqrt{\pi} m!}} \prod_{k=1}^N e^{-x_k^2/2} \prod_{1 \leq j < k \leq N} (x_j - x_k). \quad (\text{I.2.23})$$

We then have after some algebra

$$\left[ \frac{\partial \psi_F}{\partial x_k} \right]_{x_k = x_{k+1}} = \frac{1}{\sqrt{N! \prod_{m=0}^{N-1} 2^{-m} \sqrt{\pi} m!}} e^{-x_k^2} \prod_{\substack{i=1 \\ i \neq k, k+1}}^N e^{-x_i^2/2} (x_i - x_k)^2 \prod_{\substack{1 \leq j < \ell \leq N \\ j, \ell \neq k, k+1}} (x_j - x_\ell), \quad (\text{I.2.24})$$



**Figure I.2.1:** Graphic interpretation of the perturbative ansatz. The red lines correspond to the linear approximations of Eq. (I.2.18), whose slopes are given by  $-K$ .

and thus, using a Vandermonde formula:

$$\left[ \frac{\partial \psi_F}{\partial x_k} \right]_{x_k=x_{k+1}}^2 = \frac{2^{2N-3} e^{-2x_k^2}}{\pi N! (N-1)! (N-2)!} [\det [\phi_{i-1}(x_j)]]_{N-2 \times N-2}^2 \prod_{\substack{i=1 \\ i \neq k, k+1}}^N (x_i - x_k)^4, \quad (\text{I.2.25})$$

We then make use of permutational and parity invariances, and obtain:

$$\alpha_k = \frac{2^{2N-3}}{\pi N! (N-1)! (N-2)! (k-1)! (N-k-1)!} \int_{-\infty}^{+\infty} dx_k e^{-2x_k^2} \sum_{P, Q \in \mathfrak{S}_{N-2}} \epsilon(P) \epsilon(Q) \times \prod_{\substack{i=1 \\ i \neq k, k+1}}^N \int_{L_k(i)}^{U_k(i)} dx_i (x_i - x_k)^4 \phi_{P_{i-1}}(x_i) \phi_{Q_{i-1}}(x_i), \quad (\text{I.2.26})$$

where

$$(L_k(i), U_k(i)) = \begin{cases} (-\infty, x_k) & \text{if } i < k \\ (x_k, +\infty) & \text{if } i \geq k \end{cases}. \quad (\text{I.2.27})$$

Eq. (I.2.26) was obtained in [Decamp 2016a]. Alternatively, it is possible to obtain an approximate value for  $\alpha_k$  by performing a local density approximation on the homogeneous results with periodic boundary conditions [Matveev 2008, Deuretzbacher 2014].

Once the  $\alpha$  exchange constants computed in Eq. (I.2.21), the next step is to determine the  $a_P$  coefficients corresponding to each one of the states in the degenerated manifold. To do so, the idea is to notice that the lowest energy will be obtained by maximizing the energy slope functional  $K[\{a_P\}]$  (because of the minus sign in Eq. (I.2.18)). Subsequently, solving  $\partial K / \partial a_P = 0$  for all  $P \in \mathfrak{S}_N$  yields the following diagonalization problem:

$$V \vec{a} = K \vec{a}, \quad (\text{I.2.28})$$

where  $\vec{a}$  is the vector of the  $D_{N_1, \dots, N_\kappa}$  independent  $a_P$  coefficients and  $V$  is a  $D_{N_1, \dots, N_\kappa} \times$

$D_{N_1, \dots, N_\kappa}$  matrix defined in the snippet basis by

$$V_{ij} = \begin{cases} -\alpha_{i,j} & \text{if } i \neq j \\ \sum_{d, k \neq i} \alpha_{i,k} + 2 \sum_{b, k \neq i} \alpha_{i,k} & \text{if } i = j \end{cases}, \quad (\text{I.2.29})$$

where the index  $d$  means that the sum has to be taken over snippets  $k$  that transpose distinguishable particles as compared to snippet  $i$ , while  $b$  means that the sum is taken over sectors that transpose identical bosons. If the system contains only fermions, it reduces to the first sum. The parity invariance of the harmonic trap implies that  $V$  is symmetric, and thus that it can be diagonalized in an orthogonal basis. Then, the highest eigenvalue  $K_0$  and the corresponding eigenvector  $\vec{a}_0$  determines the ground-state wave function  $\psi_0$  through Eq. (I.2.16). Incidentally, all the eigenstates corresponding to the same degenerate manifold at  $g_{1D} = \infty$  are given by the orthogonal eigenvectors of  $V$ .

I provide an illustration of the method in the next paragraph. It will be further implemented in the next chapters. A graphical illustration of the method is given in Fig. I.2.1.

### A first example

As a first pedagogical example, let us consider the case of a four-particle fermionic mixtures (two spin up, two spin down), as it is done in [Volosniev 2014]. We will use this example in the next paragraph, where we give an interpretation of the method in terms of graph theory. The number of snippets, i.e. the dimension of the degenerate manifold, is given by  $D_{2,2} = 4!/(2!2!) = 6$ . Explicitly, they are given by:

$$\begin{aligned} a_1 &: \uparrow\uparrow\downarrow\downarrow \\ a_2 &: \uparrow\downarrow\uparrow\downarrow \\ a_3 &: \uparrow\downarrow\downarrow\uparrow \\ a_4 &: \downarrow\uparrow\uparrow\downarrow \\ a_5 &: \downarrow\uparrow\downarrow\uparrow \\ a_6 &: \downarrow\downarrow\uparrow\uparrow \end{aligned} \quad (\text{I.2.30})$$

where we have written the six corresponding independent  $a_P$  coefficients. For each configuration  $i \in \{1, \dots, 6\}$  of the particles, the wave function will be then given by  $\psi|_{\{i\}} = a_i \psi_F$  according to Eq. (I.2.16). The energy slope  $K$  defined in Eq. (I.2.21) is then:

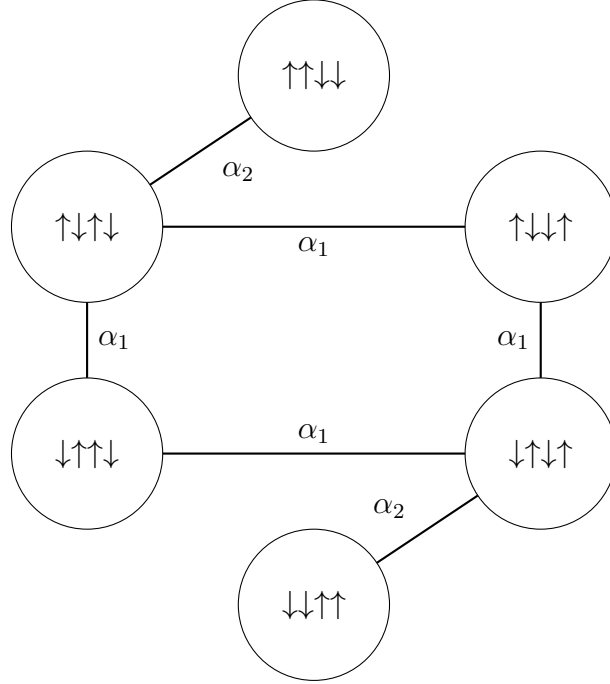
$$K = \alpha_2(a_1 - a_2)^2 + \alpha_3(a_2 - a_3)^2 + \alpha_1(a_2 - a_4)^2 + \alpha_1(a_3 - a_5)^2 + \alpha_3(a_4 - a_5)^2 + \alpha_2(a_5 - a_6)^2, \quad (\text{I.2.31})$$

where the exchange coefficients defined in Eq. (I.2.22) are:

$$\alpha_1 = \alpha_3 = \int_{x_1 < x_2 < x_3 < x_4} dx_1 dx_2 dx_3 dx_4 \delta(x_1 - x_2) \left| \frac{\partial \psi_F}{\partial x_1} \right|^2 \quad (\text{I.2.32})$$

and

$$\alpha_2 = \int_{x_1 < x_2 < x_3 < x_4} dx_1 dx_2 dx_3 dx_4 \delta(x_2 - x_3) \left| \frac{\partial \psi_F}{\partial x_2} \right|^2. \quad (\text{I.2.33})$$



**Figure I.2.2:** Weighted graph  $\mathcal{G}_V$  associated with the  $(2 + 2)$  fermionic example of the text. The laplacian matrix associated to this graph is exactly equal to  $V$  of Eq. (I.2.34).

They can be computed exactly using Eq. (I.2.26). The  $V$  matrix that has to be diagonalized in order to obtain the ground and excited states (Eq. (I.2.29)) is:

$$V = \begin{pmatrix} \alpha_2 & -\alpha_2 & 0 & 0 & 0 & 0 \\ \alpha_2 & 2\alpha_1 + \alpha_2 & -\alpha_1 & -\alpha_1 & 0 & 0 \\ 0 & -\alpha_1 & 2\alpha_1 & 0 & -\alpha_1 & 0 \\ 0 & -\alpha_1 & 0 & 2\alpha_1 & -\alpha_1 & 0 \\ 0 & 0 & -\alpha_1 & -\alpha_1 & 2\alpha_1 + \alpha_2 & \alpha_2 \\ 0 & 0 & 0 & 0 & -\alpha_2 & \alpha_2 \end{pmatrix}. \quad (\text{I.2.34})$$

The ground state energy slope  $K_0$ , given by the highest eigenvalue of  $V$ , is given by:

$$K_0 = 2\alpha_1 + \alpha_2 + \sqrt{4\alpha_1^2 - 2\alpha_1\alpha_2 + \alpha_2^2}. \quad (\text{I.2.35})$$

The lower eigenspectrum of  $V$  determines the energy slopes of the excited states.

### Graph theory interpretation

In this paragraph, we give an interpretation of the perturbative ansatz in terms of graph theory. Although this observation has not been published yet, I strongly believe this analogy can provide useful results about  $V$ 's eigenspectrum.

Let us first recall some basic definitions of graph theory [Bondy 2008]. A *graph* is a pair  $\mathcal{G} = (\mathcal{V}, \mathcal{E})$  where  $\mathcal{V}$  is a set of *vertices* (or *points*) and  $\mathcal{E}$  is a set of *edges* (or *lines*) which are unordered pairs of elements of  $\mathcal{V}$ . The *degree*  $\deg(v)$  of a vertex  $v$  is the number of vertices that are connected by an edge to  $v$ . If each element of  $\mathcal{E}$  is associated with a number, we say that  $\mathcal{G}$  is a *weighted graph*.

Given a graph  $\mathcal{G}$ , it is possible to associate matrices to  $\mathcal{G}$ , allowing to use linear algebra tools in order to analyze  $\mathcal{G}$ . The simplest matrix that we can define is the *adjacency matrix*  $A$ , whose elements  $A_{ij}$  are equal to 1 if vertex " $i$ " is connected by an edge (or *adjacent*) to vertex " $j$ " and 0 otherwise. Another interesting matrix is the *Laplacian matrix*  $L$  whose elements are given by:

$$L_{ij} = \begin{cases} \deg(v_i) & \text{if } i = j \\ -1 & \text{if } i \neq j \text{ and } v_i \text{ is adjacent to } v_j \\ 0 & \text{otherwise} \end{cases} . \quad (\text{I.2.36})$$

In the case of a weighted graph,  $L$  is defined similarly, where  $\deg(v_i)$  is the sum of the weights of the edges connected to  $v_i$ , and the off-diagonal terms in -1 are replaced by minus the weight of the edge between  $i$  and  $j$ . This matrix is extremely important in graph theory, and can be seen as a discrete version of the laplacian operator  $\Delta$ . In particular, the spectral properties of the laplacian matrices are well studied [Brouwer 2012].

Let us now go back to our physical system and apply the aforementioned definitions. Given a mixture  $N_1, \dots, N_\kappa$ , we define a weighted graph  $\mathcal{G}_V$  where each vertex is associated with a snippet, and where two snippets are adjacent with weight  $\alpha_k$  if they are equal up to a transposition of particles in positions  $k$  and  $k + 1$ . Then, the laplacian matrix  $L$  of  $\mathcal{G}_V$  is equal to the matrix  $V$  defined in Eq. (I.2.29). An illustration based on the last paragraph's example is given in Fig. I.2.2.

## Implementation

I have developed a `Mathematica` program that allows to obtain the  $V$  matrix for any kind of mixture (fermionic, bosonic or mixed), and for any number of particles  $N$ . In practice, we have chosen to study in detail the case  $N = 6$ , since the program's complexity increases extremely rapidly with increasing  $N$  (as  $\mathcal{O}(N!^2)$ ), and, as we will see, the case  $N = 6$  already allows to observe effects that are not present when  $N \leq 5$ .

For example, let us add two spin-up to our last example, so that we have a two-component fermionic mixture of the type  $\uparrow\uparrow\uparrow\uparrow\downarrow\downarrow$ . In order to compute the  $V$  matrix associated with this quantum mixture (Eq. (I.2.34)), one just need to assign a number to each component, *e.g.*  $\uparrow = 1$  and  $\downarrow = 2$ , and to enter the following vector in the program:  $\{1, 1, 1, 1, 2, 2\}$ . The program then directly computes the snippet basis and the  $V$  matrix as a function of the exchange constants  $\alpha_k$ . The output given by the program for this example is shown in Fig. I.2.3.







# CHAPTER II

---

## Symmetry analysis

### Contents

---

<b>II.1</b>	<b>Generalities</b> .....	<b>44</b>
II.1.1	Symmetries in physics . . . . .	44
II.1.1.1	What is symmetry? . . . . .	44
II.1.1.2	Importance in physics . . . . .	45
II.1.2	Exchange symmetry . . . . .	48
II.1.2.1	Identical particles . . . . .	48
II.1.2.2	The symmetric group and its representations . . . . .	49
<b>II.2</b>	<b>Symmetry analysis of strongly interacting quantum mixtures</b> .....	<b>52</b>
II.2.1	One-dimensional $SU(\kappa)$ quantum gases and quantum magnetism	52
II.2.2	The class-sum method . . . . .	54
II.2.2.1	Class-sums and central characters . . . . .	54
II.2.2.2	Description of the method . . . . .	56
II.2.2.3	Implementation for $N = 6$ mixtures and first observations . . . . .	60
II.2.3	Ordering of energy levels . . . . .	63
II.2.3.1	The Lieb-Mattis theorem . . . . .	63
II.2.3.2	Analysis in our system . . . . .	69

---

In chapter I, we have seen that we can express exact solutions for strongly repulsive one-dimensional trapped quantum mixtures by mean of a summation over the permutations of all particles. It appears clearly that the permutation symmetry is of fundamental importance in our system. This chapter is devoted to the precise symmetry analysis of the exact solutions obtained in the last chapter.

Section II.1 is a very general introduction to the concept of symmetry, with a peculiar focus on the permutational symmetry we are interested in and the mathematical properties of the associated group, namely the *symmetric group*. In section II.2, we will explain the method we used in order to characterize the symmetry of our solutions, with the will to justify it as precisely as possible in terms of group theory. We will then implement it for mixtures of  $N = 6$  particles, and analyze the results we can extract from it.

## II.1. Generalities

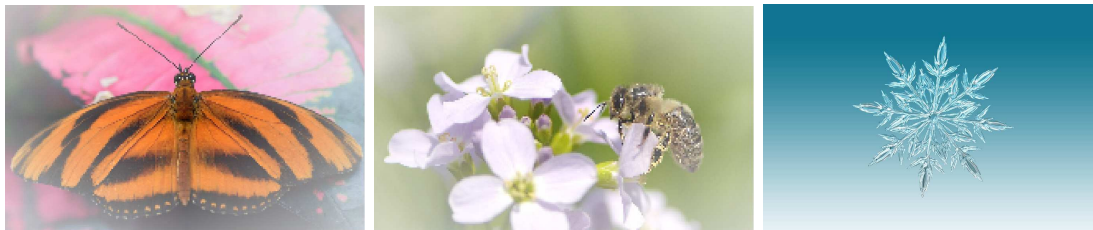
The concept of symmetry is one of the cornerstones of modern physics [Weyl 1952, Gross 1996, Gieres 1997]. It is first an extremely valuable tool in order to solve a physical problem: indeed, the fact that a classical or quantum Hamiltonian has a certain symmetry gives considerable information about the structure of the solution itself. Furthermore, the concept of symmetry appears to be so powerful and fundamental in Nature that many modern successful theories have been constructed almost only from symmetry considerations. In this section, we first discuss some very general aspects of symmetries in II.1.1. Then, we focus on the peculiar fundamental symmetry we are interested in, namely the exchange symmetry, in II.1.2.

### II.1.1. Symmetries in physics

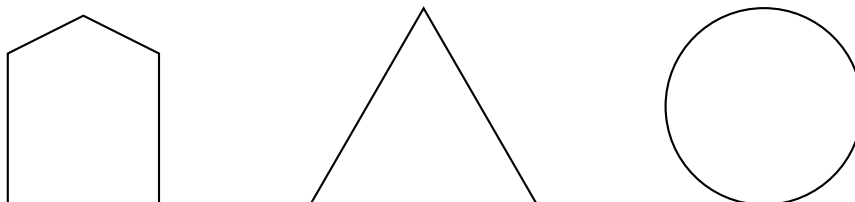
#### II.1.1.1. What is symmetry?

The notion of symmetry is very intuitive, as it is omnipresent in everyday life: human beings and animals are left-right symmetric, flowers have a *discrete* rotational symmetry, the sun has a *continuous* rotational symmetry, snowflakes have very complex symmetry structure, and so on (see Fig. II.1.1). Interestingly, on a more metaphysical point of view, it seems that "*Beauty is bound up with symmetry*" [Weyl 1952].

But how to precisely define the concept of symmetry? Roughly speaking, we can say that an object has a symmetry when you can apply some transformations to it which leaves the system invariant. More formally, this set of transformations is a group  $G$ , the *symmetry group* of the system, and this group acts on the system through the mathematical notion of linear representation  $\hat{D}_G$  [Hamermesh 1989]. The "bigger" is the group, the more symmetric is the object. Some examples of symmetric geometrical objects and their associated symmetry groups are given in Fig II.1.2. These geometrical symmetries are found in physics, for example in crystallography, where the crystals are defined by their discrete spatial periodicity and classified by their so-called *space group symmetry* [Shmueli 2006].



**Figure II.1.1:** Some examples of the symmetries encountered in Nature.



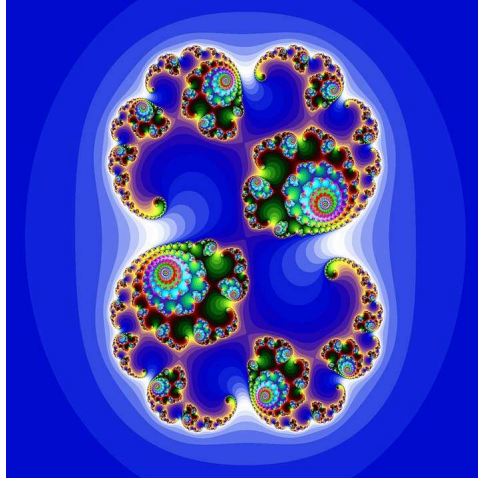
**Figure II.1.2:** Some examples of geometrical symmetries. From left to right, their symmetry group are respectively the *discrete* dihedral groups  $D_2 \simeq \mathbb{Z}_2$  and  $D_3 \simeq \mathbb{Z}_3 \times \mathbb{Z}_2$  of reflections and discrete rotations and the *continuous* orthogonal group  $O(2)$ . The groups are "bigger and bigger" from left to right, which is equivalent to the fact that the objects are more and more symmetric.

In a more fundamental way, a physical law has a symmetry when the equation describing the law, hence the Hamiltonian or equivalently the Lagrangian or the action, is invariant by a change of variables. In this case, the word *covariant* is often used. These variables can be space-time coordinates: *e.g.*, if we require that a physical law is subjected to the relativity principle [Einstein 1905], it implies that the Lagrangian must be invariant by the Lorentz group, that is the group of Lorentz transformations or equivalently the group  $O(1,3)$  of isometries of Minkowski space. Another symmetry involving a geometrical transformation is given by the *conformal group*, the group of transformations that locally conserve the angles. It involves, in particular, dilatations. Scale invariance, which is related to the mathematical notion of *fractals*, is found in many theories such as critical phenomena and quantum field theories through the notion of *renormalization* [Wilson 1975] (see Fig II.1.3).

These symmetries can be more abstract in the sense that they do not affect the space-time coordinates, in the case of the so-called *internal* symmetries. The most simple example of internal symmetry is the invariance of the electrodynamic model by a global phase-change  $U(1)$ . Another symmetry of peculiar importance in this thesis, that we will discuss more below, is the *permutational* symmetry, namely the symmetry that exchanges the states of the particles in a many-body problem.

### II.1.1.2. Importance in physics

In classical physics, already, the symmetry properties of a Hamiltonian have extremely strong implications. For example, if we know that a classical Hamiltonian  $H$  is invariant under rotation transformations and we have obtained a certain solution  $s(t)$ , we can deduce other solutions noticing that the spatially rotated  $s(t)$  is also a solution. More profoundly, the notion of symmetry is intimately linked with the notion of *conservation*



**Figure II.1.3:** A fractal, characterized by its auto-similarity, or discrete scale invariance. Fractal theory is intimately linked to the theory of critical phenomena and quantum field theories through the famous *renormalization (semi-)group*.

laws through the celebrated Noether's theorem [Noether 1918], which states that any continuous symmetry is associated with a conserved quantity. Some examples of this powerful correspondence are given in table II.1.

In quantum physics, the importance of symmetries is even higher [Landau 1981]. The intrinsic linearity of quantum physics related to the superimposition principle implies that a lot of information can be obtained from representation theory. More precisely, suppose that a quantum Hamiltonian  $\hat{H}$  has a certain symmetry group  $G$ , *i.e.* that, for every  $g \in G$ ,

$$[\hat{H}, \hat{D}(g)] = \hat{H}\hat{D}(g) - \hat{D}(g)\hat{H} = 0, \quad (\text{II.1.1})$$

where the representation  $\hat{D}$  acts on the Hilbert space  $V$  of the systems. Then, it follows from Maschke's theorem that the representation can be split<sup>1</sup> as a direct sum of *irreducible representations*, or *irreps*, *i.e.* non-zero representations that have no proper sub-representations:

$$V = \bigoplus_k V^{(k)}, \quad \hat{D}(g) = \bigoplus_k \hat{D}^{(k)}(g), \quad \hat{D}(g)V^{(k)} \subset V^{(k)}. \quad (\text{II.1.2})$$

Given Eqs. (II.1.1) and (II.1.2), it follows that  $\hat{H}$  can also be split according to the irreps of  $G$ :

$$\hat{H} = \bigoplus_k \hat{H}^{(k)}, \quad \hat{H}V^{(k)} \subset V^{(k)}, \quad (\text{II.1.3})$$

and that the spectrum of  $\hat{H}$  can be split into subspectra with degeneracies equal to the dimensions of the irreps. Thus, group theory provides *good quantum numbers* and allows to classify the spectral properties of a system. Moreover, it can provides information about the form of the corresponding eigenstates. One of the most famous examples is Bloch's theorem [Bloch 1929], which uses the translation invariance of crystals to determine the form of the wave functions. Another important application of symmetry and representations in quantum mechanics is given by selection rules. Indeed, the probability

---

<sup>1</sup>In generic cases.

Symmetry	Conserved quantity
Translation in time	Energy
Translation in space	Momentum
Rotation in space	Angular momentum
Global phase invariance $U(1)$	Electric charge

**Table II.1:** Examples of continuous symmetries and their corresponding conservation laws.

of a transition between two states associated with different irreps can be obtained by the direct product of these irreps [Hamermesh 1989]. Finally, another interesting application in terms of spectral properties is given by perturbation theory: suppose our initial Hamiltonian  $\hat{H}$  with a symmetry group  $G$  is perturbed by a Hamiltonian  $\epsilon\hat{H}_1$  with a symmetry group  $G_1 \subset G$ , *i.e.* with a lower symmetry. This case is referred as an *explicit symmetry breaking*. Then, how the spectrum of  $\hat{H}$ , whose degeneracies are given by the irreps of  $G$ , is affected? If we consider an eigenvalue  $E$  of  $\hat{H}$  with a degeneracy corresponding to the dimension  $m$  of the associated irrep  $D$  of  $G$ , this irrep  $\hat{D}$  is in general a reducible representation of  $G'$ , the symmetry group of the perturbed Hamiltonian  $\hat{H}' = \hat{H} + \epsilon\hat{H}_1$ . Then, by decomposing  $\hat{D}$  into irreps of  $G'$ , we obtain how the degeneracy of  $E$  is lifted by the perturbation.

The notion of symmetry breaking is also very useful in the case of a *spontaneous* symmetry breaking. Here, the ground-state breaks the symmetry of the Hamiltonian. This is at the origin of numerous physical phenomena such as crystals (which break translation invariance), magnets (which breaks rotational invariance) or Bose-Einstein condensates (which breaks the global phase invariance). Each global spontaneous symmetry breaking is associated with low energy fluctuations, or *Goldstone bosons* [Goldstone 1962]: sound waves or phonons for crystals, spin waves or magnons in magnets, Bogoliubov quasiparticles in Bose-Einstein condensates. Spontaneous symmetry breaking is intimately linked with the notion of phase transition: when the temperature becomes larger than a certain temperature  $T_c$ , the symmetry is restored. The Mermin–Wagner–Hohenberg theorem that we briefly discussed in section I.1.1 and that explains in particular why there is no Bose-Einstein condensation in 1D is based on the fact that the Goldstone bosons associated with a spontaneous symmetry breaking would have infrared diverging correlation functions for dimensions lower than 2 [Mermin 1966, Hohenberg 1967].

Finally, a lot of modern successful theories are *constructed from symmetries*. This is the case of special and general relativity, which are respectively based on the global and the local Lorentz covariances [Einstein 1905, Einstein 1917]. In quantum physics, and more precisely in quantum field theories, the fundamental interactions are dictated by local internal symmetries of the fields, or *gauge* symmetries:  $U(1)$  for quantum electrodynamics [Tomonaga 1946, Schwinger 1948, Feynman 1950],  $U(1) \times SU(2)$  for the electroweak theory [Glashow 1959, Salam 1959, Weinberg 1967],  $SU(3)$  for quantum chromodynamics (which describes strong interaction) [Gross 1973, Politzer 1973]. The product of these gauge symmetries  $U(1) \times SU(2) \times SU(3)$ , together with the *Higgs mechanism* which is nothing more than a spontaneous symmetry breaking explaining why the interaction bosons of the weak interaction are massive [Englert 1964, Higgs 1964], form the *standard model*, which describes all fundamental interactions except gravity. The incredible success of these theories suggests that symmetry, more than being an extremely valuable

tool for physicists, has in fact a more fundamental meaning and importance in Nature.

## II.1.2. Exchange symmetry

### II.1.2.1. Identical particles

*Identical* particles are particles with the same intrinsic properties (mass, charge, spin...), and that are therefore impossible to differentiate. For example, all the electrons of the universe are identical, and so are all the hydrogen atoms. Then, if a system is composed of identical particles, its properties must be invariant when exchanging them. This *exchange symmetry* is very important in quantum physics because it causes problems regarding its fundamental postulates [Cohen-Tannoudji 1997a, Cohen-Tannoudji 1997b]. Indeed, let us consider a system of  $N$  identical particles. If  $\mathcal{E}$  is the Hilbert space associated with one particle, the total Hilbert space of this system can be obtained by taking the tensorial product

$$\mathcal{E}_{tot} \equiv \mathcal{E}(1) \otimes \mathcal{E}(2) \otimes \cdots \otimes \mathcal{E}(N), \quad (\text{II.1.4})$$

where numbers were assigned to the particles in an arbitrary way. Let us now consider a set of  $N$  commuting observables  $(\mathcal{O}(i))_{i \in \{1, \dots, N\}}$  associated with the  $N$  particles, and with the same spectrum  $\{\sigma_n; n = 1, 2, \dots\}$ . Suppose that in an experiment we have measured simultaneously  $\mathcal{O}$  for the  $N$  particles, and that we have obtained  $\{\sigma_1, \sigma_2, \dots, \sigma_N\}$ . Then, because of the indiscernibility of the particles, it is *a priori* impossible to know to which state of  $\mathcal{E}_{tot}$  it corresponds: it can be either

$$|1 : \sigma_1\rangle \otimes |2 : \sigma_2\rangle \otimes \cdots \otimes |N : \sigma_N\rangle \in \mathcal{E}_{tot} \quad (\text{II.1.5})$$

or any of its  $N!$  permutations, *e.g.*

$$|1 : \sigma_2\rangle \otimes |2 : \sigma_1\rangle \otimes |3 : \sigma_3\rangle \otimes \cdots \otimes |N : \sigma_N\rangle \in \mathcal{E}_{tot}. \quad (\text{II.1.6})$$

This is known as the *exchange degeneracy*.

Let us consider the case of  $N = 2$  in the previous example, and let us define the permutation operator  $\hat{P}_{12}$  such that

$$\hat{P}_{12} |1 : \sigma_1\rangle \otimes |2 : \sigma_2\rangle = |1 : \sigma_2\rangle \otimes |2 : \sigma_1\rangle. \quad (\text{II.1.7})$$

It is clear then that  $\hat{P}_{12}$  is an involution ( $(\hat{P}_{12})^2 = 1$ ) and that it is self-adjoint ( $\hat{P}_{12}^\dagger = \hat{P}_{12}$ ). Therefore, its only eigenvalues are  $+1$  and  $-1$ . The corresponding orthogonal eigenstates are respectively *symmetric* and *anti-symmetric*.

In the general case, one can also define a permutation operator  $\hat{P}$  associated with every  $P \in \mathfrak{S}_N$ , where  $\mathfrak{S}_N$  is the permutation group of  $N$  objects (see section II.1.2.2). The situation is however more complicated in this case, and one can not write  $\mathcal{E}_{tot}$  as a direct sum of a completely symmetric and a completely anti-symmetric subspace. However, we can define the following projectors:

$$\begin{aligned} \hat{S} &= \frac{1}{N!} \sum_{P \in \mathfrak{S}_N} \hat{P} \\ \hat{A} &= \frac{1}{N!} \sum_{P \in \mathfrak{S}_N} \epsilon(P) \hat{P}, \end{aligned} \quad (\text{II.1.8})$$



where  $\epsilon(P)$  is the signature of permutation  $P$ , that project respectively onto a completely symmetric subspace  $\mathcal{E}_S$  and a completely anti-symmetric subspace  $\mathcal{E}_A$  of  $\mathcal{E}_{tot}$ . The symmetrization postulate states that, depending on the nature of the  $N$  identical particles, the physical  $N$ -body states belong either to  $\mathcal{E}_S$ , and in this case they are called *bosons*, or to  $\mathcal{E}_A$ , and then they are called *fermions*<sup>2</sup>. This postulate completely removes the exchange degeneracy: indeed, depending on the nature of the identical particles in our example, a measure  $\{\sigma_1, \sigma_2, \dots, \sigma_N\}$  is associated with a single possible state, which is  $\hat{S}|1 : \sigma_1\rangle \otimes \dots \otimes |N : \sigma_N\rangle \in \mathcal{E}_S$  for bosons and  $\hat{A}|1 : \sigma_1\rangle \otimes \dots \otimes |N : \sigma_N\rangle \in \mathcal{E}_A$  for fermions.

The fact that a particle is a boson or a fermion has extremely important physical consequences. To see this, let us go back to the case of two particles. In this case,  $\hat{S} = \frac{1}{2}(1 + \hat{P}_{12})$  and  $\hat{A} = \frac{1}{2}(1 - \hat{P}_{12})$ . Let us consider the state  $|u\rangle = |1 : \phi\rangle \otimes |2 : \phi\rangle$  where the two particles are in the same one-body state. Then, it is clear that  $\hat{S}|u\rangle = |u\rangle$  and  $\hat{A}|u\rangle = 0$ . In other words, it is impossible to put two identical fermions in the same quantum state. This well-known fact is known as the *Pauli exclusion principle*. It implies in particular that electrons, which are fermions, cannot be in the same state (and in particular at the same place), and therefore explains a lot of properties of matter. In contrast, there are no reason for bosons not to occupy the same quantum state. Particles will therefore have the tendency to accumulate in their individual states of lowest energy at very low temperatures, which is at the origin of spectacular quantum effects such as Bose-Einstein condensation, superfluidity and superconductivity (where electrons form bosonic *Cooper pairs*). Even at non-zero temperatures, the statistical behaviors of fermions and bosons are completely different, where the first follows the *Fermi-Dirac statistics* and the second the *Bose-Einstein statistics*.

Finally, the statistics of identical particles and their spin are related through the so-called *spin-statistics theorem* claims that particles with integer spins are bosons and particles with half-integer spins are fermions [Schwinger 1951]. This theorem can be intuitively understood as making the link between exchanging particles and rotating them — since the spin labels the irreducible representations of  $SU(2)$  (the projective group of  $SO(3)$ ), it is then intimately related to the exchange symmetry.

### II.1.2.2. The symmetric group and its representations

We have already encountered several times the *symmetric group*<sup>3</sup>, when dealing with strongly interacting mixtures (section I.2.2), or in appendix A with the Bethe ansatz. Here we recall some of the basic mathematical properties of this group and its irreps, without entering the details. For further readings, the interested reader can turn to one of the many excellent references on the subject [Fulton 2004, James 2001, Hamermesh 1989].

<sup>2</sup>In principle, one can consider identical particles which are neither bosons nor fermions. It only happens in very rare occasion, a notable exception being given by the so-called *anyons* that one encounters in 2D materials and in particular in the fractional quantum Hall effect [Wilczek 1982].

<sup>3</sup>A somehow confusing name!

### Basic properties of $\mathfrak{S}_N$

The symmetric group  $\mathfrak{S}_N$  of index  $N$  is the group of all bijections from  $\{1, 2, \dots, N\}$  to itself, or *permutations*, with the composition as an internal law. In physics, as we just saw, it has an extreme importance when dealing with identical particles. It is also very useful when studying *unitary groups* [Itzykson 1966], and therefore in gauge theories. Moreover, on a purely mathematical point of view, Cayley's theorem states that every finite group is isomorphic to a subgroup of  $\mathfrak{S}_N$  [Cayley 1854], which gives to the latter a central importance in group theory.

The group  $\mathfrak{S}_N$  has order  $N!$ . It is generated by the 2-cycles, or *transpositions*, of the form  $\tau_i = (i, i + 1)$  (that is which exchanges elements  $i$  and  $i + 1$ ). The number  $t$  of transpositions by which a permutation  $P \in \mathfrak{S}_N$  can be decomposed defines the *signature* through  $\epsilon(P) = (-1)^t$ . The kernel of this morphism is denoted  $\mathfrak{A}_N$ , the *alternating group*.

Any permutation  $P \in \mathfrak{S}_N$  can be decomposed in disjoint cycles. Moreover, the *conjugacy class* of  $P$ , that is the set

$$cc(P) = \{QPQ^{-1} \mid Q \in \mathfrak{S}_N\}, \quad (\text{II.1.9})$$

is given by the set of all permutations whose decomposition in disjoint cycles has the same structure as  $P$  (same number of cycles of every length). If this structure consists in  $k_1$  1-cycles,  $k_2$  2-cycles, ... ,  $k_m$   $m$ -cycles, the number  $|cc(P)|$  of elements in  $cc(P)$  is given by

$$|cc(P)| = \frac{N!}{1^{k_1} k_1! \dots m^{k_m} k_m!}. \quad (\text{II.1.10})$$

The number of conjugacy classes of  $\mathfrak{S}_N$  is then the number  $p(N)$  of *partitions* of the integer  $N$ . It can be obtained by expanding its *generating function* as a geometric series [Abramowitz 1965]:

$$\sum_{N=0}^{\infty} p(N) X^N = \prod_{k=1}^{\infty} \frac{1}{1 - X^k}. \quad (\text{II.1.11})$$

An asymptotic expansion for  $p(N)$  is given by [Hardy 1918]:

$$p(n) \underset{\infty}{\sim} \frac{1}{4N\sqrt{3}} \exp\left(\pi\sqrt{\frac{2N}{3}}\right). \quad (\text{II.1.12})$$

As one can see, the number of conjugacy classes of  $\mathfrak{S}_N$  grows rapidly with  $N$ , which makes its extensive study more adapted to low  $N$ .

### Irreducible representations of $\mathfrak{S}_N$ . Young formalism.

The number of non-equivalent irreps of a group is given by the number of its conjugacy classes. Therefore, the number of irreps of  $\mathfrak{S}_N$  is given by the number  $p(N)$  of partitions of  $N$ .

A convenient way of representing a partition of an integer is by a so-called *Young diagram*, which is defined as the following. Let us consider a partition of the form  $\Lambda \equiv [\lambda_1, \lambda_2, \dots, \lambda_n]$  with  $\lambda_1 \geq \lambda_2 \geq \dots \geq \lambda_n$  and  $\lambda_1 + \lambda_2 + \dots + \lambda_n = N$ . Then, we represent this partition by a left-justified set of boxes with  $n$  rows, where each row  $i \in \{1, \dots, n\}$  contains  $\lambda_i$  boxes. For example, the Young diagram associated with the partition  $\Lambda_0 = [3, 2, 2, 1]$  of 8 is given by

$$Y_{\Lambda_0} = \begin{array}{|c|c|c|} \hline & & \\ \hline & & \\ \hline & & \\ \hline & & \\ \hline \end{array} . \quad (\text{II.1.13})$$

Associated with Young diagrams are the *Young tableaux*, where the boxes are filled with symbols taken from some totally ordered set (*e.g.* integers, Latin alphabet...). If the entries are always increasing from left to right in every row and top to bottom in every column, the tableau is said to be *standard*. In the case where several symbols appear more than once, the tableau is said *semistandard* when the entries increase in the weak sense. Here are two examples of Young tableaux, one standard and one semistandard:

$$\begin{array}{|c|c|c|} \hline 1 & 3 & 5 \\ \hline 2 & 6 & \\ \hline 4 & 7 & \\ \hline 8 & & \\ \hline \end{array} \quad \text{and} \quad \begin{array}{|c|c|c|} \hline a & a & b \\ \hline b & b & \\ \hline b & c & \\ \hline c & & \\ \hline \end{array} . \quad (\text{II.1.14})$$

Thus, there is a one to one correspondence between the Young diagrams with  $N$  boxes and the irreps of  $\mathfrak{S}_N$ . This correspondence is done using the so-called *Young symmetrizers* associated with the Young diagrams [Fulton 2004]. Intuitively, it indicates that the rows are symmetrized, while the column are anti-symmetrized. In the case of  $N = 3$  for example, there are three possible Young diagrams, which are given by

$$Y_{[3]} = \begin{array}{|c|c|c|} \hline & & \\ \hline & & \\ \hline & & \\ \hline \end{array}, \quad Y_{[1,1,1]} = \begin{array}{|c|} \hline \\ \hline \\ \hline \\ \hline \end{array}, \quad \text{and} \quad Y_{[2,1]} = \begin{array}{|c|c|} \hline & \\ \hline & \\ \hline & \\ \hline \end{array}. \quad (\text{II.1.15})$$

They correspond respectively to the *trivial representation* (where every permutation is represented by the identity matrix  $\mathbb{1}$ ), to the *sign representation* (where every permutation is represented by its signature) and to the *standard representation*. In terms of identical particles,  $Y_{[3]}$  is the exchange symmetry of three identical bosons, and  $Y_{[1,1,1]}$  is the exchange symmetry of three identical fermions.  $Y_{[2,1]}$  corresponds necessarily to a mixture of non-identical particles.

The dimension of a given irrep  $D_\Lambda$  is given by the number of standard Young tableaux that one can construct from the corresponding Young diagram  $Y_\Lambda$ . This number can be obtained from the *hook length formula*. A *hook length*  $h_\Lambda(i, j)$  of a box of coordinates  $(i, j)$  of  $Y_\Lambda$  is given by the numbers of boxes below  $(i, j)$  + the number of boxes at the right of the box  $(i, j)$  + 1. For example, in  $Y_{\Lambda_0}$  of Eq. (II.1.13), the hook lengths are given by

$$\begin{array}{|c|c|c|} \hline 6 & 4 & 1 \\ \hline 4 & 2 & \\ \hline 3 & 1 & \\ \hline 1 & & \\ \hline \end{array} . \quad (\text{II.1.16})$$

Then, the hook length formula states that

$$\dim D_\Lambda = \frac{N!}{\prod_{(i,j) \in \Lambda} h_\Lambda(i,j)}. \quad (\text{II.1.17})$$

In particular, in our example we have  $\dim D_{\Lambda_0} = 8!/(6 * 4^2 * 3 * 2) = 70$ . Moreover, more generally, the trivial and sign representations, which corresponds respectively to the horizontal and vertical Young diagrams, have always a dimension 1, whereas other irreps are multidimensional. This explains why the symmetrization postulate, which states that identical particles are either bosons or fermions, removes the exchange degeneracy (see section II.1.2). Besides, two *conjugate* irreps, that is irreps whose Young diagrams are transposed, have the same dimension.

Finally, for a given irrep  $D_\Lambda$ , each element of  $\mathfrak{S}_N$  is represented by a  $(\dim D_\Lambda)$ -dimensional matrix. Then, the function

$$\chi_\Lambda : g \in \mathfrak{S}_N \mapsto \text{Tr}(D_\Lambda(g)) \in \mathbb{C} \quad (\text{II.1.18})$$

is called the *character* of  $D_\Lambda$ . These functions have many important properties that greatly help the study of irreps. In particular, there are constant on the conjugacy classes of  $\mathfrak{S}_N$ , and isomorphic representations have the same characters.

## II.2. Symmetry analysis of strongly interacting quantum mixtures

In this section we turn to the symmetry analysis of the system that we mainly studied in this thesis, that is strongly interacting quantum mixtures in one-dimensional harmonic traps (c.f. section I.2.2). We will describe the problem and its relation with quantum magnetism in II.2.1. Then, we will present the method that we used in order to solve it, namely the *class-sum method*, in II.2.2. Finally, we will analyze the ordering of energies as a function of the symmetries in II.2.3. The methods and results described in this section were published in [Decamp 2016a, Decamp 2016b] for fermionic mixtures and [Decamp 2017] for Bose-Fermi mixtures.

### II.2.1. One-dimensional $SU(\kappa)$ quantum gases and quantum magnetism

The systems we are interested in are mixtures of  $N$  atoms divided in  $\kappa$  different fermionic and/or bosonic spin species with populations  $N_1, \dots, N_\kappa$ , and submitted to the Hamiltonian of Eq. (I.2.14) that we recall here:

$$\left[ \sum_{j=1}^N \left( -\frac{\hbar^2}{2m} \frac{\partial^2}{\partial x_j^2} + \frac{1}{2} m \omega^2 x_j^2 \right) + g_{1D} \sum_{i < j} \delta(x_i - x_j) - E \right] \psi = 0. \quad (\text{II.2.1})$$

The key ingredient that allows to describe such mixtures with this Hamiltonian is that we are considering atoms whose ground-state has a purely nuclear spin. This ensures

that the interactions between particles with different spins are independent of the relative spin orientations, that collisions are not spin-flipping, and that all particles are subjected to the same external potential. This property is common to Ytterbium atoms and to fermionic alkaline-earth atoms [Gorshkov 2010]. Therefore, when exchanging fermionic (resp. bosonic) spin components, it does not affect the properties of the system. In the case of a purely fermionic or purely bosonic mixture, this is referred as the  $SU(\kappa)$  symmetry, as it constitutes a generalization of the  $SU(2)$  symmetry of spin- $\frac{1}{2}$  electronic mixtures [Laird 2017]. If the system is composed of  $\mu$  bosonic components and  $\nu$  fermionic component, the system is said to be  $SU(\mu, \nu)$ -symmetric [Kato 1995].  $SU(\kappa)$  systems with  $\kappa > 2$  display exotic features and phase diagrams that has attracted the attention of theoretical physics [Affleck 1988, Marston 1989, Read 1989], recently renewed by the experimental realization of a one-dimensional  $SU(\kappa)$  fermionic mixture described in section I.1.2.4.

The  $SU(\kappa)$ -symmetry is not transparent when just looking at Eq. (II.2.1). However, in the limit of strongly repulsive interactions  $g_{1D} \rightarrow \infty$  that we are considering, one can map this Hamiltonian onto a spin Hamiltonian [Deuretzbacher 2014, Massignan 2015, Levinsen 2015]. Indeed, if we use the same notations as in section I.2.2, we can write in the vicinity of  $1/g_{1D} = 0$  an effective Hamiltonian of the form:

$$H_S = \left( E_0 - \sum_{k=1}^{N-1} J_k \right) \mathbb{1} \pm \sum_{k=1}^{N-1} J_k \hat{P}_{k,k+1} , \quad (\text{II.2.2})$$

where the  $+$  ( $-$ ) sign is for fermions (resp. bosons), the nearest-neighbor exchange constants  $J_k = \alpha_k/g_{1D}$ , and the permutation matrices  $\hat{P}_{k,k+1}$  are defined in the snippet basis by:

$$\left( \hat{P}_{k,k+1} \right)_{ij} = \begin{cases} 1 & \text{if snippets } i \text{ and } j \text{ are equal up to a transposition } (k, k+1) \\ 0 & \text{otherwise} \end{cases} . \quad (\text{II.2.3})$$

Then, the operator  $\hat{P}_{k,k+1}$  can be re-written in terms of spin operators [Deuretzbacher 2014]: e.g. when  $\kappa = 2$ , it can be expressed in terms of the Pauli vector  $\vec{\sigma}$  by

$$\hat{P}_{k,k+1} = \frac{1}{2} \left( \vec{\sigma}^{(k)} \cdot \vec{\sigma}^{(k+1)} + \mathbb{1} \right) , \quad (\text{II.2.4})$$

and one recovers a Heisenberg Hamiltonian. When  $\kappa > 2$ ,  $\vec{\sigma}$  has to be replaced by a spin operator  $\vec{S}$  associated with the generalized generators of  $SU(\kappa)$  Lie algebra [Bourbaki 2008, Gorshkov 2010]. In any case, Eq. (II.2.2) shows that our problem (II.2.1) is equivalent to an effective  $SU(\kappa)$  spin model.

Note that in the fermionized limit  $g_{1D} \rightarrow \infty$ , Eq. (II.2.2) reduces to a trivial Hamiltonian

$$H_S^\infty = E_0 \mathbb{1} . \quad (\text{II.2.5})$$

This Hamiltonian has then a bigger symmetry, namely a  $SU(N)$  symmetry. This emergent symmetry explains the existence of degenerate manifolds at  $g_{1D} = \infty$ , and why this degeneracy is lifted whenever  $g_{1D}$  becomes finite [Harshman 2014, Harshman 2015, Harshman 2016]. Our system can then be seen as a perturbed Hamiltonian with an explicit symmetry breaking from  $SU(N)$  to  $SU(\kappa)$ .

Thus, our system is a perfect model to study *itinerant magnetism*, that is magnetism without a lattice. In the following, we will focus on the symmetry of the *spatial* wave function. This symmetry is dual to its *spin* symmetry (and thus magnetism). Indeed, the symmetry of the total wave function of identical particles is fixed by their bosonic or fermionic nature. However, if these identical particles have different spin orientations as it is the case in our model, although their total wave function still has to be totally symmetric or totally anti-symmetric, their spatial and spin wave function can be other representations of the symmetric group, as long as they are conjugate when identical fermions and equal when identical bosons. Thus, the problem that we are going to address in this section is the following: given a solution  $\psi$  of Eq. (II.2.1) in the  $g_{1D} \rightarrow \infty$  limit, given by the perturbative method described in section I.2.2 and hence by a vector of real coefficients  $\vec{a}$ , how to characterize its symmetry, or equivalently, to which representation of  $\mathfrak{S}_N$  does it belong?

## II.2.2. The class-sum method

Historically, the first description of the so-called *class-sum method* is due Dirac, who used it to study the eigenstates of a many-electron system [Dirac 1929]. It was then developed in the context of nuclear physics [Talmi 1993, Novolesky 1995], and adapted to the study of one-dimensional quantum gases in [Fang 2011, Decamp 2016a, Decamp 2016b, Decamp 2017]. After a description of the mathematical objects used in this method II.2.2.1, we will describe how this method can be adapted to our system of interest in order to answer the last paragraph's problem in II.2.2.2, and implement it in a  $N = 6$  system II.2.2.3.

### II.2.2.1. Class-sums and central characters

Let us consider a Hamiltonian  $\hat{H}$  which is invariant by permutation, as it is the case in our Hamiltonian of interest Eq. (II.2.1). More precisely, for every  $P \in \mathfrak{S}_N$ , if we define the linear operator  $\hat{P}$  by

$$\hat{P}\psi(x_1, x_2, \dots, x_N) = \psi(x_{P_1}, x_{P_2}, \dots, x_{P_N}), \quad (\text{II.2.6})$$

we then have, as in Eq. (II.1.1),

$$[\hat{H}, \hat{P}] = 0. \quad (\text{II.2.7})$$

However, since the  $N!$  permutation operators  $\hat{P}$  do not commute with each other, we cannot diagonalize  $\hat{H}$  and all the  $\hat{P}$ 's simultaneously in a common eigenbasis and use them directly in order to classify the states. We would like to define a set of operators  $\hat{C}$  as a function of the  $\hat{P}$ 's that all commute with each other and also with  $\hat{H}$ , and that completely characterize the permutational symmetry of the system: i.e. a *complete set of commuting observables* (CSCO) [Cohen-Tannoudji 1997a]. This is the same idea which leads to the definition of the *Casimir elements*  $L^2 = L_x^2 + L_y^2 + L_z^2$ , the square angular momentum, when studying the states of the Hydrogen atom which are labeled by the eigenvalues  $\{n, l, m\}$  of the CSCO  $\{\hat{H}_{Hyd}, L^2, L_z\}$ .

For every conjugacy class  $cc_\Lambda$  of  $\mathfrak{S}_N$ , where  $\Lambda \equiv [\lambda_1, \lambda_2, \dots, \lambda_n]$  is a partition of  $N$ , we now define the *conjugacy class-sum* as:

$$C_\Lambda = \sum_{P \in cc_\Lambda} P. \quad (\text{II.2.8})$$

This sum has to be understood in the context of the *group algebra* of  $\mathfrak{S}_N$ , that is the vector space whose basis is indexed by the elements of the group and that linearly extends the laws of the group [James 2001]. It is clear then that every  $Q \in \mathfrak{S}_N$  commutes with  $C_\Lambda$  and thus with each other: by definition of a conjugacy class  $QC_\Lambda Q^{-1} = C_\Lambda$  since it is the same sum in a different order. Moreover, if another linear combination of the  $P$ 's commutes with all the  $P$ 's, it is necessarily a linear combination of the  $C_\Lambda$ 's. Indeed, the condition

$$Q \left( \sum_{P \in \mathfrak{S}_N} b_P P \right) Q^{-1} = \sum_{P \in \mathfrak{S}_N} b'_P P \quad (\text{II.2.9})$$

for every  $Q \in \mathfrak{S}_N$  implies that  $b_P = b'_P$  whenever  $P$  and  $P'$  belong to the same conjugacy class. Thus we have shown that the  $C_\Lambda$ 's form a basis of the *center* of the group algebra of  $\mathfrak{S}_N$  [James 2001], which is the that the associated permutation operators  $\hat{C}_\Lambda$  form, together with  $\hat{H}$ , a CSCO.

The natural question that follows is then: what values are taken by the observables  $\hat{C}_\Lambda$ ? One can prove that it takes one constant specific value for each irreducible representation  $D_\Gamma$  of  $\mathfrak{S}_N$ , and that this value is related, up to a proportionality factor, to the irreducible character  $\chi_\Gamma$  of  $\mathfrak{S}_N$  [Novolesky 1995, Macdonald 1995]. More precisely,  $D_\Gamma(C_\Lambda)$  commutes with  $D_\Gamma(P)$  for every  $P \in \mathfrak{S}_N$ . Then, by Schur's lemma [Fulton 2004],  $D_\Gamma(C_\Lambda)$  is a *homothety*, i.e. there is a real value  $\omega_\Gamma^\Lambda$  such that:

$$D_\Gamma(C_\Lambda) = \omega_\Gamma^\Lambda \mathbb{1}_{|\Gamma|}, \quad (\text{II.2.10})$$

where  $|\Gamma| \equiv \dim D_\Gamma$  is obtained with Eq. (II.1.17). By taking traces in Eq. (II.2.10) we get

$$|\Lambda| \chi_\Gamma^\Lambda = |\Gamma| \omega_\Gamma^\Lambda, \quad (\text{II.2.11})$$

with  $\chi_\Gamma^\Lambda$  the value taken by the irreducible character  $\chi_\Gamma$  over the conjugacy class  $cc_\Lambda$ , and  $|\Lambda|$  is the number of elements in  $cc_\Lambda$ , which is given by Eq. (II.1.10). Since, from Maschke's theorem, every representation  $D$  can be written as a direct sum of irreps, the  $\omega_\Gamma^\Lambda$  values of Eq. (II.2.11) are the only eigenvalues of  $D(C_\Lambda)$ , hence the only values that are taken by the observables  $\hat{C}_\Lambda$ . Because of their link with irreducible characters, they are called the *central characters*.

In the case where  $\Lambda = [r, 1, \dots, 1] \equiv [(r)]$ , i.e. when the conjugacy class  $cc_\Lambda$  consists in a single  $r$ -cycle and  $(N - r)$  1-cycles, there are explicit expressions for the central characters  $\omega_\Gamma^{[(r)]}$ . More precisely, if  $\Gamma = [\gamma_1, \dots, \gamma_m]$  (with  $\gamma_1 \geq \gamma_2 \geq \dots \geq \gamma_m$  and  $\gamma_1 + \gamma_2 + \dots + \gamma_m = N$ ), we can define [Decamp 2017]<sup>4</sup>

$$\mu_i = \gamma_i - i + m, \quad i = 1, \dots, m. \quad (\text{II.2.12})$$

<sup>4</sup>The expression in [Katriel 1993a] contains a small notation misprint.

and then obtain, using  $\chi_{[(r)]}^\Lambda$ 's expression [Macdonald 1995, Katriel 1993a]:

$$\omega_\Gamma^{[(r)]} = \frac{1}{r} \sum_{i=1}^m \frac{\mu_i!}{(\mu_i - r)!} \prod_{j \neq i} \frac{\mu_i - \mu_j - r}{\mu_i - \mu_j}, \quad (\text{II.2.13})$$

where to product is taken to be equal to 1 when  $\Gamma$  contains only one line ( $m = 1$ ). When  $r = 2$ , one can use one of these more user-friendly formulas [Novolesky 1994]:

$$\omega_\Gamma^{[(2)]} = \begin{cases} \frac{1}{2} \sum_{i=1}^m \gamma_i (\gamma_i - 2i + 1) \\ \text{or} \\ \sum_{(i,j) \in \Gamma} (j - i) \end{cases}. \quad (\text{II.2.14})$$

Alternative ways of computing the central characters can be found in [Katriel 1993a, Katriel 1993b, Katriel 1996, Goupil 2000].

### II.2.2.2. Description of the method

Let us first precise our notations. The system  $(N_1^B, \dots, N_\mu^B, N_1^F, \dots, N_\nu^F)$  we are considering is a mixture of  $N_B = N_1^B + \dots + N_\mu^B$  bosons and  $N_F = N_1^F + \dots + N_\nu^F$  fermions divided respectively in  $\mu$  and  $\nu$  spin components, with  $N = N_B + N_F$ . Let us suppose that we have solved Eq. (II.2.1) in the  $g_{1D} \rightarrow \infty$  fermionized limit with the method of section I.2.2. Thus, we have obtained a set of  $D_{N_1^B, \dots, N_\mu^B, N_1^F, \dots, N_\nu^F}$  (c.f. Eq. (I.2.17)) vectors  $\vec{a}$  of coefficients corresponding to solutions of Eq. (II.2.1) via Eq. (I.2.16). We want to determine to which representations of  $\mathfrak{S}_N$  these vectors belong using the class-sums and central characters.

The method we have used in [Decamp 2016a, Decamp 2016b, Decamp 2017] can be decomposed into the following steps:

#### Step 1: Determine the irreps that are compatible with the mixture

When identical bosons (resp. fermions) belong to the same spin component, their spatial wave function must be symmetric (resp. anti-symmetric) when exchanging their coordinates. This reduces the number of possible irreps that are compatible with a given mixture. In practice, one has to order the different species by decreasing order of population and to assign a letter in the alphabetic order to each one of the species. Then, one has to construct all the semistandard Young tableaux with  $N$  boxes labeled by the species, imposing that no bosons (resp. fermions) belonging to the same spin component can be in the same column (resp. row).

For example, in a  $N = 4$  mixtures, there are *a priori*  $p(4) = 5$  possible irreps (c.f. Eq. (II.1.11)), given by the following Young diagrams:

$$\begin{array}{c} \square \square \square \square \\ \square \square \square \\ \square \square \\ \square \square \\ \square \end{array}, \begin{array}{c} \square \square \square \\ \square \square \\ \square \end{array}, \begin{array}{c} \square \square \\ \square \square \end{array}, \begin{array}{c} \square \square \\ \square \\ \square \end{array}, \begin{array}{c} \square \\ \square \\ \square \\ \square \end{array}. \quad (\text{II.2.15})$$



Suppose now that this mixture is given by  $(2^F, 2^F)$ . Then, the only possible semistandard Young tableaux are:

$$\begin{array}{|c|} \hline a \\ \hline a \\ \hline b \\ \hline b \\ \hline \end{array}, \quad \begin{array}{|c|c|} \hline a & b \\ \hline a & \\ \hline b & \\ \hline \end{array}, \quad \begin{array}{|c|c|} \hline a & b \\ \hline a & b \\ \hline \end{array}. \quad (\text{II.2.16})$$

If this mixture is instead  $(2^B, 2^F)$ , there are only two possible symmetries:

$$\begin{array}{|c|c|c|} \hline a & a & b \\ \hline b & & \\ \hline \end{array}, \quad \begin{array}{|c|c|} \hline a & a \\ \hline b & \\ \hline b & \\ \hline \end{array}. \quad (\text{II.2.17})$$

We now dispose of a set  $\{Y_{\Gamma_1}, \dots, Y_{\Gamma_k}\}$  of Young diagrams (with  $k \leq p(N)$ ). This initial step substantially reduces the complexity of the method.

### Step 2: Compute the central characters

We have seen in II.2.2.1 that, for a given partition  $\Lambda$  of  $N$ , the central characters  $\omega_{\Gamma}^{\Lambda}$  have a constant value on each of the irreps  $D_{\Gamma}$  of  $\mathfrak{S}_N$  because of their relation with irreducible characters (Eq. (II.2.11)). Analogously to a *character table*  $(\chi_{\Gamma}^{\Lambda})_{\Lambda, \Gamma}$  [Fulton 2004], we could construct a table  $(\omega_{\Gamma}^{\Lambda})_{\Lambda, \Gamma}$  for central characters and compute  $\omega_{\Gamma}^{\Lambda}$  for all irrep  $D_{\Gamma}$  that is compatible with the mixture and all partition  $\Lambda$ . Thus, we would be able to completely characterize the symmetry of a solution  $\vec{a}$ . This is, however, not necessary: it is sufficient to compute the central characters for  $\Lambda$ 's so that all the central characters belonging to different irreps have different values for at least one  $\Lambda$ .

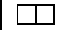
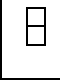
More precisely, given our set  $\{Y_{\Gamma_1}, \dots, Y_{\Gamma_k}\}$  of Young diagrams, we start by computing the central characters  $\omega_{\Gamma_1}^{\Lambda}, \dots, \omega_{\Gamma_k}^{\Lambda}$  of the transposition class-sums, i.e. when  $\Lambda = [(2)]$ , using Eq. (II.2.13) or Eq. (II.2.14). If the  $\omega_{\Gamma_i}^{[(2)]}$ 's are all different, it is sufficient in order to characterize the symmetry. If not, we compute the  $\omega_{\Gamma_i}^{[(3)]}$ 's using again Eq. (II.2.13), and so on, until a rank  $r_{\max}$  where all the irreps  $D_{\Gamma_i}$  have a different set of central characters  $\omega_{\Gamma_i}^{[(2)]}, \omega_{\Gamma_i}^{[(3)]}, \dots, \omega_{\Gamma_i}^{[r_{\max}]}$ .

In practice, when  $N \leq 5$ , it is sufficient to compute the central characters of the transposition class-sums (see table II.2). For  $N = 6$ ,  $r_{\max} = 3$  (c.f. section II.2.2.3).

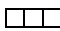
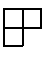
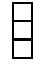
### Step 3: Compute the class-sums in the sector basis representation

The next thing to do is to construct the class-sums  $C_{[(2)]}, \dots, C_{[r_{\max}]}$  defined in Eq. (II.2.8) in the same basis as the  $\vec{a}$  vectors, that is in the sector basis. We have to be careful to the fact that, in the definition of  $\vec{a}$  (Eq. (I.2.16)), the  $a_P$  coefficients are the projection of ansatz  $\psi$  over the totally anti-symmetric wave function  $\psi_A$ : therefore, in order to characterize the symmetry of  $\psi$ , we have to compensate this anti-symmetry when constructing the class-sums. Accordingly, let us define the matrix representation  $D_{\text{sec}}$  by:

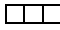
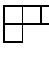
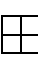

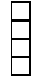
$$D_{\text{sec}} : \mathfrak{S}_N \rightarrow GL_{N!}(\mathbb{R}) \\ g \mapsto (\epsilon(g)\delta_{P, gQ})_{P, Q}, \quad (\text{II.2.18})$$

$Y_\Gamma$	$\omega_\Gamma^{[(2)]}$
	1
	-1

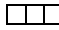
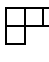



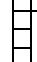
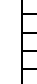
**(a)**  $N = 2$

$Y_\Gamma$	$\omega_\Gamma^{[(2)]}$
	3
	0
	-3

**(b)**  $N = 3$

$Y_\Gamma$	$\omega_\Gamma^{[(2)]}$
	6
	2
	0
	-2
	-6

**(c)**  $N = 4$

$Y_\Gamma$	$\omega_\Gamma^{[(2)]}$
	10
	5
	2
	0
	-2
	-5
	-10

**(d)**  $N = 5$

**Table II.2:** Central characters of the transposition class-sums  $\omega_\Gamma^{[(2)]}$  for  $N \leq 5$ . Since they are all different (at fixed  $N$ ), there is no need to compute  $\omega_\Gamma^\Lambda$  for other  $\Lambda$ 's. Note that conjugate diagrams have an opposite  $\omega_\Gamma^{[(2)]}$ .

with  $\epsilon$  the signature, which can be extended linearly to a morphism defined on the group algebra, where the class-sums are defined. With this definition, the cycle class-sums are represented by:

$$D_{\text{sec}} \left( C_{[(r)]} \right) = (-1)^{r-1} \sum_{\sigma \in cc_{[(r)]}} M_{\sigma}, \quad (\text{II.2.19})$$

where  $M_{\sigma}^r$  is a  $N! \times N!$  matrix whose coefficients are  $(M_{\sigma})_{PQ} = \delta_{P, \sigma Q}$ .

For the sake of clarity, let us consider the example of  $N = 3$ . There are  $3! = 6$  elements in the sector basis, that we order in the following way:

$$(e_{123}, e_{132}, e_{213}, e_{312}, e_{321}). \quad (\text{II.2.20})$$

In this basis,

$$D_{\text{sec}} \left( C_{[(2)]} \right) = - \begin{pmatrix} 0 & 1 & 1 & 0 & 0 & 1 \\ 1 & 0 & 0 & 1 & 1 & 0 \\ 1 & 0 & 0 & 1 & 1 & 0 \\ 0 & 1 & 1 & 0 & 0 & 1 \\ 0 & 1 & 1 & 0 & 0 & 1 \\ 1 & 0 & 0 & 1 & 1 & 0 \end{pmatrix}, \quad (\text{II.2.21})$$

and

$$D_{\text{sec}} \left( C_{[(3)]} \right) = \begin{pmatrix} 0 & 0 & 0 & 1 & 1 & 0 \\ 0 & 0 & 1 & 0 & 0 & 1 \\ 0 & 1 & 0 & 0 & 0 & 1 \\ 1 & 0 & 0 & 0 & 1 & 0 \\ 1 & 0 & 0 & 1 & 0 & 0 \\ 0 & 1 & 1 & 0 & 0 & 0 \end{pmatrix}. \quad (\text{II.2.22})$$

#### Step 4: Project $\vec{a}$ on the eigenbasis of the class-sum representations

As we have seen in section II.2.2.1, in each irrep  $D_{\Gamma}$ , the class-sums are homotheties whose ratios are given by the central characters (Eq. (II.2.10)). Although  $D_{\text{sec}}$  is *a priori* not an irrep, it is (up to a sign) the *regular representation* of  $\mathfrak{S}_N$  [James 2001]. Then,  $D_{\text{sec}}$  is a direct sum of all the irreps of  $\mathfrak{S}_N$  (with multiplicities equal to their degrees). In other words, the spectrum of the cycle class-sum representations is equal to the set of all the associated central characters. Therefore, by diagonalizing the  $D_{\text{sec}} \left( C_{[(r)]} \right)$  matrices, we will get a set of eigenspaces corresponding to the irreps  $D_{\Gamma}$  and with eigenvalues  $\omega_{[(r)]}^{\Lambda}$ .

Thus, the final step of this method is to diagonalize our set  $D_{\text{sec}} \left( C_{[(2)]} \right), \dots, D_{\text{sec}} \left( C_{[(r_{\text{max}})]} \right)$  of matrices and project  $\vec{a}$  in their eigenbasis. The symmetry of the associated wave function will then be completely characterized.

#### Alternative: the snippet representation

Note that for a given mixture it is also possible to write the class-sums in the lower dimensional snippet representation  $D_{\text{snip}}$  (see section I.2.2.2) by summing (or subtracting when permuting same-component bosons) over the elements of the class-sums in the

sector representation that belong to the same snippet. The only central characters that will appear when diagonalizing  $D_{\text{snip}}(C_{[(2)]}), \dots, D_{\text{snip}}(C_{[(r_{\text{max}})]})$  will then be the ones corresponding to the irreps allowed by the mixture (step 1). If we consider the fermionic mixture  $(2^F, 2^F)$  that we used as a first example in section I.2.2.2, we obtain in the same basis:

$$D_{\text{snip}}^{(2^F, 2^F)}(C_{[(2)]}) = - \begin{pmatrix} 2 & 1 & 1 & 1 & 1 & 0 \\ 2 & 2 & 1 & 1 & 0 & 1 \\ 2 & 1 & 2 & 0 & 1 & 1 \\ 2 & 1 & 0 & 2 & 1 & 1 \\ 2 & 0 & 1 & 1 & 2 & 1 \\ 0 & 1 & 1 & 1 & 1 & 2 \end{pmatrix}, \quad (\text{II.2.23})$$

which is similar to the diagonal matrix  $\text{diag}(-6, -2, -2, -2, 0, 0)$ . The corresponding central characters are, as expected, associated with the three diagrams of Eq. (II.2.16) allowed by the mixture (c.f. table II.2).

Although doing this adds a step between Step 3 and Step 4, it has the advantage of facilitating the diagonalization of Step 4 by reducing the size of the matrix representations. However, it has the inconvenient to be usable only for a given mixture, contrary to the sector representation which is usable for any mixture at given  $N$ .

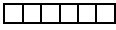
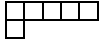
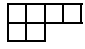
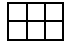
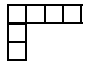
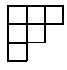
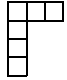
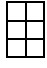
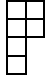


### II.2.2.3. Implementation for $N = 6$ mixtures and first observations

The  $N = 6$  case has interesting new features as compared to the  $N \leq 5$  ones. First, we will see very soon that here the central characters of the transposition class-sums  $\omega_{[(2)]}^\Lambda$  will be degenerate for two irreps, hence the need to compute the three-cycle class sum. Moreover, it allows to study various kind of mixtures, *e.g.* a completely imbalanced three-component mixtures of the type  $(3^F, 2^F, 1^F)$ . Thus, we can observe new features in these few-body systems that allow to better understand the large  $N$  behaviors of the solutions of Eq. (II.2.1). We studied these  $N = 6$  systems in detail, in [Decamp 2016a, Decamp 2016b] for fermionic mixtures and [Decamp 2017] for Bose-Fermi mixtures.

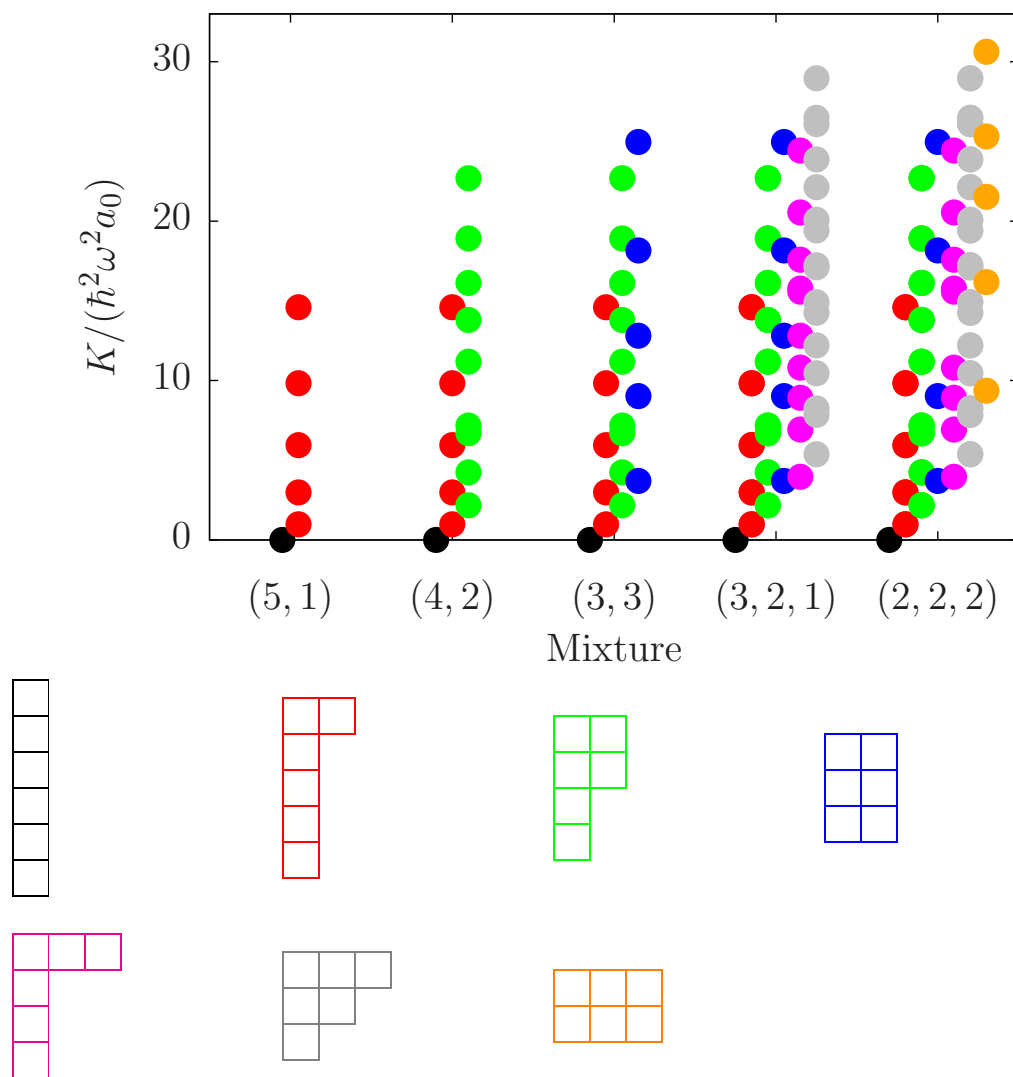
There are  $p(6) = 11$  non-isomorphic irreps of  $\mathfrak{S}_N$ . Since we will study various quantum mixtures, we will enumerate all the associated Young diagrams and compute all the corresponding central characters  $\omega_{[(2)]}^\Lambda$  and  $\omega_{[(3)]}^\Lambda$ . The results are summarized in table II.3.

We observe that conjugate irreps have equal dimensions and three-cycle central characters, and opposite transposition central characters. Moreover, as we previously mentioned, we see that there are two degeneracies in the transposition central characters, namely  $\omega_{[3,3]}^{[(2)]} = \omega_{[4,1,1]}^{[(2)]} = 3$  and  $\omega_{[3,1,1,1]}^{[(2)]} = \omega_{[2,2,2]}^{[(2)]} = -3$ . This degeneracy is no longer present for the three-cycle central characters, and therefore we do not have to compute the four-cycle central characters.

The next step is then to compute  $D_{\text{sec}}(C_{[(2)]})$  and  $D_{\text{sec}}(C_{[(3)]})$ . We have developed a `Mathematica` program similar to the one we created for the computing the  $V$  matrix (see section I.2.2.2) that computes  $D_{\text{sec}}(C_{[(2)]})$  and  $D_{\text{sec}}(C_{[(3)]})$   $N! \times N!$  matrices for any  $N$  (with a complexity of  $\mathcal{O}(N!^2)$ ), and diagonalize them. In the  $N = 6$  case it consists in

$\Gamma$	$Y_\Gamma$	$\dim D_\Gamma$	$\omega_\Gamma^{[(2)]}$	$\omega_\Gamma^{[(3)]}$
[6]		1	15	40
[5, 1]		5	9	16
[4, 2]		9	5	0
[3, 3]		5	<b>3</b>	-8
[4, 1, 1]		10	<b>3</b>	4
[3, 2, 1]		16	0	-5
[3, 1, 1, 1]		10	<b>-3</b>	4
[2, 2, 2]		5	<b>-3</b>	-8
[2, 2, 1, 1]		9	-5	0
[2, 1, 1, 1, 1]		5	-9	16
[1, 1, 1, 1, 1, 1]		1	-15	40

**Table II.3:** Central characters  $\omega_\Gamma^{[(2)]}$  and  $\omega_\Gamma^{[(3)]}$  in the  $N = 6$  case, obtained from Eqs. (II.2.13) and (II.2.14). For each partition  $\Gamma$ , the dimension of the associated irrep  $D_\Gamma$ , which corresponds to the multiplicity of the corresponding central characters as eigenvalues of the class-sums in the sector representation, is computed with the hook length formula (Eq. (II.1.17)).



**Figure II.2.1:** Energy slopes  $K$  for different kind of fermionic mixtures, with the associated symmetries given by their colors. The dots are shifted from left to right with the same order of appearance than the symmetries. These results were published in [Decamp 2016b].

a  $720 \times 720$  matrix that we will of course not present here. However, if we consider the example  $(4^F, 2^F)$  of section I.2.2.2, we can write in the snippet basis of Fig. I.2.3:

$$D_{\text{snip}}^{(4^F, 2^F)} \left( C_{[(2)]} \right) = - \begin{pmatrix} 7 & 1 & 1 & 1 & 1 & 0 & 1 & 1 & 0 & 0 & 1 & 1 & 0 & 0 & 0 \\ 1 & 7 & 1 & 1 & 0 & 1 & 1 & 0 & 1 & 0 & 1 & 0 & 1 & 0 & 0 \\ 1 & 1 & 7 & 0 & 1 & 1 & 0 & 1 & 1 & 0 & 0 & 1 & 1 & 0 & 0 \\ 1 & 1 & 0 & 7 & 1 & 1 & 1 & 0 & 0 & 1 & 1 & 0 & 0 & 1 & 0 \\ 1 & 0 & 1 & 1 & 7 & 1 & 0 & 1 & 0 & 1 & 0 & 1 & 0 & 1 & 0 \\ 0 & 1 & 1 & 1 & 1 & 7 & 0 & 0 & 1 & 1 & 0 & 0 & 1 & 1 & 0 \\ 1 & 1 & 0 & 1 & 0 & 0 & 7 & 1 & 1 & 1 & 1 & 0 & 0 & 0 & 1 \\ 1 & 0 & 1 & 0 & 1 & 0 & 1 & 7 & 1 & 1 & 0 & 1 & 0 & 0 & 1 \\ 0 & 1 & 1 & 0 & 0 & 1 & 1 & 1 & 7 & 1 & 0 & 0 & 1 & 0 & 1 \\ 0 & 0 & 0 & 1 & 1 & 1 & 1 & 1 & 1 & 7 & 0 & 0 & 0 & 1 & 1 \\ 1 & 1 & 0 & 1 & 0 & 0 & 1 & 0 & 0 & 0 & 7 & 1 & 1 & 1 & 1 \\ 1 & 0 & 1 & 0 & 1 & 0 & 0 & 1 & 0 & 0 & 1 & 7 & 1 & 1 & 1 \\ 0 & 1 & 1 & 0 & 0 & 1 & 0 & 0 & 1 & 0 & 1 & 1 & 7 & 1 & 1 \\ 0 & 0 & 0 & 1 & 1 & 1 & 0 & 0 & 0 & 1 & 1 & 1 & 1 & 7 & 1 \\ 0 & 0 & 0 & 0 & 0 & 0 & 1 & 1 & 1 & 1 & 1 & 1 & 1 & 1 & 7 \end{pmatrix}, \quad (\text{II.2.24})$$

which is similar to

$$\text{diag}(-15, -9, -9, -9, -9, -9, -5, -5, -5, -5, -5, -5, -5, -5, -5). \quad (\text{II.2.25})$$

As expected, it corresponds to the  $\omega_{\Gamma}^{[(2)]}$ 's with  $\Gamma \in \{[2, 2, 1, 1], [2, 1, 1, 1, 1], [1, 1, 1, 1, 1, 1]\}$  and with multiplicities equal to the dimensions of the associated irreps (c.f. table II.3). Note that for this mixture it is not necessary to compute  $D_{\text{snip}}^{(4^F, 2^F)} \left( C_{[(3)]} \right)$ , but it is *e.g.* for  $(2^F, 2^F, 2^F)$ . If we diagonalize the  $V$ -matrix associated with this mixture (c.f. Fig. I.2.3), we obtain a set of energy slopes  $K$  (Eqs. (I.2.21) and (I.2.28)) and  $\vec{a}$  vectors whose symmetries are obtained by projecting the  $\vec{a}$  vectors on the eigenbasis of  $D_{\text{snip}}^{(4^F, 2^F)} \left( C_{[(2)]} \right)$ .

Results for various fermionic mixtures are given in Fig. II.2.1. By comparing it to table II.3, we observe that the number of states that correspond to a given symmetry  $\Gamma$  is equal to  $\dim D_{\Gamma}$ , and that, for a given mixture  $(N_1, \dots, N_{\kappa})$  with symmetries  $\Gamma_1, \dots, \Gamma_{\kappa}$ , we have

$$\sum_{i=1}^{\kappa} \dim D_{\Gamma_i} = D_{N_1, \dots, N_{\kappa}}, \quad (\text{II.2.26})$$

where  $D_{N_1, \dots, N_{\kappa}}$  is the dimension of the degenerate manifold defined in Eq. (I.2.17). This is indeed expected from the discussion in section II.1.1.2 (see Eqs. (II.1.1), (II.1.2) and (II.1.3) with  $G = \mathfrak{S}_N$ ). Moreover, note that the set of energy slopes for a given irrep is independent of the choice of the mixture.

## II.2.3. Ordering of energy levels

### II.2.3.1. The Lieb-Mattis theorem

The Lieb-Mattis theorem [Lieb 1962] is a fundamental theorem of many-body quantum physics that links the ordering of energy levels with their relative symmetries, and that

has important consequences in condensed matter and the theory of magnetism. In this section we will enunciate and prove both versions of the theorem, following the original work of Lieb and Mattis, and then discuss some of their consequences.

### The first Lieb-Mattis theorem (LMT I)

The first and most well-known version of the Lieb-Mattis theorem, that we will refer as LMT I in the following, concerns spin-1/2 particles, or  $SU(2)$  gases. Before enunciating it, let us first define our notations. Let us consider a system of  $N$  particles divided into two fermionic components and subjected to a general Hamiltonian of the form (in units of  $\hbar = 2m = 1$ ):

$$\hat{H} = - \sum_{i=1}^N \frac{\partial^2}{\partial x_i^2} + U(x_1, \dots, x_N), \quad (\text{II.2.27})$$

where  $U$  is a real, permutational invariant potential that contains both the external and interaction potentials. The many-body wave function  $\Psi$  can be subjected to various boundary conditions:  $\Psi = 0$  or  $\partial\Psi/\partial x_i = 0$  whenever  $x_i = 0$  or  $x_i = L$  if particles are on a box of size  $L$ , or  $\Psi \in L^2(\mathbb{R}^N)$  if particles are, for example, in a harmonic trap.

We will be interested in states  $\overset{S}{M}\Psi$  with a definite total spin  $S$  and a definite total azimuthal quantum number  $M$ . These numbers are classically defined as

$$\vec{S}^2 \overset{S}{M}\Psi = S(S+1) \overset{S}{M}\Psi, \quad (\text{II.2.28})$$

and

$$\vec{S}_z \overset{S}{M}\Psi = M \overset{S}{M}\Psi, \quad (\text{II.2.29})$$

where  $\vec{S}^2 = \sum_{i=1}^N (\vec{S}^i)^2$  and  $\vec{S}_z = \sum_{i=1}^N \vec{S}_z^i$  are the usual spin operators. For given  $S$  and  $M$ , let us denote by  $E(S)$  and  $E(M)$  (resp.) the *ground-state energies* of  $S$  and  $M$  (resp.), that is the minimum eigenvalues of  $\hat{H}$  in Eq. (II.2.27) whose associated eigenstates have spin and azimuthal numbers  $S$  and  $M$  (resp.).

The first Lieb-Mattis theorem can be enunciated as follows:

**Theorem (LMT I):** *If  $S > S'$ , then  $E(S) \geq E(S')$ . Moreover,  $E(S) = E(S')$  only if  $U$  is pathological (in a sense that will be specified in the proof).*

In order to prove this theorem, remark that it is sufficient to prove that, at fixed  $M \geq 0$  (the opposite case is of course similar), the associate ground-state wave function  $\overset{M}{\Psi}$  should have  $S = M$ , and hence  $E(M) = E(S)$ . Indeed, if we consider  $S > S'$ , the ground-state  $\overset{S}{\Psi}$  corresponding to  $E(S)$  is degenerate and could have any azimuthal number  $M \in \{-S, -S+1, \dots, S-1, S\}$ , and in particular  $\overset{S}{M=S'}\Psi$  has an energy  $E(S)$ . But since the ground-state energy of states with an azimuthal number equal to  $S'$  should have a spin also equal to  $S'$ , we have  $E(S') \leq E(S)$ .

Let us consider  $M \geq 0$ . A typical total wave function  $\overset{M}{\Psi}$  with an azimuthal number  $M$  is given by:

$$\overset{M}{\Psi} = \sum_{P \in \mathfrak{S}_N} \epsilon(P) (\hat{P}_M \phi) (\hat{P}_M G), \quad (\text{II.2.30})$$



where the spin wave function  ${}_M G$  has the form

$${}_M G = (- \dots - + \dots +), \quad (\text{II.2.31})$$

with  $p \equiv N - M$  spin down ( $-$ ) and  $N - p$  spin up ( $+$ ), and the spatial wave function  ${}_M \phi$  has the form

$${}_M \phi = \phi(x_1, \dots, x_p | x_{p+1}, \dots, x_N), \quad (\text{II.2.32})$$

where  $\phi$  is anti-symmetric by permutation of  $x_1, \dots, x_p$  and  $x_{p+1}, \dots, x_N$ .

Then, we can affirm that a necessary and sufficient condition on  $\phi$  so that  $S = M$  is that  $\phi$  cannot be anti-symmetrized with respect to  $x_p, x_{p+1}, \dots, x_N$ , *i.e.* that the bar "|" in  $\phi$  cannot be moved to the left. Indeed,  $S$  can, *a priori*, take all values between  $M, M + 1, \dots, N/2$ . Then,  $S = M$  is equivalent to  $S_{+M}^M \Psi = 0$ , which means for  ${}_M G$  that one cannot transform one spin down in one spin up, and for  $\phi$  that the bar cannot be moved to the left.

Now we are going to study the properties of the ground-state wave function with azimuthal number  $M$ . We define the fundamental domain  $R_M$  of  $\mathbb{R}^N$  by

$$x_1 \leq \dots \leq x_p \quad (\text{II.2.33})$$

and

$$x_{p+1} \leq \dots \leq x_N. \quad (\text{II.2.34})$$

Then, one can prove that the Schrödinger equation  $\hat{H}\varphi = E\varphi$  in  $R_M$  with the boundary conditions  $\varphi = 0$  on the boundary of  $R_M$  has a positive ground-state solution  $\varphi_0$ . In fact, one can show that  $\varphi_0$  is strictly positive in the interior of  $R_M$  unless  $U$  is *pathological* in the sense that it contains "sufficiently strong infinities". An example of pathological potential is given by the fermionized limit  $g_{1D} \rightarrow \infty$  in our system Eq. (II.2.1), which explains why states with different symmetries have the same energy in this limit.

Given  $\varphi_0$ , we define the function  $\Phi_0$  on  $\mathbb{R}^N$  by

$$\Phi_0 = \epsilon(P)\epsilon(Q)\hat{P}\hat{Q}\varphi_0 \quad \text{in } PQ(R_M), \quad (\text{II.2.35})$$

where  $P \in \mathfrak{S}_p$  and  $Q \in \mathfrak{S}_{N-p}$ ,  $\hat{P}$  and  $\hat{Q}$  permute the variables  $x_1, \dots, x_p$  and  $x_{p+1}, \dots, x_N$  (resp.) and the domain  $PQ(R_M)$  is defined by

$$x_{P1} \leq \dots \leq x_{Pp} \quad (\text{II.2.36})$$

and

$$x_{Q(p+1)} \leq \dots \leq x_{QN}. \quad (\text{II.2.37})$$

Then,  $\Phi_0$  is a solution of the Schrödinger equation  $\hat{H}\phi = E\phi$  in  $\mathbb{R}^N$  (thanks to the boundary conditions of  $\varphi_0$ ) with an azimuthal number of  $M$  (because it is of the form of Eq. (II.2.32)). In particular, since  $\varphi_0$  is the ground state in  $R_M$ ,  $\Phi_0$  is the ground state wave function with an azimuthal number of  $M$ .

Let us show that  $\Phi_0$  verifies  $S = M$ . To do so, we define the following function on  $\mathbb{R}^N$ :

$$\mathcal{V}(x_1, \dots, x_N) = \det \begin{pmatrix} 1 & x_1 & \dots & x_1^{p-1} \\ 1 & x_2 & \dots & x_2^{p-1} \\ \vdots & \vdots & \ddots & \vdots \\ 1 & x_p & \dots & x_p^{p-1} \end{pmatrix} \det \begin{pmatrix} 1 & x_{p+1} & \dots & x_{p+1}^{N-p-1} \\ 1 & x_{p+2} & \dots & x_{p+2}^{N-p-1} \\ \vdots & \vdots & \ddots & \vdots \\ 1 & x_N & \dots & x_N^{N-p-1} \end{pmatrix}, \quad (\text{II.2.38})$$

a product of two Vandermonde determinant, which is then also equal to

$$\mathcal{V}(x_1, \dots, x_N) = \prod_{1 \leq i < j \leq p} (x_j - x_i) \prod_{p+1 \leq k < l \leq N} (x_l - x_k). \quad (\text{II.2.39})$$

It is clear that  $\mathcal{V}$  is totally anti-symmetric in the variables  $x_1, \dots, x_p$  and  $x_{p+1}, \dots, x_N$  and then is a function of the form of Eq. (II.2.32), and moreover that "the bar cannot be moved to the left": hence  $\mathcal{V}$  is characterized by an azimuthal number  $M$  and by a spin  $S = M$ . Besides  $\mathcal{V}$  is strictly positive in the fundamental domain  $R_M$ . Finally, we can define the following scalar product for functions of the type of Eq. (II.2.32):

$$\langle Mf, Mg \rangle_M = \int_{\mathbb{R}^N} Mf Mg = p!(N-p)! \int_{R_M} Mf Mg. \quad (\text{II.2.40})$$

If two functions  ${}^S_M f, {}^{S'}_M g$  have definite spin values  $S, S'$ , one can easily see that  $\langle {}^S_M f, {}^{S'}_M g \rangle_M \neq 0$  only if  $S = S'$ . We can say that the spin labels the irreps of  $SU(2)$  and that non-equivalent irreps are orthogonal. Therefore, since  $\varphi_0 \geq 0$  and  $\mathcal{V} > 0$  on  $R_M$ , we can conclude that  $\Phi_0$  verifies  $S = M$ . Thus, we have completed the proof of LMT I.

## Second Lieb-Mattis theorem (LMT II) and pouring principle

The second Lieb-Mattis theorem is a direct generalization of LMT I to  $SU(\kappa)$  systems. Although very powerful, we will see that it does not allow to compare all the ground states energies of the irreps of  $\mathfrak{S}_N$ . Here, more than giving a detailed proof, we will develop the analogy with the last paragraph.

Instead of considering two-component fermionic particles subjected to the Hamiltonian defined in Eq. (II.2.27), we do not specify the mixture and allow it to obey any statistics. In other words, it can belong to any irrep of  $\mathfrak{S}_N$ .

For LMT I, particles could belong to any irrep of the type  ${}^t [N/2 + S, N/2 - S]$ , where the notation  ${}^t [ ]$  means that we specify the number of boxes in the columns of the corresponding Young diagram<sup>5</sup>. Then the generalization of  $S$  is to specify the irrep  $D_{t\Gamma}$  associated with a partition  ${}^t \Gamma$ .

Moreover, functions with an azimuthal number  $M$  where characterized by being of the type of Eq. (II.2.32). Therefore, instead of considering  $M$ , we directly consider functions of the form:

$$\phi(x_1, \dots | \dots, x_{N-N_1-N_2} | x_{N-N_1-N_2+1}, \dots, x_{N-N_1} | x_{N-N_1+1}, \dots, x_N), \quad (\text{II.2.41})$$

where variables between two bars are anti-symmetrized. Instead of choosing  $M \geq 0$ , here we set  $N_1 \geq N_2 \geq \dots$ . Besides, bars can always be moved to the right without changing of irrep (we can always lower  $M$ ), and a necessary and sufficient condition for a function of the type of Eq. (II.2.41) to belong to the irrep  ${}^t [N_1, N_2, \dots]$  ( $S = M$  in LMT I) is that the bars cannot be moved to the left.

The central idea of the proof of LMT I was that  $E(S)$  was degenerate for  $M$  and that therefore it was sufficient to prove that the ground state wave function of azimuthal

<sup>5</sup>Notice the difference of convention with section II.1.2.2, which is appropriate here since we considered fermionic species in LMT I.

number  $M$  should have  $S = M$ . Here this degeneracy is more subtle: for a partition  ${}^t\Gamma$ , the only functions of the type of Eq. (II.2.41) that can belong to  $D_{{}^t\Gamma}$  are the ones when the bars are not moved to the left. Thus, we cannot compare all the irreps.

Accordingly, we define a partial order  $\succ$  on the irreps: considering  $D_{{}^t\Gamma}, D_{{}^t\Gamma'}$  with  ${}^t\Gamma = {}^t[N_1, N_2, N_3, \dots]$  and  ${}^t\Gamma' = {}^t[N'_1, N'_2, N'_3, \dots]$ , we say that  $D_{{}^t\Gamma}$  can be *poured* into  $D_{{}^t\Gamma'}$  and write  ${}^t\Gamma \succ {}^t\Gamma'$  if  $N_1 \geq N'_1$ ,  $(N_1 - N'_1) + N_2 \geq N'_2$ ,  $(N_1 - N'_1 + N_2 - N'_2) + N_3 \geq N'_3$ , etc. In other words,  $Y_{{}^t\Gamma}$  can be transformed into  $Y_{{}^t\Gamma'}$  by moving the boxes of the diagrams to the right. In the context of algebraic combinatorics and representation theory,  $\succ$  is known as the *dominance order* [Macdonald 1995]. For example, we have

$$\begin{array}{|c|c|c|} \hline \square & \square & \square \\ \hline \square & \square & \square \\ \hline \square & & \\ \hline \end{array} \succ \begin{array}{|c|c|c|c|} \hline \square & \square & \square & \square \\ \hline \square & \square & \square & \square \\ \hline \end{array}, \quad (\text{II.2.42})$$

or

$$\begin{array}{|c|c|} \hline \square & \square \\ \hline \square & \square \\ \hline \square & \\ \hline \end{array} \succ \begin{array}{|c|c|c|c|c|} \hline \square & \square & \square & \square & \square \\ \hline \square & & & & \\ \hline \end{array}. \quad (\text{II.2.43})$$

However, it is impossible to compare these two diagrams:

$$\begin{array}{|c|c|c|} \hline \square & \square & \square \\ \hline \square & \square & \square \\ \hline \square & \square & \\ \hline \square & & \\ \hline \square & & \\ \hline \square & & \\ \hline \end{array} \quad \text{and} \quad \begin{array}{|c|c|} \hline \square & \square \\ \hline \square & \square \\ \hline \square & \square \\ \hline \square & \square \\ \hline \square & \square \\ \hline \end{array}. \quad (\text{II.2.44})$$

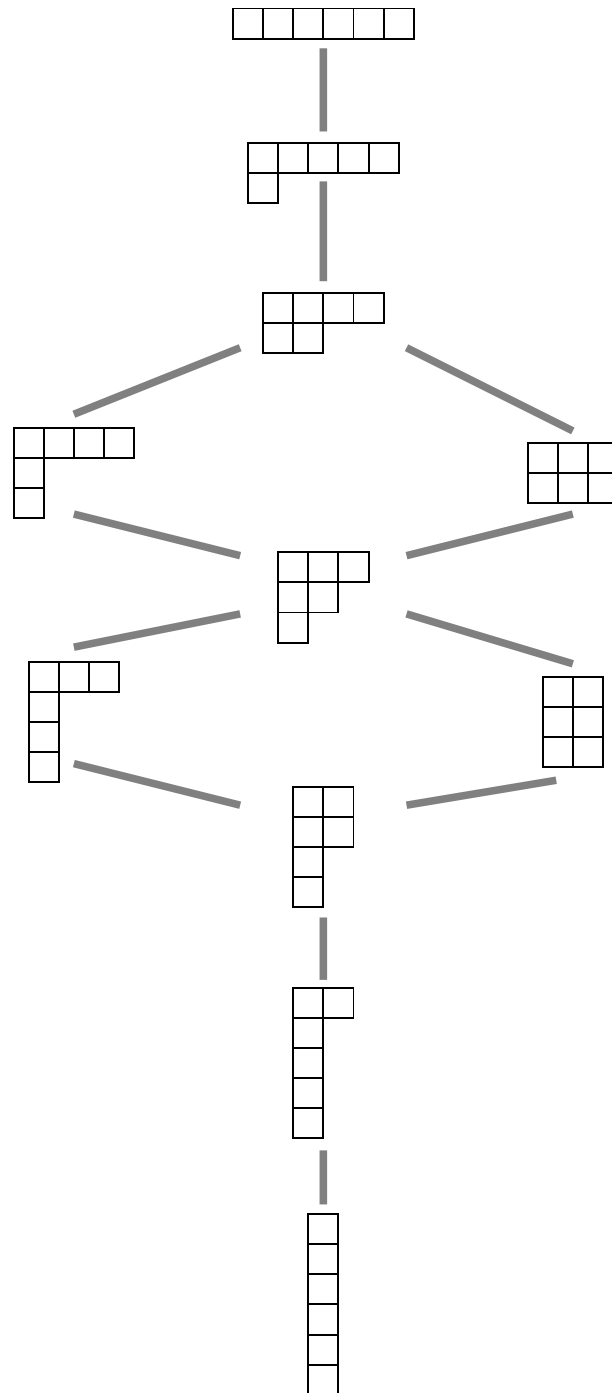
Writing  $E({}^t\Gamma)$  the ground state energy associated with the symmetry class  ${}^t\Gamma$ , we can now enunciate the second Lieb-Mattis theorem:

**Theorem (LMT II):** *If  ${}^t\Gamma \succ {}^t\Gamma'$ , then  $E({}^t\Gamma) \geq E({}^t\Gamma')$ . Moreover,  $E({}^t\Gamma) = E({}^t\Gamma')$  only if  $U$  is pathological.*

The proof of this theorem is now very similar to the proof of LMT I: considering the ground state wave function of the form of Eq. (II.2.41), we show that it is positive on the fundamental domain defined analogously to  $R_M$ . Then we consider an appropriate product of Vandermonde determinant similar to  $\mathcal{V}$ , which belongs to the irrep  $D_{{}^t\Gamma}$  with  ${}^t\Gamma = {}^t[N_1, N_2, N_3, \dots]$  and is also positive on the aforementioned fundamental domain. Thus it is not orthogonal to the ground state wave function, which therefore belongs to  $D_{{}^t\Gamma}$ .

### Consequences for the theory of magnetism

Lieb and Mattis have discussed the consequences of LMT I for the theory of magnetism, by saying that a two-component fermionic system that obeys to the Hamiltonian in Eq. (II.2.27) has an non-ferromagnetic ground state. It is clear indeed that such a



**Figure II.2.2:** Hasse diagram of the partially ordered set  $(I_6, >)$ .

system will not have a non-zero  $S$  value that grows proportionally with its size, since the ground state has a minimal spin.

In the case of a one-component Bose gas, on the contrary, since LMT II implies that the *spatial wavefunction* is as symmetric as possible and since the total wavefunction of a Bose gas is totally symmetric, it implies that the spin wavefunction is also totally symmetric. Thus, a consequence of LMT II is that the ground state of a one-dimensional Bose gas is fully polarized. It was shown in [Eisenberg 2002] that even in three-dimensional systems at finite temperature, it is also the case as long as there are no spin-dependent forces.

Moreover, Lieb and Mattis have shown, with the help of LMT II, that it is possible to extend LMT I to higher dimensions if the potential  $U$  is *separably symmetric* (e.g. for a two-dimensional potential  $U(x_1, \dots, x_N; y_1, \dots, y_N)$ ,  $U$  is symmetric in the  $x_i$  coordinates of the  $N$  particles, and also in the  $y_i$ ). Therefore, it does not apply, for example, to three-dimensional systems with central forces among the particles.

More generally, the Lieb-Mattis theorems do not apply to systems with momentum-dependent or spin-dependent forces. It does apply, however, to one-dimensional quantum gases that can be simulated with cold-atom experiments such as the ones discussed in this thesis.

### II.2.3.2. Analysis in our system

First of all, let us note that, although the  $1/g_{1D} = 0$  point corresponds to a pathological case of Lieb-Mattis theorem and is degenerate for the irreps, the set of energy slopes  $K$  allows to deduce the ordering of energy levels in the vicinity of that point (see e.g. Fig. I.2.1). Notice also that, because of the minus sign in  $K$ 's definition (Eq. (I.2.18)), the ground state energies will correspond to the maximum  $K$  values. Accordingly, given a symmetry class  $\Gamma$ , we define  $K(\Gamma)$  as the maximum  $K$  whose corresponding state belongs to  $D_\Gamma$ . With this notation, LMT II becomes, in our context:

$$\Gamma \succ \Gamma' \quad \Rightarrow \quad K(\Gamma) < K(\Gamma'), \quad (\text{II.2.45})$$

where we have written " $<$ " instead of " $\leq$ " since the interaction potential in Eq. (II.2.1) is non-pathological in the vicinity of the degenerate manifold  $1/g_{1D} = 0$ <sup>6</sup>.

Before analyzing our results, let us first see how the set  $I_6$  of irreps of  $\mathfrak{S}_6$  is partially ordered by the dominance order  $\succ$ . The conventional way of representing a partially ordered  $(E, \leq)$  set is through a *Hasse diagram* [Simovici 2014], i.e. a graph (see section I.2.2.2) where each vertex is an element of  $E$ , and if an edge relies two vertices  $A$  and  $B$  where if  $A$  is above  $B$ , then  $A \geq B$ . The Hasse diagram of  $(I_6, \succ)$  is given in Fig. II.2.2.

Now, a direct comparison of Fig. II.2.2 and Fig. II.2.1 shows that our system, in the fermionic case, verifies LMT II. In [Decamp 2017], we extended this result to Bose-Fermi mixtures, as one can see in table II.4. On a side note, remark that three-component

---

<sup>6</sup>Since the interaction potential is pathological in the degenerate manifold, the energetic counterpart should still be written  $\Gamma \succ \Gamma' \Rightarrow E(\Gamma) \geq E(\Gamma')$ .

Mixture	$Y_\Gamma$	$K(\Gamma)/(\hbar^2\omega^2a_0)$
$(2^B, 2^F)$		10.66
		7.08
$(3^B, 3^F)$		30.37
		24.43

(a) Two-component Bose-Fermi mixtures.

Mixtures	$Y_\Gamma$	$K(\Gamma)/(\hbar^2\omega^2a_0)$
$(2^B, 2^B, 2^F)$		33.35
		32.16
		30.63
		30.37
		28.96
		24.97
		24.43
		22.69
$(2^B, 2^F, 2^F)$		14.60

(b) Three-component Bose-Fermi mixtures.

**Table II.4:** Symmetry classes  $\Gamma$  and corresponding ground-state energy slopes  $K(\Gamma)$  for two- (II.4a) and three- (II.4b) component Bose-Fermi mixtures. In table II.4b, the black diagrams are common to both mixtures, whereas the blue (resp. red) diagrams are specifically associated to  $(2^B, 2^B, 2^F)$  (resp.  $(2^B, 2^F, 2^F)$ ). These results were published in [Decamp 2017].

Bose-Fermi mixtures display much more complex symmetry structures than their two-component counterparts. Indeed, mixtures of the type  $(N_1^B, N_1^F)$  have only two possible conjugate irreps associated with  $\Gamma = [N_1^B, 1, \dots, 1]$  and  $\Gamma = [N_1^B + 1, 1, \dots, 1]$  [Fang 2011]. Besides, the  $K(\Gamma)$  depend only on  $\Gamma$  and are independent of the mixture, which shows the fundamental importance of symmetries in our system.

Moreover, we are able to compare energy levels that goes beyond the scope of LMT II and that are not comparable by the dominance order  $\succ$  and the pouring principle. Indeed, we observe in Fig. II.2.1 and table II.4 that, although that the symmetry classes  $[4, 1, 1]$  (resp.  $[3, 1, 1, 1]$ ) are not comparable with  $[3, 3]$  (resp.  $[2, 2, 2]$ ) by the dominance order  $\succ$  (c.f. Fig II.2.2), we have proved:

$$K([3, 3]) > K([4, 1, 1]) \quad \text{and} \quad K([2, 2, 2]) > K([3, 1, 1, 1]). \quad (\text{II.2.46})$$

This ordering was also obtained for fermionic mixtures using Bethe ansatz equations in the homogeneous case and local density approximation in the harmonic trap [Pan 2017].

Interestingly, the two pairs of irreps that are not comparable by the dominance order are also the ones who have identical transposition central characters  $\omega_\Gamma^{[(2)]}$  (c.f. table II.3). Moreover, we observe that:

$$\Gamma \succ \Gamma' \quad \Leftrightarrow \quad \omega_\Gamma^{[(2)]} < \omega_{\Gamma'}^{[(2)]} \quad (\text{II.2.47})$$

This suggests that a profound analysis of the central characters would allow to predict the energy ordering beyond LMT II. The idea would be to define an order " $\triangleright$ " on the set of  $\omega_\Gamma^{[\Lambda]}$ 's that would, unlike  $\succ$ , be a *total order*. For the moment, we only have conjectures of the type of Eq. (II.2.47). A deeper analysis, using the full power of representation theory, is required and in progress.

Let us conclude this section by two remarks: first, the *a priori* knowledge of the irrep  $D_\Gamma$  of the ground-state of our system is extremely valuable information in terms of practical computing. Indeed, the dimension  $\dim D_\Gamma$  of this irrep is much lesser than the dimension of the total space, which implies faster and less memory-expensive programs [Nataf 2014, Nataf 2016, Wan 2017]. Second, although our analysis is done in the fermionized limit  $g_{1D} \rightarrow \infty$ , there are good reasons to think that the energy ordering is the same for all  $0 < g_{1D} < \infty$ . Indeed, since the degeneracies of  $\hat{H}$  are equal to the dimensions of the irreps of its symmetry group (c.f. section II.1.1.2), there are no energy level crossings unless there is an additional symmetry for a certain value of  $g_{1D}$  [Harshman 2014], which is unlikely (but would require however a rigorous proof).





# CHAPTER III

---

## One-body correlations. Tan's contact

### Contents

---

<b>III.1 One-body correlations</b> .....	<b>74</b>
III.1.1 Generalities .....	74
III.1.1.1 Definitions .....	74
III.1.1.2 Experimental probes .....	76
III.1.2 Exact one-body correlations for strongly repulsive systems . . .	77
III.1.2.1 A formula for the one-body density matrix .....	77
III.1.2.2 Density profile analysis .....	79
III.1.2.3 Momentum distributions .....	82
<b>III.2 Short-range correlations: Tan's contact</b> .....	<b>84</b>
III.2.1 Introduction .....	85
III.2.1.1 Brief historical review .....	85
III.2.1.2 Asymptotic behavior of the momentum distributions in one-dimensional quantum gases .....	85
III.2.1.3 Tan sweep theorem .....	87
III.2.2 Exact results in the fermionized limit .....	88
III.2.2.1 Exact contact from the perturbative ansatz .....	88
III.2.2.2 Discussion: Tan's contact as a symmetry probe . . . .	90
III.2.3 Scaling laws for Tan's contact .....	90
III.2.3.1 Contact at finite interaction strength .....	90
III.2.3.2 Contact at finite temperature .....	95
III.2.3.3 Influence of the transverse confinement .....	99

---

Correlation functions are extremely important quantities in many-body quantum physics: Usually easier to compute than the total wave functions, they are involved in the characterization of many exotic properties of quantum matter, ranging for the celebrated Bose-Einstein condensation to the quasi-long range order in one dimension. Moreover, they can be extracted in a typical ultracold atom experiment.

In this chapter, we focus on the properties of the first order correlation functions, from which a large number of properties of the system can be deduced. In particular, we analyze what are the effects of the strong interactions and of the permutational symmetry that we have characterized in chapter II. The leitmotiv of this study is the following: How to extract uniquely the symmetry of the system from a measure of the one-body correlation? In section III.1, we analyze in detail the exact density and momentum profiles of few body strongly interacting quantum mixtures from the exact solution computed in chapter I, trying to extract some general features. Then, in section III.2, we focus on the so-called *Tan's contact*, a quantity that governs the high-momentum behavior and has become a pivot in the study of short-range interacting quantum gases, showing especially that it allows to answer this chapter's main question. Furthermore, in order to be the more experimentally relevant as possible, we derive Tan's contact dependences on the interaction strength, temperature, and transverse confinement.

## III.1. One-body correlations

In this section, we discuss the properties of the one-body correlations in strongly repulsive one-dimensional quantum mixtures. After theoretically defining this quantity and recalling the experimental ways that are used in order to measure it in cold atom set ups in III.1.1, we will then explain in III.1.2 how we obtained it from the exact solutions computed in section I.2. In particular, we compute and analyze the density profiles and momentum distributions of  $N = 6$  mixtures, focusing on the effects of strong interactions and symmetries.

### III.1.1. Generalities

#### III.1.1.1. Definitions

The notion of correlation was first introduced in the mathematical theory of statistics [Feller 1947]. Intuitively, given several random/statistical variables, it allows to measure how these variables are linked together on average. This notion is extensively used in many areas of science, ranging from financial analysis and sociology to optics and statistical physics. In the latter, the universal behaviors of correlation functions in the vicinity of critical points are at the heart of the theory of phase transitions.

In quantum physics, which is an intrinsically probabilistic theory, quantum correlation functions have proven to be a very efficient theoretical tool. They are for example exten-

sively used in quantum field theories<sup>1</sup>, where the Feynman paradigm of path integrals and Feynman diagrams have proven to be a very efficient computational tool.

Now, let us give some general definitions. Suppose that a one-dimensional quantum system is described, in the second quantization formalism, by quantum field creation and annihilation operators  $\hat{\Psi}^\dagger(x)$  and  $\hat{\Psi}(x)$  (respectively), where  $x$  is the spatial coordinate. Then, the *first order* correlation function  $G^{(1)}$ , also called *one-body density matrix* or *one-point correlators*, is defined as [Pitaevskii 2016]:

$$G^{(1)}(x, x') = \langle \hat{\Psi}^\dagger(x) \hat{\Psi}(x') \rangle. \quad (\text{III.1.1})$$

If the system can be described by a normalized  $N$ -particle many-body wave function  $\Psi(x_1, \dots, x_N)$ , the first quantization analogue of Eq. (III.1.1) is

$$G^{(1)}(x, x') = N \int dx_2 \dots x_N \Psi^*(x, x_2, \dots, x_N) \Psi(x', x_2, \dots, x_N). \quad (\text{III.1.2})$$

In a similar way we can define the second order correlation function as

$$G^{(2)}(x, x') = \langle \hat{\Psi}^\dagger(x) \hat{\Psi}^\dagger(x') \hat{\Psi}(x) \hat{\Psi}(x') \rangle, \quad (\text{III.1.3})$$

and so on.

A lot of information can be obtained just from  $G^{(1)}$ . The diagonal part  $n(x)$  of  $G^{(1)}$  is the *density profile* and is associated with the probability (normalized to  $N$ ) of finding a particle at point  $x$ :

$$n(x) = G^{(1)}(x, x) = N \int dx_2 \dots x_N |\Psi(x, x_2, \dots, x_N)|^2. \quad (\text{III.1.4})$$

The off-diagonal part of  $G^{(1)}$  can be related to the *momentum distribution*  $n(k)$ , associated with the probability of having a particle with a momentum  $k$ , by the following formula:

$$\begin{aligned} n(k) &= \langle \hat{\Psi}^\dagger(k) \hat{\Psi}(k) \rangle \\ &= \frac{1}{2\pi} \iint dx dx' G^{(1)}(x, x') e^{-\frac{i}{\hbar} k(x-x')}, \end{aligned} \quad (\text{III.1.5})$$

which is simply due to  $\hat{\Psi}(k) = \frac{1}{2\pi} \int dx \hat{\Psi}(x) e^{-\frac{i}{\hbar} kx}$ . Note that we have

$$\int dx n(x) = \int dk n(k) = N. \quad (\text{III.1.6})$$

Notice also that we can extract the total kinetic energy  $E_K$  from the momentum distribution by

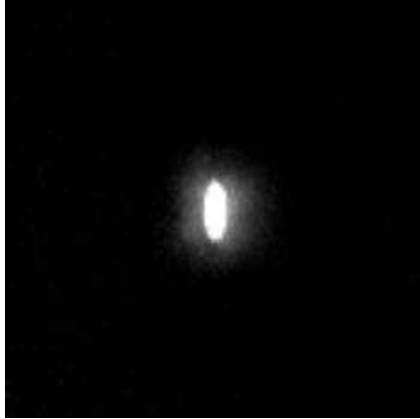
$$E_K = \int dk \frac{k^2}{2} n(k), \quad (\text{III.1.7})$$

which is convergent only if we have

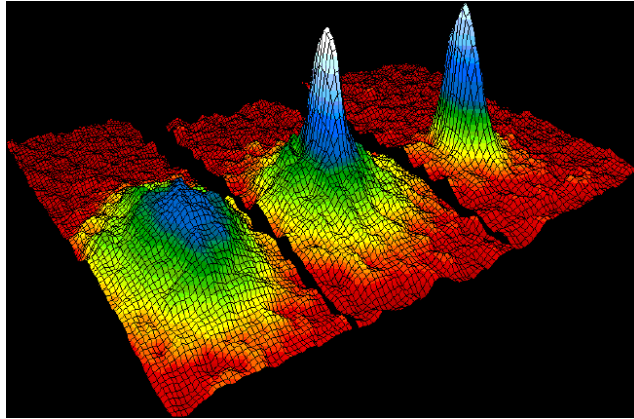
$$n(k) = \underset{k \rightarrow \infty}{o} \left( \frac{1}{k^3} \right). \quad (\text{III.1.8})$$

---

<sup>1</sup>In this context, correlation functions are sometimes called "Green functions", which must not be confused with the Green functions defined in functional analysis as the inverses of differential operators!



(a) Image obtained by absorption imaging of a Bose-Einstein condensate of Rubidium atoms (courtesy of Guillaume Labeyrie).



(b) Momentum distributions obtained by TOF and absorption imaging on a Rubidium gas. The two images on the right correspond to a Bose-Einstein condensate. From [Anderson 1995].

**Figure III.1.1:** Absorption imaging of Bose-Einstein condensates of Rubidium atoms.

We will see in section III.2 that in fact  $n(k) \sim \mathcal{C}/k^4$ . This asymptotic behavior for  $n(k)$  is associated with the *short-range* correlations of the system. Conversely, the asymptotic behavior  $|x - y| \rightarrow \infty$  of  $G^{(1)}(x, y)$  is associated with the *long-range order*. It can serve as a characterization of the coherence properties of the system, and e.g. intervenes in the definition of a Bose-Einstein condensate [Penrose 1956, Yang 1962]. Since it is equivalent to the low-momentum properties, it is well described by the Luttinger liquid theory and the bosonization method that we briefly mentioned in section I.1.1. In this thesis, we focus more on the short-range properties, which go beyond the scope of Luttinger paradigm.

### III.1.1.2. Experimental probes

Not only correlation functions have a great theoretical importance and are often easier to calculate than the total wave functions, they also happen to be very efficiently measurable in cold atoms experiments [Bloch 2008, Cazalilla 2011].

The main method to measure the density profile of an atomic cloud is the *in-situ* absorption imaging. It basically consists in measuring the absorbed light with a CCD camera when the cloud is submitted to a resonant laser beam. Examples of images obtained with this method are given in Fig. III.1.1.

The usual way of measuring the momentum distribution  $n(\vec{p})$  is called the *time-of-flight* (TOF) technique. The idea is to suddenly release the trapping potential, and to measure with absorption imaging the density profile  $n_{TOF}(\vec{r}, \tau)$  after a time  $\tau \gg mL^2/\hbar$ , where  $L$  is the linear size of the cloud before switching off the trap. If interactions can be safely neglected during the expansion so that it can be considered as ballistic, the momentum distribution in the trap  $n(\vec{p})$  can be related to  $n_{TOF}(\vec{r}, \tau)$  by the simple formula:

$$n_{TOF}(\vec{r}, \tau) = \left(\frac{m}{\hbar\tau}\right)^3 n(\vec{p}(\vec{r})), \quad (\text{III.1.9})$$

where  $\vec{p}(\vec{r}) = m\vec{r}/\hbar\tau$ . For example, in the case of a Bose-Einstein condensate, the

absorption image after a TOF will display a typical central peak (see Fig III.1.1b).

### III.1.2. Exact one-body correlations for strongly repulsive systems

#### III.1.2.1. A formula for the one-body density matrix

In this section we provide an expression we have obtained for the one-body density matrix  $G^{(1)}(x, x')$  for the strongly interacting limit  $g_{1D} \rightarrow +\infty$  of our model, using the notations of section I.2.2.2. This is the formula we used in order to plot the exact density profiles and exact momentum distributions in [Decamp 2016a, Decamp 2016b, Decamp 2017]. Here we will use units of  $a_0 = \sqrt{\hbar/m\omega}$  for length and  $\hbar\omega$  for energy.

Suppose that our system is of the form  $(N_1, \dots, N_\kappa)$  and that we want, for a given solution and thus a given vector  $\vec{a}$  of size  $N!$ , and for a given spin-component  $\sigma \in \{1, \dots, \kappa\}$ , to compute the associated one-body density matrix:

$$G_\sigma^{(1)}(x, x') = N_\sigma \int dx_2 \dots dx_N \Psi^*(x, x_2, \dots, x_N) \Psi(x', x_2, \dots, x_N), \quad (\text{III.1.10})$$

where "particle 1" belongs to component  $\sigma$ ,  $\Psi$  is given by Eq. (I.2.16) and we have normalized  $G_\sigma^{(1)}(x, x')$  to  $N_\sigma$  so that the total one-body density verifies

$$G^{(1)}(x, x') = \sum_{\sigma=1}^{\kappa} G_\sigma^{(1)}(x, x'). \quad (\text{III.1.11})$$

Let us organize the set of permutations  $\mathfrak{S}_N$  in a convenient way: each permutation will be written

$$P_{\{i,k\}}, \quad i \in \{1, \dots, N\}, \quad k \in \{1, \dots, (N-1)!\}, \quad (\text{III.1.12})$$

where  $i$  denotes the position of particle 1 after permutation and  $k$  labels the permutation of the  $N-1$  other particles. With this notation, Eq. (I.2.16) becomes

$$\Psi(x_1, \dots, x_N) = \sum_{i=1}^N \sum_{k=1}^{(N-1)!} a_{\{i,k\}} \theta_{\{i,k\}}(x_1, \dots, x_N) \psi_F(x_1, \dots, x_N), \quad (\text{III.1.13})$$

where  $a_{P_{\{i,k\}}} \equiv a_{\{i,k\}}$  and  $\theta(x_{P_{\{i,k\}}1} < \dots < x_{P_{\{i,k\}}N}) \equiv \theta_{\{i,k\}}(x_1, \dots, x_N)$ .

We can now write  $G_\sigma^{(1)}(x, x')$  by supposing  $x \leq x'$  (which is possible since  $G_\sigma^{(1)}(x, x') = G_\sigma^{(1)}(x', x)$ ) and using Eq. (III.1.13):

$$G_\sigma^{(1)}(x, x') = N_\sigma \sum_{1 \leq i \leq j \leq N} \int dx_2 \dots dx_N \left[ \sum_{k=1}^{(N-1)!} a_{\{i,k\}} \theta_{\{i,k\}}(x, x_2, \dots, x_N) \right. \\ \left. \times \psi_F(x, x_2, \dots, x_N) \right] \left[ \sum_{l=1}^{(N-1)!} a_{\{j,l\}} \theta_{\{j,l\}}(x', x_2, \dots, x_N) \psi_F(x', x_2, \dots, x_N) \right]. \quad (\text{III.1.14})$$

Moreover, remark that

$$\int dx_2 \dots dx_N \theta_{\{i,k\}}(x, x_2, \dots, x_N) \theta_{\{j,l\}}(x', x_2, \dots, x_N) (\dots) \propto \delta_{kl}, \quad (\text{III.1.15})$$

where  $(\dots)$  is an arbitrary function of  $x, x', x_2, \dots, x_N$ . Notice also that the following product

$$\psi_F(x, x_2, \dots, x_N)\psi_F(x', x_2, \dots, x_N), \quad (\text{III.1.16})$$

is symmetric by any permutation of the variables  $x_2, \dots, x_N$ . Therefore, Eq. (III.1.14) becomes:

$$\begin{aligned} G_\sigma^{(1)}(x, x') = & N_\sigma \sum_{1 \leq i \leq j \leq N} C_{ij} \int_{-\infty}^x dx_2 \dots dx_i \int_x^{x'} dx_{i+1} \dots dx_j \\ & \times \int_{x'}^{+\infty} dx_{j+1} \dots dx_N \psi_F(x, x_2, \dots, x_N) \psi_F(x', x_2, \dots, x_N), \end{aligned} \quad (\text{III.1.17})$$

where

$$C_{ij} = \frac{1}{(i-1)!(j-i)!(N-j)!} \sum_{k=1}^{(N-1)!} a_{\{i,k\}} a_{\{j,k\}}. \quad (\text{III.1.18})$$

The last step is to use again the Vandermonde trick that we used in order to obtain the exchange coefficient  $\alpha_k$  (Eq. (I.2.26))<sup>2</sup>. More precisely, by noticing the Vandermonde determinant expression in Eq. (I.2.23), we get:

$$\begin{aligned} \psi_F(x, x_2, \dots, x_N) &= \frac{1}{\sqrt{N!} \prod_{m=0}^{N-1} 2^{-m} \sqrt{\pi m!}} \prod_{k=2}^N e^{-x_k^2/2} \prod_{2 \leq j < k \leq N} (x_j - x_k) \prod_{l=2}^N (x_l - x) e^{-x^2/2} \\ &= \frac{2^{(N-1)/2}}{\sqrt{\pi} N! (N-1)!} \begin{vmatrix} \phi_0(x_2) & \dots & \phi_{N-2}(x_2) \\ \vdots & \ddots & \vdots \\ \phi_0(x_N) & \dots & \phi_{N-2}(x_N) \end{vmatrix} \prod_{l=2}^N (x_l - x) e^{-x^2/2} \\ &= \frac{2^{(N-1)/2}}{\sqrt{\pi} N! (N-1)!} \sum_{P \in \mathfrak{S}_{N-1}} \epsilon(P) \prod_{l=2}^N \phi_{P(l)-2}(x_l) (x_l - x) e^{-x^2/2}. \end{aligned} \quad (\text{III.1.19})$$

Finally, by putting this expression for  $\psi_F$  into Eq. (III.1.17), we get

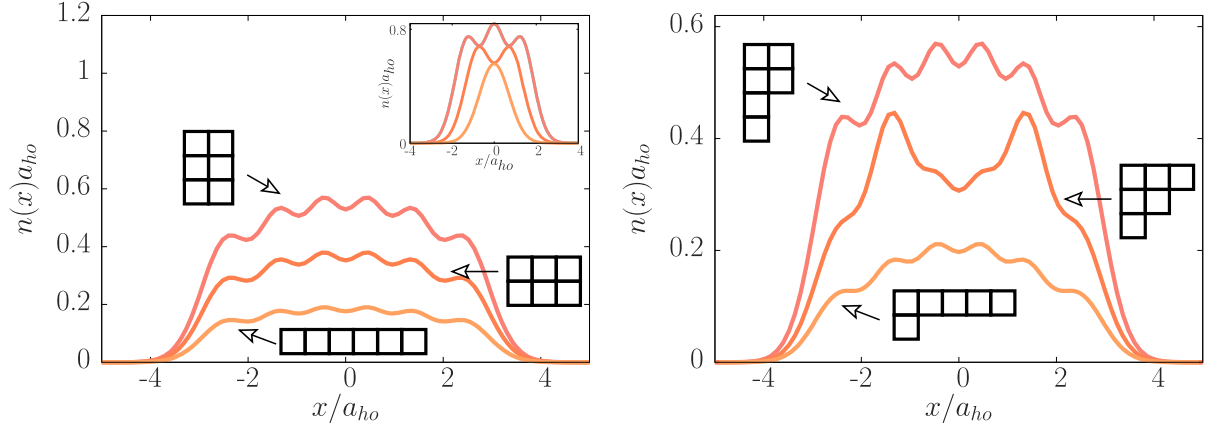
$$\begin{aligned} G_\sigma^{(1)}(x, x') = & N_\sigma \frac{2^{(N-1)/2}}{\sqrt{\pi} N! (N-1)!} \sum_{1 \leq i \leq j \leq N} C_{ij} \sum_{P, Q \in \mathfrak{S}_{N-1}} \epsilon(P) \epsilon(Q) \\ & \times \prod_{l=2}^N \int_{L_{ij}(l)}^{U_{ij}(l)} dz (z - x)(z - x') \phi_{P(l)-2}(z) \phi_{Q(l)-2}(z), \end{aligned} \quad (\text{III.1.20})$$

with the integration limits given by

$$(L_{ij}(l), U_{ij}(l)) = \begin{cases} (-\infty, x) & \text{if } l \leq i \\ (x, x') & \text{if } i < l \leq j \\ (x', +\infty) & \text{if } l > j \end{cases}. \quad (\text{III.1.21})$$

I implemented Eq. (III.1.20) in a *Mathematica* program, that runs typically 20 minutes for  $N = 6$  systems. Notice that it has a complexity of  $O(N^2((N-1)!)^2)$ , so that  $N > 6$  systems are very time-consuming.

<sup>2</sup>This idea was suggested by Matteo Rizzi, and allows to consider sums over  $\mathfrak{S}_{N-1}$  instead of  $\mathfrak{S}_N$ .



**Figure III.1.2:** Ground state (left panel) and first excited state with a different symmetry (right panel) density profiles in units of  $a_{ho}^{-1} = \sqrt{m\omega/\hbar}$  for three strongly interacting balanced mixtures of  $N = 6$  fermions, normalized to the number  $N/\kappa$  of particles in each spin-component (from top to bottom:  $\kappa = 2, 3, 6$ ). For a given balanced mixture, the  $\kappa$  spin-components have the same density profile. The corresponding symmetries  $Y_{\Gamma}$  that were determined in chapter II are associated with each profile. In order to observe the effects of fermionization, the density profiles of the same mixtures in the non-interacting cases are shown in the insets. From [Decamp 2016a].

### III.1.2.2. Density profile analysis

Let us now analyze exact density profiles  $n(x) = G^{(1)}(x, x)$  obtained from Eq. (III.1.20) for quantum mixtures with  $N = 6$  atoms. Results for purely fermionic mixtures were published in [Decamp 2016a], and for Bose-Fermi mixtures in [Decamp 2017]. Density profiles for the ground state and first excited with a different symmetry than the ground state of balanced (respectively imbalanced) fermionic mixtures are given in Fig. III.1.2 and III.1.3. Ground state density profiles of Bose-Fermi mixtures are given in Fig. III.1.4.

## Discussion

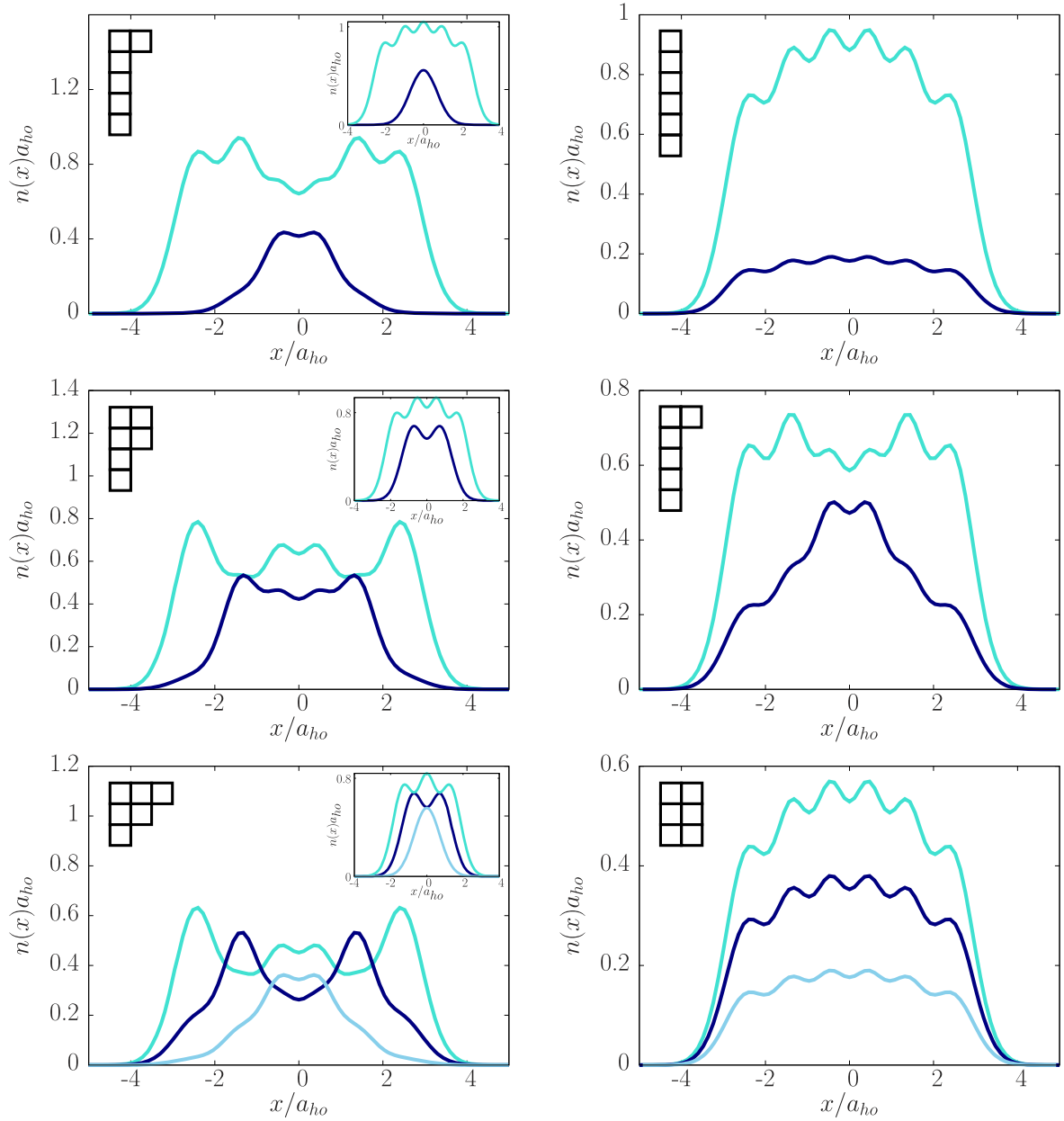
A first observation is that the total density profiles, defined by

$$n(x) = \sum_{\sigma=1}^{\kappa} n_{\sigma}(x), \quad (\text{III.1.22})$$

are always equal, for the ground state, to the density profile of  $N$  spinless fermions (see also Eq. (I.2.12)):

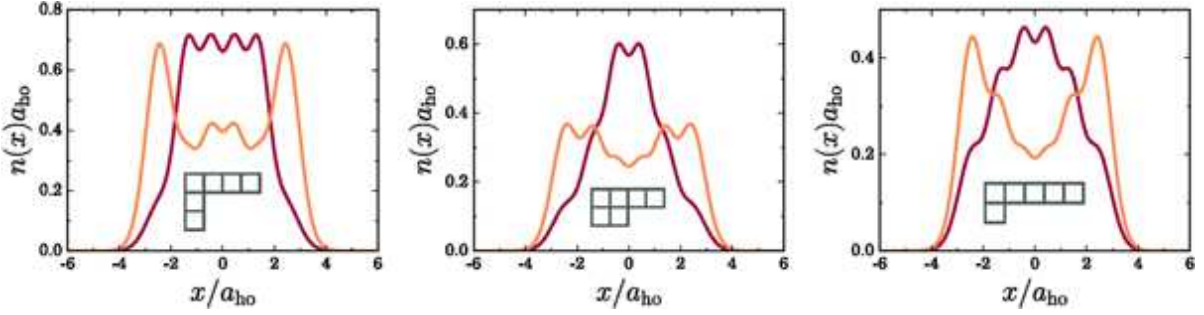
$$\begin{aligned} n_F(x) &= N \int dx_2 \dots dx_N \Psi_F(x, x_2, \dots, x_N)^2 \\ &= \frac{1}{\sqrt{\pi a_0}} \sum_{k=0}^{N-1} \frac{1}{2^k k!} H_k^2(x/a_0) e^{-(x/a_0)^2}, \end{aligned} \quad (\text{III.1.23})$$

characterized by a global parabolic shape and  $N$  small density oscillations [Vignolo 2000, Kolomeisky 2000]. This observation, that was also reported in [Grining 2015a], is a



**Figure III.1.3:** Ground state (left panel) and first excited state with a different symmetry (right panel) density profiles in units of  $a_{ho}^{-1} = \sqrt{m\omega/\hbar}$  for three strongly interacting imbalanced mixtures of  $N = 6$  fermions, normalized to the number  $N_\sigma$  of particles in the corresponding spin-component (from top to bottom:  $(5^F, 1^F)$ ,  $(4^F, 2^F)$ ,  $(3^F, 2^F, 1^F)$ ). The corresponding symmetries  $Y_\Gamma$  that were determined in chapter II are associated with each panel. In order to observe the effects of fermionization, the density profiles of the same mixtures in the non-interacting cases are shown in the insets. From [Decamp 2016a].





**Figure III.1.4:** Ground state density profiles in units of  $a_{ho}^{-1} = \sqrt{m\omega/\hbar}$  for three strongly interacting Bose-Fermi mixtures of  $N = 6$  particles, normalized to the number  $N_\sigma$  of particles in the corresponding spin-component (from left to right:  $(3^B, 3^F)$ ,  $(2^B, 2^F, 2^F)$ ,  $(2^B, 2^B, 2^F)$ ). For a given mixture, spin-components with the same number of particles and same statistics have the same density profile. The corresponding symmetries  $Y_\Gamma$  that were determined in chapter II are associated with each panel. From [Decamp 2017].

generalization of the equivalence between the density profiles of a bosonic Tonks gas and a spinless Fermi gas. Consequently, if the mixture is decomposed in  $\kappa$  species with equal number of particles per spin-component, the ground-state density profile for every spin-component  $\sigma$  will verify

$$n_\sigma(x) = \frac{1}{\kappa} n_F(x), \quad (\text{III.1.24})$$

as we can observe in the left panel Fig. III.1.2.

Interestingly, as one can see in the right panel of Fig. III.1.2, it is no longer true in general when considering the total density profile of excited states. Instead, we observe that the excited state of  $(2^F, 2^F, 2^F)$ , which belongs to the  $\Gamma = [3, 2, 1]$  symmetry class, has the same density profile as the ground state density profile of the two-particle component of  $(3^F, 2^F, 1^F)$  (c.f. Fig III.1.3), which belongs to the same symmetry class. Conversely, the excited states of  $(5^F, 1^F)$ ,  $(4^F, 2^F)$  and  $(3^F, 2^F, 1^F)$ , which belong respectively to the  $[1, 1, 1, 1, 1, 1]$ ,  $[2, 1, 1, 1, 1]$  and  $[2, 2, 2]$  symmetry classes, have similar density profiles than the ground state density profiles of  $(6^F)$ ,  $(5^F, 1^F)$  and  $(3^F, 3^F)$  (respectively). Remark however that the excited state of  $(3^F, 3^F)$ , with symmetry class  $\Gamma = [2, 2, 1, 1]$ , has not the same density profile as the ground state of  $(4^F, 2^F)$ .

The ground state density profiles of imbalanced fermionic mixtures (right panel of Fig III.1.3) and balanced Bose-Fermi mixtures (Fig. III.1.4) have a more complex structure than in the balanced fermionic case. In the cases  $(5^F, 1^F)$  of a polaron and of Bose-Fermi mixtures, we observe a partial spatial separation between the polaron (respectively bosonic component(s)) in the center of the trap and the majority component (respectively fermionic component) pushed toward the edges. This spatial separation for Bose-Fermi mixtures was predicted by Luttinger theory for homogeneous systems [Cazalilla 2003] and by local density approximation [Imambekov 2006a, Imambekov 2006b], and exact diagonalization [Deuretzbacher 2017] for harmonically trapped systems. It was also obtained in [Dehkharghani 2017] by a similar method and DMRG simulations. In the cases of  $(4^F, 2^F)$  and  $(3^F, 2^F, 1^F)$ , the spatial separation of the ground state density profiles is even more complex. In the first case, the system displays an alternance between the two components. This can be seen as a realization of an antiferromagnet [Murmam 2015].

In the imbalanced three-component system, the density profiles are similar to the ones corresponding to the same number of particles in  $(4^F, 2^F)$  and  $(5^F, 1^F)$ .

In any case, the shape of the density profiles can be seen as a consequence of two complementary phenomena. First, by looking at the insets of Fig. III.1.2 and Fig III.1.3, and remembering that the density profile of non-interacting bosons is just a simple central peak, we clearly see the effect of fermionization. Indeed, particles that are not subjected to the Pauli principle (like identical bosons or fermions of different spin-components) tend to be pushed away in different peaks because of the strong repulsion between them. Second, from the spatial separation discussed in the last paragraph, we observe that particles subjected to the Pauli principle, that is fermions belonging to the same spin-component, tend to avoid each other. This can be intuitively understood by analyzing the form of Eq. (I.2.21), that we recall here:

$$K = \sum_{P,Q \in \mathfrak{S}_N} (a_P - a_Q)^2 \alpha_{P,Q}, \quad (\text{III.1.25})$$

where  $\alpha_{P,Q} = \alpha_k$  are the nearest-neighbor exchange constants between particles at positions  $k$  and  $k + 1$ . Recalling that in the perturbative ansatz we used (section I.2.2.2), the ground-state configuration is associated with the maximum value for  $K$ , and noting that an anti-symmetric exchange corresponds to a zero contribution in Eq. (III.1.25), we can enunciate the following rule:

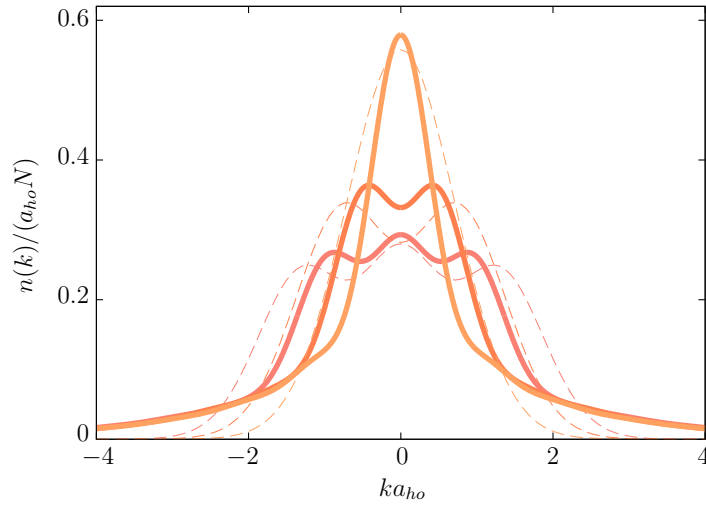
*The spatial configuration of strongly interacting one-dimensional quantum mixtures is such that the number of anti-symmetric exchanges between nearest-neighbors is minimized. In particular, for the ground-state, the Lieb-Mattis theorem implies that these anti-symmetric exchanges only occur between fermions belonging to the same spin-component.*

This fact, together with the parity symmetry of the trap and the fact that the sum of the density profiles is  $n_F(x)$ , allows to qualitatively predict the shape of the ground-state density profiles.

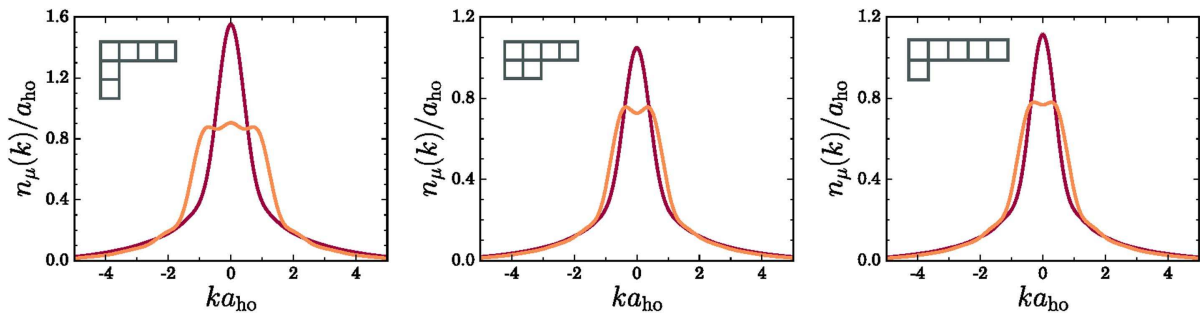
To conclude this discussion, we have seen that the spatial symmetries investigated in chapter II allow to understand qualitative effects on the shape of the density profiles. We stress, however, that this correspondence is not unequivocal: different symmetry classes can be associated with the same spatial distribution. Thus, the knowledge of the density profile, *e.g.* by an absorption imaging in a cold atom experiment, does not allow to deduce the symmetry class of the system.

### III.1.2.3. Momentum distributions

Let us study the momentum distributions  $n_\sigma(k) = \frac{1}{2\pi} \iint dx dx' G_\sigma^{(1)}(x, x') e^{-\frac{i}{\hbar} k(x-x')}$ , where  $G_\sigma^{(1)}$  is as defined in Eq. (III.1.10). Results for  $N = 6$  fermionic (resp. Bose-Fermi) mixtures were published in [Decamp 2016b] (resp. [Decamp 2017]). The corresponding momentum distributions are respectively shown in Fig. III.1.5 and Fig. III.1.6. Here, we discuss the general qualitative aspects of the momentum distributions — the asymptotic behaviors will be studied in much details in section III.2.



**Figure III.1.5:** Ground state momentum distributions  $n(k) = \kappa n_\sigma(k)$  in units of  $a_{ho} = \sqrt{\hbar/m\omega}$  for three strongly interacting balanced mixtures of  $N = 6$  fermions, normalized to unity (solid lines,  $\kappa = 2, 3, 6$ ). For a given balanced mixture, the  $\kappa$  spin-components have the same momentum distributions. In order to observe the effects of fermionization, the momentum distributions of the same mixtures in the non-interacting cases are shown in dashed lines.



**Figure III.1.6:** Ground state momentum distributions  $n_\mu(k)$  in units of  $a_{ho} = \sqrt{\hbar/m\omega}$  for three strongly interacting Bose-Fermi mixtures of  $N = 6$  particles, normalized to the number  $N_\mu$  of particles in the corresponding spin-component (from left to right:  $(3^B, 3^F)$ ,  $(2^B, 2^F, 2^F)$ ,  $(2^B, 2^B, 2^F)$ ). For a given mixture, spin-components with the same number of particles and same statistics have the same momentum distributions. The corresponding symmetries  $Y_\Gamma$  that were determined in chapter II are associated with each panel. From [Decamp 2017].

## Discussion

It is a well known fact that the momentum distribution  $n_F(k)$  of harmonically trapped spinless non-interacting fermions is equal to its density profile  $n_F(x)$  (Eq. (III.1.23)) and is characterized by  $N$  peaks [Vignolo 2000]. This is a consequence of the duality between  $x$  and  $k$  in the harmonic oscillator Hamiltonian. On the contrary, the momentum distribution  $n_B(k)$  of a Tonks gas is characterized by a single central peak at  $k=0$  [Papenbrock 2003], showing in passing the limits of the Bose-Fermi mapping discussed in section I.2.1.

In our systems, we observe in Fig. III.1.6 that the bosonic components in Bose-Fermi mixtures always display one central peak, while the fermionic components have a number of peaks equal to the number of fermions in the considered species, as also observed in [Deuretzbacher 2016]. In particular, the momentum distribution of the ground state of  $(1^F, 1^F, 1^F, 1^F, 1^F, 1^F)$  is equal to  $n_B(k)$  (Fig. III.1.5). Thus, similarly to what we discussed for the density profiles, the exchange symmetry and the Pauli principle allow to predict qualitative effects on the momentum distributions of strongly interacting one-dimensional quantum mixtures. Here again, however, different exchange symmetries can have similar distributions.

The effect of interactions on momentum distributions is more subtle than on the spatial distributions, as one can observe in Fig. III.1.5. Indeed, the global structure is similar, with the fermionized momentum distributions displaying the same number of peaks as the non-interacting ones. We observe however a significant reduction of width of these peaks, which is dual to the broadening of the density profiles observed in section III.1.2.2. Moreover, complementary to this reduction, the large momentum tails are enhanced by interactions. The quantitative analysis of these asymptotic behaviors is the subject of section III.2.

## III.2. Short-range correlations: Tan's contact

This section is devoted to study of *Tan's contact*, a quantity that governs the large  $k$  behavior of the momentum distributions  $n(k)$ , or equivalently the short-range correlations, and therefore goes beyond the Luttinger liquid theory paradigm. After defining this quantity for one-dimensional quantum gases and showing how it is universally related to thermodynamic variables of the system in III.2.1, we will study its properties in fermionized one-dimensional mixtures in III.2.2. We will argue, in particular, that Tan's contact is an indicator of the symmetry class of the system. Finally, in III.2.3, in order to be relevant for actual experiments, we will derive a set of universal scaling laws as functions of interaction, temperature, and the transverse confinement.

### III.2.1. Introduction

#### III.2.1.1. Brief historical review

In systems interacting via a  $\delta$ -potential, the momentum distributions  $n(k)$  display the following asymptotic algebraic behavior:

$$n(k) \underset{k \rightarrow \infty}{\sim} \mathcal{C}k^{-4}, \quad (\text{III.2.1})$$

where  $\mathcal{C}$  is called the *contact*, or *Tan's contact*. Historically, this behavior was initially highlighted for one-dimensional bosonic Tonks gases in [Minguzzi 2002], and for any value of the interaction strength in [Olshanii 2003]. In three-dimensional systems of spin- $\frac{1}{2}$  fermions, Tan has also shown that  $\mathcal{C}$  is related to thermodynamic quantities of the system — the so-called *Tan relations* — such as the dependence of the energy on the scattering length, the quantum pressure or the static structure factor [Tan 2008a, Tan 2008c, Tan 2008b] (see also [Braaten 2008b, Braaten 2008a, Zhang 2009, Combescot 2009]). These results were then extended to two-dimensional [Werner 2012b, Valiente 2011, Valiente 2012] and one-dimensional [Barth 2011] spin- $\frac{1}{2}$  gases, and to arbitrary quantum mixtures in two and three dimensions [Werner 2012a], and in one dimension [Pătu 2017].

On the experimental side, Tan's contact measurements were performed in three-dimensional strongly interacting fermionic and bosonic ultracold gases, by a direct TOF [Stewart 2010, Chang 2016], or indirectly by *rf spectroscopy* [Stewart 2010, Wild 2012, Sagi 2012] (exploiting the relation between the contact and the fraction of atoms in a given unoccupied state when applying large frequency pulses [Pieri 2009, Braaten 2008a]) or making use of *Bragg spectroscopy* [Kuhnle 2011, Hoinka 2013] (exploiting the relation between the contact and the structure factor). A precise measurement of Tan's contact in one-dimension remains an experimental challenge because of the enhanced fluctuations at large momenta. However, metastable Helium, which allows extremely precise correlation detections (see *e.g.* [Keller 2014]), appears to be a promising candidate.

#### III.2.1.2. Asymptotic behavior of the momentum distributions in one-dimensional quantum gases

We now proceed to re-derive Eq. (III.2.1) for one-dimensional quantum mixtures, following [Olshanii 2003, Pătu 2017]. Their approach is based on the cusp condition (section I.1.3.3). Other more quantum-field-oriented methods rely on the definition of a *generalized function* [Tan 2008a, Tan 2008c, Tan 2008b], or in a so-called *operator product expansion* [Braaten 2008b, Barth 2011].

We consider a system of  $N$  one-dimensional particles of coordinates  $x_1, \dots, x_N$  of same mass  $m$ , subjected to an arbitrary (continuous) external potential  $V_{ext}$ , and then verifying the following Schrödinger equation:

$$\left( -\frac{\hbar^2}{2m} \sum_{i=1}^N \frac{\partial^2}{\partial x_i^2} + g_{1D} \sum_{i < j} \delta(x_i - x_j) + V_{ext}(x_1, \dots, x_N) - E \right) \psi(x_1, \dots, x_N) = 0. \quad (\text{III.2.2})$$

For the moment, we suppose that these particles are identical bosons.

Defining the reduced coordinates  $X_{ij} = \frac{x_i + x_j}{2}$  and  $x_{ij} = x_i - x_j$  and the reduced masses  $M = 2m$  and  $\mu = m/2$ , the  $N$ -body analogue of Eq. (I.1.34) implies

$$\begin{aligned} \psi(x_1, \dots, x_i, \dots, x_j, \dots, x_N) &\underset{x_i \rightarrow x_j}{=} \psi(x_1, \dots, X_{ij}, \dots, X_{ij}, \dots, x_N) \\ &\times \left[ 1 - \frac{|x_{ij}|}{a_{1D}} + \mathcal{O}(x_{ij}^2) \right], \end{aligned} \quad (\text{III.2.3})$$

where  $a_{1D} = -\hbar^2/\mu g_{1D}$ .

Moreover, we know from Fourier analysis that, for a Lebesgue integrable function  $f(x) = |x - x_0|F(x)$  (with  $F$  a smooth function), we have [Bleistein 2010]:

$$\int dx e^{-ikx} f(x) \underset{k \rightarrow \infty}{=} -\frac{2e^{-ikx_0}}{k^2} + \mathcal{O}\left(\frac{1}{|k|^3}\right). \quad (\text{III.2.4})$$

Then, Eq. (III.2.3) implies

$$\begin{aligned} \int dx_1 e^{-ikx_1} \psi(x_1, x_2, \dots, x_N) &\underset{k \rightarrow \infty}{\sim} \int dx_1 e^{-ikx_1} \sum_{j=2}^N \psi(X_{1j}, \dots, X_{1j}, \dots, x_N) \left[ 1 - \frac{|x_{1j}|}{a_{1D}} \right] \\ &\underset{k \rightarrow \infty}{\sim} \frac{2}{a_{1D}k^2} \sum_{j=2}^N e^{-ikx_j} \psi(x_j, \dots, x_j, \dots, x_N), \end{aligned} \quad (\text{III.2.5})$$

where we have removed one of the terms using the fact that the Fourier transform of a differentiable function with continuous derivative falls to 0 as  $o\left(\frac{1}{k^2}\right)$  when  $k \rightarrow \infty$  [Bracewell 1999]. Therefore, using  $n(k)$ 's definition (Eq. (III.1.5)), we find

$$\begin{aligned} n(k) &\underset{k \rightarrow \infty}{\sim} \frac{2N}{\pi a_{1D}^2 k^4} \int dx_2 \dots x_N \sum_{2 \leq j \leq l \leq N} e^{-k(x_j - x_l)} \psi(x_j, \dots, x_j, \dots, x_N) \psi(x_l, \dots, x_l, \dots, x_N) \\ &\underset{k \rightarrow \infty}{\sim} \frac{2N}{\pi a_{1D}^2 k^4} \sum_{j=2}^N \int dx_2 \dots x_N \psi(x_j, \dots, x_j, \dots, x_N)^2, \end{aligned} \quad (\text{III.2.6})$$

where again we have neglected the off-diagonal terms because of the smoothness of the integrand.

Furthermore, the first-quantized version of  $G^{(2)}(x, x')$  (c.f. Eq. (III.1.3)) can be written

$$G^{(2)}(x, x') = \int dx_1 \dots dx_N \psi(x_1, \dots, x_N)^2 \sum_{i \neq j} \delta(x - x_i) \delta(x' - x_j). \quad (\text{III.2.7})$$

Thus, exploiting the permutational symmetry of the integrand, Eq. (III.2.6) implies Eq. (III.2.1) with

$$\mathcal{C} = \frac{2}{\pi a_{1D}^2} \int dx G^{(2)}(x, x). \quad (\text{III.2.8})$$

With this definition, we see that the contact can be interpreted as a measure of the probability of finding two particles in the same region of space.

The generalization to the  $\kappa$ -component case is straightforward, by restricting the summations on specific components rather than summing over all the  $N$  particles. More explicitly, for two spin-components  $\sigma$  and  $\sigma'$ , we define

$$G_{\sigma\sigma'}^{(2)}(x, x') = \int dx_1 \dots dx_N \psi(x_1, \dots, x_N)^2 \sum_{i \in I_\sigma, j \in I_{\sigma'}, i \neq j} \delta(x - x_i) \delta(x' - x_j), \quad (\text{III.2.9})$$

where  $I_\sigma$  is the subset of  $\{1, \dots, N\}$  associated with particles of type  $\sigma$ . Then, it is easy to prove that

$$n_\sigma(k) \underset{k \rightarrow \infty}{\sim} \mathcal{C}_\sigma k^{-4}, \quad (\text{III.2.10})$$

where we have

$$\mathcal{C}_\sigma = \frac{2}{\pi a_{1D}^2} \int dx \sum_{\sigma'=1}^{\kappa} G_{\sigma\sigma'}^{(2)}(x, x), \quad (\text{III.2.11})$$

which can be seen as a measure of the probability of finding a particle of type  $\sigma$  in the same region of space than another particle. Notice that if  $\sigma$  is a fermionic component, the term in  $\sigma' = \sigma$  cancels out. Moreover, if the mixture is completely balanced, or of it contains only two components, all the contacts are equal. In every case, we can define the *total contact* as:

$$\begin{aligned} \mathcal{C}_{tot} &= \sum_{\sigma}^{\kappa} \mathcal{C}_\sigma \\ &= \frac{2}{\pi a_{1D}^2} \int dx G^{(2)}(x, x). \end{aligned} \quad (\text{III.2.12})$$

### III.2.1.3. Tan sweep theorem

Also known as *Tan adiabatic theorem* in the spin- $\frac{1}{2}$  case, this theorem allows to relate the contact to the derivative of the the energy as a function of the scattering length. It is a simple consequence of the Hellmann-Feynman theorem [Feynman 1939]. More precisely, we have:

$$\begin{aligned} \frac{\partial E}{\partial a_{1D}} &= \frac{2\hbar^2}{ma_{1D}^2} \int dx_1 \dots dx_N \psi(x_1, \dots, x_N)^2 \sum_{i < j} \delta(x_i - x_j) \\ &= \frac{\hbar^2}{ma_{1D}^2} \int dx G^{(2)}(x, x), \end{aligned} \quad (\text{III.2.13})$$

and therefore, using the definition of the total contact (Eq. (III.2.12)), we obtain

$$\frac{\partial E}{\partial a_{1D}} = \frac{\pi\hbar^2}{2m} \mathcal{C}_{tot}. \quad (\text{III.2.14})$$

In order to write the equivalent of Eq. (III.2.14) for  $\mathcal{C}_\sigma$ , we have to modify the definition of our interaction potential, by writing  $a_{1D}\delta(x_i - x_j) \equiv a_{\sigma\sigma'}\delta(x_i - x_j)$  when either  $(i, j)$  or  $(j, i)$  is in  $I_\sigma \times I_{\sigma'}$ . Then, the Hellmann-Feynman theorem implies

$$\frac{\partial E}{\partial a_{\sigma\sigma'}} = \frac{2\hbar^2}{ma_{\sigma\sigma'}^2(1 + \delta_{\sigma\sigma'})} \int dx G_{\sigma\sigma'}^{(2)}(x, x), \quad (\text{III.2.15})$$

where  $\delta_{\sigma\sigma'}$  is the Kronecker symbol, and therefore

$$\mathcal{C}_\sigma = \frac{m}{\pi\hbar^2} \sum_{\sigma'=1}^{\kappa} (1 + \delta_{\sigma\sigma'}) \frac{\partial E}{\partial a_{\sigma\sigma'}}. \quad (\text{III.2.16})$$

Note the term in  $\sigma = \sigma'$  is non-zero only in the case where we consider a bosonic component.

## III.2.2. Exact results in the fermionized limit

### III.2.2.1. Exact contact from the perturbative ansatz

Given Eq. (III.2.14), we can relate the total contact in the  $g_{1D} \rightarrow \infty$  limit to the  $K = -\lim_{g_{1D} \rightarrow \infty} \frac{\partial E}{\partial g_{1D}^{-1}}$  parameter that we introduced in the perturbative ansatz (section I.2.2.2) by the simple relation:

$$\mathcal{C}_{tot}(\infty) = \frac{m^2}{\pi\hbar^4} K. \quad (\text{III.2.17})$$

Given a solution, characterized by a vector  $\vec{a}$  of coefficients (c.f. the definition of the ansatz in Eq. (I.2.16) and the relation (I.2.21) between  $K$  and  $\vec{a}$ ), we can write  $\mathcal{C}_{tot}(\infty)$ :

$$\mathcal{C}_{tot}(\infty) = \frac{m^2}{\pi\hbar^4} \sum_{k=1}^{N-1} \sum_{P \in \mathfrak{S}_N} (a_P - a_{P(k,k+1)})^2 \alpha_k, \quad (\text{III.2.18})$$

where  $(k, k+1)$  is the transposition between particles at positions  $k$  and  $k+1$  and  $\alpha_k$  are the exchange coefficients defined in Eq. (I.2.22).

Moreover, the contact for a given spin-component can be extracted from Eq. (III.2.16) by restricting the second sum in Eq. (III.2.18) over the subset  $\tilde{\mathfrak{S}}_N(k|\sigma, \sigma')$  of permutations so that the indexes in positions  $k$  and  $k+1$  correspond to particles belonging to components  $\sigma$  and  $\sigma'$ :

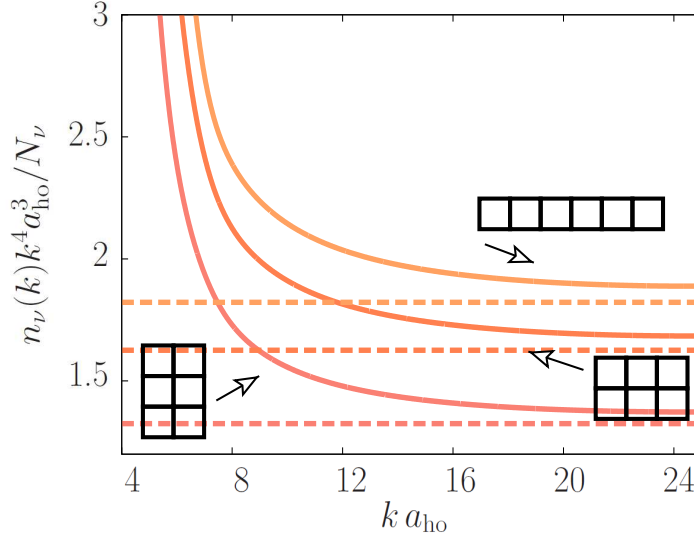
$$\tilde{\mathfrak{S}}_N(k|\sigma, \sigma') = \{P \in \mathfrak{S}_N | (P(k), P(k+1)) \in I_\sigma \times I_{\sigma'} \cup I_{\sigma'} \times I_\sigma\}. \quad (\text{III.2.19})$$

With these notations, we have:

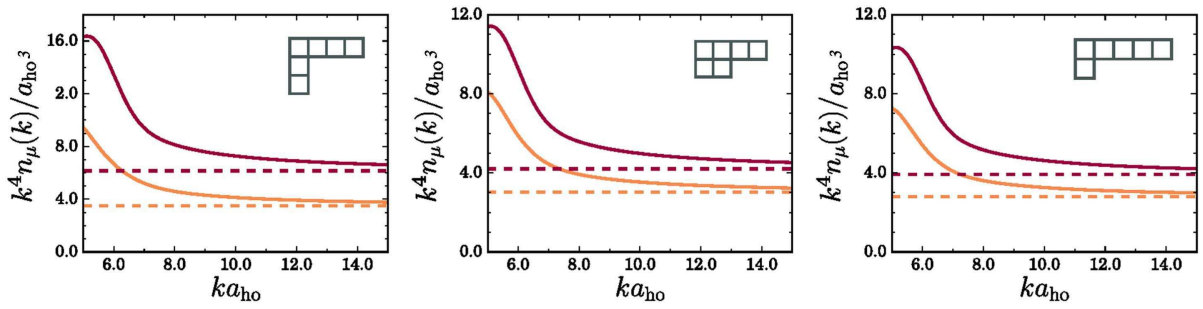
$$\mathcal{C}_\sigma(\infty) = \frac{m^2}{2\pi\hbar^4} \sum_{\sigma'=1}^{\kappa} (1 + \delta_{\sigma\sigma'}) \sum_{k=1}^{N-1} \sum_{P \in \tilde{\mathfrak{S}}_N(k|\sigma, \sigma')} (a_P - a_{P(k,k+1)})^2 \alpha_k. \quad (\text{III.2.20})$$

In Figs. III.2.1 and III.2.2, the  $\mathcal{C}_\sigma(\infty)$  for balanced fermionic mixtures and Bose-Fermi mixtures (respectively) computed from Eq. (III.2.20) are plotted and compared with the  $n_\sigma(k)k^4$  functions computed in section III.1.2.3. We observe that the asymptotic behaviors verify Eq. (III.2.10), which comfort us on the consistence of our calculations.





**Figure III.2.1:** Ground state  $n_\nu(k)k^4 a_{ho}^3 / N_\nu$  functions as functions of  $ka_{ho}$  where  $a_{ho} = \sqrt{\hbar/m\omega}$  for three strongly interacting balanced mixtures of  $N = 6$  fermions (solid lines,  $N_\nu = 3, 2, 1.$ ). The corresponding symmetries  $Y_\Gamma$  that were determined in chapter II are associated with each panel. The contacts  $C_\nu(\infty)$  computed from Eq. (III.2.20) are shown in dashed lines.



**Figure III.2.2:** Ground state  $n_\mu(k)k^4 a_{ho}^3 / N_\nu$  functions as functions of  $ka_{ho}$  where  $a_{ho} = \sqrt{\hbar/m\omega}$  for three strongly interacting Bose-Fermi mixtures of  $N = 6$  particles (from left to right:  $(3^B, 3^F)$ ,  $(2^B, 2^F, 2^F)$ ,  $(2^B, 2^B, 2^F)$ ). For a given mixture, spin-components with the same number of particles and same statistics have the same distributions. The corresponding symmetries  $Y_\Gamma$  that were determined in chapter II are associated with each panel. The contacts  $C_\mu(\infty)$  computed from Eq. (III.2.20) are shown in dashed lines. From [Decamp 2017].

### III.2.2.2. Discussion: Tan's contact as a symmetry probe

In Fig. III.2.1, we see that the contact of balanced fermionic mixtures increases as a function of the number  $\kappa$  of components. This behavior was qualitatively observed in the LENS experiment [Pagano 2014]. This property is directly related to the global symmetry of the mixture: when the number of spin-components increases, the mixture is more and more spatially symmetric. As discussed in chapter II, the (generalized) Lieb-Mattis theorem implies that the energy of the system decreases, and more precisely that the energy slope  $\partial E/\partial a_{1D}$  increases. Therefore, because of Tan sweep theorem (Eq. (III.2.16)), we can conclude that the contact also increases with the number of components. In the fermionized limit, this statement is readily obtained by observing Eq. (III.2.20). Besides, it also allows to understand why the bosonic contact of a balanced Bose-Fermi mixture is bigger than the fermionic one, as one can see in Fig. III.2.2.

Thus, we see that the contact constitutes an experimentally accessible quantity in order to compare spatial symmetries. In fact, because of Eq. (III.2.17) and the fact that the  $K$  coefficients label the states of the system, a precise measurement of  $\mathcal{C}_{tot}$  via a standard time-of-flight technique would allow to determine uniquely the state of the system, and thus its spatial symmetry (c.f. Fig. II.2.1). Besides, as discussed in section II.2.1, because of the duality between the spatial symmetry and the spin symmetry, the contact can also be seen as a magnetic structure probe [Decamp 2016b].

Finally, we stress that our discussion is based on strong assumptions: zero temperature, infinite interactions, purely one-dimensional system. Section III.2.3 is devoted to studying finite corrections to the contact. However, Tan's contact is associated with high momenta. As argued in [Olshanii 2003], it is then a more robust experimental parameter as compared to low-momentum related quantities, as it is less sensitive to temperature and to residual three-dimensional effects in optical lattices (c.f. Fig. I.1.3).

### III.2.3. Scaling laws for Tan's contact

The results presented in this section were published in [Decamp 2016b] (paragraphs III.2.3.1 and III.2.3.2) and [Decamp 2018] (paragraph III.2.3.3).

#### III.2.3.1. Contact at finite interaction strength

##### Preliminary discussion: scaling parameter in the harmonic trap

In this paragraph, we discuss what is the dimensionless parameter we have to consider when going to the thermodynamic limit.

To do so, let us first analyze the Lieb-Liniger case (c.f. appendix A), whose Hamiltonian is given by

$$\hat{H}_{LL} = \sum_{i=1}^N -\frac{\hbar^2}{2m} \frac{\partial^2}{\partial x_i^2} + g_{1D} \sum_{i<j} \delta(x_i - x_j), \quad (\text{III.2.21})$$

where the particle coordinates verify  $x_i \in [0, L]$ . The thermodynamic limit consists in considering  $N, L \rightarrow \infty$  with the lineic density  $n \equiv N/L$  being kept constant. By writing the coordinates in terms of the typical inter-particle distance  $y_i \equiv nx_i \in [0, N]$ , it is natural to write:

$$\hat{H}_{LL} = \frac{\hbar^2 n^2}{2m} \left[ \sum_{i=1}^N -\frac{\partial^2}{\partial y_i^2} + 2\gamma \sum_{i<j} \delta(y_i - y_j) \right], \quad (\text{III.2.22})$$

where

$$\gamma = \frac{mg_{1D}}{\hbar^2 n} \quad (\text{III.2.23})$$

is the dimensionless interaction strength. Then, we see that the total energy per particle will verify, in the thermodynamic limit, the following scaling behavior:

$$\frac{E}{N} = \frac{\hbar^2 n^2}{2m} e(\gamma), \quad (\text{III.2.24})$$

with  $e(\gamma)$  a dimensionless function, that can be obtained, at least perturbatively, by Bethe ansatz (c.f. section A.2.2). For more complicated statistics than a one-component bosonic system, the function  $e$  will also depend on the single-species polarizations  $\{p_\sigma\} \equiv \{N_\sigma/N\}_{\sigma \in \{1, \dots, \kappa\}}$ . The take-home message is that we have factorized  $\hat{H}_{LL}$  by the typical energy  $\hbar^2 n^2/2m$ , which corresponds to the Fermi energy in the Tonks thermodynamic limit, in order to obtain the adimensional scaling parameter  $\gamma$  (Eq. (III.2.23)) and Eq. (III.2.24).

In the case where the system is trapped by a harmonic potential of frequency  $\omega$ , we recall that the Hamiltonian is given by

$$\hat{H} = \sum_{i=1}^N \left( -\frac{\hbar^2}{2m} \frac{\partial^2}{\partial x_i^2} + \frac{1}{2} m \omega^2 x_i^2 \right) + g_{1D} \sum_{i<j} \delta(x_i - x_j). \quad (\text{III.2.25})$$

Naively, one could think of re-scaling  $\hat{H}$  in terms of  $\hbar\omega$  for the energy and  $x_i/a_0$  for length (where  $a_0 = \sqrt{\hbar/m\omega}$  is the harmonic oscillator length). However, keeping in mind the reasoning that we had in the absence of harmonic potential, we see that we have to factorize by the Fermi energy in the Tonks thermodynamic limit, which is given by  $\hbar\omega N$ . Thus, by re-scaling the spatial coordinates by  $y_i \equiv x_i/a_0\sqrt{N}$ , we obtain:

$$\hat{H} = \hbar\omega N \left[ \sum_{i=1}^N \left( -\frac{\partial^2}{\partial y_i^2} + \frac{1}{2N^2} y_i^2 \right) + \alpha_0 \sum_{i<j} \delta(y_i - y_j) \right], \quad (\text{III.2.26})$$

where the adimensional interaction strength relevant for our problem is given by

$$\alpha_0 = \frac{a_0 m g_{1D}}{\sqrt{N} \hbar^2} = -\frac{2a_0}{\sqrt{N} a_{1D}}. \quad (\text{III.2.27})$$

Therefore, analogously to Eq. (III.2.24) the total energy per particle in the thermodynamic limit of the harmonically trapped system is of the form (in the multi-component case)

$$\frac{E}{N} = \hbar\omega N f(\alpha_0, \{p_\sigma\}), \quad (\text{III.2.28})$$

with  $f$  an adimensional function.

Note that from these simple arguments, together with Tan adiabatic theorem (Eq. (III.2.14)), we already see that Eq. (III.2.28) implies that the total contact  $\mathcal{C}_{tot}$  verifies

$$\mathcal{C}_{tot}(\alpha_0) = \frac{N^{5/2}}{\pi a_0^3} \alpha_0^2 \frac{\partial f(\alpha_0, \{p_\sigma\})}{\partial \alpha_0}. \quad (\text{III.2.29})$$

We now proceed to find an explicit expression for this scaling.

### A local density approximation approach

The Local Density Approximation (LDA) consists in stating that when the harmonic potential is sufficiently shallow as compared to the typical length of the system, as it is the case in a typical cold atom experiment, we can consider the system as "locally homogeneous". Then, if we have an expression in the homogeneous case for  $e(\gamma)$  (Eq. (III.2.24)), we can obtain results in the harmonically trapped case by considering the following density functional:

$$E[n] = \int n(x) dx \left( \frac{\hbar^2 n(x)^2}{2m} e(\gamma) + \frac{1}{2} m \omega^2 x^2 - \mu \right), \quad (\text{III.2.30})$$

where the density profile  $n(x)$  is now a function of  $x$  that has to be determined, and the chemical potential  $\mu$  is a Lagrange multiplier allowing to fix the total number of particles:

$$\int n(x) dx = N. \quad (\text{III.2.31})$$

LDA is a peculiar class of approximation in density functional theory [Parr 1980].

Then, we obtain the ground-state density profile by minimizing  $E[n]$ , i.e. by solving  $\delta E[n]/\delta n = 0$ . This yields

$$\frac{3\hbar^2}{2m} e(\gamma) n(x)^2 - \frac{g_{1D}}{2} e'(\gamma) n(x) = \mu \left( 1 - \frac{x^2}{R_{TF}^2} \right), \quad (\text{III.2.32})$$

where  $R_{TF} \equiv \sqrt{2\mu/(m\omega^2)}$  is the Thomas-Fermi radius.

Once the ground-state density profile  $n(x)$  is known, it is easy to obtain Tan's contact by combining Eq. (III.2.30) to Tan adiabatic theorem (Eq. (III.2.14)):

$$\mathcal{C}_{tot} = \frac{g_{1D}^2 m^2}{2\pi \hbar^4} \int dx n(x)^2 e' \left( \frac{mg_{1D}}{\hbar^2 n(x)} \right). \quad (\text{III.2.33})$$

Note that in this paragraph we have considered only one density profile  $n(x)$ . This corresponds to the case of a single-component bosonic system or of a balanced fermionic or bosonic mixture. If different density profiles  $n_1, \dots, n_\kappa$  have to be considered, one will have to define a density functional  $E[n_1, \dots, n_\kappa]$  and the chemical potentials accordingly. This situation is a little bit more intricate, and in this thesis we have only considered the case of a balanced fermionic mixture [Decamp 2016b] (c.f. next paragraph), which is relevant for the LENS experiment [Pagano 2014]. Our method was adapted to the single-component bosonic case in [Lang 2017].

### Expression for strongly interacting balanced fermionic mixtures

In the homogeneous regime [Guan 2012], we dispose of an explicit Laurent expansion for  $e(\gamma)$  when  $\gamma \rightarrow \infty$  in the case of a balanced fermionic mixture. It is given by:

$$e(\gamma) \underset{\gamma \rightarrow \infty}{=} \frac{\pi^2}{3} \left[ 1 - \frac{4Z_1(\kappa)}{\gamma} + \frac{12Z_1(\kappa)^2}{\gamma^2} - \frac{32}{\gamma^3} \left( Z_1(\kappa)^3 - \frac{Z_3(\kappa)\pi^2}{15} \right) + \mathcal{O}\left(\frac{1}{\gamma^4}\right) \right], \quad (\text{III.2.34})$$

with

$$Z_1(\kappa) = -\frac{1}{\kappa} \left( \psi\left(\frac{1}{\kappa}\right) + C_{Euler} \right), \quad (\text{III.2.35})$$

and

$$Z_3(\kappa) = \frac{1}{\kappa^3} \left( \zeta\left(3, \frac{1}{\kappa}\right) - \zeta(3) \right), \quad (\text{III.2.36})$$

where  $C_{Euler} \approx 0.577$  is the Euler constant and  $\psi$  and  $\zeta$  are respectively the Digamma and Riemann Zeta functions [Abramowitz 1965]. In section A.3.3.2, we provide a sketch of the proof of relation (III.2.34).

The next step is to write the chemical potential  $\mu$  and the density profile  $n(x)$  as similar  $1/\gamma$ -expansions whose coefficients are unknown, and plugging these expansions into Eqs (III.2.32) and (III.2.31). Then, solving it order by order using Eq. (III.2.34) and applying Eq. (III.2.33), we find the strong-coupling expansion for the Tan's contact of a balanced fermionic mixture:

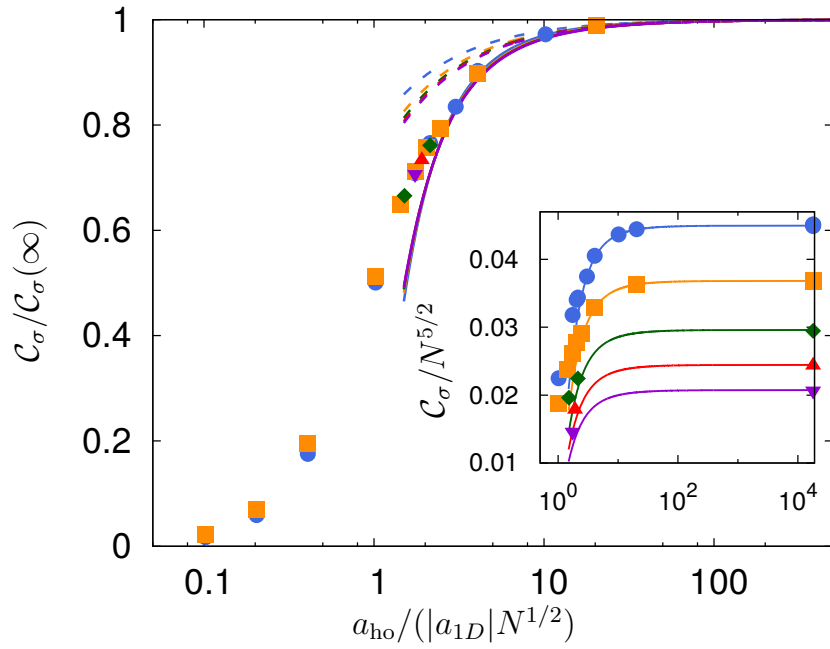
$$\mathcal{C}_{tot}(\alpha_0) \underset{\alpha_0 \rightarrow \infty}{=} \frac{N^{5/2}}{\pi a_0^3} \left[ \frac{128\sqrt{2}Z_1(\kappa)}{45\pi^2} + \frac{2(315\pi^2 - 4096)Z_1(\kappa)^2}{81\pi^4\alpha_0} - \frac{64\sqrt{2}[25(1437\pi^2 - 14336)Z_1(\kappa)^3 + 1728\pi^4 Z_3(\kappa)]}{14175\pi^6\alpha_0^2} + \mathcal{O}\left(\frac{1}{\alpha_0^3}\right) \right]. \quad (\text{III.2.37})$$

In particular, in the fermionized limit, Eq. (III.2.37) implies

$$\mathcal{C}_{tot}(\infty) = \frac{N^{5/2}}{a_0^3} \frac{128\sqrt{2}Z_1(\kappa)}{45\pi^3}. \quad (\text{III.2.38})$$

Notice that these expressions have the same form as Eq. (III.2.29), which was predicted only by physical arguments. Besides, by taking the  $\kappa \rightarrow \infty$  limit of an infinite number of components, since  $\lim_{\kappa \rightarrow \infty} Z_1(\kappa) = 1$ , we see that we obtain the strong-coupling expansion for the contact in the bosonic case [Olshanii 2003, Lang 2017]. This suppression of the effects of internal degrees of freedom when  $\kappa \rightarrow \infty$ , also known as *high-spin bosonization* was also highlighted in [Yang 2011, Guan 2012, Liu 2014]. Experimentally, this phenomenon was observed by analyzing the collective mode frequencies when increasing the number  $\kappa$  of fermionic components up to  $\kappa = 6$  [Pagano 2014].

The  $N^{5/2}$ -dependence of the contact was also observed in Monte Carlo numerical simulations [Matveeva 2016], these results thus constituting an analytical proof. Moreover, we observe that  $\mathcal{C}_{tot}$  is an increasing function of the number of components  $\kappa$ , as observed in the LENS experiment [Pagano 2014] and explained qualitatively by symmetry arguments in section III.2.2.2.



**Figure III.2.3:** Comparison between the strong-coupling expansion (Eq. (III.2.37)) to first and second order in  $1/\alpha_0$  (dashed and continuous lines, respectively), and the DMRG simulations performed by Matteo Rizzi and Johannes Jünemann for the contacts  $\mathcal{C}_\nu$  of different balanced fermionic mixtures ( $N_\nu = 2$ ; blue circles:  $\kappa = 2$ , orange squares:  $\kappa = 3$ , green diamonds:  $\kappa = 4$ , red up-triangles:  $\kappa = 5$ , violet down-triangles:  $\kappa = 6$ ), as functions of  $\alpha_0/2 = a_0/(|a_{1D}|N^{1/2})$ . By removing the  $N^{5/2}$ -dependence (inset) and then the asymptotic value of  $\mathcal{C}_\nu$  (main panel), we see that the data collapse, thus displaying a very weak dependence on the number  $\kappa$  of components. From [Decamp 2016b].

In Fig. III.2.3, we compare the contact strong-coupling expansion of Eq. (III.2.37) with numerical DMRG data obtained by Matteo Rizzi and Johannes Jünemann [Decamp 2016b]. The agreement between the two is extremely good, although we have used strong assumptions in order to perform the LDA. Indeed, our result should, in principle, work only for a very large number of atoms, but we see that it is already very accurate for few-body systems ( $4 \leq N \leq 12$ ). This property, that was recently discussed in the bosonic case [Rizzi 2018], suggests that few-body systems, that are hence more accessible for numerical and analytical calculations, already capture the essential behaviors of many-body systems (see also [Grining 2015b]). Moreover, by re-scaling the contacts by their values at infinite interactions, we note that all the plots collapse almost perfectly and therefore display a very weak dependence on  $\kappa$ .

### III.2.3.2. Contact at finite temperature

In section III.2.1, when introducing Tan's contact and Tan sweep theorem, we have only considered pure states. However, when temperature is finite, statistical mixtures have to be considered. Hopefully, this generalization is pretty straightforward. In particular, the finite-temperature version of Eq. (III.2.16) in the grand canonical ensemble becomes [Pătu 2017]:

$$\mathcal{C}_\sigma(T) = \frac{m}{\pi \hbar^2} \sum_{\sigma'=1}^{\kappa} (1 + \delta_{\sigma\sigma'}) \left( \frac{\partial \Omega}{\partial a_{\sigma\sigma'}} \right)_{\mu_\sigma, T}, \quad (\text{III.2.39})$$

where  $\Omega$  is the grand potential defined by

$$\Omega = -k_B T \ln \mathcal{Z}, \quad (\text{III.2.40})$$

with the grand partition function given by

$$\mathcal{Z} = \text{Tr} \left[ e^{(\sum_{\sigma=1}^{\kappa} \mu_\sigma \hat{N}_\sigma - \hat{H})/k_B T} \right]. \quad (\text{III.2.41})$$

### Virial expansion at high temperatures

In general,  $\Omega$  is hard to compute exactly in our system. However, in the limit of high temperatures, *i.e.*

$$\frac{\hbar\omega}{k_B T} \ll 1, \quad (\text{III.2.42})$$

it can be expanded in powers of the *fugacity*, which verifies in this limit [Landau 1980]

$$z_\sigma \equiv e^{\frac{\mu_\sigma}{k_B T}} \ll 1. \quad (\text{III.2.43})$$

Such an expansion is known as a *virial expansion*, and its coefficients can be computed analytically in the strongly repulsive limit [Ho 2004, Liu 2009, Liu 2010]. It has allowed to compute the high-temperature contact in the fermionized regime in three-dimensional  $SU(2)$  systems [Hu 2011], in one-dimensional bosonic Tonks gas [Vignolo 2013] and  $SU(\kappa)$  systems [Decamp 2016b]. In the following, we will first explain how this expansion works in the simplest case of the one-dimensional Tonks gas, and then show how it can be extended to other statistics.

In a one-component Bose gas, in the limit of high temperatures, we can forget the  $\sigma$  index and write

$$\mathcal{Z} \underset{z \rightarrow 0}{=} 1 + zQ_1 + z^2Q_2 + \mathcal{O}(z^3), \quad (\text{III.2.44})$$

with  $Q_n$  the partial partition function of clusters of size  $n$ , *i.e.*

$$Q_n = \text{Tr}_n \left[ e^{-\hat{H}_n/k_B T} \right]. \quad (\text{III.2.45})$$

By taking the logarithm, we can write  $\Omega$  as

$$\Omega \underset{z \rightarrow 0}{=} -k_B T Q_1 \left( z + b_2 z^2 \right) + \mathcal{O}(z^3), \quad (\text{III.2.46})$$

with the *second virial coefficient* given by

$$b_2 = (Q_2 - Q_1^2/2)/Q_1. \quad (\text{III.2.47})$$

Then, the one-component version of Eq. (III.2.39) implies

$$\begin{aligned} \mathcal{C}(T) &= \frac{2m}{\pi \hbar^2} \frac{\partial \Omega}{\partial a_{1D}} \\ &\underset{z \rightarrow 0}{=} \frac{2m}{\pi \hbar^2 \lambda_{dB}} k_B T Q_1 c_2 z^2 + \mathcal{O}(z^3), \end{aligned} \quad (\text{III.2.48})$$

where  $\lambda_{dB} = \sqrt{2\pi \hbar^2 / m k_B T}$  and the adimensional coefficient  $c_2$  is defined by

$$c_2 = -\frac{\partial b_2}{\partial (a_{1D} / \lambda_{dB})}. \quad (\text{III.2.49})$$

In the strongly interacting and high temperature limit, the following relations hold:

$$\begin{aligned} Q_1 &= \sum_{k=0}^{+\infty} e^{-\frac{\hbar \omega}{k_B T} (k+1/2)} \\ &\sim \frac{k_B T}{\hbar \omega}, \end{aligned} \quad (\text{III.2.50})$$

and

$$z \sim \frac{N \hbar \omega}{k_B T}, \quad (\text{III.2.51})$$

which can be deduced from

$$N = \int d\epsilon \rho_S(\epsilon) \frac{1}{e^{(\epsilon-\mu)/(k_B T)} + 1} \quad (\text{III.2.52})$$

with the density of states given by  $\rho_S(\epsilon) = 1/(\hbar \omega)$  and by taking the high  $T$  limit. Moreover, we have

$$c_2 \sim \frac{1}{\sqrt{2}}. \quad (\text{III.2.53})$$

This last relation is obtained using the fact that

$$Q_2 = Q_1 \sum_{\nu} e^{-\epsilon_{\nu}^{rel} / k_B T}, \quad (\text{III.2.54})$$



where  $\epsilon_\nu^{rel}$  are the energies of the two-body problem. In the harmonic trap, one can prove that [Busch 1998]

$$\epsilon_\nu^{rel} = \hbar\omega \left( \nu + \frac{1}{2} \right), \quad (\text{III.2.55})$$

with  $\nu$  the solution of the following transcendental equation:

$$f(\nu) \equiv \frac{\Gamma(-\nu/2)}{\Gamma(-\nu/2 + 1/2)} = \frac{\sqrt{2}a_{1D}}{a_0}. \quad (\text{III.2.56})$$

In the fermionized regime  $a_{1D}$ , this implies  $\nu \in 2\mathbb{N} + 1$ . Then, Eq. (III.2.53) becomes

$$c_2 = -\lambda_{dB} \sum_\nu \frac{\hbar\omega}{k_B T} \frac{\partial \epsilon_\nu^{rel}}{\partial a_{1D}} e^{-\epsilon_\nu^{rel}/k_B T}, \quad (\text{III.2.57})$$

and

$$\begin{aligned} \frac{\partial \epsilon_\nu^{rel}}{\partial a_{1D}} &= \frac{\epsilon_\nu^{rel}}{\partial \nu} \frac{\partial \nu}{\partial f} \frac{\partial f}{\partial a_{1D}} \\ &= \frac{\sqrt{2}\hbar\omega}{a_0} \frac{\partial \nu}{\partial f}. \end{aligned} \quad (\text{III.2.58})$$

Using Eq. (III.2.56) and some algebraic relations on the Euler function  $\Gamma$  yields, taking  $\nu = 2n + 1$  with  $n \in \mathbb{N}$ :

$$\frac{\partial \nu}{\partial f} = \frac{2}{\pi} \frac{\Gamma\left(\frac{3}{2} + n\right)}{n!}. \quad (\text{III.2.59})$$

Then, we have to evaluate the following sum:

$$\sum_{n \in \mathbb{N}} \frac{\Gamma\left(\frac{3}{2} + n\right)}{n!} e^{-\frac{\hbar\omega}{k_B T} (2n + \frac{3}{2})}, \quad (\text{III.2.60})$$

which can be performed exactly and is equal to [Hu 2011]

$$\frac{\sqrt{\pi}}{4 \left[ 2 \frac{\hbar\omega}{k_B T} \sinh\left(\frac{\hbar\omega}{k_B T}\right) \right]^{3/2}}. \quad (\text{III.2.61})$$

Thus, taking the  $\hbar\omega \ll k_B T$  limit, we readily obtain Eq. (III.2.53).

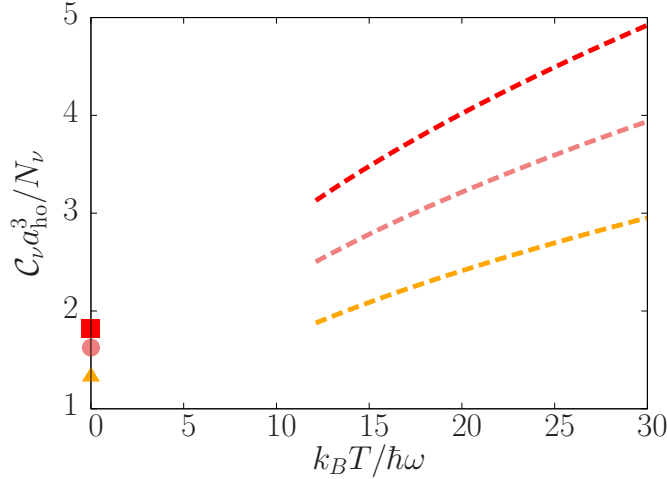
Finally, putting Eqs. (III.2.50), (III.2.51) and (III.2.53) into Eq. (III.2.48), we find the high-temperature dependence of the Tan's contact of the Tonks gas:

$$\mathcal{C}(T) = \frac{N^2}{\pi^{3/2} a_0^3} \sqrt{\frac{k_B T}{\hbar\omega}}. \quad (\text{III.2.62})$$

Refinements for this formula can be found in [Yao 2018].

In [Decamp 2016b], we have generalized Eq. (III.2.62) to fermionic mixtures. Here, we will describe how to generalize it to Bose-Fermi mixtures, which is straightforward. Instead of writing the grand partition function as in Eq. (III.2.44), we write

$$\mathcal{Z} \underset{z \rightarrow 0}{=} 1 + \sum_{\sigma=1}^{\kappa} z_\sigma Q_1 + \sum_{\sigma, \sigma'} z_\sigma z_{\sigma'} Q_{2\sigma\sigma'} + \mathcal{O}(z^3), \quad (\text{III.2.63})$$



**Figure III.2.4:** Ground state normalized Tan's contacts as functions of  $k_B T / \hbar \omega$  for three strongly interacting balanced mixtures of  $N = 6$  fermions (solid lines,  $N_\nu = 3, 2, 1$ ). The dashed lines correspond to Eq. (III.2.65) while the  $T = 0$  points are given by the exact solution (Eq. (III.2.20)). From [Decamp 2016b].

with

$$z_\sigma \sim N_\sigma \frac{\hbar \omega}{k_B T} \quad (\text{III.2.64})$$

in the high temperature and strongly repulsive limit. Note that  $Q_{2\sigma\sigma} = 0$  if  $\sigma$  is a fermionic component, and otherwise  $Q_{2\sigma\sigma'} = Q_2$  as found in the Tonks gas. Then, applying the same procedure than before to the generalized Tan sweep relation (Eq. (III.2.39)) yields

$$C_\sigma(T) = \frac{N_\sigma}{\pi^{3/2} a_0^3} \sqrt{\frac{k_B T}{\hbar \omega}} \sum_{\sigma'=1}^{\kappa} \chi_{\sigma\sigma'} N_{\sigma'}, \quad (\text{III.2.65})$$

where

$$\chi_{\sigma\sigma'} = \begin{cases} 0 & \text{if } \sigma = \sigma' \text{ and } \sigma \text{ is a fermionic component} \\ 1 & \text{otherwise} \end{cases} . \quad (\text{III.2.66})$$

Notice that in the case of a balanced fermionic mixture, Eq. (III.2.65) implies

$$C_{tot}(T) = \frac{N^2}{\pi^{3/2} a_0^3} \sqrt{\frac{k_B T}{\hbar \omega}} \frac{\kappa - 1}{\kappa} \quad (\text{III.2.67})$$

and once again we recover the Tonks result (Eq. (III.2.62)) in the  $\kappa \rightarrow \infty$  limit.

In Fig. III.2.4 are plotted the high-temperature dependencies of balanced fermionic mixtures. The high-temperature curves are given by Eq. (III.2.65) and the  $T = 0$  results correspond to the exact solution (Eq. (III.2.20)).

## Discussion

Several interesting facts are worth noticing. First of all, in the fermionized limit  $g_{1D} \rightarrow \infty$ , the contact is an increasing function of temperature. This is a typical one-dimensional effect: indeed, one would expect that the correlations (and thus the contact) would be

destroyed by the high temperatures. This is indeed the fact for three dimensional systems [Hu 2011], but the dimensional constraint implies an opposite behavior for one-dimensional systems (c.f. section I.1.1). Note that we did not discuss the case where interactions are finite, where we expect the presence of maximum, as recently obtained in the bosonic case [Yao 2018]. Moreover, we observe that the normalized contact is still an increasing function of the number of components, in agreement with the experimental observations [Pagano 2014]. Finally, the fact that the second virial coefficient is a constant (Eq. (III.2.53)) implies that the contact at infinite interactions is a *universal* quantity, and thus, as already pointed out in section III.2.2.2, a robust experimental observable.

An alternative way of deriving Tan's contact temperature dependence consists in performing, analogously to what we did in section III.2.3.1, an LDA on the thermal version of the Bethe ansatz equations (See appendix A, sections A.2.3 and A.3.4). This was done recently in [Yao 2018] for the harmonically trapped Lieb-Liniger gas. This method has the advantage of allowing to express the contact simultaneously as a function of the temperature and the interaction strength, and for all temperatures. Nevertheless, extension to multi-component systems appears to be more intricate, given the complexity of the thermodynamic Bethe ansatz equations in this case, which involve an infinite set of coupled equations (c.f. Eq. (A.3.44)). A promising alternative to these equations has however been proposed in [Păţu 2016] for the Gaudin-Yang model.

### III.2.3.3. Influence of the transverse confinement

In section I.1.2.2, we have seen that experimentalists are able to construct quasi-1D traps for ultracold atoms by superimposing counter-propagating lasers with frequencies  $(\omega_x, \omega_y, \omega_z)$  where  $\omega_x = \omega_y = \omega_\perp$  such that the aspect ratio  $\lambda = \omega_z/\omega_\perp$  is very small. Therefore, the energy gap between the transverse ground state and the first excited state is higher than all the typical energies of the system, and the systems behaves essentially like a one-dimensional system oriented in the  $z$  direction. Nevertheless, one should not forget that, even if the system in this regime can be described by one-dimensional Hamiltonian, the interactions between particles are intrinsically three-dimensional. This can be seen in the derivation and expression of the effective one-dimensional scattering length  $a_{1D}$  [Olshanii 1998], which is a function of the three-dimensional scattering length  $a_{3D}$  (c.f. Eq. (I.1.29)).

Tan's contact, that we defined in Eq. (III.2.11), is a two-body quantity. Then, it depends crucially on the three-dimensional nature of the contact interactions. Thus, it is natural to ask ourselves how the contact behaves as a function of  $\lambda$ , *i.e.* in the *dimensional crossover* consisting in allowing progressively the transverse states to be populated. In the following, we describe how this behavior can be studied in the case of a dilute Bose gas trapped in a potential of the form  $V(x, y, z) = m/2(\omega_\perp^2 x^2 + \omega_\perp^2 y^2 + \omega_z^2 z^2)$  with  $\lambda \gg 1$ , as published [Decamp 2018]. This is a bit different from what we studied until now, that is strongly interacting mixtures. However, it constitutes a first step toward the characterization of the dimensional crossover behavior of the contact in these systems.

### Effective one-dimensional Gross-Pitaevskii equation

The Gross-Pitaevskii theory is a mean-field theory describing dilute degenerate Bose gases [Gross 1961, Pitaevskii 1961]. In the  $\lambda = \omega_z/\omega_\perp \ll 1$  regime, an effective stationary Gross-Pitaevskii equation can be written [Leboeuf 2001, Gerbier 2004, Muñoz Mateo 2006]:

$$\left[ -\frac{\hbar^2}{2m} \frac{\partial^2}{\partial z^2} + U(z) + \epsilon(n_1) - E \right] \psi(z) = 0, \quad (\text{III.2.68})$$

where the 1D order parameter  $\psi(z)$  is associated to the effective 1D density profile through  $n_1(z) = |\psi(z)|^2$ ,  $U(z)$  is an external potential, and  $\epsilon(n_1)$  is given by [Fuchs 2003, Gerbier 2004]

$$\epsilon(n_1) = \hbar\omega_\perp \sqrt{1 + 4a_{3D}n_1}. \quad (\text{III.2.69})$$

The role of this parameter is to describe the effective one-dimensional interactions in the dimensional crossover. Indeed, in the regime where  $a_\perp n_1 \ll 1$ ,  $\epsilon(n_1) \simeq \hbar\omega_\perp + 2\hbar\omega_\perp a_{3D}n_1$ , which corresponds to the standard non-linearity  $\propto \psi|\psi|^2$  and thus to the 1D equivalent of the 3D Gross-Pitaevskii equation. In this regime, which is referred as the *mean field regime* (MF) in the following, the transverse wave function is in the ground state of the transverse harmonic oscillator. On the contrary, when  $a_{3D}n_1 \gg 1$ , we have  $\epsilon(n_1) \simeq 2\hbar\omega_\perp \sqrt{a_{3D}n_1}$ , the non-linearity  $\propto \psi|\psi|$  is no longer standard and many transverse excited states are populated, thus displaying a Thomas-Fermi profile: this is referred as the *transverse Thomas-Fermi regime* (TTF).

### Homogeneous contact from the quantum fluctuations

We now turn to the calculation of Tan's contact in the homogeneous case, corresponding to  $U(z) = 0$  in Eq. (III.2.68). In this case the contact is a constant function of  $z$ , and we rather consider the *homogeneous contact*, defined as

$$\tilde{\mathcal{C}} = \frac{2}{\pi a_{1D}^2} G^{(2)}(0, 0). \quad (\text{III.2.70})$$

In the homogeneous case where the gas is in a box of length  $L$ , we simply have  $\mathcal{C} = L\tilde{\mathcal{C}}$ .  $\tilde{\mathcal{C}}$  is also called *contact density*.

Note that the correlations  $G^{(2)}(0, 0)$  can not be deduced from Eq. (III.2.68), which is a mean-field model. In order to do so, we have to take into account the quantum fluctuations by a Bogoliubov method [Gerbier 2004]. Usually, in a 1D quantum model, one should not only take into account the density fluctuations, but also the phase fluctuations. It is indeed these phase fluctuations, related to the collective nature of excitations, which explain for example the impossibility of finite-temperature phase transitions in 1D (see section I.1.1 and the MWH theorem). However they are related to the long-range order, or equivalently the low-momenta: since the contact is associated to the high-momentum behavior, we can safely neglect them in what follows.

The Bogoliubov expansion in our case is then very similar to its 3D counterpart. The idea is to consider that the system is highly degenerate, with  $N_0 \equiv N$  particles in the

ground-state solution  $\psi_0$  of Eq. (III.2.68), and add a quantum fluctuation  $\delta\hat{\Psi}$  to the field operator of the system [Pitaevskii 2016]:

$$\hat{\Psi}(z) = \sqrt{N_0}\psi_0(z) + \sum_{k \neq 0} \psi_k(z)\hat{a}_k, \quad (\text{III.2.71})$$

where  $\hat{a}_k$  annihilates a particle with momentum  $\hbar k$  (with an analogous equation for the creation field operator  $\hat{\Psi}^\dagger$ ). After expanding Eq. (III.2.68) on this basis up to the second order in  $\delta\hat{\Psi}$ , we can perform the celebrated *Bogoliubov transformation* [Bogoliubov 1947] which consists in diagonalizing the Hamiltonian in terms of the bosonic operator  $\hat{b}_k = u_k\hat{a}_k + v_{-k}\hat{a}_{-k}^\dagger$ , where  $u_k$  and  $v_k$  obey the *Bogoliubov-de Gennes equations*:

$$\hbar\omega \begin{pmatrix} u_k \\ v_k \end{pmatrix} = \begin{pmatrix} \frac{\hbar^2 k^2}{2m} + mc^2 & mc^2 \\ -mc^2 & -\frac{\hbar^2 k^2}{2m} - mc^2 \end{pmatrix} \begin{pmatrix} u_k \\ v_k \end{pmatrix}, \quad (\text{III.2.72})$$

as well as  $u_k^2 - v_k^2 = 1$ , which is a consequence of the bosonic commutation relations. In Eq. (III.2.72),  $c$  is the *effective velocity of sound*, and is given in our system by [Stringari 1996, Zaremba 1998]

$$mc^2 = n_1 \epsilon'(n_1). \quad (\text{III.2.73})$$

Then, solving Eq. (III.2.72) yields the famous *Bogoliubov spectrum*, given by

$$\hbar\omega(k) = \sqrt{\hbar^2 k^2 c^2 + \left(\frac{\hbar^2 k^2}{2m}\right)^2}. \quad (\text{III.2.74})$$

The momentum distribution for  $k \neq 0$  at zero temperature can then be obtained in the Bogoliubov paradigm as:

$$\begin{aligned} n(k) &= \langle \hat{a}_k^\dagger \hat{a}_k \rangle = v_k^2 \\ &= \frac{\hbar^2 k^2 / 2m + mc^2}{2\hbar\omega(k)} - \frac{1}{2}. \end{aligned} \quad (\text{III.2.75})$$

The homogeneous contact is then extracted from Eqs. (III.2.73), (III.2.74) and (III.2.75), giving

$$\tilde{C} = \frac{4}{a_\perp^4} \frac{a_{3D}^2 n_1^2}{1 + 4a_{3D} n_1}, \quad (\text{III.2.76})$$

where  $a_\perp = \sqrt{\hbar/m\omega_\perp}$  is the radial harmonic oscillator length.

Notice that the contact goes from a  $\mathcal{O}(a_{3D} n_1)$  to a  $\mathcal{O}((a_{3D} n_1)^2)$  behavior when going from the TTF to the MF regime.

### Comparison with Lieb-Liniger theory

Here we compare Eq. (III.2.76) to the results obtained from a completely different paradigm, that is the Lieb-Liniger theory (c.f. appendix A, section A.2).

Tan sweep theorem (Eq. (III.2.16)) allows to express the homogeneous contact as a function of the adimensional coupling strength  $\gamma = -2/a_{1D} n_1$  and the adimensional

ground-state energy  $e$  (which is obtained solving the Bethe ansatz equations of the Lieb-Liniger model, Eqs (A.2.9), (A.2.13), (A.2.14)):

$$\tilde{\mathcal{C}} = \frac{4n_1^2}{a_{1D}^2} e'(\gamma), \quad (\text{III.2.77})$$

where  $a_{1D}$ 's expression is given in Eq. (I.1.29). Moreover, if  $a_{\perp} \gg a_{3D}$ , one can consider simultaneously the  $\gamma \ll 1$  (i.e.  $a_{1D}n_1 \gg 1$ ) regime and the MF regime  $a_{3D}n_1 \ll 1$ . In this case, Eq. (I.1.29) implies  $a_{1D} \approx -a_{\perp}^2/a_{3D}$  and the low-coupling expression of  $e$  (Eq. (A.2.17)) yields

$$\tilde{\mathcal{C}} \sim \frac{4a_{3D}^2 n_1^2}{a_{\perp}^4}, \quad (\text{III.2.78})$$

which corresponds exactly to the  $a_{3D}n_1 \ll 1$  equivalent of  $\tilde{\mathcal{C}}$  in Eq. (III.2.76).

In the other regimes, it is not possible to compare analytically the one-dimensional Lieb-Liniger theory with our approach. However, a variational gaussian ansatz, known as the *generalized Lieb-Liniger theory* (GLL), was proposed in [Salasnich 2004, Salasnich 2005] in order to take into account the effects of the transverse confinement. It consists in supposing that the 3D wave function  $\Phi(\vec{r}_1, \dots, \vec{r}_N)$  (where  $\vec{r}_i \equiv (x_i, y_i, z_i)$  is the 3D coordinate of particle  $i$ ) is given by:

$$\Phi(\vec{r}_1, \dots, \vec{r}_N) = \psi(z_1, \dots, z_N) \prod_{i=1}^N \frac{\exp\left(-\frac{x_i^2 + y_i^2}{2\sigma^2}\right)}{\sqrt{\pi}\sigma}. \quad (\text{III.2.79})$$

Here, the variational parameter  $\sigma$  corresponds to the transverse width of the cloud. The lineic total energy  $\mathcal{E}$  can then be extracted within this hypothesis and is equal to

$$\mathcal{E} = \frac{\hbar^2}{2m} n_1^3 e \left( \frac{2a_{3D}}{a_{\perp}^2 n_1 \sigma^2} \right) + \frac{\hbar\omega_{\perp}}{2} n_1 \left( \frac{1}{\sigma^2} + \sigma^2 \right), \quad (\text{III.2.80})$$

where  $e$  is obtained by solving numerically the Bethe ansatz equations. Then,  $\delta\mathcal{E}/\delta\sigma = 0$  yields

$$\sigma^4 = 1 + 2a_{3D}n_1 e' \left( \frac{2a_{3D}}{a_{\perp}^2 n_1 \sigma^2} \right). \quad (\text{III.2.81})$$

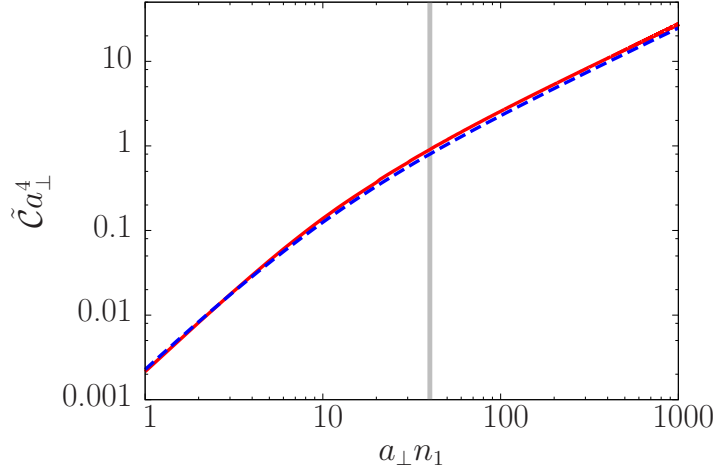
Once  $\mathcal{E}$  is obtained by solving Eqs. (III.2.80) and (III.2.81) consistently, we can extract the homogeneous contact from Eq. (III.2.75) as well as the relation [Stringari 1996, Zaremba 1998]:

$$c = \sqrt{\frac{n_1}{m} \frac{\partial^2 \mathcal{E}}{\partial n_1^2}}. \quad (\text{III.2.82})$$

In Fig. (III.2.5) we have plotted the homogeneous contact obtained by this method and compared it to the analytic result of Eq. (III.2.76). As one can see, the two methods give mutually consistent results.

### Trapped one-dimensional contact

Here we extract the contact  $\mathcal{C}$  from the homogeneous contact  $\tilde{\mathcal{C}}$  in the realistic case where  $U(z) = m\omega_z z^2/2$ . To do so, in the same spirit as what we did in section III.2.3.1,



**Figure III.2.5:** Homogeneous contact  $\tilde{\mathcal{C}}$  in units of  $a_{\perp}^{-4}$  as a function of  $a_{\perp}n_1$ , with  $a_{3D}/a_{\perp} = 0.025$ . The dashed blue line is plotted using Eq. (III.2.76) and we obtained the solid red line numerically by the GLL method. The vertical gray line represents  $a_{\perp}n_1 = 1$  and corresponds to the transition from the MF to the TTF regime.

the idea is to perform a LDA. However, in the present case, we dispose of an analytic expression for the density profile [Muñoz Mateo 2006]:

$$n_1(z) = \frac{1}{4a_{3D}} \left( \frac{\lambda Z}{a_{\perp}} \right)^2 \left[ 1 - \left( \frac{z}{Z} \right)^2 \right] + \frac{1}{16a_{3D}} \left( \frac{\lambda Z}{a_{\perp}} \right)^4 \left[ 1 - \left( \frac{z}{Z} \right)^2 \right]^2, \quad (\text{III.2.83})$$

where  $Z$ , the axial Thomas-Fermi radius, verifies

$$\frac{1}{15} \left( \frac{\lambda Z}{a_{\perp}} \right)^5 + \frac{1}{3} \left( \frac{\lambda Z}{a_{\perp}} \right)^3 = \frac{\lambda N a_{3D}}{a_{\perp}} \equiv \chi_1, \quad (\text{III.2.84})$$

and can be approximated by [Muñoz Mateo 2008]

$$\frac{\lambda Z}{a_{\perp}} \simeq \left( \frac{1}{(15\chi_1)^{4/5} + \frac{1}{3}} + \frac{1}{57\chi_1 + 345} + \frac{1}{(3\chi_1)^{4/3}} \right)^{-1/4}. \quad (\text{III.2.85})$$

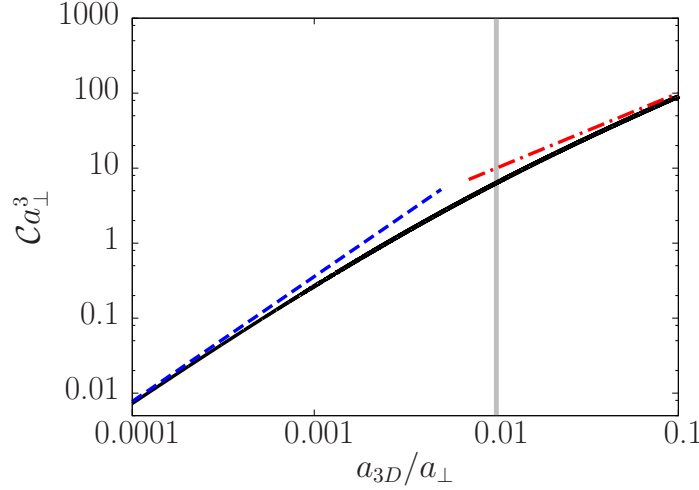
The  $\chi_1$  parameter characterizes the transition between the TTF regime ( $\chi_1 \gg 1$ ) and the MF regime ( $\chi_1 \ll 1$ ) in the harmonic trap [Menotti 2002].

Then, the LDA approximation implies  $\mathcal{C} = \int dz \tilde{\mathcal{C}}(n_1(z))$ , which yields

$$\mathcal{C} = \left\{ \lambda Z \sqrt{\lambda^2 Z^2 + 2a_{\perp}^2} (2\lambda^6 Z^6 + 14a_{\perp}^2 Z^4 \lambda^4 + 5a_{\perp}^4 \lambda^2 Z^2 - 15a_{\perp}^6) + 30a_{\perp}^8 \operatorname{artanh} \left( \frac{\lambda Z}{\sqrt{\lambda^2 Z^2 + 2a_{\perp}^2}} \right) \right\} \frac{1}{30a_{\perp}^8 \lambda (\lambda^2 Z^2 + 2a_{\perp}^2)^{3/2}}. \quad (\text{III.2.86})$$

In the TTF and MF regimes, Eq. (III.2.86) admits respectively the more compact forms:

$$\mathcal{C} \underset{\chi_1 \gg 1}{\sim} \frac{a_{3D} N}{a_{\perp}^4} \equiv \mathcal{C}_{TTF}, \quad (\text{III.2.87})$$



**Figure III.2.6:** Tan's contact  $\mathcal{C}$  in units of  $a_{\perp}^{-3}$  as a function of  $a_{3D}/a_{\perp}$ . The black curve is plotted using Eq. (III.2.86), while the dashed blue and dot-dashed red curves correspond to the MF and TTF expansions from Eqs (III.2.87) and (III.2.88), respectively. The vertical gray line verifies  $\chi_1 = 1$  and is associated with the transition from the MF to the TTF regime. The set of parameters used in these plots is ( $N = 1000, \lambda = 0.1$ ).

and

$$\mathcal{C} \underset{\chi_1 \ll 1}{\sim} \frac{4(3\lambda)^{2/3}}{5a_{\perp}^{14/3}} a_{3D}^{5/3} N^{5/3}. \quad (\text{III.2.88})$$

This last expression is, as expected, compatible with the contact obtained by LDA on the weak coupling Lieb-Liniger expansion of the homogeneous contact [Olshanii 2003, Lang 2017].

We observe that the contact has clearly distinct scaling behaviors in the TTF regime (where it is linear in  $a_{3D}N$ ) and the MF regime (where  $\mathcal{C} \propto (a_{3D}N)^{5/3}$ ). It can thus be used as an experimental characterization of the dimensional regime in highly anisotropic traps. Notice that, in the TTF regime, which is associated with a three-dimensional system, the contact does not depend on the aspect ratio  $\lambda$ . In Fig. III.2.6, we have plotted  $\mathcal{C}$  as a function of  $a_{3D}$ .

If we plot the contact as a function of the number of bosons, we can plot on a same graph the TTF, MF and one-dimensional strongly interacting regimes. The relevant parameter in order to characterize the transition from the strongly-interacting regime to the MF regime in the 1D trap is  $\xi_1 \equiv Na_{1D}^2/a_z^2 = N\lambda a_{\perp}^2/a_{3D}^2$  [Menotti 2002, Petrov 2000, Dunjko 2001]<sup>3</sup>. The strong-coupling expansion of the trapped bosonic contact, obtained by a similar method as in section III.2.3.1, is given by [Lang 2017]:

$$\mathcal{C} = \frac{N^{5/2}\lambda^{3/2}}{a_{\perp}^3} \left[ \frac{256\sqrt{2}}{45\pi^2} + \sqrt{\xi_1} \left( \frac{70}{9\pi^2} - \frac{8192}{81\pi^4} \right) \right]. \quad (\text{III.2.89})$$

The transition between the three regimes is plotted in Fig. III.2.7.

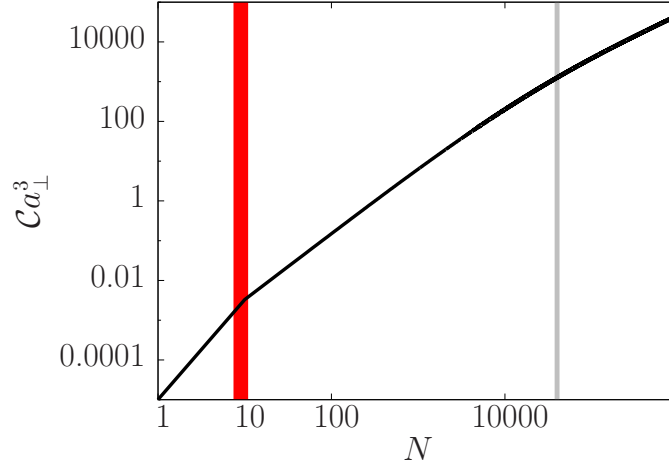
We have summarized the main results for the bosonic contact in highly elongated traps in table III.1.

<sup>3</sup>Alternatively, we could have chosen the  $\alpha_0$  parameter defined in section III.2.3.1.



Regime	TTF	TTF $\rightarrow$ MF	MF	SI
Parameters	$\chi_1 \gg 1$	$\chi_1 \simeq 1$	$\chi_1 \ll 1, \xi_1 \gg 1$	$\xi_1 \ll 1$
$n_1(z)$	$\propto (1 - z^2/Z^2)^2$	$\frac{1}{4a} \left(\frac{\lambda Z}{a_\perp}\right)^2 \left[1 - \left(\frac{z}{Z}\right)^2\right] + \frac{1}{16a} \left(\frac{\lambda Z}{a_\perp}\right)^4 \left[1 - \left(\frac{z}{Z}\right)^2\right]^2$	$\propto (1 - z^2/Z^2)$	$\propto (1 - z^2/Z^2)^{1/2}$
$\tilde{\mathcal{C}}$	$\frac{a_{3D} n_1}{a_\perp^4}$	$\frac{4}{a_\perp^4} \frac{a_{3D}^2 n_1^2}{1 + 4a_{3D} n_1}$	$\frac{4a_{3D}^2 n_1^2}{a_\perp^4}$	$4\pi^2 n_1^4 \left(\frac{1}{3} + 3a_{1D} n_1\right)$
$\mathcal{C}$	$\frac{a_{3D} N}{a_\perp^4}$	Eq. (III.2.86)	$\frac{4(3\lambda)^{\frac{2}{3}}}{5} a_\perp^{-\frac{14}{3}} a_{3D}^{\frac{5}{3}} N^{\frac{5}{3}}$	$\frac{N^{\frac{5}{2}} \lambda^{\frac{3}{2}}}{a_\perp^3} \left[ \frac{256\sqrt{2}}{45\pi^2} + \frac{a_{1D}\sqrt{N\lambda}}{a_\perp} \left( \frac{70}{9\pi^2} - \frac{8192}{81\pi^4} \right) \right]$

**Table III.1:** Contacts  $\tilde{\mathcal{C}}$  and  $\mathcal{C}$  and density profiles in the TTF, MF and 1D strongly interacting (SI) regimes. The transition parameters are given by  $\chi_1 = N\lambda a/a_\perp$  and  $\xi_1 = N\lambda a_\perp^2/a^2$ . In the intermediate regime  $\xi_1 \simeq 1$  between MF and SI, the expressions are not known analytically.



**Figure III.2.7:** Tan's contact  $\mathcal{C}$  (black line) in units of  $a_{\perp}^{-3}$  as a function of the number of bosons  $N$ . The thick vertical red line represents  $\xi_1 = N\lambda a_{\perp}^2/a_{3D}^2 = 1$  and corresponds to the transition from the strongly interacting regime to the MF regime. The left part is plotted using Eq. (III.2.89), the right part using Eq. (III.2.86). The small shift at the transition is due to corrections to Eq. (III.2.89) in the intermediate regime (which are not known analytically). The vertical gray line corresponds to the transition from the MF regime to the TTF regime at  $\chi_1 = N\lambda a_{3D}/a_{\perp} = 1$ . The set of parameters used in these plots is  $(\lambda = 0.0005, a_{3D}/a_{\perp} = 0.05)$ .

### Three-dimensional contact

As we discussed in section III.2.1, Tan's contact paradigm is not specific to 1D. We can indeed define a 3D contact  $\mathcal{C}_{3D}$  analogously to what we did for the 1D contact, which will also verify the (3D) Tan relations. In highly anisotropic traps, it is then natural to wonder how the 1D contact is related to the 3D one. In the quasi-1D regime, which correspond to the MF regime in our case, it can be shown that they are related by a simple geometric factor [Valiente 2012, He 2017]:

$$\mathcal{C}_{3D} = \pi a_{\perp}^2 \mathcal{C}. \quad (\text{III.2.90})$$

Quite remarkably, despite the high non-uniformity of the system in the radial direction, Eq. (III.2.90) shows that, in the quasi-1D regime, the system behaves as if it were a cylinder of radius  $a_{\perp}$  with a constant lineic contact.

In the TTF regime, the numerous excited states should imply non-negligible non-uniformity effects. Indeed, if we perform a 3D treatment similar to what we just did, *i.e.* by doing a LDA on the homogeneous contact obtained by Bogoliubov theory, one obtain in the 3D Thomas-Fermi regime [Chang 2016]:

$$\mathcal{C}_{3D} = \frac{64\pi^2}{7} a_{3D}^2 N n_0, \quad (\text{III.2.91})$$

where  $n_0$  is the atomic density in the center of the trap. Using its expression in highly elongated traps [Baym 1996], we get

$$\mathcal{C}_{3D} = \frac{8\pi}{7} \frac{a_{3D} N}{a_{\perp}^2} \left( \frac{15\lambda N a_{3D}}{a_{\perp}} \right)^{5/2}. \quad (\text{III.2.92})$$

Moreover, in the TTF regime, the radial Thomas-Fermi radius is given by [Pitaevskii 2016]

$$R_{\perp} = 2a_{\perp}(an_1(0))^{1/4}. \quad (\text{III.2.93})$$

Therefore, we have found

$$\begin{aligned} \mathcal{C}_{3D} &= \frac{8}{7}\pi R_{\perp}^2 \frac{a_{3D}N}{a_{\perp}^2} \\ &= S\mathcal{C}_{TTF}, \end{aligned} \quad (\text{III.2.94})$$

where  $S \equiv \frac{8}{7}\pi R_{\perp}^2$  is the cross section of the trap up to a numerical factor that can be accounted for the non-uniformity of the system. This last relation is the generalization of Eq. (III.2.90) to the TTF regime.



---

# Conclusion

---

This thesis has been devoted to the theoretical study of one-dimensional quantum mixtures, in the experimentally relevant case of particles with short-range and strong repulsions trapped in a harmonic potential. These particles are moreover supposed to have equal masses and to be subjected to the same external and interaction potentials regardless of their spin-component, which confers highly symmetric properties to the system. This can be realized using ultracold atoms with a purely nuclear spin, as it was recently achieved in the groundbreaking experiment of the group of L. Fallani in Florence [Pagano 2014].

In the absence of an external harmonic potential, the system is integrable and one disposes of an extremely powerful theoretical tool, namely the Bethe ansatz, which allows in principle to obtain exact results in the system for any range of the interaction strength and temperature. Although integrability is destroyed by the presence of the harmonic potential, the system is also exactly solvable in the fermionized limit of infinite repulsions. In chapter I, we have explained how, exploiting a perturbative ansatz, we have obtained numerically the exact solutions for various few-body systems. Our program works in principle for any number of particles and any kind of quantum mixture. Moreover, we have provided a graph theory interpretation of the perturbative ansatz. Combined with graph spectral theory, an analysis of our system using this interpretation would be an interesting and potentially fruitful perspective.

Once these exact solutions are known exactly, a natural question is to characterize their exchange symmetry. Indeed, although the spatial exchange symmetry of particles belonging to the same component is fixed by their bosonic or fermionic nature, the question is more tricky to address when considering particles belonging to different components. In chapter II, we have described how we have adapted the so-called class-sum method, which allows to characterize to which irreducible representation a wave function belongs, to the perturbative ansatz. We have studied in particular the symmetries of systems with six particles, and analyzed the relation between the ordering of the energy levels and the symmetries. We have shown that our system verifies the celebrated Lieb-Mattis theorem, which states intuitively that it wants to be as symmetric as possible, whatever the kind of mixture (bosonic, fermionic or mixed). Besides, we were able to compare energy levels that are not comparable with this theorem. Moreover, we have highlighted a connection between this energy ordering and the central characters, *i.e.* the eigenvalues of the class-sum operators. If proven, this connection would allow to compare systematically the ordering of energy levels belonging to different symmetry class beyond the scope of the Lieb-Mattis theorem. A possible use of this *a priori* knowledge would then be to

adapt the perturbative ansatz consequently, which would considerably reduce the cost of our calculations.

In the last and longest chapter of this thesis (chapter III), we have studied the one-body correlations in our system. This quantity is of extreme theoretical importance, and can be measured quite easily in a typical ultracold experiment by standard methods such as *in-situ* absorption imaging and time-of-flight techniques. We have obtained a very general formula in order to extract it from a solution obtained by the aforementioned perturbative ansatz. Then, we have analyzed the exact density profiles and momentum distributions of various few-body systems, highlighting the effects of the strong interactions and of the symmetry. We have, in particular, obtained simple rules in order to guess qualitatively the shape of these profiles from symmetry arguments. Thus, the density profiles are so that particles which are submitted to an anti-symmetric exchange (like fermions belonging to the same spin-component) tend to avoid each other, and the momentum distributions contain as many peaks as the number of anti-symmetric exchanges. However, although the role of symmetry is obvious, we have shown that a measurement of the density profile or of the central part of the momentum distribution does not allow to extract uniquely the symmetry class of the system.

Then, we have shown that this experimental symmetry characterization can be realized by a measurement of the so-called Tan's contact, a quantity that governs the algebraic asymptotic behavior of the momentum distributions in short-range interacting quantum gases. Indeed, we have proved that Tan's contact is an increasing function of the symmetry, and thus of the number of components, as observed in [Pagano 2014], which makes it a tool in order to compare symmetries. Moreover, provided that the experiment is sufficiently accurate, we have shown that a measure of Tan's contact allows to infer uniquely the spatial and spin symmetries, and thus that it can be used as a magnetic structure probe.

The previous results were derived in the perfect case of infinite repulsions and zero temperature. In order to be as relevant as possible for experiment, we have then derived scaling laws for Tan's contact.

First, we have obtained a strong coupling expansion for the contact of a balanced fermionic mixture at zero temperature. To do so, we have performed a local density approximation on results obtained in the homogeneous case by Bethe ansatz. Interestingly, although it is derived for a large number of particles, this law is in perfect agreement with the exact results we obtained at infinite interactions and with finite-interaction DMRG results obtained by our collaborators Matteo Rizzi and Johannes Jünemann. This agreement is certainly due to a scale invariance in our system, that would require a deeper treatment, for instance using the renormalization group theory or conformal field theory. Moreover, we have shown that the dependence we have obtained as a function of the number of particles and the number of components is in agreement with previous Monte Carlo simulations [Matveeva 2016] and experimental observations [Pagano 2014].

Second, using a virial expansion, we have obtained an expression for the contact at high temperature and infinite interaction that is valid for any kind of quantum mixture. As in the zero temperature case, we have obtained that the contact is an increasing function of the number of components. Besides, we have shown that it is also an increasing function of

temperature, which is a striking consequence of the dimensional constraint. Furthermore, the contact displays a universal behavior as a function of temperature, since it does not depend explicitly on interactions. A natural perspective would then be to analyze deeper these universal properties by deriving a scaling law for the contact at finite temperature and finite interaction strength simultaneously. This was recently achieved in the simpler case of a one-component Bose gas, in which the presence of a maximum as a function of the temperature for finite interactions was highlighted [Yao 2018].

Finally, we have taken into account the intrinsically three-dimensional nature of interactions in a realistic quasi-one-dimensional trap by studying the influence of the transverse confinement. Using an approach based on Gross-Pitaveskii and Bogoliubov theories combined with a local density approximation, we have obtained a scaling law for the contact of a dilute Bose gas in a highly elongated trap as a function of the aspect ratio, three-dimensional scattering length and number of particles. Moreover, we have checked that it is compatible with results obtained using Lieb-Liniger theory. We have highlighted that the contact has completely different behaviors in the quasi-one-dimensional and three-dimensional cases, and that it can thus be used as an experimental characterization of the dimensional regime. The next step would then be to derive such a scaling for more general quantum mixtures as the ones considered earlier in this thesis.

In addition to the perspectives we mentioned above, many compelling questions remain for further prospects. For example, what happens if we consider systems with unequal masses? In this case, integrability is broken even in the absence of an external confinement, and very little is known on the properties of such systems, although recent semi-analytical developments using hyperspherical coordinates offer promising results for few-body systems [Dehkharghani 2016, Harshman 2017]. More realistic for the case of Bose-Fermi mixtures, an extension of the results discussed in this thesis to these models appears to be a challenging but interesting task.

Furthermore, another interesting issue would be to study the robustness of these features to disorder and quantum chaos by adding a kicked rotor-type potential [Izrailev 1990]. This is motivated by the theoretical observation of  $k^{-4}$  tails in the evolution operator of a system of two interacting bosons in an atomic kicked rotor potential [Qin 2017], suggesting an interesting analogy with Tan's contact physics. In these systems, integrability, correlations, disorder and symmetries would interplay in a non-trivial way, and would possibly allow the occurrence of fascinating many-body features, such as, for example, *many-body localization* [Abanin 2017].





# Appendices



# APPENDIX A

---

## Coordinate Bethe ansatz

In this appendix, we consider a system of  $N$  particles in 1D interacting via the  $\delta$ -type potential (I.1.30), without any external potential. This system is often referred as a *quantum integrable system*. The definition of integrability in quantum physics is not as clear as in classical physics, but one can say, following [Sutherland 2004], that a system is integrable when the scattering events occur without any diffraction. In other words, any scattering will simply result in an exchange of the momenta of the particles. In practice, this implies that the system can be solved using a closed set of equations that is valid for a wide range of parameters — without the need of a perturbative method. The usual way to obtain this set of equations is through the so-called *Bethe ansatz*, an educated guess for the form of the many-body wave-function that was first used by Hans Bethe to solve the 1D Heisenberg XXX model [Bethe 1931]. Since then, the number of models that have been solved with this very powerful and elegant method has been flourishing, ranging from 1D quantum gases in the continuum [Lieb 1963, Gaudin 1967, Yang 1967, Sutherland 1968] and the 1D Hubbard model [Lieb 1968], to 2D classical spin chains [Sutherland 1967, Baxter 1971], or in more recent theories such as string theory in the context of AdS/CFT correspondence [Ambjørn 2006]. Here we obviously focus on the first category of systems, and we try to build an intuitive understanding of this method rather than trying to be exhaustive and perfectly rigorous. After a first general description of the model in A.1, we then describe Lieb and Liniger’s solution for the interacting Bose gas as a pedagogical example in A.2. In the third and biggest part of this appendix, we analyze the more intricate case of a multi-component system in A.3<sup>1</sup>

### A.1. Model and first considerations

We consider a one-dimensional homogeneous (i.e. with no external potential) system of finite size  $L$  containing  $N$  particles of same masses  $m$ , interacting via a  $\delta$ -type potential with an interaction strength  $g_{1D} = 2c$  with  $c > 0$ . In this section, in order to simplify the expressions, we will write the equations in units of  $\hbar = 2m = 1$ . The Schrödinger equation for the many-body wave-function  $\psi(x_1, \dots, x_N)$ , where  $x_j \in [0, L]$  is the coordinate

---

<sup>1</sup>NB: Although only specific results of this appendix will be used in the main text of this thesis (in particular the Bethe ansatz equations of the Lieb-Liniger model and the strong-coupling expansion of the energy in the multi-component case), we have decided to write it as a self-sufficient introduction to coordinate Bethe ansatz. We indeed have the feeling that a complete set of derivations of this method without the use of involved algebraic tools is missing in the literature, despite its importance in the study of one-dimensional quantum gases.

of particle  $j$ , is given by

$$-\sum_{j=1}^N \frac{\partial^2 \psi}{\partial x_j^2} + 2c \sum_{i < j} \delta(x_i - x_j) \psi = E \psi. \quad (\text{A.1.1})$$

As explained in section I.1.3.3, we do not need to specify the symmetry of the many-body wave-function here. Let us suppose that the  $N$  particles are in a given configuration, i.e. that the vector  $\{x\} = (x_1, \dots, x_N)$  is in a given *sector*  $D_Q = x_{Q_1} < x_{Q_2} < \dots < x_{Q_N}$  of  $[0, L]^N$ , where  $Q = (Q_1, \dots, Q_N)$  is a permutation of  $\{1, \dots, N\}$ . Eq. (A.1.1) can be reduced to a free-wave Helmholtz equation

$$\left( \sum_{j=1}^N \frac{\partial^2}{\partial x_j^2} + E \right) \psi = 0, \quad (\text{A.1.2})$$

together with the  $N - 1$  boundaries conditions, for  $j \in \{1, \dots, N - 1\}$ :

$$\psi|_{x_{Q(j+1), Q_j}=0^+} = \psi|_{x_{Q(j+1), Q_j}=0^-} \quad (\text{A.1.3})$$

and

$$\left( \frac{\partial \psi}{\partial x_{Q(j+1)}} - \frac{\partial \psi}{\partial x_{Q_j}} \right) \Big|_{x_{Q(j+1), Q_j}=0^+} - \left( \frac{\partial \psi}{\partial x_{Q(j+1)}} - \frac{\partial \psi}{\partial x_{Q_j}} \right) \Big|_{x_{Q(j+1), Q_j}=0^-} = 2c \psi|_{x_{Q(j+1), Q_j}}, \quad (\text{A.1.4})$$

with  $x_{Q(j+1), Q_j} = x_{Q(j+1)} - x_{Q_j}$ . Eq. (A.1.3) is simply a continuity equation and Eq. (A.1.4) is the cusp condition (I.1.34). Therefore, the *Bethe's hypothesis* consists, in a pretty natural way, in supposing that the solution of Eq. (A.1.1) in the sector  $D_Q$  will be given by a combination of plane waves:

$$\psi|_{\{x\} \in D_Q} = \sum_{P \in \mathfrak{S}_N} \langle Q || P \rangle e^{i(x_{Q_1} k_{P_1} + \dots + x_{Q_N} k_{P_N})}, \quad (\text{A.1.5})$$

where  $\mathfrak{S}_N$  is the set of all permutations of  $\{1, \dots, N\}$  (see section II.1.2.2) and  $\{k\} \in \mathbb{R}^N$  is a set of distinct parameters (pseudo-momenta) associated with the energy

$$E = \sum_{j=1}^N k_j^2. \quad (\text{A.1.6})$$

Now, all the game will consist in finding the coefficients  $\langle Q || P \rangle$  which satisfy the boundary conditions (A.1.3) and (A.1.4) (in order to do that, we will have to have one more set of boundary conditions in  $Q_N - Q_1 = 0$ , which is possible if we ask the particles to be on a circle of size  $L$  and impose  $\psi$  to be periodic). Although the apparent simplicity of Bethe's hypothesis, the considerations allowing to achieve this can be pretty involved. However, if the wave-function  $\psi$  is symmetric by exchange of coordinates, as it is the case in the one-component Bose gas, we will have  $\langle Q || P \rangle = \langle Q' || P \rangle$  for any  $Q, Q' \in \mathfrak{S}_N$ , which will considerably simplify the discussion. This case will be studied in section A.2, and its extension to multi-component systems in section A.3. In both sections, we will derive the sets of *Bethe ansatz equations*, allowing us to extract the ground state and finite-temperature properties in the limit  $N, L \rightarrow \infty$  with  $n = N/L$  kept constant.

## A.2. One-component Bose gas: the Lieb-Liniger model

### A.2.1. Deriving the Bethe ansatz equations

The method employed in this section is pretty much the same as the one used in the original paper of E.H. Lieb and W. Liniger [Lieb 1963]. As told in section A.1, in the one-component Bose gas we have, for any  $Q \in \mathfrak{S}_N$ ,  $\psi|_{\{x\} \in D_Q} = \psi|_{\{x\} \in I}$  where  $D_I = x_1 < \dots < x_N$  is the *fundamental sector* of  $[0, L]^N$ : it is therefore sufficient to obtain the solution (A.1.5) in  $D_I$  and we can write it:

$$\psi|_{\{x\} \in D_I} = \sum_{P \in \mathfrak{S}_N} a(P) e^{i(x_1 k_{P1} + \dots + x_N k_{PN})}, \quad (\text{A.2.1})$$

where  $a(P) = \langle I || P \rangle$  has to satisfy Eqs (A.1.3) and (A.1.4). Moreover, the cusp condition (A.1.4) simply becomes

$$\left( \frac{\partial}{\partial x_{j+1}} - \frac{\partial}{\partial x_j} \right) \psi \Big|_{x_{j+1}=x_j} = c \psi|_{x_{j+1}=x_j}. \quad (\text{A.2.2})$$

Considering  $P \in \mathfrak{S}_N$  and  $P' = P(j, j+1)$  (i.e.  $P$  and  $P'$  are the same except  $P(j+1) = P'j$  and  $Pj = P'(j+1)$ ), Eqs (A.2.1) and (A.2.2) give

$$\begin{aligned} \frac{a(P')}{a(P)} &= \frac{k_{Pj} - k_{P(j+1)} - ic}{k_{Pj} - k_{P(j+1)} + ic} \\ &= -e^{-i\theta(k_{Pj} - k_{P(j+1)})}, \end{aligned} \quad (\text{A.2.3})$$

with

$$\theta(k_{Pj} - k_{P(j+1)}) = -2 \arctan \left( \frac{k_{Pj} - k_{P(j+1)}}{c} \right). \quad (\text{A.2.4})$$

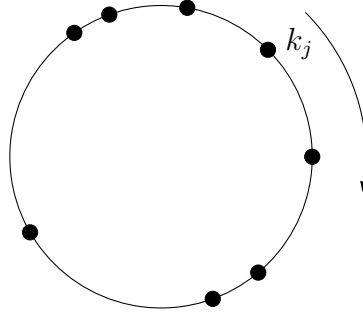
Thus, the two-body scattering between two identical bosons just reduces to a phase factor.

In order to obtain the so-called Bethe ansatz equations, we will have to impose that our system is in fact on a ring of circumference  $L$ , with periodic boundaries conditions for  $\psi$ . This may appear to be strange at first sight, as it seems to restrict a lot the geometry of the system. However, because we are going to consider eventually the thermodynamic limit  $N, L \rightarrow \infty$ , the boundary conditions can be chosen adequately without affecting the relevance of the problem (as often in physics, c.f. quantum field theories). More precisely, the periodic boundary condition on  $\psi$  can be written in  $D_I$ :

$$\psi(x_N - L, x_1, \dots, x_{N-1}) = \psi(x_1, x_2, \dots, x_N). \quad (\text{A.2.5})$$

If we put this condition into Eq. (A.2.1), given Eq. (A.2.3), it implies that for every  $j \in \{1, \dots, N\}$  we have:

$$e^{ik_j L} (-1)^{N-1} \prod_{l=1, l \neq j}^N e^{-i\theta(k_j - k_l)} = 1. \quad (\text{A.2.6})$$



**Figure A.2.1:** Semi-classical interpretation of the Bethe ansatz equations of the Lieb-Liniger model. A boson with pseudo-momentum  $k_j$  scatters with the  $N - 1$  other particles and returns to its initial position after a whole turn around the ring. After this operation, the wave-function will acquire a phase factor  $e^{ik_j L}$  due to turn, and a phase factor  $(-1)^{N-1} \prod_{l=1, l \neq j}^N e^{-i\theta(k_j - k_l)}$  due to the two-body scatterings. The periodic boundary conditions imply that this global phase factor must be equal to 1.

This can be interpreted as the scattering of a particle with pseudo-momentum  $k_j$  with the  $N - 1$  other particles after a whole turn around the ring (see Fig. A.2.1). Then, putting Eq. (A.2.6) in a logarithmic form, we obtain a set of  $N$  coupled equations, namely the Bethe ansatz equations for the Lieb-Liniger model:

$$k_j L = 2\pi I_j + \sum_{l=1, l \neq j}^N \theta(k_j - k_l), \quad (\text{A.2.7})$$

where  $I_j$  is an integer when  $N$  is odd and a half-odd integer otherwise.

What do the numbers  $I_j$  represent? They have to be taken into account in order to remove the ambiguity of the phase when going from Eq. (A.2.6) to Eq. (A.2.7), but they happen to have a deeper physical meaning: they are the *quantum numbers* of the system. In order to understand that, we consider the Tonks limit  $c \rightarrow \infty$  of hardcore bosons. In this case, we observe that  $\theta(k_j^\infty - k_l^\infty) = 0$ , so that the Bethe ansatz equations (A.2.7) simply implies  $k_j^\infty = \frac{2\pi}{L} I_j$  for any  $j \in \{1, \dots, N\}$ . Since we want the  $k_j$  to be different (as it is the case in a one-component Fermi gas), we see that the  $I_j$  have to be different. Thus, the  $I_j$  label the  $k_j$ , and a given set of these numbers will completely characterize the state  $\{k\}$  of the system through the Bethe ansatz equations.

## A.2.2. The ground state

Since  $\theta(\Delta k)$  monotonically increases with  $\Delta k$ , it is clear given Eqs. (A.1.6) and (A.2.7) that the energy  $E$  of the system is minimized when the set of quantum numbers  $I_j$  is as compactly centered around 0 as possible. Therefore, the ground state of the Lieb-Liniger model is characterized by  $I_j \in \{-\frac{N-1}{2}, \dots, \frac{N-1}{2}\}$ . If we choose the  $I_j$  so that  $I_1 < I_2 < \dots < I_N$  we also have

$$\frac{2\pi I_1}{L} < k_1 < \dots < k_N < \frac{2\pi I_N}{L}. \quad (\text{A.2.8})$$

We can now consider the thermodynamic limit, where  $N, L \rightarrow \infty$  with a fixed density  $n = \frac{N}{L}$ . In this case, we define the quasi-momentum distribution  $\rho(k)$  so that the number

of  $k$ 's between in a small interval  $[k, k + dk]$  is  $L\rho(k) dk$ . Similarly to Eq. (A.2.8), the  $k$ 's will be distributed symmetrically between  $q$  and  $-q$ , with  $q$  verifying

$$\int_{-q}^q \rho(k) dk = n. \quad (\text{A.2.9})$$

Then, the discrete summation over  $k$  will become an integral:

$$\sum_{k=1}^N \rightarrow L \int_{-q}^q \rho(k) dk. \quad (\text{A.2.10})$$

The thermodynamic equivalent of the quantum number is found noticing that  $I_j$  counts the number of  $k$ 's between 0 and  $k_j$  (with the same sign as  $k_j$ ). Therefore, we can write Eq. (A.2.7) in the thermodynamic limit:

$$k = 2\pi \int_0^k \rho(k') dk' + \int_{-q}^q \theta(k - k') \rho(k') dk', \quad (\text{A.2.11})$$

which becomes after differentiation

$$1 = 2\pi\rho(k) + \int_{-q}^q \theta'(k - k') \rho(k') dk'. \quad (\text{A.2.12})$$

Using the explicit expression for  $\theta(\Delta k)$  we get

$$1 + 2c \int_{-q}^q \frac{\rho(k') dk'}{c^2 + (k - k')^2} = 2\pi\rho(k). \quad (\text{A.2.13})$$

The ground state energy density  $e = \frac{E}{L}$  can then be obtained with

$$e = \int_{-q}^q k^2 \rho(k) dk. \quad (\text{A.2.14})$$

Together with Eq. (A.2.9), Eq. (A.2.13) completely determines the ground state of the Lieb-Liniger gas in the thermodynamic limit. It is a Fredholm integral equation of the second kind with a kernel of the form

$$K(x, y) = \frac{1}{c^2 + (x - y)^2}. \quad (\text{A.2.15})$$

This kernel, and hence Eq. (A.2.13), is non singular for any  $c > 0$ , guarantying a unique analytic solution. If  $c = 0$  however it becomes singular. This implies in practice that the numerical resolution of Eq. (A.2.13) becomes more and more difficult as one approaches the  $c \rightarrow 0$  limit, and that it is very difficult to obtain small  $c$  asymptotic expansions of physical quantities like the energy. On the contrary, when one approaches the Tonks limit  $c \rightarrow \infty$ , we have  $K(x, y) \approx c^{-2}$ , which leads to

$$e(\gamma) \approx \frac{\pi^2}{3} \left( \frac{\gamma}{\gamma + 2} \right)^2, \quad (\text{A.2.16})$$

where  $\gamma = \frac{c}{n}$  is the natural interaction parameter of our system. The  $\gamma \ll 1$  is a little bit more tricky, but one can check that

$$e(\gamma) \underset{0}{\approx} \gamma. \quad (\text{A.2.17})$$

### A.2.3. Finite temperature thermodynamics

The so-called *thermodynamic Bethe ansatz* was derived by C.N. Yang and C.P. Yang in [Yang 1969]. They observed that in an excited state, the quantum numbers  $I_j$  will still be a set of integers/half-odd integers, but not as compact as possible. There will be omitted lattice sites  $J_j$ , and equivalently omitted  $k$  values. These omitted  $k$  values are called *holes*. Then, in the same way than in section A.2.2, we can define a density  $\rho(k)$  for the number of particles with pseudo-momentum  $k$ , but also a density  $\rho_h(k)$  for the holes. In a similar fashion than for Eq. (A.2.13), we obtain an integral equation for  $\rho$  and  $\rho_h$ :

$$1 + 2c \int_{-\infty}^{\infty} \frac{\rho(k') dk'}{c^2 + (k - k')^2} = 2\pi (\rho(k) + \rho_h(k)), \quad (\text{A.2.18})$$

with  $\rho$  verifying

$$\int_{-\infty}^{\infty} \rho(k) dk = n. \quad (\text{A.2.19})$$

Note that this time we do not restrict the boundaries of integration.

Contrary to the case of the ground state, there is here a degeneracy of the quantum states, which implies a non-zero entropy  $S$ . This degeneracy is given by

$$\frac{[L(\rho + \rho_h) dk]!}{[L\rho dk]![L\rho_h dk]!} \approx \exp [L dk ((\rho + \rho_h) \ln(\rho + \rho_h) - \rho \ln \rho - \rho_h \ln \rho_h)]. \quad (\text{A.2.20})$$

Putting the Boltzmann constant equal to 1, the entropy density is then

$$\frac{S}{L} = \int_{-\infty}^{\infty} ((\rho + \rho_h) \ln(\rho + \rho_h) - \rho \ln \rho - \rho_h \ln \rho_h) dk. \quad (\text{A.2.21})$$

We can therefore write the quantum pressure  $p = \frac{1}{L}[TS - E + \mu N]$ :

$$p = \int_{-\infty}^{\infty} [T((\rho + \rho_h) \ln(\rho + \rho_h) - \rho \ln \rho - \rho_h \ln \rho_h) + (\mu - k^2)\rho] dk. \quad (\text{A.2.22})$$

Then, minimizing  $p$  according to  $\rho$  gives with the help of Eq. (A.2.18):

$$\ln\left(\frac{\rho_h}{\rho}\right) + \frac{c}{\pi} \int_{-\infty}^{\infty} \frac{dk'}{c^2 + (k - k')^2} \ln\left(1 + \frac{\rho}{\rho_h}\right) + \frac{1}{T}[\mu - k^2] = 0. \quad (\text{A.2.23})$$

Defining the *pseudo-energy*  $\epsilon(k) = T \ln\left(\frac{\rho_h}{\rho}\right)$ , Eq. (A.2.23) can be re-written as an integral equation for  $\epsilon$ :

$$\epsilon(k) = -\mu + k^2 - \frac{Tc}{\pi} \int_{-\infty}^{\infty} \frac{dk'}{c^2 + (k - k')^2} \ln\left(1 + e^{-\epsilon(k)/T}\right). \quad (\text{A.2.24})$$

Using Eqs. (A.2.18), (A.2.22) and (A.2.24) yields a very simple expression for the quantum pressure:

$$p = \frac{T}{2\pi} \int_{-\infty}^{\infty} \ln\left(1 + e^{-\epsilon(k)/T}\right) dk. \quad (\text{A.2.25})$$

Thus, given  $\mu$  and  $T$ , one can solve the integral equation (A.2.24) in order to find  $\epsilon$ , and then obtain  $p$  with Eq. (A.2.25). The thermodynamic quantities of interest can then be obtained using

$$L dp = S dT + N d\mu. \quad (\text{A.2.26})$$

Analytics expressions for the Yang-Yang thermodynamics can be found in [Guan 2011].





**Figure A.3.1:** Two possible scattering diagrams for distinguishable particles. The black particle (thick line) can either be reflected against the white one (thin line) or transmitted, corresponding respectively to the left and the right diagram.

## A.3. Extension to the multi-component case

### A.3.1. Scattering operators and consistency

Let us now consider that the particles are no longer identical. In this case, the scattering between two particles with different internal states (let us say a black one and a white one) will have two possible outcomes: either they will transmit or reflect (see Fig. A.3.1). Equivalently, we can say that they can exchange their colors, or not. Then, the scattering processes will no longer be described by a phase factor, as it was the case in the Lieb-Liniger model, but they will have to be described by a *scattering matrix*  $S$ .

In order to construct the  $S$ -matrices of our  $N$ -body problem, we consider the boundary conditions Eqs. (A.1.3) and (A.1.4), as well as  $P, P', Q, Q' \in \mathfrak{S}_N$  with  $P' = P(j, j + 1)$  and  $Q' = Q(j, j + 1)$ . We then obtain the following relations between the coefficients:

$$\langle Q||P \rangle + \langle Q||P' \rangle = \langle Q'||P \rangle + \langle Q'||P' \rangle \quad (\text{A.3.1})$$

for the continuity equation and

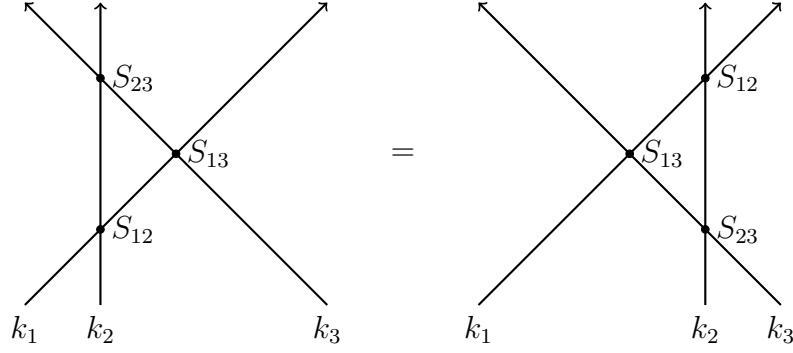
$$i(k_{j+1} - k_j) (\langle Q||P \rangle - \langle Q||P' \rangle + \langle Q'||P \rangle - \langle Q'||P' \rangle) = 2c (\langle Q||P \rangle + \langle Q||P' \rangle) \quad (\text{A.3.2})$$

for the cusp condition. Putting these two relations together brings

$$\langle Q||P' \rangle = \frac{ic}{k_{j+1} - k_j - ic} \langle Q||P \rangle + \frac{k_j - k_{j+1}}{k_j - k_{j+1} + ic} \langle Q'||P \rangle. \quad (\text{A.3.3})$$

Before interpreting this equation, let us first observe that there are  $(N-1)(N!)^2$  equations of this type (since  $j \in \{1, \dots, N-1\}$  and  $P, Q \in \mathfrak{S}_N$ ,  $\mathfrak{S}_N$  having  $N!$  elements), but there are only  $(N!)^2$  coefficients  $\langle Q||P \rangle$ . Therefore, it is a priori not obvious that these equations are consistent with each other and characterize uniquely the coefficients. We postpone this question of consistency to a little bit later.

We see in Eq. (A.3.3) that  $\frac{ic}{k_{j+1} - k_j - ic} \equiv R_{j+1,j}$  is a reflection coefficient ("Q remains Q") and  $\frac{k_j - k_{j+1}}{k_j - k_{j+1} + ic} \equiv T_{j+1,j}$  is a transmission coefficient ("Q becomes  $Q' = Q(j, j + 1)$ "). Let



**Figure A.3.2:** Diagrammatic interpretation of the Yang-Baxter equations, insuring the consistency of our problem.

us organize the  $\langle Q||P \rangle$  coefficients in a  $N! \times N!$  matrix, and denote its columns by  $\zeta_P$ . Considering  $P, P' \in \mathfrak{S}_N$  with  $P' = P(j, l)$ , we can write using Eq. (A.3.3)

$$\zeta_P = \left( R_{l,j} \mathbb{1} + T_{l,j} \hat{P}_{lj} \right) \zeta_{P'}, \quad (\text{A.3.4})$$

where  $\mathbb{1}$  is the identity matrix and  $\hat{P}_{lj}$  is the permutation operator of  $l$  and  $j$ , i.e. with 0 coefficients except when the permutations corresponding to the coordinates are equal up to a transposition  $(j, l)$ . Thus, in all generality, considering two particles  $a$  and  $b$  with momenta  $k_j$  and  $k_l$ , we can define the scattering operator  $S_{jl}^{ab}$  by:

$$S_{jl}^{ab} = R_{jl} \mathbb{1} + T_{jl} \hat{P}_{ab}. \quad (\text{A.3.5})$$

This is called the *reflection representation* of the scattering matrix, because we are considering the columns  $\zeta_P$  and the  $Q$  remains unchanged, so that the reflection coefficients are on the diagonal. Alternatively, we could have defined the *transmission representation* of the scattering matrix  $\tilde{S}_{jl}^{ab} \equiv \hat{P}_{ab} S_{jl}^{ab} = T_{jl} \mathbb{1} + R_{jl} \hat{P}_{ab}$  relating  $\zeta_{P'}$  to  $\hat{P}_{ab} \zeta_P$ .

As told before, in order to be consistent, the set of  $(N-1)(N!)^2$  equations of the form (A.3.3), describing two-body scatterings, should lead to a unique set of  $\langle Q||P \rangle$  coefficients. In other words, if we want to obtain  $\langle Q'||P' \rangle$  from  $\langle Q||P \rangle$  where  $P, Q, P', Q' \in \mathfrak{S}_N$ , it should not depend on the sequence of two-body scatterings we choose. It is sufficient to check this for the three-body case. If we consider an initial state  $(ijk)$  and a final state  $(kji)$ , we want the following diagram to be commutative:

$$\begin{array}{ccccc} (ijk) & \xrightarrow{S_{ij}} & (jik) & \xrightarrow{S_{ik}} & (jki) \\ S_{jk} \downarrow & & & & S_{jk} \downarrow \\ (ikj) & \xrightarrow{S_{ik}} & (kij) & \xrightarrow{S_{ij}} & (kji) \end{array} \quad (\text{A.3.6})$$

In terms of the scattering matrices of Eq. (A.3.5), the consistency equations then read:

$$S_{ij}^{bc} S_{ik}^{ab} S_{jk}^{bc} = S_{jk}^{ab} S_{ik}^{bc} S_{ij}^{ab}. \quad (\text{A.3.7})$$

This set of ternary relations constitute the celebrated Yang-Baxter equations [Yang 1967]. It is easy to check that they are verified in our system, confirming that our problem is consistent and can be reduced to two-body scatterings. Note that this consistency was trivially verified in the Lieb-Liniger gas of section A.2, as the scattering only consisted in a phase change. A graphical interpretation of Eq. (A.3.7) is given in Fig. A.3.2.

Thus, if we obtain  $\zeta_I$  for a given set of pseudo-momentum, all the  $\zeta_P$ 's are determined. We can now suppose that we have the periodic boundary conditions and do the same procedure as in section A.2, i.e. we let a particle with pseudo-momentum  $k_j$  make a whole turn around the ring (see Fig. A.3.3), and we get for all  $j \in \{1, \dots, N\}$ :

$$e^{ik_j L} \zeta_I = \tilde{S}_{(j+1)j}^{(j+1)j} \times \tilde{S}_{(j+2)j}^{(j+2)j} \times \cdots \times \tilde{S}_{Nj}^{Nj} \times \tilde{S}_{1j}^{1j} \times \cdots \times \tilde{S}_{(j-1)j}^{(j-1)j} \zeta_I. \quad (\text{A.3.8})$$

In this form, the Bethe ansatz equations are a set of  $N$  coupled eigenvalue equations, with the same eigenvector  $\zeta_I$ . In the thermodynamic limit, this set of equations is impossible to solve in practice. Hopefully, there are some clever methods to simplify it, when taking into account the fundamental symmetries of our multi-component system. The most complete and efficient method to do it is called the *Quantum Inverse Scattering Method* [Korepin 1993], but is not very intuitive. Rather than expose it here, which would be unnecessary long and involved, we will try to justify the shape of the equations in order to have a intuitive understanding of their meaning. We start with the Gaudin-Yang model for the two-component fermionic model in section A.3.2, and extend it to the general case in section A.3.3.

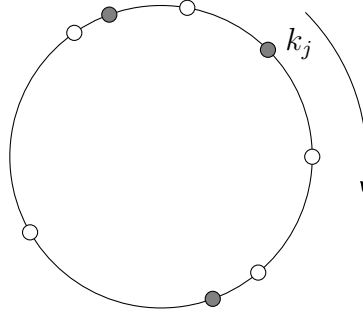
## A.3.2. Two-component fermions: the Gaudin-Yang model

### A.3.2.1. The Bethe-Yang hypothesis

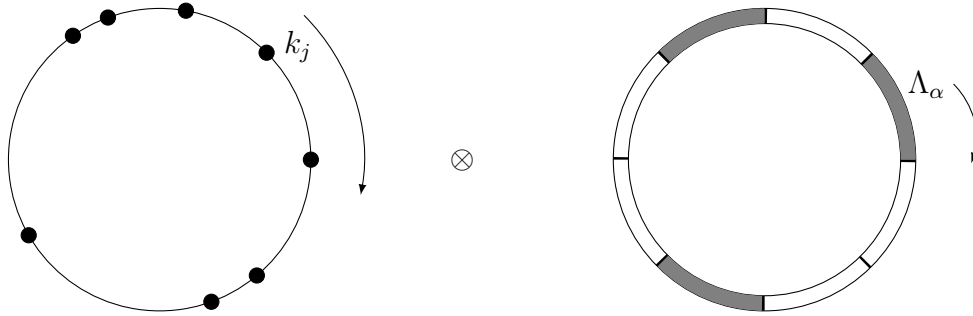
We consider the case of  $N$  spin- $\frac{1}{2}$  particles, divided in  $M$  spins down and  $N - M$  spins up (these numbers are fixed). This model was solved by Gaudin in [Gaudin 1967] and C.N. Yang in [Yang 1967]. They noticed that the problem can be separated between the configuration/spin part on the one side and the pseudo-momentum/spatial part where we forget the color/spin of the particles (i.e. analogous to the Lieb-Liniger case) on the other side. Both sides of the problem are of course coupled through the scattering processes. Due to the anti-symmetric nature of same-component fermions, for a given  $P \in \mathfrak{S}_N$ , there will be only  $C_M^N$  independent coefficients of the form  $\langle Q||P \rangle$ . Then, it is sufficient to know  $\langle Q||P \rangle$  for a given set of positions  $\{y_1 < \cdots < y_M\} \subset \{1, \dots, N\}$  of the  $M$  spin downs. Therefore, the quantity of interest for this model, called the *spin wave function* by Yang, can be written:

$$\phi(y_1, \dots, y_M || P) = \epsilon_P \langle Q||P \rangle, \quad (\text{A.3.9})$$

where  $y_1 < \cdots < y_M$  are the positions of the  $M$  spins down and  $\epsilon_P$  is the signature of the permutation  $P$  which takes into account the fermionic nature of the problem. Thus, the spin part of the problem can be seen as a discrete problem of down spins on a chain of length  $N$ . Similarly to the continuous spatial part where each particle has a pseudo-momentum  $k_j$ , each spin down  $y_\alpha$  will carry a momentum-like quantity, namely a *rapidity*



**Figure A.3.3:** Semi-classical interpretation of the Bethe ansatz equations for the two-component model ( $N = 8$  and  $M = 3$ ). Contrary to the Lieb-Liniger case, the scatterings would have to take into account the possibility of a reflection and a transmission, and would therefore be described by  $S$ -matrices.



**Figure A.3.4:** Another way to interpret the two-component model, equivalent to Fig. A.3.3. Here, the problem is separated between two coupled parts, a spatial part (left), and a spin part (right). The spin part can be seen as  $M$  spin downs on a discrete chain of length  $N$ . A rapidity  $\Lambda_\alpha$  is associated with each spin down.

$\Lambda_\alpha$ , which will characterize how the spins will evolve through the scattering processes (this affirmation will be further justified below). Using this observation, Yang made the following generalized Bethe hypothesis (often called the *Bethe-Yang hypothesis*) for the form of  $\phi$ :

$$\phi(y_1, \dots, y_M || P) = \sum_{R \in \mathfrak{S}_M} b(R) F_P(y_1, \Lambda_1) F_P(y_2, \Lambda_2) \cdots F_P(y_M, \Lambda_M), \quad (\text{A.3.10})$$

where the  $F_P$  function and the  $b(R)$  coefficients remain to be determined, and  $\Lambda_1, \dots, \Lambda_M$  are a set of unequal numbers. We summarize these considerations in Fig. A.3.4.

In order to determine  $F_P$ , let us first consider the two-body problem where  $N = 2$  and  $M = 1$ . Using previous notations (see section A.3.1), the scattering process reduces to

$$\zeta_{(21)} = S_{12}^{-1} \zeta_{(12)}. \quad (\text{A.3.11})$$

One can check that, for every value of  $\Lambda \in \mathbb{R}$ , the following set of coefficients verifies Eq. (A.3.11) [Colome-Tatche 2008]:

$$\begin{aligned} \phi(1 || (12)) &= k_1 - \Lambda - \frac{ic}{2}, \\ \phi(2 || (12)) &= -(k_2 - \Lambda + \frac{ic}{2}). \end{aligned} \quad (\text{A.3.12})$$

We see that the parameter  $\Lambda$  is homogeneous to a momentum. If we consider the  $N = 3$ ,  $M = 1$  case, the boundary conditions for  $\phi$  can be written for  $j \in 1, 2, 3$  and  $P, P' \in \mathfrak{S}_3$  where  $P' = P(j, j + 1)$ :

$$\begin{aligned}\phi(y||P) &= \phi(y||P') \quad \text{if } y \neq j, j + 1, \\ \phi(j||P) &= -R_{j+1,j}\phi(j||P') + T_{j+1,j}\phi(j + 1||P'), \\ \phi(j + 1||P) &= -R_{j+1,j}\phi(j + 1||P') + T_{j+1,j}\phi(j||P').\end{aligned}\tag{A.3.13}$$

For any  $\Lambda, b \in \mathbb{R}$ , a solution is given by:

$$\begin{aligned}\phi(1||P) &= b(k_{P2} - \Lambda - \frac{ic}{2})(k_{P3} - \Lambda - \frac{ic}{2}), \\ \phi(2||P) &= b(k_{P1} - \Lambda + \frac{ic}{2})(k_{P3} - \Lambda - \frac{ic}{2}), \\ \phi(3||P) &= b(k_{P1} - \Lambda + \frac{ic}{2})(k_{P2} - \Lambda + \frac{ic}{2}).\end{aligned}\tag{A.3.14}$$

Generalizing to  $N$  particles with  $M = 1$  down spin, we have obtained the form of the functions  $F_P(y, \Lambda)$ :

$$F_P(y, \Lambda) = \prod_{j=1}^{y-1} (k_{Pj} - \Lambda + \frac{ic}{2}) \prod_{l=y+1}^N (k_{Pl} - \Lambda - \frac{ic}{2}).\tag{A.3.15}$$

We are now able to determine  $b(R)$ . We can write the boundary conditions in the general case in terms of  $\bar{\phi} \equiv \phi(y_1, \dots, y_M||P)$ , for  $P, P' \in \mathfrak{S}_N$  with  $P' = P(j, j + 1)$  and  $j \in \{1, \dots, N\}$ :

$$\begin{aligned}\bar{\phi} &= \phi(y_1, \dots, y_M||P') \quad \text{if } \forall l, y_l \neq j, j + 1 \quad \text{or if } \exists l, y_l = j, y_{l+1} = j + 1, \\ \bar{\phi} &= -R_{j+1,j}\phi(y_1, \dots, y_l, \dots, y_M||P') + T_{j+1,j}\phi(y_1, \dots, y_l + 1, \dots, y_M||P') \\ &\quad \text{if } y_l = j, y_{l+1} \neq j + 1, \\ \bar{\phi} &= -R_{j+1,j}\phi(y_1, \dots, y_l, \dots, y_M||P') + T_{j+1,j}\phi(y_1, \dots, y_l - 1, \dots, y_M||P') \\ &\quad \text{if } y_l \neq j, y_{l+1} = j + 1.\end{aligned}\tag{A.3.16}$$

Then, if we consider  $R, R' \in \mathfrak{S}_M$  with  $R' = R(l, l + 1)$  and  $P, P' \in \mathfrak{S}_N$  with  $P' = P(y_l, y_{l+1})$ , we get using Eq. (A.3.10):

$$\begin{aligned}b(R)F_P(y_l, \Lambda_{Rl})F_P(y_l + 1, \Lambda_{R(l+1)}) &+ b(R')F_P(y_l, \Lambda_{R(l+1)})F_P(y_l + 1, \Lambda_{Rl}) \\ &= b(R)F_{P'}(y_l, \Lambda_{Rl})F_{P'}(y_l + 1, \Lambda_{R(l+1)}) + b(R')F_{P'}(y_l, \Lambda_{R(l+1)})F_{P'}(y_l + 1, \Lambda_{Rl}),\end{aligned}\tag{A.3.17}$$

which becomes, using  $F$ 's expression of Eq. (A.3.15):

$$b(R)(\Lambda_{R(l+1)} - \Lambda_{Rl} - ic) = -b(R')(\Lambda_{Rl} - \Lambda_{R(l+1)} - ic).\tag{A.3.18}$$

In order for this condition to be satisfied in the general case, we can choose:

$$b(R) = \epsilon_R \prod_{j < l} (\Lambda_{Rj} - \Lambda_{Rl} - ic).\tag{A.3.19}$$

Thus, Eqs. (A.3.10), (A.3.15) and (A.3.19) completely determine the solution for the Gaudin-Yang model as a function of the rapidities and pseudo-momenta. We can now apply the periodic boundary conditions in order to determine these parameters.

### A.3.2.2. Bethe ansatz equations and ground state

Similarly to the Lieb-Liniger model, we suppose now that the total wave function follows the periodic boundary condition of Eq. (A.2.5), namely  $\psi(x_N - L, x_1, \dots, x_{N-1}) = \psi(x_1, x_2, \dots, x_N)$ . Equivalently, we say that the particle  $N$  with momentum  $k_j$  will make a whole turn around the ring (c.f. Fig. A.3.3). Here, we have to distinct two possibilities: the case where particle  $N$  is a spin up and the case where it is a spin down. In terms of  $\phi$ , for  $P, P' \in \mathfrak{S}_N$  where  $P' = (PN, P1, P2, \dots, P(N-1))$ , these cases can be written respectively:

$$\phi(y_1, \dots, y_M) ||P\rangle e^{ik_{PN}L} = \phi(y_1 + 1, \dots, y_M + 1) ||P'\rangle, \quad (\text{A.3.20})$$

and

$$\phi(y_1, \dots, y_{M-1}, N) ||P\rangle e^{ik_{PN}L} = \phi(1, y_1 + 1, \dots, y_{M-1} + 1) ||P'\rangle. \quad (\text{A.3.21})$$

Using  $\phi$ 's complete expression within the Bethe-Yang hypothesis (Eqs. (A.3.10), (A.3.15) and (A.3.19)) yields

$$\begin{aligned} e^{ik_{PN}L} &= \prod_{\beta=1}^M \frac{k_{PN} - \Lambda_\beta + \frac{ic}{2}}{k_{PN} - \Lambda_\beta - \frac{ic}{2}}, \\ \prod_{j=1}^N \frac{k_j - \Lambda_{RM} + \frac{ic}{2}}{k_j - \Lambda_{RM} - \frac{ic}{2}} &= - \prod_{\beta=1}^M \frac{\Lambda_{RM} - \Lambda_\beta - ic}{\Lambda_{RM} - \Lambda_\beta + ic}. \end{aligned} \quad (\text{A.3.22})$$

Taking the logarithmic form, we obtain the  $N + M$  Bethe ansatz equations for the Gaudin-Yang model:

$$\begin{aligned} k_j L &= 2\pi I_j + \sum_{\beta=1}^M \theta(2k_j - 2\Lambda_\beta), \quad j \in \{1, \dots, N\}, \\ - \sum_{j=1}^N \theta(2\Lambda_\alpha - 2k_j) &= 2\pi J_\alpha - \sum_{\beta=1}^M \theta(\Lambda_\alpha - \Lambda_\beta), \quad \alpha \in \{1, \dots, M\}, \end{aligned} \quad (\text{A.3.23})$$

where the phase  $\theta$  is defined as in Eq. (A.2.4), and  $I_j, J_\alpha$  are the quantum numbers of this model. We can observe the power of Bethe-Yang hypothesis by comparing Eqs (A.3.23) and (A.3.8): here, we have only added  $M$  scalar equations as compared to the one-component case!

Just like for the Lieb-Liniger model, the quantum numbers will define the ground state when  $I_j \in \{-\frac{N-1}{2}, \dots, \frac{N-1}{2}\}$  and  $J_\alpha \in \{-\frac{M-1}{2}, \dots, \frac{M-1}{2}\}$ . We can then take the thermodynamic limit  $N, M, L \rightarrow \infty$  keeping  $n = \frac{N}{L}$  and  $n_\downarrow = \frac{M}{L}$  constant, and define the quasi-momentum and spin distributions verifying respectively

$$\int_{-q}^q \rho(k) dk = n, \quad (\text{A.3.24})$$

and

$$\int_{-s}^s \sigma(\Lambda) d\Lambda = n_\downarrow. \quad (\text{A.3.25})$$

We finally get the integral equations for the ground state:

$$\begin{aligned} 1 + 4c \int_{-s}^s \frac{\sigma(\Lambda) d\Lambda}{c^2 + 4(k - \Lambda)^2} &= 2\pi \rho(k), \\ - 2c \int_{-s}^s \frac{\sigma(\Lambda') d\Lambda'}{c^2 + (k - \Lambda')^2} + 4c \int_{-q}^q \frac{\rho(k) dk}{c^2 + 4(k - \Lambda)^2} &= 2\pi \sigma(\Lambda). \end{aligned} \quad (\text{A.3.26})$$

The ground state energy density can then be obtained using

$$e = \int_{-q}^q k^2 \rho(k) dk. \quad (\text{A.3.27})$$

### A.3.3. General case: the nested Bethe ansatz

#### A.3.3.1. Bethe ansatz equations

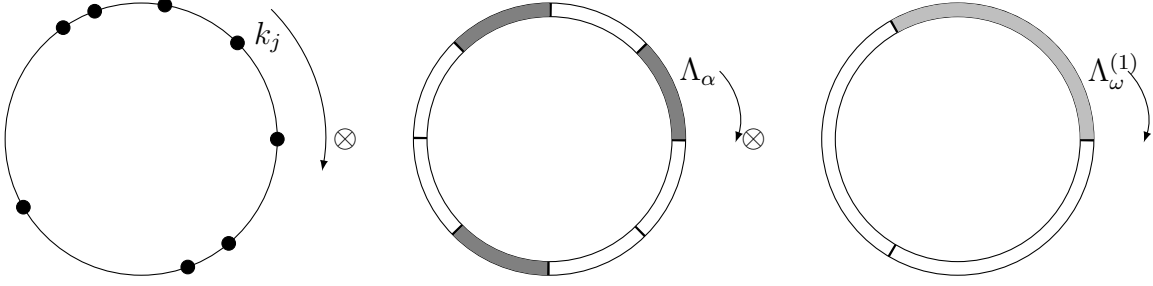
The model of  $\kappa$ -component fermions was solved by Sutherland in [Sutherland 1968]. Without entering the details, the idea is to apply successively the Bethe-Yang hypothesis to the coefficients of the spin wave-functions, resulting in Bethe ansatz equations of smaller and smaller dimensions (hence the name of *nested Bethe ansatz*). More precisely, let us consider the case of a three-component model of  $N$  particles with  $N - M$  particles of type 1,  $M - M_1$  particles of type 2 and  $M_1$  particles of type 3. We can first separate the  $N - M$  type-1 particles and the  $M$  other, and treat the problem similarly to the Gaudin-Yang model of section A.3.2. Since the  $M$  "other particles" are of different type, we will have to write the Bethe-Yang hypothesis of Eq. (A.3.10) in a different form, taking into account the permutations of the  $M$  particles. This is exactly what we did when we went from the Lieb-Liniger model of section A.2 to the Gaudin-Yang model of two-component fermions. Thus, if  $Q \in \mathfrak{S}_M$ , the spin wave-function  $\phi$  for the  $M$  particles is written in the (discrete) sector  $1 \leq y_{Q1} < \dots < y_{QM} \leq N$ :

$$\phi = \sum_{P \in \mathfrak{S}_M} \langle Q || P \rangle F(\Lambda_{P1}, y_{Q1}) \cdots F(\Lambda_{PM}, y_{QM}). \quad (\text{A.3.28})$$

We can then repeat the same procedure as in section A.3.1, namely we arrange the coefficients  $\langle Q || P \rangle$  in a  $M! \times M!$  matrix, translate the boundary conditions in terms of scattering matrices and check the consistency of our problem guaranteed by the Yang-Baxter equations. Then, we can separate the  $M$  particles between the  $M - M_1$  type-2 and the  $M_1$  type-3 particles and re-apply the Bethe-Yang hypothesis for the coefficients  $\langle Q || P \rangle$ , introducing rapidities  $\Lambda^{(1)}$  for the type-3 particles. Finally, after applying the usual periodic boundary conditions, we find:

$$\begin{aligned} e^{ik_j L} &= \prod_{\beta=1}^M \frac{k_j - \Lambda_\beta + \frac{ic}{2}}{k_j - \Lambda_\beta - \frac{ic}{2}}, \quad j \in \{1, \dots, N\}, \\ \prod_{j=1}^N \frac{k_j - \Lambda_\alpha + \frac{ic}{2}}{k_j - \Lambda_\alpha - \frac{ic}{2}} &= - \prod_{\beta=1}^M \frac{\Lambda_\alpha - \Lambda_\beta - ic}{\Lambda_\alpha - \Lambda_\beta + ic} \prod_{\gamma=1}^{M_1} \frac{\Lambda_\alpha - \Lambda_\gamma^{(1)} + \frac{ic}{2}}{\Lambda_\alpha - \Lambda_\gamma^{(1)} - \frac{ic}{2}}, \quad \alpha \in \{1, \dots, M\}, \\ \prod_{\beta=1}^M \frac{k_j - \Lambda_\beta + \frac{ic}{2}}{k_j - \Lambda_\beta - \frac{ic}{2}} &= - \prod_{\gamma=1}^{M_1} \frac{\Lambda_\omega^{(1)} - \Lambda_\gamma^{(1)} - ic}{\Lambda_\omega^{(1)} - \Lambda_\gamma^{(1)} + ic}, \quad \omega \in \{1, \dots, M_1\}. \end{aligned} \quad (\text{A.3.29})$$

Long story short, we can again consider the logarithm form of Eq. (A.3.29), introducing the  $N + M + M_1$  quantum numbers  $I_j, J_\alpha, K_\omega$  for the three-component model, which have to be as compactly centered as possible around the origin when considering the ground state. After that, we can consider the thermodynamic limit with fixed densities, in a very similar manner as we did before, resulting in three coupled integral equations



**Figure A.3.5:** Semi-classical interpretation of the nested Bethe ansatz equations for the 3-component gas, with five particles of type 1, two particles of type 2 and one particle of type 3. A pseudo-momentum  $k_j$  is associated with each of the eight particles (left), a rapidity  $\Lambda_\alpha$  with each of the three particles of type 2 and 3 (center), and a rapidity  $\Lambda_\omega^{(1)}$  for the particle of type 3 (right).

for the distributions  $\rho(k)$ ,  $\sigma(\Lambda)$ , and  $\tau(\Lambda^{(1)})$ . An illustration of the nested Bethe ansatz is given in Fig. A.3.5.

Following these ideas, in the case of a  $\kappa$ -component Fermi gas divided in  $[m_1, \dots, m_\kappa]$  particles per species, we can define a set of  $\kappa$  rapidities, distributions and integration limits denoted respectively  $k_i$ ,  $\rho_i(k_i)$  and  $B_i$ . Defining  $M_i = \sum_{j=i}^{\kappa} m_j$  for all  $i \in \{1, \dots, \kappa\}$ , we can write the  $\kappa$  coupled integral Bethe ansatz equations for the ground state in the thermodynamic limit:

$$\begin{aligned}
 2\pi\rho_1 &= 1 + 4c \int_{-B_2}^{B_2} \frac{\rho_2 dk_2}{c^2 + 4(k_1 - k_2)^2}, \\
 \int_{-B_{i+1}}^{B_{i+1}} \frac{4c\rho_{i+1} dk_{i+1}}{c^2 + 4(k_i - k_{i+1})^2} + \int_{-B_{i-1}}^{B_{i-1}} \frac{4c\rho_{i-1} dk_{i-1}}{c^2 + 4(k_i - k_{i-1})^2} &= 2\pi\rho_i + \int_{-B_i}^{B_i} \frac{2c\rho_i dk'_i}{c^2 + (k_i - k'_i)^2} \\
 &\quad \text{for } i \in \{2, \dots, \kappa - 1\}, \\
 \int_{-B_{\kappa-1}}^{B_{\kappa-1}} \frac{4c\rho_{\kappa-1} dk_{\kappa-1}}{c^2 + 4(k_\kappa - k_{\kappa-1})^2} &= 2\pi\rho_\kappa + \int_{-B_\kappa}^{B_\kappa} \frac{2c\rho_\kappa dk'_\kappa}{c^2 + (k_\kappa - k'_\kappa)^2},
 \end{aligned} \tag{A.3.30}$$

together with the following normalization conditions:

$$\frac{M_i}{L} = \int_{-B_i}^{B_i} \rho_i dk_i, \quad i \in \{1, \dots, \kappa\}, \tag{A.3.31}$$

and the formula for the ground state energy density:

$$e = \int_{-B_1}^{B_1} \rho_1 k_1^2 dk_1. \tag{A.3.32}$$

### A.3.3.2. Strong-coupling expansion in the balanced fermionic case

In general, Eqs. (A.3.30) are very hard to solve in practice. In particular, the boundaries  $B_i$  are not easy to evaluate. Hopefully, in the balanced case, there are some simplifications that allow to access a strong-coupling expansion for the ground-state



energy (Eq. (A.3.32)). Here, we provide the ideas for the proof of this expansion, following [Guan 2012].

First, the key property is that the fact that a fermionic mixture is balanced implies that the boundaries verify  $B_i \rightarrow \infty$  for every  $i \geq 2$ . Indeed, by integrating Eq. (A.3.30) we obtain for every  $i \geq 2$ :

$$\int_{-\infty}^{\infty} \rho_i(k) dk = \frac{M_{i-1}}{L} - \frac{M_i}{L} + \frac{M_{i+1}}{L} = \frac{M_i}{L} \quad (\text{A.3.33})$$

in the balanced case. It is then clear, by comparing to Eq. (A.3.32), that all boundaries except  $B_1$  go to infinity.

Writing the Fourier transform of  $\rho_i(k)$  as  $\tilde{\rho}_i(\omega)$  and introducing the function  $\rho_{1in}(k) \equiv \theta_{[-B_1, B_1]}(k) \rho_1(k)$  where  $\theta_{[-B_1, B_1]}$  is the indicator function of  $[-B_1, B_1]$ , we can now Fourier transform Eqs. (A.3.30) and find after some algebra, for every  $i \geq 2$ :

$$\tilde{\rho}_i(\omega) = \frac{\tilde{\rho}_{1in}(\omega) \sinh \left[ \frac{1}{2}(\kappa - i + 1)|\omega|c \right]}{\sinh \left[ \frac{1}{2}\kappa|\omega|c \right]}. \quad (\text{A.3.34})$$

Then, the condition  $c \gg 1$  allows to perform perturbative developments of the kernels of integrals in Eqs. (A.3.30) (c.f. the Lieb-Liniger case, section A.2.2). By doing so and using Eqs. (A.3.34), (A.3.31) and (A.3.32), Guan *et al* have obtained:

$$\tilde{\rho}_{1in}(\omega) \approx n - \frac{e\omega^2}{2}, \quad \tilde{\rho}_2(\omega) \approx \frac{\sinh \left[ \frac{1}{2}(\kappa - 1)|\omega|c \right]}{\sinh \left[ \frac{1}{2}\kappa|\omega|c \right]} \left[ n - \frac{e\omega^2}{2} \right]. \quad (\text{A.3.35})$$

Plugging this equation into the first line of Eq. (A.3.30) yields:

$$\rho_1(k) = \frac{1}{2\pi} + \frac{nY_0(k)}{2\pi} - \frac{eY_2(k)}{4\pi} + \mathcal{O}(c^{-4}), \quad (\text{A.3.36})$$

with

$$Y_\alpha(k) = \int d\omega \frac{\sinh \left[ \frac{1}{2}(\kappa - 1)|\omega|c \right]}{\sinh \left[ \frac{1}{2}\kappa|\omega|c \right]} \exp(i\omega k - c|\omega|/2) \omega^\alpha. \quad (\text{A.3.37})$$

In the  $c \rightarrow \infty$  limit, it can be shown that

$$Y_0(k) = \frac{2Z_1(\kappa)}{c} - \frac{2Z_3(\kappa)k^2}{c^3} + \mathcal{O}(c^{-4}) \quad (\text{A.3.38})$$

and

$$Y_2(k) = \frac{4Z_3(\kappa)}{c^3} + \mathcal{O}(c^{-4}), \quad (\text{A.3.39})$$

with

$$Z_1(\kappa) = -\frac{1}{\kappa} \left( \psi \left( \frac{1}{\kappa} \right) + C_{Euler} \right), \quad (\text{A.3.40})$$

and

$$Z_3(\kappa) = \frac{1}{\kappa^3} \left( \zeta \left( 3, \frac{1}{\kappa} \right) - \zeta(3) \right), \quad (\text{A.3.41})$$

where  $C_{Euler} \approx 0.577$  is the Euler constant and  $\psi$  and  $\zeta$  are respectively the Digamma and Riemann Zeta functions [Abramowitz 1965]. Then, plugging Eq. (A.3.36) into Eqs (A.3.31) and (A.3.32) gives, after some calculations, Eq. (III.2.34) of the main text.

### A.3.4. Thermodynamic Bethe ansatz

The thermodynamic Bethe ansatz for multi-component fermions was obtained by Takahashi and Lai for two-component fermions [Takahashi 1971, Lai 1971] and was extended to  $\kappa$  components by Schlottmann [Schlottmann 1993]. Although the global idea is similar to the Yang-Yang case of section A.2.3, that is considering the excited states in terms of particle and hole densities, there is one fundamental difference. Indeed, in section A.2.3 we were only considering real pseudo-momenta: a complex pseudo-momentum means the an exponentially decreasing wave-function as a function of the relative distance between particles, which is not the case when  $c > 0$ . When considering multicomponent fermions however, we have introduced spin rapidities  $\Lambda$  which have no reason to be real numbers for excited states. The so-called *string hypothesis* assumes that the complex spin-rapidities of excited states form discrete strings of arbitrary length  $(2m - 1)$  where  $m \geq 1$ :

$$\Lambda_m = \xi_m + i\nu \frac{c}{2} + \delta(L), \quad \nu \in \{-(m-1), \dots, m-1\}, \quad (\text{A.3.42})$$

where  $\xi \in \mathbb{R}$  and  $\delta(L)$  vanishes in the thermodynamic limit. The intuitive idea behind this hypothesis is that if a spin rapidity has an imaginary part, it will result in exponentially vanishing terms in the Bethe ansatz equations which would have to be compensated by poles in the  $\frac{\Lambda-k-\frac{ic}{2}}{\Lambda-k+\frac{ic}{2}}$  factors, which is achieved when the complex rapidities are separated by  $\frac{ic}{2}$ . As compared with the Yang-Yang case when we were going from Eq. (A.2.13) for the ground state to Eq. (A.2.18) for the excited states, the excited analogous of Eq. (A.3.30) will contain sums over strings of arbitrary length for each class of spin rapidities. We adapt the notations of Eq. (A.3.30) in the following way:  $\rho \equiv \rho_1$  and  $\sigma_m^{(l)}(\Lambda)$  is the density for strings of length  $m$  associated with real rapidities  $k_{l+1}$ , so that

$$\begin{aligned} \frac{N}{L} &= \frac{M_1}{L} = \int dk \rho(k), \\ \frac{M_{l+1}}{L} &= \sum_{m=1}^{\infty} m \int d\Lambda \sigma_m^{(l)}(\Lambda), \quad l \in \{1, \dots, \kappa - 1\}. \end{aligned} \quad (\text{A.3.43})$$

We define the associated hole densities  $\rho_h$  and  $\sigma_{mh}^{(l)}(\Lambda)$  analogously to section A.2.3, as well as the pseudo-energies  $\epsilon(k) = T \ln \left( \frac{\rho_h}{\rho} \right)$  and  $\varphi_m^{(l)}(\Lambda) = T \ln \left( \frac{\sigma_{mh}^{(l)}}{\sigma_m^{(l)}} \right) = T \ln(\eta_m^{(l)})$ . We can then define an entropy density for each class of excitations, and minimize the free energy of the system given the constraints of Eq. (A.3.43), each of them being associated with a Lagrange multiplier  $A_l$  ( $A_0$  is the chemical potential  $\mu$  of section A.2.3). After some (tedious) algebra, we find the analogous of the integral equation (A.2.24) in the

multicomponent case:

$$\begin{aligned}
\epsilon(k) &= k^2 - A_0 - \frac{T}{\pi} \sum_{m=1}^{\infty} \int d\Lambda \frac{\frac{mc}{2}}{(\Lambda - k)^2 + \left(\frac{mc}{2}\right)^2} \ln \left(1 + \eta_m^{(1)}(\Lambda)^{-1}\right), \\
\ln \left(1 + \eta_m^{(l)}(\Lambda)\right) &= -\frac{mA_l}{T} \sum_{n=1}^{\infty} \int d\Lambda' D_{mn}(\Lambda - \Lambda') \ln \left(1 + \eta_n^{(l)}(\Lambda')^{-1}\right) \\
&\quad - \sum_{n=1}^{\infty} \int d\Lambda' C_{mn}(\Lambda - \Lambda') \ln \left(1 + \eta_n^{(l+1)}(\Lambda')^{-1}\right) \ln \left(1 + \eta_n^{(l-1)}(\Lambda')^{-1}\right) \\
&\hspace{15em} \text{for } l \in \{1, \dots, \kappa - 1\} \text{ and } m \in \mathbb{N}^*,
\end{aligned} \tag{A.3.44}$$

where we have  $D_{mn}(\Lambda) = \mathcal{F} [\coth(|\omega c|/2) \{ \exp(-|n - m||\omega c|/2) - \exp(-(n + m)|\omega c|/2) \}]$  and  $C_{mn}(\Lambda) = \mathcal{F} [\hat{D}_{mn}(\omega)/(2 \cosh(\omega c/2))]$  ( $\mathcal{F}$  being the Fourier transform operator),  $\eta_1^{(0)} = \exp(\epsilon/T)$  and  $\eta_m^{(0)} = \infty$  for  $m \geq 2$ , and  $\eta_m^{(\kappa)} = \infty$ . We see that in this case, the pseudo-energies are given by an *infinite* set of coupled integral equations! Then, one can extract the quantum pressure using Eq. (A.2.25).



# APPENDIX B

---

## List of publications

- **J. Decamp**, P. Armagnat, B. Fang, M. Albert, A. Minguzzi and P. Vignolo, *Exact density profiles and symmetry classification for strongly interacting multi-component Fermi gases in tight waveguides*, New J. Phys. **18**, 055011 (2016)
- **J. Decamp**, J. Jünemann, M. Albert, M. Rizzi, A. Minguzzi, P. Vignolo, *High-momentum tails as magnetic-structure probes for strongly correlated  $SU(\kappa)$  fermionic mixtures in one-dimensional traps*, Phys. Rev. A **94**, 053614 (2016)
- **J. Decamp**, J. Jünemann, M. Albert, M. Rizzi, A. Minguzzi, P. Vignolo, *Strongly correlated one-dimensional Bose-Fermi quantum mixtures: symmetry and correlations*, New J. Phys. **19**, 125001 (2017)
- **J. Decamp**, M. Albert, P. Vignolo, *Tan's contact in a cigar-shaped dilute Bose gas*, Phys. Rev. A **97**, 033611 (2018)



---

# Bibliography

---

- [Abanin 2017] Dmitry A. Abanin and Zlatko Papić. *Recent progress in many-body localization*. *Annalen der Physik*, vol. 529, 2017.
- [Abramowitz 1965] Milton Abramowitz and Irene Stegun. *Handbook of mathematical functions: with formulas, graphs, and mathematical tables*. Dover Publications, 1965.
- [Affleck 1988] Ian Affleck and J. Brad Marston. *Large- $n$  limit of the Heisenberg-Hubbard model: Implications for high- $T_c$  superconductors*. *Phys. Rev. B*, vol. 37, pages 3774–3777, Mar 1988.
- [Ambjørn 2006] J. Ambjørn, R.A. Janik and C. Kristjansen. *Wrapping interactions and a new source of corrections to the spin-chain/string duality*. *Nuclear Physics B*, vol. 736, no. 3, pages 288 – 301, 2006.
- [Anderson 1995] M. H. Anderson, J. R. Ensher, M. R. Matthews, C. E. Wieman and E. A. Cornell. *Observation of Bose-Einstein Condensation in a Dilute Atomic Vapor*. *Science*, vol. 269, no. 5221, pages 198–201, 1995.
- [Auerbach 1994] Assa Auerbach. *Interacting electrons and quantum magnetism*. Springer New York, 1994.
- [Auslaender 2005] O. M. Auslaender. *Spin-Charge Separation and Localization in One Dimension*. *Science*, vol. 308, no. 5718, pages 88–92, apr 2005.
- [Banerjee 2013] D. Banerjee, M. Bögli, M. Dalmonte, E. Rico, P. Stebler, U.-J. Wiese and P. Zoller. *Atomic Quantum Simulation of  $U(N)$  and  $SU(N)$  Non-Abelian Lattice Gauge Theories*. *Phys. Rev. Lett.*, vol. 110, page 125303, Mar 2013.
- [Barth 2011] M. Barth and W. Zwerger. *Tan relations in one dimension*. *Annals of Physics*, vol. 326, page 2544, 2011.
- [Baxter 1971] R. J. Baxter. *Eight-Vertex Model in Lattice Statistics*. *Phys. Rev. Lett.*, vol. 26, pages 832–833, Apr 1971.
- [Baym 1996] Gordon Baym and C. J. Pethick. *Ground-State Properties of Magnetically Trapped Bose-Condensed Rubidium Gas*. *Phys. Rev. Lett.*, vol. 76, pages 6–9, Jan 1996.
- [Bethe 1931] H. Bethe. *Zur Theorie der Metalle*. *Zeitschrift für Physik*, vol. 71, no. 3, pages 205–226, Mar 1931.

- [Bleistein 2010] Norman Bleistein and Richard A Handelsman. *Asymptotic expansions of integrals*. Dover Publications, 2010.
- [Bloch 1929] Felix Bloch. *Über die Quantenmechanik der Elektronen in Kristallgittern*. *Zeitschrift für Physik*, vol. 52, no. 7-8, pages 555–600, jul 1929.
- [Bloch 2008] Immanuel Bloch, Jean Dalibard and Wilhelm Zwerger. *Many-body physics with ultracold gases*. *Rev. Mod. Phys.*, vol. 80, pages 885–964, Jul 2008.
- [Bloch 2012] Immanuel Bloch, Jean Dalibard and Sylvain Nascimbène. *Quantum simulations with ultracold quantum gases*. *Nature Physics*, vol. 8, no. 4, pages 267–276, apr 2012.
- [Bockrath 1999] Marc Bockrath, David H. Cobden, Jia Lu, Andrew G. Rinzler, Richard E. Smalley, Leon Balents and Paul L. McEuen. *Luttinger-liquid behaviour in carbon nanotubes*. *Nature*, vol. 397, no. 6720, pages 598–601, feb 1999.
- [Bogoliubov 1947] N. Bogoliubov. *On the theory of superfluidity*. *J. Phys. USSR*, vol. 11, page 23, 1947.
- [Bondy 2008] J.A. Bondy and U.S.R. Murty. *Graph theory*. Springer-Verlag London, 2008.
- [Bourbaki 2008] Nicolas Bourbaki. *Lie groups and lie algebras*. Springer Publishing Company, Incorporated, 2008.
- [Braaten 2008a] Eric Braaten, Daekyoung Kang and Lucas Platter. *Universal relations for a strongly interacting Fermi gas near a Feshbach resonance*. *Phys. Rev. A*, vol. 78, page 053606, Nov 2008.
- [Braaten 2008b] Eric Braaten and Lucas Platter. *Exact Relations for a Strongly Interacting Fermi Gas from the Operator Product Expansion*. *Phys. Rev. Lett.*, vol. 100, page 205301, May 2008.
- [Bracewell 1999] Ronald Bracewell. *The fourier transform & its applications*. McGraw-Hill Science/Engineering/Math, 1999.
- [Bradley 1995] C. C. Bradley, C. A. Sackett, J. J. Tollett and R. G. Hulet. *Evidence of Bose-Einstein Condensation in an Atomic Gas with Attractive Interactions*. *Phys. Rev. Lett.*, vol. 75, pages 1687–1690, Aug 1995.
- [Brouwer 2012] Andries E. Brouwer and Willem H. Haemers. *Spectra of graphs*. Springer-Verlag New York, 2012.
- [Busch 1998] Thomas Busch, Berthold-Georg Englert, Kazimierz Rzażewski and Martin Wilkens. *Two Cold Atoms in a Harmonic Trap*. *Foundations of Physics*, vol. 28, no. 4, pages 549–559, Apr 1998.
- [Cayley 1854] A. Cayley. *VII. On the theory of groups, as depending on the symbolic equation  $\theta_n = 1$* . *The London, Edinburgh, and Dublin Philosophical Magazine and Journal of Science*, vol. 7, no. 42, pages 40–47, 1854.



- [Cazalilla 2003] M.A. Cazalilla and A.F. Ho. *Instabilities in Binary Mixtures of One-Dimensional Quantum Degenerate Gases*. Phys. Rev. Lett., vol. 91, page 150403, 2003.
- [Cazalilla 2011] M. A. Cazalilla, R. Citro, T. Giamarchi, E. Orignac and M. Rigol. *One dimensional bosons: From condensed matter systems to ultracold gases*. Rev. Mod. Phys., vol. 83, pages 1405–1466, Dec 2011.
- [Chang 2016] R. Chang, Q. Bouton, H. Cayla, C. Qu, A. Aspect, C. I. Westbrook and D. Clément. *Momentum-Resolved Observation of Thermal and Quantum Depletion in a Bose Gas*. Phys. Rev. Lett., vol. 117, page 235303, Dec 2016.
- [Cohen-Tannoudji 1997a] C. Cohen-Tannoudji, B. Diu and F. Laloë. *Mécanique quantique*, tome 1. Hermann, 1997.
- [Cohen-Tannoudji 1997b] C. Cohen-Tannoudji, B. Diu and F. Laloë. *Mécanique quantique*, tome 2. Hermann, 1997.
- [Colome-Tatche 2008] Maria Colome-Tatche. *Finite size effects and dynamics in one-dimensional integrable systems*. Theses, Université Paris Sud - Paris XI, December 2008.
- [Combescot 2009] R. Combescot, F. Alzetto and X. Leyronas. *Particle distribution tail and related energy formula*. Phys. Rev. A, vol. 79, page 053640, May 2009.
- [Davis 1995] Kendall B. Davis, Marc-Oliver Mewes, Michael A. Joffe, Michael R. Andrews and Wolfgang Ketterle. *Evaporative Cooling of Sodium Atoms*. Phys. Rev. Lett., vol. 74, pages 5202–5205, Jun 1995.
- [Decamp 2016a] Jean Decamp, Pacome Armagnat, Bess Fang, Mathias Albert, Anna Minguzzi and Patrizia Vignolo. *Exact density profiles and symmetry classification for strongly interacting multi-component Fermi gases in tight waveguides*. New Journal of Physics, vol. 18, page 055011, 2016.
- [Decamp 2016b] Jean Decamp, Johannes Junemann, Mathias Albert, Matteo Rizzi, Anna Minguzzi and Patrizia Vignolo. *High-momentum tails as magnetic-structure probes for strongly correlated  $SU(\kappa)$  fermionic mixtures in one-dimensional traps*. Physical Review A, vol. 94, page 053614, 2016.
- [Decamp 2017] Jean Decamp, Johannes Jünemann, Mathias Albert, Matteo Rizzi, Anna Minguzzi and Patrizia Vignolo. *Strongly correlated one-dimensional Bose–Fermi quantum mixtures: symmetry and correlations*. New Journal of Physics, vol. 19, no. 12, page 125001, 2017.
- [Decamp 2018] Jean Decamp, Mathias Albert and Patrizia Vignolo. *Tan’s contact in a cigar-shaped dilute Bose gas*. Phys. Rev. A, vol. 97, page 033611, Mar 2018.
- [Dehkharghani 2016] A S Dehkharghani, A G Volosniev and N T Zinner. *Impenetrable mass-imbalanced particles in one-dimensional harmonic traps*. Journal of Physics B: Atomic, Molecular and Optical Physics, vol. 49, no. 8, page 085301, 2016.
- [Dehkharghani 2017] A S Dehkharghani, F F Bellotti and N T Zinner. *Analytical and numerical studies of Bose–Fermi mixtures in a one-dimensional harmonic trap*.

- Journal of Physics B: Atomic, Molecular and Optical Physics, vol. 50, no. 14, page 144002, 2017.
- [Deuretzbacher 2008] F. Deuretzbacher, K. Fredenhagen, D. Becker, K. Bongs, K. Sengstock and D. Pfannkuche. *Exact solution of strongly interacting quasi-one-dimensional spinor Bose gases*. Phys. Rev. Lett., vol. 100, page 160405, 2008.
- [Deuretzbacher 2014] F. Deuretzbacher, D. Becker, J. Bjerlin, S. Reimann and L. Santos. *Quantum magnetism without lattices in strongly interacting one-dimensional spinor gases*. Phys. Rev. A, vol. 90, page 013611, 2014.
- [Deuretzbacher 2016] F. Deuretzbacher, D. Becker and L. Santos. *Momentum distributions and numerical methods for strongly interacting one-dimensional spinor gases*. Phys. Rev. A, vol. 94, page 023606, Aug 2016.
- [Deuretzbacher 2017] F. Deuretzbacher, D. Becker, J. Bjerlin, S. M. Reimann and L. Santos. *Spin-chain model for strongly interacting one-dimensional Bose-Fermi mixtures*. Phys. Rev. A, vol. 95, page 043630, Apr 2017.
- [Dirac 1929] P. A. M. Dirac. *Quantum Mechanics of Many-Electron Systems*. Proceedings of the Royal Society A: Mathematical, Physical and Engineering Sciences, vol. 123, no. 792, pages 714–733, apr 1929.
- [Dunjko 2001] V. Dunjko, V. Lorent and M. Olshanii. *Bosons in Cigar-Shaped Traps: Thomas-Fermi Regime, Tonks-Girardeau Regime, and In Between*. Phys. Rev. Lett., vol. 86, pages 5413–5416, Jun 2001.
- [Dyson 1967] Freeman J. Dyson and A. Lenard. *Stability of Matter. I*. Journal of Mathematical Physics, vol. 8, no. 3, pages 423–434, 1967.
- [Dzyaloshinskii 1961] I E Dzyaloshinskii, E M Lifshitz and Lev P Pitaevskii. *General theory of van der Waals' forces*. Soviet Physics Uspekhi, vol. 4, no. 2, page 153, 1961.
- [Eckel 2018] S. Eckel, A. Kumar, T. Jacobson, I. B. Spielman and G. K. Campbell. *A Rapidly Expanding Bose-Einstein Condensate: An Expanding Universe in the Lab*. Phys. Rev. X, vol. 8, page 021021, Apr 2018.
- [Einstein 1905] A. Einstein. *Zur Elektrodynamik bewegter Körper*. Annalen der Physik, vol. 322, no. 10, pages 891–921, 1905.
- [Einstein 1917] A. Einstein. *Kosmologische Betrachtungen zur allgemeinen Relativitätstheorie*. Sitzungsberichte der Königlich Preußischen Akademie der Wissenschaften (Berlin), Seite 142-152., 1917.
- [Eisenberg 2002] Eli Eisenberg and Elliott H. Lieb. *Polarization of Interacting Bosons with Spin*. Phys. Rev. Lett., vol. 89, page 220403, Nov 2002.
- [Englert 1964] F. Englert and R. Brout. *Broken Symmetry and the Mass of Gauge Vector Mesons*. Phys. Rev. Lett., vol. 13, pages 321–323, Aug 1964.
- [Fang 2011] Bess Fang, Patrizia Vignolo, Mario Gattobigio, Christian Miniatura and Anna Minguzzi. *Exact solution for the degenerate ground-state manifold of a*

- strongly interacting one-dimensional Bose-Fermi mixture*. Phys. Rev. A, vol. 84, page 023626, Aug 2011.
- [Fano 1961] U. Fano. *Effects of Configuration Interaction on Intensities and Phase Shifts*. Phys. Rev., vol. 124, pages 1866–1878, Dec 1961.
- [Fedichev 1996] P. O. Fedichev, Yu. Kagan, G. V. Shlyapnikov and J. T. M. Walraven. *Influence of Nearly Resonant Light on the Scattering Length in Low-Temperature Atomic Gases*. Phys. Rev. Lett., vol. 77, pages 2913–2916, Sep 1996.
- [Feller 1947] Will Feller. *Review: Harald Cramer, Mathematical Methods of Statistics*. Ann. Math. Statist., vol. 18, no. 1, pages 136–139, 03 1947.
- [Feshbach 1958] Herman Feshbach. *Unified theory of nuclear reactions*. Annals of Physics, vol. 5, no. 4, pages 357 – 390, 1958.
- [Feynman 1939] R. P. Feynman. *Forces in Molecules*. Phys. Rev., vol. 56, pages 340–343, Aug 1939.
- [Feynman 1950] R. P. Feynman. *Mathematical Formulation of the Quantum Theory of Electromagnetic Interaction*. Phys. Rev., vol. 80, pages 440–457, Nov 1950.
- [Feynman 1982] Richard P. Feynman. *Simulating Physics with Computers*. International Journal of Theoretical Physics, vol. 21, pages 467–488, June 1982.
- [Feynman 1986] Richard P. Feynman. *Quantum mechanical computers*. Foundations of Physics, vol. 16, no. 6, pages 507–531, Jun 1986.
- [Folman 2002] Ron Folman, Peter Krüger, Jörg Schmiedmayer, Johannes Denschlag and Carsten Henkel. *Microscopic Atom Optics: From Wires to an Atom Chip*. Journal of Modern Optics, vol. 48, pages 263 – 356, 2002.
- [Forrester 2003] P. J. Forrester, N. E. Frankel, T. M. Garoni and N. S. Witte. *Finite one-dimensional impenetrable Bose systems: Occupation numbers*. Phys. Rev. A, vol. 67, page 043607, Apr 2003.
- [Fuchs 2003] J. N. Fuchs, X. Leyronas and R. Combescot. *Hydrodynamic modes of a one-dimensional trapped Bose gas*. Phys. Rev. A, vol. 68, page 043610, Oct 2003.
- [Fukuhara 2009] Takeshi Fukuhara, Seiji Sugawa, Yosuke Takasu and Yoshiro Takahashi. *All-optical formation of quantum degenerate mixtures*. Phys. Rev. A, vol. 79, page 021601, 2009.
- [Fulton 2004] William Fulton and Joe Harris. Representation theory. Springer New York, 2004.
- [Gaudin 1967] M. Gaudin. *Un système à une dimension de fermions en interaction*. Physics Letters A, vol. 24, no. 1, pages 55 – 56, 1967.
- [Gerbier 2004] F. Gerbier. *Quasi-1D Bose-Einstein condensates in the dimensional crossover regime*. EPL (Europhysics Letters), vol. 66, no. 6, page 771, 2004.
- [Gerlach 1922] Walther Gerlach and Otto Stern. *Der experimentelle Nachweis der Richtungsquantelung im Magnetfeld*. Zeitschrift für Physik, vol. 9, no. 1, pages 349–352, Dec 1922.

- [Giamarchi 2003] T. Giamarchi. *Quantum physics in one dimension*. Clarendon Press, Oxford, 2003.
- [Gieres 1997] F. Gieres, M. Kinler, C. Lucchesi and O. Piguet. *Symmetries in physics*. Editions Frontières, Paris, 1997.
- [Girardeau 1960] M. D. Girardeau. *Relationship between Systems of Impenetrable Bosons and Fermions in One Dimension*. *J. Math. Phys.*, vol. 1, page 516, 1960.
- [Girardeau 2001] M. D. Girardeau, E. M. Wright and J. M. Triscari. *Ground-state properties of a one-dimensional system of hard-core bosons in a harmonic trap*. *Phys. Rev. A*, vol. 63, page 033601, Feb 2001.
- [Glashow 1959] Sheldon L. Glashow. *The renormalizability of vector meson interactions*. *Nuclear Physics*, vol. 10, pages 107 – 117, 1959.
- [Goldstone 1962] Jeffrey Goldstone, Abdus Salam and Steven Weinberg. *Broken Symmetries*. *Phys. Rev.*, vol. 127, pages 965–970, Aug 1962.
- [Gorshkov 2010] A. V. Gorshkov, M. Hermele, V. Gurarie, C. Xu, P. S. Julienne, J. Ye, P. Zoller, E. Demler, M. D. Lukin and A. M. Rey. *Two-orbital  $SU(N)$  magnetism with ultracold alkaline-earth atoms*. *Nature Physics*, vol. 6, no. 4, pages 289–295, feb 2010.
- [Goupil 2000] Alain Goupil, Dominique Poulalhon and Gilles Schaeffer. *Central Characters and Conjugacy Classes of the Symmetric Group or On some Conjectures of J. Katriel*. In *Formal Power Series and Algebraic Combinatorics*, pages 238–249. Springer Berlin Heidelberg, 2000.
- [Greiner 2002] Markus Greiner, Olaf Mandel, Tilman Esslinger, Theodor W. Hänsch and Immanuel Bloch. *Quantum phase transition from a superfluid to a Mott insulator in a gas of ultracold atoms*. *Nature*, vol. 415, no. 6867, pages 39–44, jan 2002.
- [Grimm 2000] Rudolf Grimm, Matthias Weidemüller and Yurii B. Ovchinnikov. *Optical Dipole Traps for Neutral Atoms*. *Advances In Atomic, Molecular, and Optical Physics*, vol. 42, pages 95 – 170, 2000.
- [Grining 2015a] T. Grining, M. Tomza, M. Lesiuk, M. Przybytek, M. Musia, P. Massignan, M. Lewenstein and R. Moszynski. *Many interacting fermions in a one-dimensional harmonic trap: a quantum-chemical treatment*. *New Journal of Physics*, vol. 11, 2015.
- [Grining 2015b] Tomasz Grining, Michał Tomza, Michał Lesiuk, Michał Przybytek, Monika Musiał, Robert Moszynski, Maciej Lewenstein and Pietro Massignan. *Crossover between few and many fermions in a harmonic trap*. *Phys. Rev. A*, vol. 92, page 061601, Dec 2015.
- [Gross 1961] E. P. Gross. *Structure of a quantized vortex in boson systems*. *Il Nuovo Cimento (1955-1965)*, vol. 20, no. 3, pages 454–477, May 1961.
- [Gross 1973] David J. Gross and Frank Wilczek. *Ultraviolet Behavior of Non-Abelian Gauge Theories*. *Phys. Rev. Lett.*, vol. 30, pages 1343–1346, Jun 1973.

- [Gross 1996] David J. Gross. *The role of symmetry in fundamental physics*. Proceedings of the National Academy of Sciences, vol. 93, no. 25, pages 14256–14259, 1996.
- [Guan 2011] X-W Guan and M T Batchelor. *Polylogs, thermodynamics and scaling functions of one-dimensional quantum many-body systems*. Journal of Physics A: Mathematical and Theoretical, vol. 44, no. 10, page 102001, 2011.
- [Guan 2012] Xi-Wen Guan, Zhong-Qi Ma and Brendan Wilson. *One-dimensional multicomponent fermions with  $\delta$ -function interaction in strong- and weak-coupling limits:  $\kappa$ -component Fermi gas*. Phys. Rev. A, vol. 85, page 033633, Mar 2012.
- [Haldane 1981] F D M Haldane. *'Luttinger liquid theory' of one-dimensional quantum fluids. I. Properties of the Luttinger model and their extension to the general 1D interacting spinless Fermi gas*. Journal of Physics C: Solid State Physics, vol. 14, no. 19, page 2585, 1981.
- [Hamermesh 1989] M. Hamermesh. Group theory and its applications to physical problems. Dover, New York, 1989.
- [Hardy 1918] G. H. Hardy and S. Ramanujan. *Asymptotic Formulae in Combinatory Analysis*. Proceedings of the London Mathematical Society, vol. s2-17, no. 1, pages 75–115, 1918.
- [Harshman 2014] N. L. Harshman. *Spectroscopy for a few atoms harmonically trapped in one dimension*. Phys. Rev. A, vol. 89, page 033633, Mar 2014.
- [Harshman 2015] N. L. Harshman. *One-Dimensional Traps, Two-Body Interactions, Few-Body Symmetries: I. One, Two, and Three Particles*. Few-Body Systems, vol. 57, no. 1, pages 11–43, sep 2015.
- [Harshman 2016] N. L. Harshman. *One-Dimensional Traps, Two-Body Interactions, Few-Body Symmetries. II. N Particles*. Few-Body Systems, vol. 57, no. 1, pages 45–69, 2016.
- [Harshman 2017] N. L. Harshman, Maxim Olshanii, A. S. Dehkharghani, A. G. Volosniev, Steven Glenn Jackson and N. T. Zinner. *Integrable Families of Hard-Core Particles with Unequal Masses in a One-Dimensional Harmonic Trap*. Phys. Rev. X, vol. 7, page 041001, Oct 2017.
- [He 2017] M. He and Q. Zhou. *s-wave Contacts of Quantum Gases in Quasi-one and Quasi-two Dimensions*. ArXiv 1708.00135, 2017.
- [Higgs 1964] Peter W. Higgs. *Broken Symmetries and the Masses of Gauge Bosons*. Phys. Rev. Lett., vol. 13, pages 508–509, Oct 1964.
- [Ho 2004] Tin-Lun Ho and Erich J. Mueller. *High Temperature Expansion Applied to Fermions near Feshbach Resonance*. Phys. Rev. Lett., vol. 92, page 160404, Apr 2004.
- [Hohenberg 1967] P. C. Hohenberg. *Existence of Long-Range Order in One and Two Dimensions*. Phys. Rev., vol. 158, pages 383–386, Jun 1967.
- [Hoinka 2013] Sascha Hoinka, Marcus Lingham, Kristian Fenech, Hui Hu, Chris J. Vale, Joaquín E. Drut and Stefano Gandolfi. *Precise Determination of the Structure*

- Factor and Contact in a Unitary Fermi Gas*. Phys. Rev. Lett., vol. 110, page 055305, Jan 2013.
- [Hu 2011] Hui Hu, Xia-Ji Liu and Peter D Drummond. *Universal contact of strongly interacting fermions at finite temperatures*. New Journal of Physics, vol. 13, no. 3, page 035007, 2011.
- [Huang 1957] Kerson Huang and C. N. Yang. *Quantum-Mechanical Many-Body Problem with Hard-Sphere Interaction*. Phys. Rev., vol. 105, pages 767–775, Feb 1957.
- [Imambekov 2006a] Adilet Imambekov and Eugene Demler. *Applications of exact solution for strongly interacting one-dimensional Bose–Fermi mixture: Low-temperature correlation functions, density profiles, and collective modes*. Annals of Physics, vol. 321, no. 10, pages 2390 – 2437, 2006.
- [Imambekov 2006b] Adilet Imambekov and Eugene Demler. *Exactly solvable case of a one-dimensional Bose–Fermi mixture*. Phys. Rev. A, vol. 73, page 021602, Feb 2006.
- [Itzykson 1966] C. Itzykson and M. Nauenberg. *Unitary Groups: Representations and Decompositions*. Rev. Mod. Phys., vol. 38, pages 95–120, Jan 1966.
- [Izrailev 1990] F. M. Izrailev. *Simple models of quantum chaos: Spectrum and eigenfunctions*. Physics Reports, vol. 196, pages 299–392, 1990.
- [Jacqmin 2011] Thibaut Jacqmin, Julien Armijo, Tarik Berrada, Karen V. Kheruntsyan and Isabelle Bouchoule. *Sub-Poissonian Fluctuations in a 1D Bose Gas: From the Quantum Quasicondensate to the Strongly Interacting Regime*. Phys. Rev. Lett., vol. 106, page 230405, Jun 2011.
- [James 2001] Gordon James and Martin Liebeck. Representations and characters of groups (2nd ed.). Cambridge University Press, Cambridge, London, 2001.
- [Kato 1995] Yusuke Kato and Yoshio Kuramoto. *Exact Solution of the Sutherland Model with Arbitrary Internal Symmetry*. Phys. Rev. Lett., vol. 74, pages 1222–1225, Feb 1995.
- [Katriel 1993a] J. Katriel. *Representation-free evaluation of the eigenvalues of the class-sums of the symmetric group*. J. Phys. A, vol. 26, page 135, 1993.
- [Katriel 1993b] Jacob Katriel and Ruben Pauncz. *Eigenvalues of single-cycle class-sums in the symmetric group. II*. International Journal of Quantum Chemistry, vol. 48, no. 2, pages 125–134, oct 1993.
- [Katriel 1996] Jacob Katriel. *Explicit expressions for the central characters of the symmetric group*. Discrete Applied Mathematics, vol. 67, no. 1, pages 149 – 156, 1996. Chemistry and Discrete Mathematics.
- [Keller 2014] Michael Keller, Mateusz Kotyrba, Florian Leupold, Mandip Singh, Maximilian Ebner and Anton Zeilinger. *Bose-Einstein condensate of metastable helium for quantum correlation experiments*. Phys. Rev. A, vol. 90, page 063607, Dec 2014.

- [Ketterle 1992] W. Ketterle and D. E. Pritchard. *Trapping and focusing ground state atoms with static fields*. Applied Physics B, vol. 54, no. 5, pages 403–406, May 1992.
- [Kinoshita 2004] Toshiya Kinoshita, Trevor Wenger and David S. Weiss. *Observation of a One-Dimensional Tonks-Girardeau Gas*. Science, vol. 305, no. 5687, pages 1125–1128, 2004.
- [Kolomeisky 2000] Eugene B. Kolomeisky, T. J. Newman, Joseph P. Straley and Xiaoya Qi. *Low-Dimensional Bose Liquids: Beyond the Gross-Pitaevskii Approximation*. Phys. Rev. Lett., vol. 85, pages 1146–1149, Aug 2000.
- [Korepin 1993] V. E. Korepin, N. M. Bogoliubov and A. G. Izergin. Quantum inverse scattering method and correlation functions. Cambridge Monographs on Mathematical Physics. Cambridge University Press, Cambridge, 1993.
- [Kuhnle 2011] E D Kuhnle, S Hoinka, H Hu, P Dyke, P Hannaford and C J Vale. *Studies of the universal contact in a strongly interacting Fermi gas using Bragg spectroscopy*. New Journal of Physics, vol. 13, no. 5, page 055010, 2011.
- [Lahav 2010] Oren Lahav, Amir Itah, Alex Blumkin, Carmit Gordon, Shahar Rinott, Alona Zayats and Jeff Steinhauer. *Realization of a Sonic Black Hole Analog in a Bose-Einstein Condensate*. Phys. Rev. Lett., vol. 105, page 240401, Dec 2010.
- [Lai 1971] C. K. Lai. *Thermodynamics of Fermions in One Dimension with a  $\delta$ -Function Interaction*. Phys. Rev. Lett., vol. 26, pages 1472–1475, Jun 1971.
- [Laird 2017] E. K. Laird, Z.-Y. Shi, M. M. Parish and J. Levinsen.  *$SU(N)$  fermions in a one-dimensional harmonic trap*. Phys. Rev. A, vol. 96, page 032701, Sep 2017.
- [Lake 2005] Bella Lake, D. Alan Tennant, Chris D. Frost and Stephen E. Nagler. *Quantum criticality and universal scaling of a quantum antiferromagnet*. Nature Materials, vol. 4, no. 4, pages 329–334, apr 2005.
- [Landau 1957] L. D. Landau. *The Theory of a Fermi Liquid*. JETP, vol. 3, pages 920–925, 1957.
- [Landau 1980] L. D. Landau and E.M. Lifshitz. Statistical physics. Course of Theoretical Physics, Volume 5. Butterworth-Heinemann, 1980.
- [Landau 1981] L. D. Landau and L. M. Lifshitz. Quantum mechanics, third edition: Non-relativistic theory (volume 3). Butterworth-Heinemann, 1981.
- [Lang 2017] Guillaume Lang, Patrizia Vignolo and Anna Minguzzi. *Tan’s contact of a harmonically trapped one-dimensional Bose gas: Strong-coupling expansion and conjectural approach at arbitrary interactions*. The European Physical Journal Special Topics, vol. 226, no. 7, pages 1583–1591, May 2017.
- [Leboeuf 2001] P. Leboeuf and N. Pavloff. *Bose-Einstein beams: Coherent propagation through a guide*. Phys. Rev. A, vol. 64, page 033602, Aug 2001.
- [Levinsen 2015] Jesper Levinsen, Pietro Massignan, Georg M. Bruun, and Meera M. Parish. *Strong-coupling Ansatz for the one-dimensional Fermi gas in a harmonic potential*. Science Advances, 2015.

- [Lieb 1962] Elliott Lieb and Daniel Mattis. *Theory of Ferromagnetism and the Ordering of Electronic Energy Levels*. Phys. Rev., vol. 125, pages 164–172, Jan 1962.
- [Lieb 1963] E.H. Lieb and W. Liniger. *Exact Analysis of an Interacting Bose Gas. I. The General Solution and the Ground State*. Phys. Rev., vol. 130, page 1605, 1963.
- [Lieb 1968] Elliott H. Lieb and F. Y. Wu. *Absence of Mott Transition in an Exact Solution of the Short-Range, One-Band Model in One Dimension*. Phys. Rev. Lett., vol. 20, pages 1445–1448, Jun 1968.
- [Lin 2011] Y.-J. Lin, R. L. Compton, K. Jiménez-García, W. D. Phillips, J. V. Porto and I. B. Spielman. *A synthetic electric force acting on neutral atoms*. Nature Physics, vol. 7, no. 7, pages 531–534, mar 2011.
- [Liu 2009] Xia-Ji Liu, Hui Hu and Peter D. Drummond. *Virial Expansion for a Strongly Correlated Fermi Gas*. Phys. Rev. Lett., vol. 102, page 160401, Apr 2009.
- [Liu 2010] Xia-Ji Liu and Hui Hu. *Virial expansion for a strongly correlated Fermi gas with imbalanced spin populations*. Phys. Rev. A, vol. 82, page 043626, Oct 2010.
- [Liu 2014] Xia-Ji Liu and Hui Hu. *Collective mode evidence of high-spin bosonization in a trapped one-dimensional atomic Fermi gas with tunable spin*. Annals of Physics, vol. 350, pages 84 – 94, 2014.
- [Macdonald 1995] I. G. Macdonald. Symmetric functions and hall polynomials. Oxford Mathematical Monographs. Oxford University Press, USA, 2 édition, 1995.
- [Marston 1989] J. Brad Marston and Ian Affleck. *Large- $n$  limit of the Hubbard-Heisenberg model*. Phys. Rev. B, vol. 39, pages 11538–11558, Jun 1989.
- [Massignan 2015] Pietro Massignan, Jesper Levinsen and Meera M. Parish. *Magnetism in Strongly Interacting One-Dimensional Quantum Mixtures*. Phys. Rev. Lett., vol. 115, page 247202, Dec 2015.
- [Matveev 2008] K. A. Matveev and A. Furusaki. *Spectral Functions of Strongly Interacting Isospin- $\frac{1}{2}$  Bosons in One Dimension*. Phys. Rev. Lett., vol. 101, page 170403, Oct 2008.
- [Matveeva 2016] N. Matveeva and G.E. Astrakharchik. *One-dimensional multicomponent Fermi gas in a trap: quantum Monte Carlo study*. New Journal of Physics, vol. 18, page 065009, 2016.
- [Menotti 2002] Chiara Menotti and Sandro Stringari. *Collective oscillations of a one-dimensional trapped Bose-Einstein gas*. Phys. Rev. A, vol. 66, page 043610, Oct 2002.
- [Mermin 1966] N. D. Mermin and H. Wagner. *Absence of Ferromagnetism or Antiferromagnetism in One- or Two-Dimensional Isotropic Heisenberg Models*. Phys. Rev. Lett., vol. 17, pages 1133–1136, Nov 1966.
- [Milliken 1996] F.P. Milliken, C.P. Umbach and R.A. Webb. *Indications of a Luttinger liquid in the fractional quantum Hall regime*. Solid State Communications, vol. 97, no. 4, pages 309 – 313, 1996.



- [Minguzzi 2002] A. Minguzzi, P. Vignolo and M.P. Tosi. *High momentum tail in the Tonks gas under harmonic confinement*. Phys. Lett. A, vol. 294, page 222, 2002.
- [Moritz 2003] Henning Moritz, Thilo Stöferle, Michael Köhl and Tilman Esslinger. *Exciting Collective Oscillations in a Trapped 1D Gas*. Phys. Rev. Lett., vol. 91, page 250402, Dec 2003.
- [Muñoz Mateo 2006] A. Muñoz Mateo and V. Delgado. *Extension of the Thomas-Fermi approximation for trapped Bose-Einstein condensates with an arbitrary number of atoms*. Phys. Rev. A, vol. 74, page 065602, Dec 2006.
- [Muñoz Mateo 2008] A. Muñoz Mateo and V. Delgado. *Effective mean-field equations for cigar-shaped and disk-shaped Bose-Einstein condensates*. Phys. Rev. A, vol. 77, page 013617, Jan 2008.
- [Murmans 2015] S. Murmann, F. Deuretzbacher, G. Zürn, J. Bjerlin, S. M. Reimann, L. Santos, T. Lompe and S. Jochim. *Antiferromagnetic Heisenberg Spin Chain of a Few Cold Atoms in a One-Dimensional Trap*. Phys. Rev. Lett., vol. 115, page 215301, Nov 2015.
- [Nataf 2014] Pierre Nataf and Frédéric Mila. *Exact Diagonalization of Heisenberg  $SU(N)$  Models*. Phys. Rev. Lett., vol. 113, page 127204, Sep 2014.
- [Nataf 2016] Pierre Nataf and Frédéric Mila. *Exact diagonalization of Heisenberg  $SU(N)$  chains in the fully symmetric and antisymmetric representations*. Phys. Rev. B, vol. 93, page 155134, Apr 2016.
- [Noether 1918] E. Noether. *Invariante Variationsprobleme*. Nachrichten von der Gesellschaft der Wissenschaften zu Göttingen, Mathematisch-Physikalische Klasse, vol. 1918, pages 235–257, 1918.
- [Novolesky 1994] A. Novolesky and J. Katriel. *Hyperspherical functions with arbitrary permutational symmetry*. Phys. Rev. A, vol. 49, page 833, 1994.
- [Novolesky 1995] A. Novolesky and J. Katriel. *Symmetry analysis of many-body wave functions, with applications to the nuclear shell model*. Phys. Rev. C, vol. 51, page 412, 1995.
- [Olshanii 1998] M. Olshanii. *Atomic Scattering in the Presence of an External Confinement and a Gas of Impenetrable Bosons*. Phys. Rev. Lett., vol. 81, pages 938–941, Aug 1998.
- [Olshanii 2003] Maxim Olshanii and Vanja Dunjko. *Short-Distance Correlation Properties of the Lieb-Liniger System and Momentum Distributions of Trapped One-Dimensional Atomic Gases*. Phys. Rev. Lett., vol. 91, page 090401, 2003.
- [Pagano 2014] G. Pagano, M. Mancini, P. Lombardi, G. Cappellini, P. Lombardi, K.-J. Liu, F. Schafer, H. Hu, J. Catani, C. Sias, M. Inguscio and L. Fallani. *A one-dimensional liquid of Fermions with tunable spin*. Nature Physics, vol. 10, page 198–201, 2014.

- [Pătu 2016] Ovidiu I. Pătu and Andreas Klümper. *Thermodynamics, contact, and density profiles of the repulsive Gaudin-Yang model*. Phys. Rev. A, vol. 93, page 033616, Mar 2016.
- [Pătu 2017] Ovidiu I. Pătu and Andreas Klümper. *Universal Tan relations for quantum gases in one dimension*. Phys. Rev. A, vol. 96, page 063612, Dec 2017.
- [Pan 2017] Lei Pan, Yanxia Liu, Haiping Hu, Yunbo Zhang and Shu Chen. *Exact ordering of energy levels for one-dimensional interacting Fermi gases with  $SU(N)$  symmetry*. Phys. Rev. B, vol. 96, page 075149, Aug 2017.
- [Papenbrock 2003] T. Papenbrock. *Ground-state properties of hard-core bosons in one-dimensional harmonic traps*. Phys. Rev. A, vol. 67, page 041601, Apr 2003.
- [Paredes 2004] B Paredes, A Widera, V Murg, O Mandel, S Folling, I Cirac, GV Shlyapnikov, TW Hansch and I Bloch. *Tonks-Girardeau gas of ultracold atoms in an optical lattice*. Nature, vol. 429, page 277, 2004.
- [Parr 1980] Robert G. Parr. *Density Functional Theory of Atoms and Molecules*. In Horizons of Quantum Chemistry, pages 5–15, Dordrecht, 1980. Springer Netherlands.
- [Peano 2005] V Peano, M Thorwart, C Mora and R Egger. *Confinement-induced resonances for a two-component ultracold atom gas in arbitrary quasi-one-dimensional traps*. New Journal of Physics, vol. 7, no. 1, page 192, 2005.
- [Penrose 1956] Oliver Penrose and Lars Onsager. *Bose-Einstein Condensation and Liquid Helium*. Phys. Rev., vol. 104, pages 576–584, Nov 1956.
- [Petrich 1995] Wolfgang Petrich, Michael H. Anderson, Jason R. Ensher and Eric A. Cornell. *Stable, Tightly Confining Magnetic Trap for Evaporative Cooling of Neutral Atoms*. Phys. Rev. Lett., vol. 74, pages 3352–3355, Apr 1995.
- [Petrov 2000] D.S. Petrov, G.V. Shlyapnikov and J.T.M. Walraven. *Regimes of quantum degeneracy in trapped 1D gases*. Phys. Rev. Lett., vol. 85, page 3745, 2000.
- [Pieri 2009] Pierbiagio Pieri, Andrea Perali and Giancarlo Calvanese Strinati. *Enhanced paraconductivity-like fluctuations in the radiofrequency spectra of ultracold Fermi atoms*. Nature Physics, vol. 5, no. 10, pages 736–740, aug 2009.
- [Pitaevskii 1961] L. P. Pitaevskii. *Vortex lines in imperfect Bose gas*. JETP, vol. 13, pages 451–454, 1961.
- [Pitaevskii 2016] L. Pitaevskii and S. Stringari. *Bose-einstein condensation and superfluidity*. Oxford University Press, Oxford, United Kingdom, 2016.
- [Politzer 1973] H. David Politzer. *Reliable Perturbative Results for Strong Interactions?* Phys. Rev. Lett., vol. 30, pages 1346–1349, Jun 1973.
- [Qin 2017] Pinquan Qin, Alexei Andreanov, Hee Chul Park and Sergej Flach. *Interacting ultracold atomic kicked rotors: loss of dynamical localization*. Scientific Reports, vol. 7, 2017.

- [Raab 1987] E. L. Raab, M. Prentiss, Alex Cable, Steven Chu and D. E. Pritchard. *Trapping of Neutral Sodium Atoms with Radiation Pressure*. Phys. Rev. Lett., vol. 59, pages 2631–2634, Dec 1987.
- [Read 1989] N. Read and Subir Sachdev. *Some features of the phase diagram of the square lattice  $SU(N)$  antiferromagnet*. Nuclear Physics B, vol. 316, no. 3, pages 609 – 640, 1989.
- [Reichel 1999] J. Reichel, W. Hänsel and T. W. Hänsch. *Atomic Micromanipulation with Magnetic Surface Traps*. Phys. Rev. Lett., vol. 83, pages 3398–3401, Oct 1999.
- [Rizzi 2018] Matteo Rizzi, Christian Miniatura, Anna Minguzzi and Patrizia Vignolo. *Contact and ground-state energy for harmonically-trapped one-dimensional interacting bosons: from two to many*. ArXiv 1805.02463, May 2018.
- [Sagi 2012] Yoav Sagi, Tara E. Drake, Rabin Paudel and Deborah S. Jin. *Measurement of the Homogeneous Contact of a Unitary Fermi Gas*. Phys. Rev. Lett., vol. 109, page 220402, Nov 2012.
- [Salam 1959] Abdus Salam and J. C. Ward. *Weak and electromagnetic interactions*. II Nuovo Cimento (1955-1965), vol. 11, no. 4, pages 568–577, Feb 1959.
- [Salasnich 2004] L. Salasnich, A. Parola and L. Reatto. *Transition from three dimensions to one dimension in Bose gases at zero temperature*. Phys. Rev. A, vol. 70, page 013606, Jul 2004.
- [Salasnich 2005] L. Salasnich, A. Parola and L. Reatto. *Quasi-one-dimensional bosons in three-dimensional traps: From strong-coupling to weak-coupling regime*. Phys. Rev. A, vol. 72, page 025602, Aug 2005.
- [Schlottmann 1993] P Schlottmann. *Thermodynamics of the one-dimensional multicomponent Fermi gas with a delta -function interaction*. Journal of Physics: Condensed Matter, vol. 5, no. 32, page 5869, 1993.
- [Schwinger 1948] Julian Schwinger. *Quantum Electrodynamics. I. A Covariant Formulation*. Phys. Rev., vol. 74, pages 1439–1461, Nov 1948.
- [Schwinger 1951] Julian Schwinger. *The Theory of Quantized Fields. I*. Phys. Rev., vol. 82, pages 914–927, Jun 1951.
- [Shmueli 2006] U. Shmueli, editor. *International tables for crystallography*. International Union of Crystallography, oct 2006.
- [Simovici 2014] Dan A. Simovici and Chabane Djeraba. *Mathematical tools for data mining: Set theory, partial orders, combinatorics*. Springer London, 2014.
- [Stewart 2010] J. T. Stewart, J. P. Gaebler, T. E. Drake and D. S. Jin. *Verification of Universal Relations in a Strongly Interacting Fermi Gas*. Phys. Rev. Lett., vol. 104, page 235301, Jun 2010.
- [Stöferle 2004] Thilo Stöferle, Henning Moritz, Christian Schori, Michael Köhl and Tilman Esslinger. *Transition from a Strongly Interacting 1D Superfluid to a Mott Insulator*. Phys. Rev. Lett., vol. 92, page 130403, Mar 2004.

- [Stringari 1996] S. Stringari. *Collective Excitations of a Trapped Bose-Condensed Gas*. Phys. Rev. Lett., vol. 77, pages 2360–2363, Sep 1996.
- [Sutherland 1967] B. Sutherland, C. N. Yang and C. P. Yang. *Exact Solution of a Model of Two-Dimensional Ferroelectrics in an Arbitrary External Electric Field*. Phys. Rev. Lett., vol. 19, pages 588–591, Sep 1967.
- [Sutherland 1968] Bill Sutherland. *Further Results for the Many-Body Problem in One Dimension*. Phys. Rev. Lett., vol. 20, pages 98–100, Jan 1968.
- [Sutherland 2004] B. Sutherland. Beautiful models: 70 years of exactly solved quantum many-body problems. World Scientific Press, Singapore, 2004.
- [Tagliacozzo 2013] L. Tagliacozzo, A. Celi, P. Orland, M. W. Mitchell and M. Lewenstein. *Simulation of non-Abelian gauge theories with optical lattices*. Nature Communications, vol. 4, no. 1, oct 2013.
- [Taie 2010] Shintaro Taie, Yosuke Takasu, Seiji Sugawa, Rekishu Yamazaki, Takuya Tsujimoto, Ryo Murakami and Yoshiro Takahashi. *Realization of a  $SU(2) \times SU(6)$  System of Fermions in a Cold Atomic Gas*. Phys. Rev. Lett., vol. 105, page 190401, Nov 2010.
- [Takahashi 1971] Minoru Takahashi. *One-Dimensional Electron Gas with Delta-Function Interaction at Finite Temperature*. Progress of Theoretical Physics, vol. 46, no. 5, pages 1388–1406, 1971.
- [Talmi 1993] Talmi. Simple models of complex nuclei. Harwood Academic, Chur, Switzerland, 1993.
- [Tan 2008a] Shina Tan. *Energetics of a strongly correlated Fermi gas*. Annals of Physics, vol. 323, no. 12, pages 2952 – 2970, 2008.
- [Tan 2008b] Shina Tan. *Generalized virial theorem and pressure relation for a strongly correlated Fermi gas*. Annals of Physics, vol. 323, no. 12, pages 2987 – 2990, 2008.
- [Tan 2008c] Shina Tan. *Large momentum part of a strongly correlated Fermi gas*. Annals of Physics, vol. 323, no. 12, pages 2971 – 2986, 2008.
- [Tiesinga 1993] E. Tiesinga, B. J. Verhaar and H. T. C. Stoof. *Threshold and resonance phenomena in ultracold ground-state collisions*. Phys. Rev. A, vol. 47, pages 4114–4122, May 1993.
- [Tollett 1995] J. J. Tollett, C. C. Bradley, C. A. Sackett and R. G. Hulet. *Permanent magnet trap for cold atoms*. Phys. Rev. A, vol. 51, pages R22–R25, Jan 1995.
- [Tomonaga 1946] S. Tomonaga. *On a Relativistically Invariant Formulation of the Quantum Theory of Wave Fields*. Progress of Theoretical Physics, vol. 1, no. 2, pages 27–42, 1946.
- [Tonks 1936] Lewi Tonks. *The Complete Equation of State of One, Two and Three-Dimensional Gases of Hard Elastic Spheres*. Phys. Rev., vol. 50, pages 955–963, Nov 1936.

- [Valiente 2011] Manuel Valiente, Nikolaj T. Zinner and Klaus Mølmer. *Universal relations for the two-dimensional spin-1/2 Fermi gas with contact interactions*. Phys. Rev. A, vol. 84, page 063626, Dec 2011.
- [Valiente 2012] Manuel Valiente, Nikolaj T. Zinner and Klaus Mølmer. *Universal properties of Fermi gases in arbitrary dimensions*. Phys. Rev. A, vol. 86, page 043616, Oct 2012.
- [Vignolo 2000] Patrizia Vignolo, Anna Minguzzi and M. P. Tosi. *Exact Particle and Kinetic-Energy Densities for One-Dimensional Confined Gases of Noninteracting Fermions*. Phys. Rev. Lett., vol. 85, pages 2850–2853, Oct 2000.
- [Vignolo 2001] Patrizia Vignolo, Anna Minguzzi and M. P. Tosi. *Light scattering from a degenerate quasi-one-dimensional confined gas of noninteracting fermions*. Phys. Rev. A, vol. 64, page 023421, Jul 2001.
- [Vignolo 2013] Patrizia Vignolo and Anna Minguzzi. *Universal Contact for a Tonks-Girardeau Gas at Finite Temperature*. Phys. Rev. Lett., vol. 110, page 020403, Jan 2013.
- [Voit 1995] J Voit. *One-dimensional Fermi liquids*. Reports on Progress in Physics, vol. 58, no. 9, page 977, 1995.
- [Volosniev 2013] A.G. Volosniev, A.S. Jensen D.V. Fedorov, N.T. Zinner and M. Valiente. *Multicomponent Strongly Interacting Few-Fermion Systems in One Dimension*. Few-Body Systems, vol. 55, page 839, 2013.
- [Volosniev 2014] A.G. Volosniev, D.V. Fedorov, A.S. Jensen, N.T. Zinner and M. Valiente. *Strongly interacting confined quantum systems in one dimension*. Nature Communications, vol. 5, page 5300, 2014.
- [Wan 2017] Kianna Wan, Pierre Nataf and Frédéric Mila. *Exact diagonalization of  $SU(N)$  Heisenberg and Affleck-Kennedy-Lieb-Tasaki chains using the full  $SU(N)$  symmetry*. Phys. Rev. B, vol. 96, page 115159, Sep 2017.
- [Weinberg 1967] Steven Weinberg. *A Model of Leptons*. Phys. Rev. Lett., vol. 19, pages 1264–1266, Nov 1967.
- [Werner 2012a] Félix Werner and Yvan Castin. *General relations for quantum gases in two and three dimensions. II. Bosons and mixtures*. Phys. Rev. A, vol. 86, page 053633, Nov 2012.
- [Werner 2012b] Félix Werner and Yvan Castin. *General relations for quantum gases in two and three dimensions: Two-component fermions*. Phys. Rev. A, vol. 86, page 013626, Jul 2012.
- [Weyl 1952] Hermann Weyl. *Symmetry*. Princeton University Press, 1952.
- [Wilczek 1982] Frank Wilczek. *Quantum Mechanics of Fractional-Spin Particles*. Phys. Rev. Lett., vol. 49, pages 957–959, Oct 1982.
- [Wild 2012] R. J. Wild, P. Makotyn, J. M. Pino, E. A. Cornell and D. S. Jin. *Measurements of Tan’s Contact in an Atomic Bose-Einstein Condensate*. Phys. Rev. Lett., vol. 108, page 145305, Apr 2012.

- [Wilson 1975] Kenneth G. Wilson. *The renormalization group: Critical phenomena and the Kondo problem*. Rev. Mod. Phys., vol. 47, pages 773–840, Oct 1975.
- [Yang 1962] C. N. Yang. *Concept of Off-Diagonal Long-Range Order and the Quantum Phases of Liquid He and of Superconductors*. Rev. Mod. Phys., vol. 34, pages 694–704, Oct 1962.
- [Yang 1967] C. N. Yang. *Some Exact Results for the Many-Body Problem in one Dimension with Repulsive Delta-Function Interaction*. Phys. Rev. Lett., vol. 19, pages 1312–1315, Dec 1967.
- [Yang 1969] C. N. Yang and C. P. Yang. *Thermodynamics of a One-Dimensional System of Bosons with Repulsive Delta-Function Interaction*. Journal of Mathematical Physics, vol. 10, no. 7, pages 1115–1122, 1969.
- [Yang 2011] C. N. Yang and You Yi-Zhuang. *One-Dimensional  $w$ -Component Fermions and Bosons with Repulsive Delta Function Interaction*. Chinese Physics Letters, vol. 28, no. 2, page 020503, 2011.
- [Yao 2018] H. Yao, D. Clément, A. Minguzzi, P. Vignolo and L. Sanchez-Palencia. *Tan’s Contact for Trapped Lieb-Liniger Bosons at Finite Temperature*. ArXiv 1804.04902, April 2018.
- [Zaremba 1998] E. Zaremba. *Sound propagation in a cylindrical Bose-condensed gas*. Phys. Rev. A, vol. 57, pages 518–521, Jan 1998.
- [Zhang 2009] Shizhong Zhang and Anthony J. Leggett. *Universal properties of the ultracold Fermi gas*. Phys. Rev. A, vol. 79, page 023601, Feb 2009.
- [Zohar 2013] Erez Zohar, J. Ignacio Cirac and Benni Reznik. *Cold-Atom Quantum Simulator for  $SU(2)$  Yang-Mills Lattice Gauge Theory*. Phys. Rev. Lett., vol. 110, page 125304, Mar 2013.